National Library of Canada
Collections Development Branch

Canadian Theses on
Microfiche Service

Bibliothèque nationale du Canada
Direction du développement des collections

Service des thèses canadiennes
sur microfiche

NOTICE

The quality of this microfiche is heavily dependent upon the quality of the original thesis submitted for microfilming. Every effort has been made to ensure the highest quality of reproduction possible.

If pages are missing, contact the university which granted the degree.

Some pages may have indistinct print especially if the original pages were typed with a poor typewriter ribbon or if the university sent us a poor photocopy.

Previously copyrighted materials (journal articles, published tests, etc.) are not filmed.

Reproduction in full or in part of this film is governed by the Canadian Copyright Act, R.S.C. 1970, c. C-30. Please read the authorization forms which accompany this thesis.

THIS DISSERTATION
HAS BEEN MICROFILMED
EXACTLY AS RECEIVED

AVIS

La qualité de cette microfiche dépend grandement de la qualité de la thèse soumise au microfilmage. Nous avons tout fait pour assurer une qualité supérieure de reproduction.

S'il manque des pages, veuillez communiquer avec l'université qui a conféré le grade.

La qualité d'impression de certaines pages peut laisser à désirer, surtout si les pages originales ont été dactylographiées à l'aide d'un ruban usé ou si l'université nous a fait parvenir une photocopie de mauvaise qualité.

Les documents qui font déjà l'objet d'un droit d'auteur (articles de revue, examens publiés, etc.) ne sont pas microfilmés.

La reproduction, même partielle, de ce microfilm est soumise à la Loi canadienne sur le droit d'auteur, SRC 1970, c. C-30. Veuillez prendre connaissance des formules d'autorisation qui accompagnent cette thèse.

LA THÈSE A ÉTÉ
MICROFILMÉE TELLE QUE
NOUS L'AVONS REÇUE

Ottawa, Canada
K1A 0N4

NL-339 (Rev. 8/80)

LASER ACTION IN C IV, N V, AND O VI PLASMAS COOLED BY ADIABATIC EXPANSION

by

Pierre A. Millette

Thesis submitted
to the School of Graduate Studies
of the University of Ottawa
in partial fulfillment of the
requirements for the degree of
Master of Science
in
Physics

Ottawa, Ontario, 1980

Pierre A. Millette, 1980

© Pierre A. Millette, Ottawa, Canada, 1980.

ABSTRACT

The population densities of the discrete levels of the lithium-like ions C IV, N V, and O VI in optically thin plasmas cooled by adiabatic expansion have been calculated with the Collisional-Radiative (CR) plasma model, suitably modified to account for the samll energy separation of the ground and the first excited states of these ions. The following elementary processes have been included in the CR model: electron impact ionization, excitation, and de-excitation, three-body and radiative recombination, and spontaneous transitions. The data and calculations available on these processes have been analysed and extended by various methods. The resulting rate coefficients are compared with the corresponding hydrogenic values, and a discussion of their accuracy is given.

Population inversions have been found to occur in many of the transitions of these ions. We have concentrated our attention to such transitions of the ion C IV between levels with $n \leq 6$ which give rise to emission lines in the visible region of the spectrum. The gain α' of the inversely populated transitions is presented in the form of n_e-T_e diagrams.

The C IV $\lambda\lambda$4646,4658 lines arising from the 6f→5d and 6g→5f transitions respectively, are found to be strongly inverted and should be excellent candidates for producing laser action in laboratory plasmas cooled by adiabatic expansion techniques. In addition, the behavior of the line C IV λ4650 observed in the WC category of the Wolf-Rayet stars is found to be in agreement with that expected from the model calculations. The present investigation thus provides an understanding of the unusual strength of the C IV λ4650 emission in Wolf-Rayet stars, and provides a strong basis for believing that laser action is responsible for it.

ACKNOWLEDGEMENTS

Thanks are due to many individuals, too numerous to be all mentioned here. In particular, I'd like to address special thanks to the following persons.

To Professor Y.P. Varshni, for suggesting the problem and for his constant assistance and encouragement throughout the course of this work. Many an interesting discussion resulted in valuable insights into various problems. Partial financial support from his NRC grant is also gratefully acknowledged.

To the staff and graduate students of this department for a very pleasant stay.

And finally to my wife Suzette for her courage throughout these years, and for her typing of this thesis on a Wylbur terminal.

INTRODUCTION

Under ordinary terrestrial conditions, plasmas are quite rare and unusual. However, most of the matter in the observable universe exists in an ionized state. The investigation of plasmas is thus a necessity if we are to achieve a fuller understanding of nature especially since they are the seat of many varied and unexpected phenomena. In recent years, the investigation of both laboratory and astrophysical plasmas has intensified and gained in importance. Previously uncharted regions are being explored and new territories opened to our investigations.

Non-equilibrium processes play an important role in plasmas under certain physical conditions. The purpose of this work is to study the adiabatic expansion of C IV, N V, and O VI plasmas and to identify the conditions under which population inversions are likely to result in the levels of these ions. This work is of interest in that it provides an indication of the lines which are likely candidates for undergoing laser action by this process in laboratory plasmas. In addition, this mechanism may provide an explanation of the intensity anomalies of C IV lines in Wolf-Rayet stars.

In Chapter I, the calculation of the population densities of the energy levels of a hydrogen-like monatomic plasma is considered. Under equilibrium conditions, the Local Thermodynamic Equilibrium (LTE) model is used and the population densities are calculated from the Boltzmann

and the Saha equations. For non-equilibrium conditions, the Collisional-Radiative (CR) model is used to calculate the level population densities, and the work of House (1964) to obtain the ion densities. The model used to simulate the adiabatic expansion of the plasma and the mechanism giving rise to laser action are then considered.

In Chapter II, the calculation of the rate coefficients needed in the CR model are presented for hydrogenic ions. These coefficients are well known and their calculation is relatively simple. The following coefficients are included: electron impact ionization, excitation, and de-excitation rate coefficients, three-body and radiative recombination rate coefficients, and spontaneous transition probabilities.

Chapter III is devoted to the lithium-like ions C IV, N V, and O VI. These are compared to the hydrogenic ions and the differences between them are noted. Such differences arise in the structure, the energy eigenvalues, and the effective quantum numbers of these ions, and require that the CR model be modified. In particular, the relatively small energy separation of the ground and the first excited states requires that these two levels be considered as two ground states in the CR model. The data available on these ions is then summarized. The data are scarce and consist mostly of theoretical calculations; very little experimental data have been published.

Chapters IV to VIII deal with the calculation of the rate coefficients of the lithium-like ions C IV, N V, and O VI. The following coefficients are included: electron impact ionization (Chapter V), excitation (Chapter VI), and de-excitation (Chapter VII) rate coeffi-

cients, the three-body (Chapter VII) and radiative (Chapter VIII) recombination rate coefficients, and the oscillator strengths (Chapter IV). These Chapters include an analysis of the available data and calculations, a description of the methods used to extend the data, a comparison with the corresponding hydrogenic values, and a discussion of the accuracy of the resulting rate coefficients.

In Chapter IX, results for such lines which arise from transitions between levels of the ion C IV with $n \leq 6$, which lie in the visible region of the spectrum, and for which laser action is possible, are presented in the form of n_e-T_e diagrams. These show the gain α of the lasing process as a function of the free electron density n_e and the free electron temperature T_e of the plasma. These lines are compared with the lines of C IV observed in Wolf-Rayet stars which display anomalous intensities. In particular, the evidence available on the Wolf-Rayet spectral line C IV λ4650 is summarized and the behavior of the line is compared with the expectations of the model calculations.

In conclusion, we find that the present investigation provides an understanding of the unusual strength of the C IV λ4650 emission in Wolf-Rayet stars and provides a strong basis for believing that laser action is responsible for it. In addition, we find that the C IV $\lambda\lambda$4646, 4658 lines will be excellent candidates for producing laser action in laboratory plasmas by adiabatic expansion techniques.

NOTATION

A few words on the notation used in this work are necessary. The symbols n' and n are used to denote quantum numbers whereas p and q are used as state labels. We use the convention n' < n; no such condition is imposed on p and q. Subscripted n's on the other hand denote population densities. When it is important to distinguish between the initial and final states of a transition, an arrow is used such as in $f_{p\to q}$; however, if the order is not important, no arrow is used: E_{pq}. Significant digits are denoted by a capital S as used by Cody and Thatcher (1968). $\ln$ denotes natural or napierian logarithms while log denotes base ten logarithms.

It should also be noted that the expression "average state" is used to denote a state in which the orbital angular momentum splitting of the level is neglected. Similarly, the expression "average rate coefficient" denotes a coefficient which involves an average state.

Atomic units are often used in this work due to the convenience of such units to describe processes occurring at the level of the atom. They can be easily converted to SI units with the following conversion factors:

Length: Bohr radius, $a_0 = \frac{\hbar^2}{me^2} = 5.29177 \times 10^{-11}$ m.

Area: $\pi a_0^2 = 8.79735 \times 10^{-21}$ m^2.

Energy: 1 eV = 1.60219×10^{-19} J;

1 Rydberg = hcR_∞ = 13.6058 eV;

$= 2.177991 \times 10^{-18}$ J;

$1\ cm^{-1} = 1.23985 \times 10^{-4}$ eV;

$= 1.98648 \times 10^{-23}$ J.

Temperature: 1 eV = 11605 K.

Values of the fundamental constants are taken from Taylor et al. (1969).

GLOSSARY OF IMPORTANT PHYSICAL SYMBOLS

$a_p(\nu)$: cross-section for the photoionization of state p

$A_{q\to p}$: Einstein spontaneous transition probability coefficient of the q->p transition

$C_{p\to q}(T)$: electron impact excitation rate coefficient of the p->q transition

E: free electron kinetic energy

E_{pq}: energy separation of levels p and q

f(v): free electron velocity distribution

f_c: cooling factor of the plasma

f_e: expansion factor of the plasma

$f_{p\to q}$: oscillator strength of the p->q transition

$F_{q\to p}(T)$: electron impact de-excitation rate coefficient of the q->p transition

g: Kramers-Gaunt factor

I_H: ionization potential of hydrogen

I_p: ionization potential of level p

k^2: ejected electron kinetic energy

n: quantum number

n': quantum number

n^*: effective quantum number

n_{gd}: ground state quantum number

n_A: population density of species A

n_e: free electron population density

n_i: ionic population density

n_p: population density of state p

n_p^e: Saha equilibrium value of the population density of state p

n_p^{ss}: steady state value of the population density of state p

p: state label

q: state label

$r_p^{(0)}$, $r_p^{(1)}$, and $r_p^{(2)}$: population coefficients of level p.

$R_{n'l'}^{nl}$: radial matrix element of the $n'l' \rightarrow nl$ transition

S_{CR}: collisional-radiative ionization rate coefficient

$S_p(T)$: electron impact ionization rate coefficient of level p

$S_{p\rightarrow q}$: line strength of the p->q transition

T_A: temperature of species A

U: normalized kinetic energy

$U^{(A)}$: partition function of species A

U_i: ionic partition function

y_p: population density per unit statistical weight of level p

Z_A: core charge of species A

$Z_{N,A}$: nuclear charge of species A

$Z_p(T) = n_p^e/n_e n_i$

α: fractional gain per unit distance

$\alpha' = \alpha \Delta\nu$

α_{CR}: collisional-radiative recombination rate coefficient

$\alpha_p(T)$: three-body recombination rate coefficient of level p

$\beta_p(T)$: radiative recombination rate coefficient of level p

γ: ratio of the specific heats at constant pressure and at constant volume

$\Delta\nu$: linewidth

ϵ: energy divided by Z^2

θ: energy divided by kT

λ: line wavelength in Angstroms

μ_n: quantum defect of state n

ν: line frequency

ξ_p: number of equivalent electrons in state p

ρ_p: normalized population density of level p

$\sigma_p(E)$: cross-section for the ionization of state p by electron impact

$\sigma_{p\to q}(E)$: cross-section for the excitation of the p->q transition by electron impact

$\sigma_{n'\ell'\to n\ell}$: transition integral of the $n'\ell'$->$n\ell$ transition

τ_p: relaxation time of level p

ω_p: statistical weight of level p

CONTENTS

LIST OF TABLES

LIST OF FIGURES

STATEMENT OF ORIGINALITY

To the best of the author's knowledge, the following investigations constitute original work performed at the Department of Physics of the University of Ottawa.

The CR model

The CR model is modified for lithium-like ions to account for the small energy separation of the ground and the first excited states of these ions. The relatively large population densities of these two states (ρ_1 and ρ_2 respectively) as compared to the population densities of the other excited states (ρ_p) are accounted for in the model by letting ρ_p be a function of ρ_1 and ρ_2, and by introducing a new population coefficient $r_p^{(2)}$. The derivation of the systems of equations satisfied by the population coefficients $r_p^{(0)}$, $r_p^{(1)}$, and $r_p^{(2)}$, and the explicit form of the solutions $n_1(t)$, $n_2(t)$, and of the collisional-radiative rate coefficients α_1^{CR}, α_2^{CR}, S_1^{CR}, S_2^{CR}, M_{21}^{CR}, and M_{12}^{CR} are also developed in this work.

Adiabatic cooling of the plasma

The model which simulates the adiabatic cooling of the plasma is also modified for lithium-like ions. The steady state solution of the rate equations of the CR model is included as an intermediate step in the cooling process. This permits the determination of the population den-

sities of the ground and the first excited states. In addition, the assumptions and the limitations of the model are considered in greater detail. Detailed calculations are carried out on the lithium-like ions C IV, N V, and O VI, using this model.

Analysis of the inversely populated transitions

A new quantity $\alpha' = \alpha \Delta\nu$ is introduced to allow for the study of the fractional gain per unit length (α) of the amplifying medium without knowledge of the linewidth ($\Delta\nu$). n_e-T_e diagrams are obtained for the $6\ell' \rightarrow 5\ell$ transitions of C IV which display population inversions under adiabatic expansion conditions.

Ionization equilibrium

The conditions under which the model of House (1964) can be used to calculate the ionization equilibrium of a plasma are studied extensively. The validity condition specified by House is found to be only one of several conditions which must be satisfied if the model is to provide good approximations.

Lithium-like ions

Seaton's Quantum Defect Theory is applied to the lithium-like ions C IV, N V, and O VI. A table of the fit parameters for the s and p states of these ions, from which the quantum defect function can be calculated for negative and positive energy states of the valence electron, is provided.

Rate coefficients

A compilation of the data available on the rate coefficients of the lithium-like ions C IV, N V, and O VI up to 1975 is carried out. A critical analysis of the formulas available to generate the unknown rate coefficients is performed. Semi-empirical representations of the lithium-like cross-sections are developed and tables of fit parameters are provided to permit the calculation of all needed coefficients from relatively simple but reliable analytical formulas.

Radiative recombination rate coefficients

A semi-empirical expression is proposed to represent the photoionization cross-sections of the lithium-like ions. An analytical formula to calculate the radiative recombination rate coefficients is then developed and tables of fit parameters are given for the lithium-like ions C IV, N V, and O VI.

Electron impact ionization rate coefficients

Evidence is presented to justify the application of a formula proposed by Lotz (1967, 1968) for ground-state ionization, to the calculation of ionization rate coefficients of excited states.

Electron impact excitation rate coefficients

Semi-empirical cross-section formulas proposed by Drawin (1963, 1964, 1966) for allowed and forbidden transitions are modified to account for the finite value of the excitation cross-sections of positively charged ions at the threshold. Analytical expressions to calculate the rate coefficients are then developed and tables of fit parameters are given for the lithium-like ions C IV, N V, and O VI.

Evaluation of integrals

Accurate analytical approximations to integrals often encountered in atomic physics have been developed for use on computers. Among the more important ones, we have

$$\int_a^b \ln x\, e^{-x}\, dx,$$

$$\int_a^b (\ln x / x) e^{-x}\, dx,$$

$$\int_a^\infty E_1(x)/x\, dx = \epsilon_1(a),$$

where $E_1(x)$ is the exponential integral,

and $$\int_1^\infty x^\mu e^{-ax}\, dx = S_\mu(a)$$

for integral or half-integral, and positive or negative values of μ.

Chapter I

POPULATION DENSITIES OF THE ENERGY LEVELS OF A MONATOMIC PLASMA

1. INTRODUCTION

A plasma consists of one or more elements in various stages of ionization. Its main constituents are positively charged ions, free electrons, neutral atoms, and electromagnetic radiation from discrete and continuous spectra.

In this work, we consider a monatomic (element A), stationary, and spatially homogeneous plasma, free of magnetic fields. Label A refers to all ionization stages of element A: neutral (A I), singly-ionized (A II), doubly-ionized (A III), ... Element A is characterized by a density n_A cm^{-3} and a temperature T_A Kelvin , and the free electrons by a density n_e and a temperature T_e. Furthermore, each stage of ionization X of element A is characterized by a density $n_A^{(x)}$; then

$$n_A = \sum_x n_A^{(x)} . \qquad \ldots(1.1)$$

All particles of the plasma are assumed to be at the same temperature T:

$$T = T_e = T_A \qquad \ldots(1.2)$$

Under the plasma conditions considered in this work, this is a reasonable approximation, especially since T_A is used only to calculate the ionization equilibrium of element A (see Section 4.2 of this Chapter),

2. ENERGY DISTRIBUTION OF THE FREE ELECTRONS

The mass of the electron is much smaller than that of any ion. The electrons are thus much more mobile than the ions. Their energy distribution in a plasma is described by Maxwell-Boltzmann statistics:

$$\frac{dn_e}{n_e} = f_{MB}(\theta)\, d\theta \qquad \ldots(1.3)$$

where $f_{MB}(\theta)$ is the Maxwell-Boltzmann distribution function

$$f_{MB}(\theta) = \frac{2}{\sqrt{\pi}}\, \theta^{1/2}\, e^{-\theta}, \qquad \ldots(1.4)$$

$$\theta = E / kT, \qquad \ldots(1.5)$$

E is the free electron kinetic energy, and k is Boltzmann's constant.

This distribution function holds if the mean de Broglie wavelength of the plasma electrons is appreciably smaller than the mean distance between them (Vedenov, 1965, p.235). As derived in Appendix A, this puts an approximate upper limit on n_e of

$$n_e \ll 1.2 \times 10^{15}\ T^{3/2}\ \ cm^{-3}. \qquad \ldots(1.6)$$

This condition is illustrated graphically in Fig.A.1. In all cases studied in this work, we are well below this upper limit of validity.

An approximate lower limit of validity can be derived as follows. An electronic Maxwellian distribution will hold if a sufficient number of

elastic collisions occurs between the free electrons to allow enough energy exchanges between them to establish a Maxwellian energy distribution. This will be the case if the plasma is sufficiently dense. A crude estimate of the lower limiting value of n_e is accordingly obtained in Appendix A and illustrated graphically in Fig.A.1 as a function of T for atomic hydrogen, for a hydrogenic ion with Z = 10, and for the lithium-like ion C IV. For a hydrogenic or lithium-like plasma with $n_A = 10^{14}$ cm^{-3}, the distribution will be close to Maxwellian if

$$n_e > 10^{10} \text{ cm}^{-3}. \qquad \ldots(1.7)$$

Since we consider plasmas with

$$n_e \sim 10^{12} - 10^{15} \text{ cm}^{-3}, \qquad \ldots(1.8)$$

we expect the Maxwellian distribution to be a reasonable approximation to the actual distribution function of the free electrons in the plasma. A sufficiently dense plasma also insures that the time of response of the distribution to a change in the plasma parameters is sufficiently rapid that the distribution remains Maxwellian at all times.

However, the validity conditions can be quite complex and departures from a Maxwellian distribution are possible even if eqs.(1.6) and (1.7) are valid. Recent work (Shoub, 1977) suggests that departures from a free electron Maxwellian distribution in a pure hydrogen gas can occur in the high-energy tail of the distribution if the ionization level is very low ($n_e/n_H \lesssim 1\%$) and if the ground state population is far from

its equilibrium value. Drawin (1975, p.596) also mentions that departures are possible when the degree of ionization is smaller than approximately 0.5%. Some additional work on this subject may be found in Oxenius (1970a, b), Shaw et al. (1970a, b), Suckewer (1970), and Drawin (1970a, 1971).

3. EQUILIBRIUM POPULATION OF THE LEVELS

3.1. The Local Thermodynamic Equilibrium (LTE) model

Plasmas in complete thermodynamic equilibrium (CTE) only exist under very special conditions and are thus very rarely observed. However, there exists a large class of plasmas in which each volume element fulfills all thermodynamic equilibrium laws derived for plasmas in CTE except for Planck's radiation law. Such plasmas are said to be in local thermodynamic equilibrium (LTE).

In these plasmas, the level population densities are determined solely by collisional processes which are assumed to occur rapidly enough that the population densities respond instantaneously to any change in the plasma conditions. The population densities thus depend entirely on local values of the plasma parameters. Furthermore, each physical process is then accompanied by its inverse and, by the principle of detailed balancing (see Section 6 of Chapter II), these pairs of processes occur at equal rates. The advantage of this model is that the atomic cross-sections of the various physical processes are not needed to calculate the population densities. These are determined solely by the laws of statistical mechanics which we now consider.

3.2. The Boltzmann equation

Consider a particular ionization stage of element A which we label X. We then use "ion X" to denote the X-times ionized atom of element A. Its total electric charge is +Xe where e is the electronic charge. We label two states of ion X as p and q; $p \gtrless q$ unless otherwise indicated. The ground state is labelled as 1, the first excited state as 2, and so on in order of increasing level energy.

The number of ions X that have an electron in state q relative to those with an electron in state p ($p < q$) is then given by the Boltzmann equation (Novotny, 1973, p.108)

$$\frac{n_q^{(x)}}{n_p^{(x)}} = \frac{\omega_q^{(x)}}{\omega_p^{(x)}} e^{-E_{pq}^{(x)}/kT} \qquad \ldots(1.9)$$

where $n_q^{(x)}$ and $n_p^{(x)}$ are the population densities of ions X with an electron in levels q and p respectively, $\omega_q^{(x)}$ and $\omega_p^{(x)}$ are the corresponding statistical weights,

$$E_{pq}^{(x)} = E_p^{(x)} - E_q^{(x)} \qquad \ldots(1.10)$$

is the energy separation of levels p and q, and $E_q^{(x)}$ and $E_p^{(x)}$ are the absolute values of the energy eigenvalues of levels q and p respectively. The Boltzmann equation can also be written as the fraction of ions X that have an electron in state p:

$$\frac{n_p^{(x)}}{n^{(x)}} = \frac{\omega_p^{(x)}}{u^{(x)}} e^{-E_{ip}^{(x)}/kT} \qquad \ldots(1.11)$$

where $n^{(x)}$ is the population density of ion X and $u^{(x)}$ is the partition function of ion X:

$$u^{(x)} = \sum_{q=1}^{\infty} \omega_q^{(x)} e^{-E_{1q}^{(x)} / kT} \qquad \ldots(1.12)$$

Its evaluation is discussed in Appendix B.

3.3. The Saha equation

The Saha equation (Unsöld, 1977, p.154; Griem, 1964, p.135) can be formulated in many ways. In general, it gives the relative population densities of various stages of ionization of an element. The following examples illustrate its use.

The relative population densities of ions X and X+1 in their ground states are given by

$$\frac{n_1^{(x+1)}}{n_1^{(x)}} n_e = \frac{\omega_1^{(x+1)}}{\omega_1^{(x)}} \frac{2(2\pi m kT)^{3/2}}{h^3} e^{-I_1^{(x)}/kT} . \qquad \ldots(1.13)$$

where $I_1^{(x)}$ is the ionization potential of ion X in its ground state and all other symbols have their usual meaning. The relative densities of ions X and X+1 in various states are given by

$$\frac{n_q^{(x+1)}}{n_p^{(x)}} n_e = \frac{\omega_q^{(x+1)}}{\omega_p^{(x)}} \frac{2(2\pi m kT)^{3/2}}{h^3} e^{-\frac{I_p^{(x)} + E_{1q}^{(x+1)}}{kT}} \qquad \ldots(1.14)$$

where $I_p^{(x)}$ is the ionization potential of ion X in excited state p and $E_{1q}^{(x+1)}$ is the energy separation of the ground and the q^{th} state of ion X+1. The relative densities of all ions X and X+1 are given by

$$\frac{n^{(x+1)}}{n^{(x)}} n_e = \frac{u^{(x+1)}}{u^{(x)}} \frac{2(2\pi m kT)^{3/2}}{h^3} e^{-I_i^{(x)}/kT} \quad \ldots(1.15)$$

Various combinations of these equations produce alternate forms of the Saha equation.

In this work, the equation is used as follows. Since we concentrate on one particular ionization stage (X) of element A, we simplify the notation by neglecting the superscript X. The various symbols then become:

$n_p^{(x)} \longrightarrow n_p$: population density of level p;

$n^{(x+1)} \longrightarrow n_i$: ionic density;

$\omega_p^{(x)} \longrightarrow \omega_p$: statistical weight of level p;

$u^{(x+1)} \longrightarrow u_i$: ionic partition function;

$I_p^{(x)} \longrightarrow I_p$: ionization potential of state p.

Combining eqs.(1.14) and (1.15) we then obtain the following form of the Saha equation:

$$n_p^\varepsilon = Z_p(T)\, n_i\, n_e \quad \ldots(1.16)$$

where n_p^ε is the Saha equilibrium population density of level p and

$$Z_p(T) = \frac{\omega_p}{u_i} \frac{h^3}{2(2\pi m kT)^{3/2}} e^{I_p/kT} \quad \ldots(1.17)$$

Numerically,

$$Z_p(T) = \frac{2.071 \times 10^{-16}}{T^{3/2}} \frac{\omega_p}{u_i} e^{I_p/kT} \quad \ldots(1.18)$$

For hydrogenic ions, U_i is the partition function of the bare nucleus and, as discussed in Appendix B,

$$U_i \simeq 1. \qquad \ldots(1.19)$$

The same holds for lithium-like ions since U_i is then the partition function of a closed shell ion.

3.4. Validity of the LTE model

A combination of the Boltzmann and Saha equations completely describes the population densities of the energy levels of a monatomic plasma in LTE. The conditions under which such a description is valid have been investigated extensively. Examples of the work that has been carried on include Böhm (1960) who discusses the validity of the Boltzmann equation (p.104), the Saha equation (p.100), and the LTE model (p.96), Griem (1964, p.145), McWhirter (1965, p.205), and Drawin (1975, p.591).

The conditions under which the LTE model is valid are complex. However, a simple but crude criterion can be obtained by considering the fact that LTE conditions will prevail if the plasma is dominated by collisional processes. Thus there is a lower limiting value of n_e below which radiative processes are not negligible and LTE is not valid. This approach is used by McWhirter (1965, p.206) to derive the values of n_e above which radiative processes cause less than a 10% departure of the plasma from LTE. For T in Kelvin and E_{pq} in eV, this condition is given by

$$n_e \geq 1.6 \times 10^{12} \sqrt{T}\, E_{pq}^3 \ \text{cm}^{-3}. \qquad \ldots(1.20)$$

for all values of p and q. This criterion is least likely to be satisfied for the largest energy gap in the term scheme of the ion considered. For hydrogen, the largest energy gap lies between states 1 and 2: $E_{1,2} = 10.2$ eV. Thus a hydrogenic plasma will be in LTE for

$$n_e \geq 1.7 \times 10^{15} \sqrt{T} \ \text{cm}^{-3}. \qquad \ldots(1.21)$$

The upper limiting value of n_e above which LTE is not valid can be obtained from the validity conditions of the Boltzmann and Saha equations. The applicability of these two equations is limited by the validity conditions of Maxwell-Boltzmann statistics. As derived in Appendix A, the upper limit on n_e is thus given by eq.(1.6), viz.

$$n_e \ll 1.2 \times 10^{15} \, T^{3/2} \ \text{cm}^{-3}.$$

The limits given by eqs.(1.21) and (1.6) are illustrated graphically in Fig.1.1. As can also be seen in this figure, the free electron densities of the plasmas studied in this work, and given by eq.(1.8), are well outside the domain of applicability of the LTE model. This model is thus not useful to us as a general plasma model; however, its value lies in the fact that it can be applied to high-lying quantum states. This is due to the fact that collision cross-sections increase rapidly as the principal quantum number increases, whereas radiative decay rates

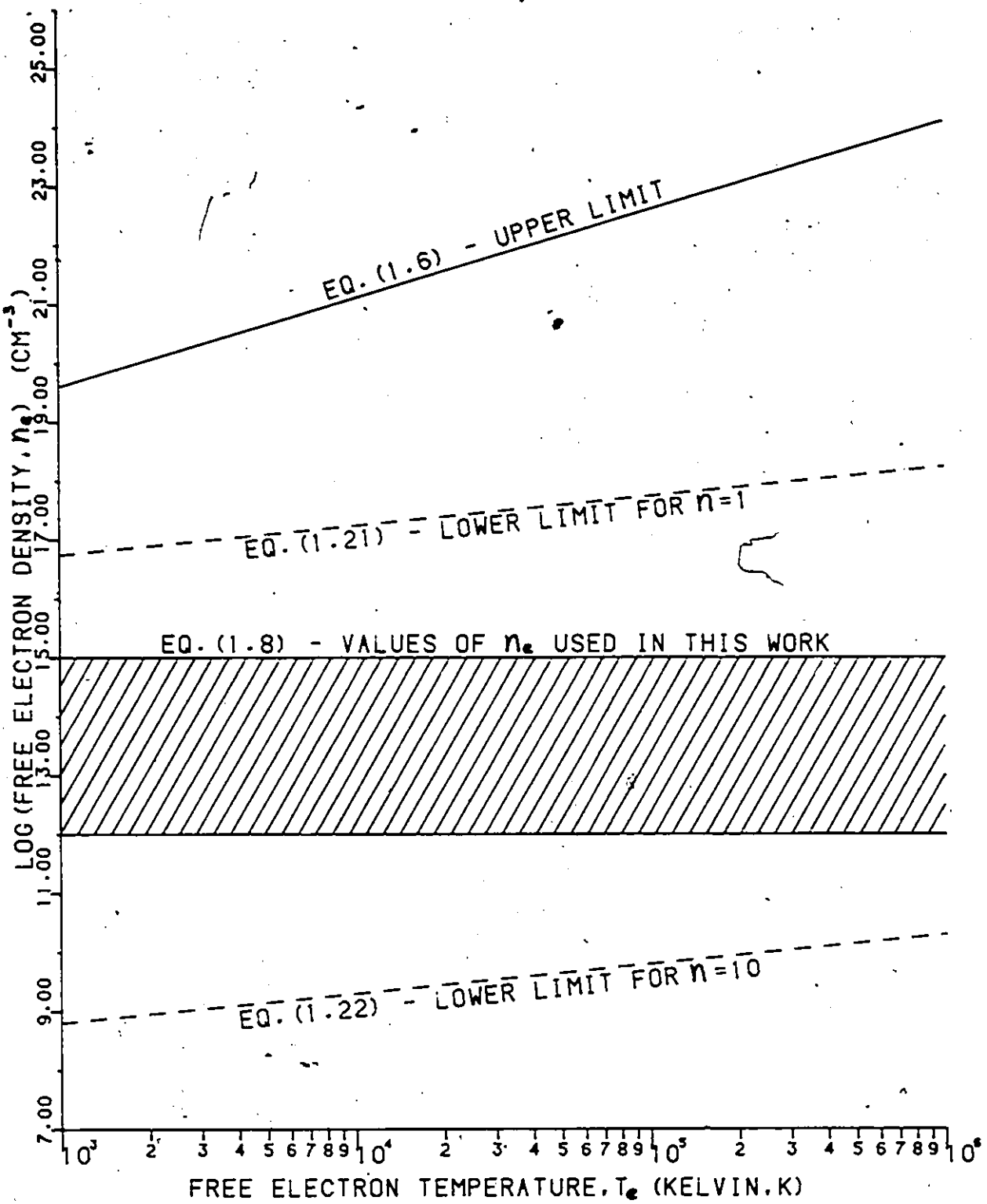

FIGURE 1.1 - APPROXIMATE LIMITS OF APPLICABILITY OF THE LTE MODEL TO HYDROGEN PLASMAS.

decrease under such conditions. A level is thus eventually reached for which collisional processes dominate the population of the levels. Then all excited states lying between the ionization limit and this lowest LTE state are in LTE and their population densities can be obtained from the Boltzmann and Saha equations (Giovanelli, 1948; Drawin, 1975, p.595). A crude estimate of the limit of validity of this approach can be obtained by applying McWhirter's criterion, eq.(1.20). For example, suppose we wish to take level 10 as the lowest LTE state of a hydrogen plasma. Then since the largest energy gap in the term scheme of hydrogen above level 10 lies between states 10 and 11 for which $E_{10,11} = 0.0236$ eV, the value of n_e above which the radiative processes will cause less than a 10% departure of the population of level 10 from LTE is given by

$$n_e \geq 2.1 \times 10^7 \sqrt{T} \ cm^{-3}. \qquad \ldots(1.22)$$

This lower limit is also shown in Fig.1.1. We see that this approach can be very useful for the plasmas considered in this work.

4. NON-EQUILIBRIUM POPULATION OF THE LEVELS

4.1. The Collisional-Radiative (CR) model

4.1.a. Introduction

Plasmas that do not obey the LTE model are called non-LTE plasmas. The population densities of the energy levels of ions in non-LTE plasmas

must be obtained from the rate coefficients of the individual collisional and radiative processes occurring within the plasma. Several models which take into account some or most of these processes have been proposed; of these, the most useful and general is the Collisional-Radiative (CR) model.

This model was first proposed and applied to hydrogenic ions by Bates et al. (1962a, b). It was subsequently used by Bates and Kingston (1963) and McWhirter and Hearn (1963). Since then, much work has been done on and with the CR model, too numerous to be all mentioned in this work. Drawin (1969) reformulated the model within the context of the Boltzmann collision equation. It was first applied to helium by Drawin and Emard (1970), to lithium by Gordiets et al. (1968), and to cesium by Norcross and Stone (1968). Fujimoto et al. (1972) performed calculations on hydrogenic ions with the best data available on the rate coefficients; they published extensive tables of results and discussed these at length. We thus follow their notation as closely as possible. Stevefelt and Robben (1972) found that the collisional-radiative recombination coefficients calculated by Bates et al. (1962a, b) with the CR model agree within a factor of two with experimental values they obtained for helium plasmas. This agreement is reasonable, especially since Bates et al. (1962a, b) calculated all electron impact cross-sections with classical formulas given by Gryzinski (1959). The CR model can thus be expected to provide a reasonable description of certain types of non-LTE plasmas; these are specified in Section 4.1.h of this Chapter.

4.1.b. Physical processes occurring in a plasma

Let e denote an electron, $h\upsilon$ a photon, and N_p^x an X-times ionized atom (ion X) in state p. Then the physical processes occurring within the plasma and included in the CR model can be described as follows (these are schematically represented in Fig.1.2):

i. Collisional ionization by electron impact:

$$N_p^x + e \rightarrow N^{x+1} + e + e. \qquad \ldots(1.23)$$

The rate coefficient of this process is denoted by:

$$S_p(T) \quad cm^3 s^{-1}. \qquad \ldots(1.24)$$

The number of such processes occurring per unit volume per unit time is given by:

$$n_p n_e S_p(T) \quad cm^{-3} s^{-1}. \qquad \ldots(1.25)$$

ii. Three-body recombination: inverse of process (i):

$$N^{x+1} + e + e \rightarrow N_p^x + e. \qquad \ldots(1.26)$$

Rate coefficient: $\alpha_p(T) \quad cm^6 s^{-1}$. $\ldots(1.27)$

Number of processes: $n_e^2 n_i \alpha_p(T) \quad cm^{-3} s^{-1}$. $\ldots(1.28)$

iii. Radiative recombination: predominates over process (ii) in low-density plasmas:

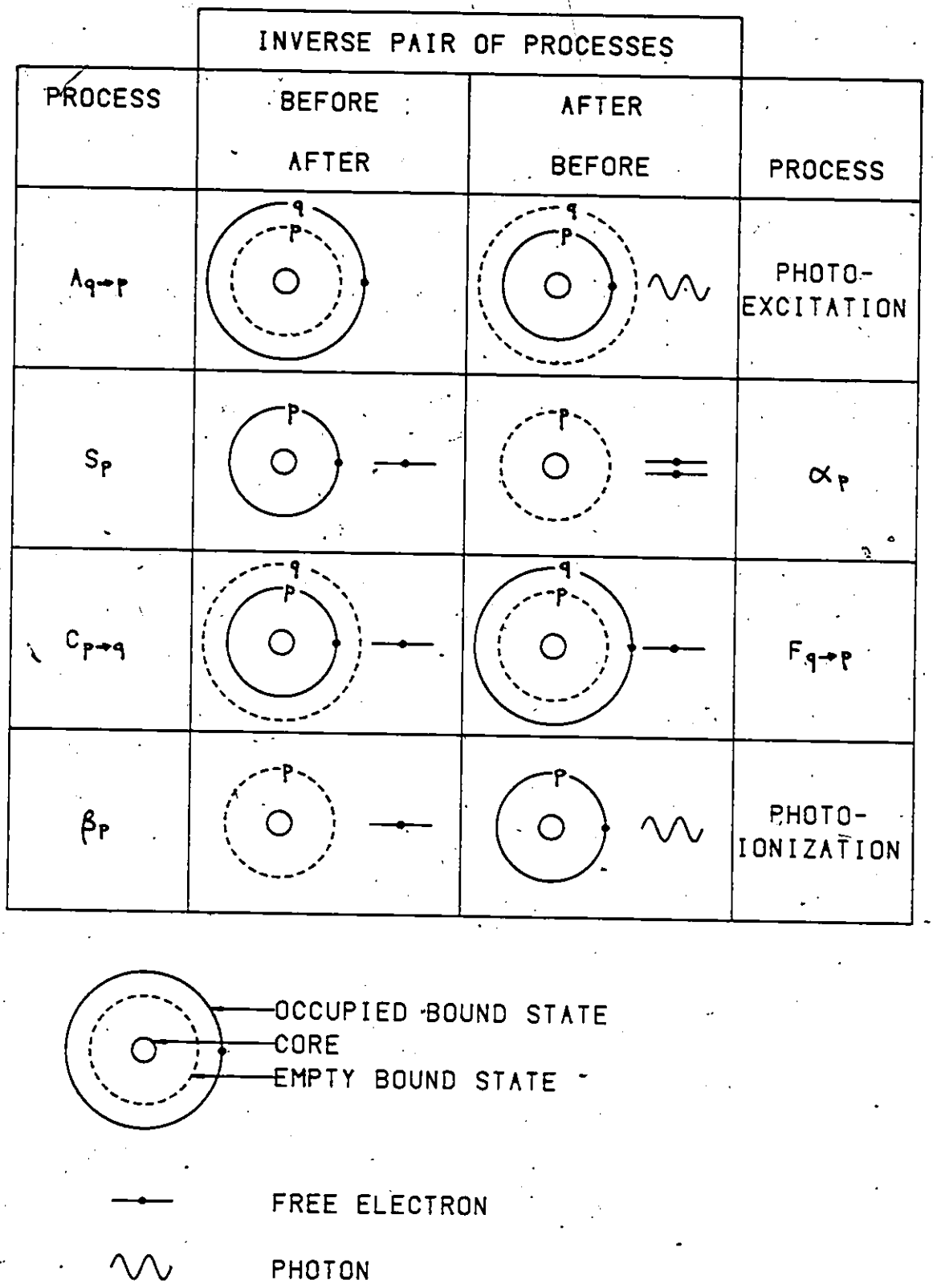

FIGURE 1.2 - PHYSICAL PROCESSES OCCURRING IN A PLASMA.

$$N^{x+1} + e \rightarrow N_p^x + h\nu. \qquad \ldots(1.29)$$

Rate coefficient: $\beta_p(T)$ $cm^3 s^{-1}$. $\ldots(1.30)$

Number of processes: $n_e n_i \beta_p(T)$ $cm^{-3} s^{-1}$. $\ldots(1.31)$

iv. Collisional excitation by electron impact ($p < q$):

$$N_p^x + e \rightarrow N_q^x + e. \qquad \ldots(1.32)$$

Rate coefficient: $C_{p\rightarrow q}(T)$ $cm^3 s^{-1}$. $\ldots(1.33)$

Number of processes: $n_p n_e C_{p\rightarrow q}(T)$ $cm^{-3} s^{-1}$. $\ldots(1.34)$

v. Collisional de-excitation by electron impact ($p < q$): inverse of process (iv):

$$N_q^x + e \rightarrow N_p^x + e. \qquad \ldots(1.35)$$

Rate coefficient: $F_{q\rightarrow p}(T)$ $cm^3 s^{-1}$. $\ldots(1.36)$

Number of processes: $n_q n_e F_{q\rightarrow p}(T)$ $cm^{-3} s^{-1}$. $\ldots(1.37)$

vi. Spontaneous transition ($p < q$):

$$N_q^x \rightarrow N_p^x + h\nu. \qquad \ldots(1.38)$$

Einstein probability coefficient: $A_{q\rightarrow p}$ s^{-1}. $\ldots(1.39)$

Number of processes: $n_q A_{q\rightarrow p}$ $cm^{-3} s^{-1}$. $\ldots(1.40)$

These are the main physical processes which occur in a plasma under most conditions. Other processes are possible, but since they occur less frequently, they are neglected. For example, all processes involv-

ing electron transitions due to heavy particle collisions such as proton-atom, proton-ion, atom-atom, atom-ion, or ion-ion collisions are neglected. However, the effect of some types of heavy particle collisions has been investigated by Drawin (1969a, b), Drawin and Emard (1974), and others.

For the sake of simplicity, the plasma is also assumed to be optically thin such that all radiation emitted within the plasma escapes without being absorbed. The following physical processes are thus neglected:

vii. Photoexcitation ($p < q$): inverse of process (vi):

$$N_p^x + h\upsilon \rightarrow N_q^x. \qquad \ldots(1.41)$$

viii. Photoionization: inverse of process (iii):

$$N_p^x + h\upsilon \rightarrow N^{x+1} + e. \qquad \ldots(1.42)$$

However, plasmas in which radiation absorption occurs are important and have been investigated by many workers. For example, Bates et al. (1962b) consider a hydrogenic plasma which is optically thick toward the lines of certain series. Drawin (1969a, b, c, 1970b) and Drawin and Emard (1970, 1972, 1973, 1974) have investigated radiation absorption in non-LTE plasmas extensively. The effects of radiation absorption are numerous and very complex.

4.1.c. Equations governing the level population densities

We consider level p of ion X and look at the processes of Fig.1.2 which contribute to the filling or emptying of level p as shown in Fig.1.3. The differential equation describing the time variation of the population density of level p is given by

$$\frac{dn_p}{dt} = \begin{pmatrix} \text{electrons entering} \\ \text{level p} \end{pmatrix} - \begin{pmatrix} \text{e's leaving} \\ \text{level p} \end{pmatrix} \quad \ldots(1.43)$$

The terms of eq.(1.43) in parentheses include contributions from all levels $q < p$, $q > p$, and continuum states. Using eqs.(1.25), (1.28), (1.31), (1.34), (1.37), and (1.40) to include all the processes of Fig.1.3 in eq.(1.43), we obtain the differential equation

$$\begin{aligned} \dot{n}_p = & \sum_{q=1}^{p-1} C_{q\to p}\, n_e\, n_q \\ & - \left\{ \left[\sum_{q=1}^{p-1} F_{p\to q} + S_p + \sum_{q=p+1}^{\infty} C_{p\to q} \right] n_e + \sum_{q=1}^{p-1} A_{p\to q} \right\} n_p \\ & + \sum_{q=p+1}^{\infty} \left\{ F_{q\to p}\, n_e + A_{q\to p} \right\} n_q \\ & + \left\{ \alpha_p\, n_e + \beta_p \right\} n_e\, n_i \end{aligned} \quad \ldots(1.44)$$

where the dot over n_p represents differentiation with respect to time. There is such an equation for each and every level $p = 1, 2, \ldots, \infty$ of ion X. We thus obtain an infinite number of coupled first order differential equations in the population densities of the discrete levels of ion X.

The normalized population density of level p is defined by

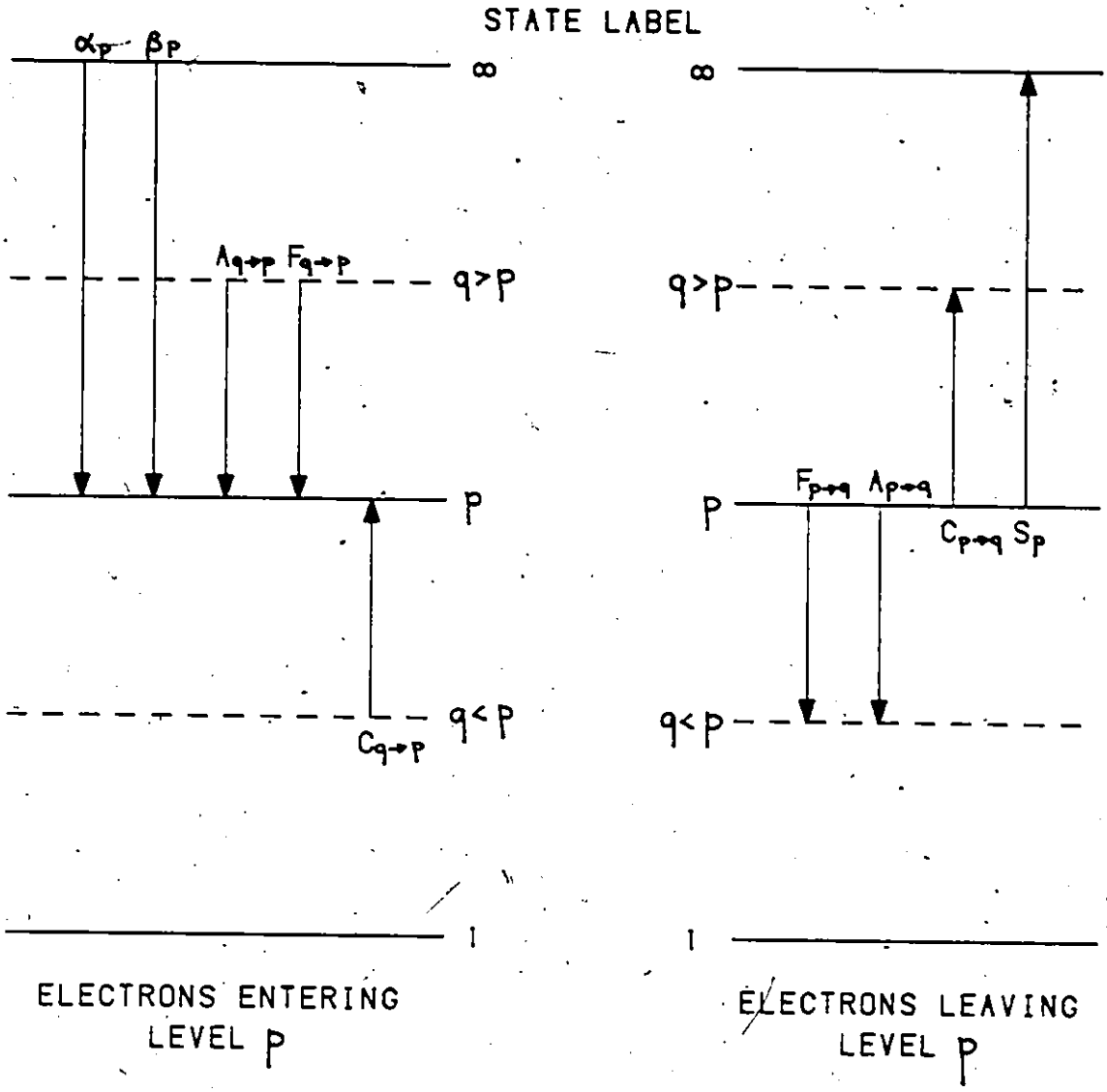

FIGURE 1.3 - CONTRIBUTIONS TO THE POPULATION DENSITY OF LEVEL p.

$$\rho_p = \frac{n_p}{n_p^\epsilon} \qquad \ldots(1.45)$$

where n_p^ϵ is the Saha equilibrium value of the population density of level p given by eq.(1.16). Dividing eq.(1.44) by n_p^ϵ and using eq.(1.45), the set of equations (1.44) becomes

$$\dot{\rho}_p = \sum_{q=1}^{p-1} C_{q\to p} \frac{n_q^\epsilon}{n_p^\epsilon} n_e \rho_q$$

$$-\left\{\left[\sum_{q=1}^{p-1} F_{p\to q} + S_p + \sum_{q=p+1}^{\infty} C_{p\to q}\right] n_e + \sum_{q=1}^{p-1} A_{p\to q}\right\} \rho_p$$

$$+\sum_{q=p+1}^{\infty} \left\{ F_{q\to p} \frac{n_q^\epsilon}{n_p^\epsilon} n_e + A_{q\to p} \frac{n_q^\epsilon}{n_p^\epsilon} \right\} \rho_q$$

$$+\left\{\alpha_p n_e + \beta_p\right\} \frac{n_e n_i}{n_p^\epsilon} \quad ; \; p = 1, 2, \ldots, \infty. \qquad \ldots(1.46)$$

For levels in LTE, detailed balancing between the collisional excitation and de-excitation processes holds; then

$$n_q^\epsilon F_{q\to p} = n_p^\epsilon C_{p\to q}. \qquad \ldots(1.47)$$

Using eqs.(1.47) and (1.16), eq.(1.46) becomes

$$\dot{\rho}_p = \sum_{q=1}^{p-1} F_{p\to q} n_e \rho_q$$

$$-\left\{\left[\sum_{q=1}^{p-1} F_{p\to q} + S_p + \sum_{q=p+1}^{\infty} C_{p\to q}\right] n_e + \sum_{q=1}^{p-1} A_{p\to q}\right\} \rho_p$$

$$+\sum_{q=p+1}^{\infty} \left\{ C_{p\to q} n_e + \frac{Z_q}{Z_p} A_{q\to p} \right\} \rho_q$$

$$+ \frac{1}{Z_p}\{\alpha_p n_e + \beta_p\} \; ; \; p = 1, 2, \ldots, \infty. \qquad \ldots(1.48)$$

As mentioned previously in Section 3.4 of this Chapter, there exists a high-lying quantum state r above which the discrete levels are in LTE. The population density of these levels is then given by

$$\rho_{p>r} = 1. \qquad \ldots(1.49)$$

The infinite set of equations (1.48) thus becomes a finite set of r coupled equations which can be solved for ρ_p, $p = 1, 2, \ldots, r$. The infinite sums appearing in eq.(1.48) can be cut off at a sufficiently high-lying level $s > r$ above which the rate coefficients involving these states contribute little to the infinite sums of eq.(1.48). The set of equations (1.48) then becomes

$$\dot{\rho}_p = \sum_{q=1}^{p-1} F_{p\to q}\, n_e\, \rho_q$$

$$- \left\{ \left[\sum_{q=1}^{p-1} F_{p\to q} + S_p + \sum_{q=p+1}^{s} C_{p\to q} \right] n_e + \sum_{q=1}^{p-1} A_{p\to q} \right\} \rho_p$$

$$+ \sum_{q=p+1}^{r} \left\{ C_{p\to q}\, n_e + \frac{Z_q}{Z_p} A_{q\to p} \right\} \rho_q + \frac{1}{Z_p}\{\alpha_p n_e + \beta_p\}$$

$$+ \sum_{q=r+1}^{s} \left\{ C_{p\to q}\, n_e + \frac{Z_q}{Z_p} A_{q\to p} \right\} \; ; \; p = 1, 2, \ldots, r. \qquad \ldots(1.50)$$

4.1.d. Solution of the system of equations (1.50)

The exact solution of the system of equations (1.50), $\rho_p(t)$, the time evolution of the population densities of levels p = 1, 2, ..., r of ion X, is very difficult to obtain. It requires a set of initial conditions $\rho_p(t=0)$ and can only be calculated numerically. Such a solution would be time consuming and of limited use. A simpler solution, known as the quasi-steady state (QSS) approximation, holds for a large class of plasmas and is used extensively in the literature (Bates et al. 1962a, b, and subsequent papers mentioned previously in Section 4.1.a of this Chapter).

The simplest solution to the set of equations (1.50) is the steady state (SS) solution which is obtained by putting

$$\dot{\rho}_p^{ss}(t) = 0 \quad ; \quad p = 1, 2, \ldots, r. \qquad \ldots(1.51)$$

This time-independent solution holds when the rate at which the electrons enter level p equals the rate at which they leave level p. Once the steady state solution is established, a perturbation of the population density of level p will be followed by a return to its steady state value in a time of order

$$\tau_p \sim \left\{ \left[\sum_{q=1}^{p-1} F_{p\to q} + S_p + \sum_{q=p+1}^{s} C_{p\to q} \right] n_e + \sum_{q=1}^{p-1} A_{p\to q} \right\}^{-1}. \qquad \ldots(1.52)$$

τ_p is the relaxation time of level p. McWhirter and Hearn (1963) have calculated τ_p for a wide range of plasma parameters. They conclude that the relaxation time of the ground state is always much greater than

that of any of the excited states, even if the plasma is not near its steady state. This is due to two main reasons: a) the electron collision rate coefficients between excited states are much greater than those involving the ground state; b) the ground state cannot decay by spontaneous radiative transitions. Consequently, the population densities of the excited levels of ion X come into equilibrium with particular values of the population densities of the ground state, of the free electrons, and of the ions X+1 in a time which is very short as compared to the ground state relaxation time. This is the basis of the QSS solution.

4.1.e. The population coefficients

We thus express the population densities of the excited states as a function of the ground state population density:

$$\rho_p = r_p^{(o)} + r_p^{(1)} \rho_1 \quad ; \quad p = 2, 3, \ldots, r. \qquad \ldots(1.53)$$

$r_p^{(o)}$ and $r_p^{(1)}$ are called the population coefficients of level p. Furthermore, since the population densities of the excited states are in equilibrium with that of the ground state, we solve the system of coupled equations (1.50) by putting

$$\dot{\rho}_{p>2} = 0 \qquad \ldots(1.54)$$

and $$\dot{\rho}_1 \neq 0 \qquad \ldots(1.55)$$

since, in general, the ground state is not in equilibrium. In our calculations, we also assume that the free electron and ionic densities, n_e and n_i respectively, do not change substantially during the time of establishment of the QSS. This restricts the applicability of the approximation and is discussed more extensively in Section 4.1.h of this Chapter.

Substituting the trial solution (1.53) in the system of equations (1.50), and using the condition (1.54), we obtain

$$\Big[\sum_{q=1}^{p-1} F_{p\to q}\, n_e\, r_q^{(0)}$$

$$-\Big\{\Big[\sum_{q=1}^{p-1} F_{p\to q} + S_p + \sum_{q=p+1}^{s} C_{p\to q}\Big] n_e + \sum_{q=1}^{p-1} A_{p\to q}\Big\}\, r_p^{(0)}$$

$$+\sum_{q=p+1}^{r}\Big\{C_{p\to q}\, n_e + \frac{Z_q}{Z_p} A_{q\to p}\Big\}\, r_q^{(0)}$$

$$+\sum_{q=r+1}^{s}\Big\{C_{p\to q}\, n_e + \frac{Z_q}{Z_p} A_{q\to p}\Big\} + \frac{1}{Z_p}\{\alpha_p n_e + \beta_p\}\Big]$$

$$+\Big[\sum_{q=1}^{p-1} F_{p\to q}\, n_e\, r_q^{(1)}$$

$$-\Big\{\Big[\sum_{q=1}^{p-1} F_{p\to q} + S_p + \sum_{q=p+1}^{s} C_{p\to q}\Big] n_e + \sum_{q=1}^{p-1} A_{p\to q}\Big\}\, r_p^{(1)}$$

$$+\sum_{q=p+1}^{r}\Big\{C_{p\to q}\, n_e + \frac{Z_q}{Z_p} A_{q\to p}\Big\}\, r_q^{(1)}\Big]\rho_1 = 0 \quad ; p = 2,3,\ldots,r. \qquad \ldots(1.56)$$

This set of equations is of the form

$$a_p + b_p \rho_1 = 0 \quad ; \quad p = 2, 3, \ldots, r. \qquad \ldots(1.57)$$

The general solution of eq.(1.57), for an arbitrary value of ρ_1, is

$$a_p = 0$$

$$b_p = 0 \quad \ldots(1.58)$$

Before proceeding with the solution of eq.(1.58), certain limiting conditions must be imposed on the population coefficients $r_p^{(0)}$ and $r_p^{(1)}$ corresponding to the cases when $p = 1$ and $p > r$. Substituting $p = 1$ in eq.(1.53), we obtain the condition

$$r_1^{(0)} = 0$$

$$r_1^{(1)} = 1 \quad \ldots(1.59)$$

The other condition, which is obtained by putting $p > r$ in eq.(1.53), has already been imposed on the set of equations (1.56):

$$r_{p>r}^{(0)} = 1$$

$$r_{p>r}^{(1)} = 0 \quad \ldots(1.60)$$

Substituting for a_p and b_p in eq.(1.58) from eq.(1.56), and imposing the condition (1.59), we obtain the following two sets of r-1 equations in the population coefficients $r_p^{(0)}$ and $r_p^{(1)}$ respectively:

$$\sum_{q=2}^{p-1} F_{p\to q}\, n_c\, r_{bq}^{(0)}$$

$$-\left\{\left[\sum_{q=2}^{p-1} F_{p\to q} + S_p + \sum_{q=p+1}^{s} C_{p\to q}\right] n_c + \sum_{q=1}^{p-1} A_{p\to q}\right\} r_p^{(0)}$$

$$+\sum_{q=p+1}^{r}\left\{C_{p\to q}\,n_e+\frac{Z_q}{Z_p}A_{q\to p}\right\}r_q^{(0)}=-\frac{1}{Z_p}\left\{\alpha_p\,n_e+\beta_p\right\}$$

$$-\sum_{q=r+1}^{s}\left\{C_{p\to q}\,n_e+\frac{Z_q}{Z_p}A_{q\to p}\right\}\;; \qquad \ldots(1.61)$$

$$\sum_{q=2}^{p-1}F_{p\to q}\,n_e\,r_q^{(1)}$$

$$-\left\{\left[\sum_{q=1}^{p-1}F_{p\to q}+S_p+\sum_{q=p+1}^{s}C_{p\to q}\right]n_e+\sum_{q=1}^{p-1}A_{p\to q}\right\}r_p^{(1)}$$

$$+\sum_{q=p+1}^{r}\left\{C_{p\to q}\,n_e+\frac{Z_q}{Z_p}A_{q\to p}\right\}r_q^{(1)}$$

$$=-F_{p\to 1}\,n_e\;;\quad p=2,3,\ldots,r. \qquad \ldots(1.62)$$

4.1.f. The population densities

Once the population coefficients $r_p^{(0)}$ and $r_p^{(1)}$ have been obtained from the sets of equations (1.61) and (1.62) respectively, they are substituted in eq.(1.53). For any value of p_i, the population densities p_p can then be calculated. From eqs.(1.45) and (1.16),

$$p_p=\frac{n_p}{Z_p\,n_i\,n_e}\;; \qquad \ldots(1.63)$$

substituting eq.(1.63) in eq.(1.53), we obtain

$$n_p=Z_p\,n_i\,n_e\,r_p^{(0)}+\frac{Z_p}{Z_1}\,n_i\,r_p^{(1)}\;;\quad p=2,3,\ldots,r. \qquad \ldots(1.64)$$

As required by the QSS approximation, the population density of the excited state p depends on the value of the ground state population density n_1, the free electron density n_e, and the ionic density n_i. The population density per unit statistical weight is given by

$$y_p = \frac{n_p}{\omega_p} \qquad \ldots(1.65)$$

where ω_p is the statistical weight of level p. The population density per unit statistical weight must be used when the population densities of different states are compared.

4.I.g. The collisional-radiative rate coefficients

The time evolution of the population density of the ground state can be studied with eq.(1.50) when p = 1. Substituting for ρ_p from eq.(1.53), and using the previously calculated population coefficients and eq.(1.45), we obtain the differential equation

$$\dot{n}_1 = - S_{cR}\, n_e\, n_1 + \alpha_{cR}\, n_e\, n_i . \qquad \ldots(1.66)$$

S_{cR} and α_{cR} are called the collisional-radiative ionization and recombination rate coefficients respectively. They are the effective ionization and recombination rate coefficients of the plasma. They are related to the individual atomic rate coefficients by the following expressions:

$$S_{cR} = S_1 + \sum_{q=2}^{s} C_{1\to q}$$

$$- \frac{1}{z_1 n_e} \sum_{q=2}^{s} z_q \left(F_{q\to 1} n_e + A_{q\to 1} \right) r_q^{(1)} ; \qquad \ldots(1.67)$$

$$\alpha_{CR} = \alpha_1 n_e + \beta_1 + \sum_{q=2}^{s} z_q \left(F_{q\to 1} n_e + A_{q\to 1} \right) r_q^{(0)} . \qquad \ldots(1.68)$$

The solution of eq.(1.66) can easily be shown to be given by

$$n_1(t) = \frac{\alpha_{CR}}{S_{CR}} n_i + \left[n_1(t=0) - \frac{\alpha_{CR}}{S_{CR}} n_i \right] e^{-S_{CR} n_e t} . \qquad \ldots(1.69)$$

The steady state population density of the ground state is obtained in the limit $t \to \infty$:

$$n_1^{ss} = \frac{\alpha_{CR}}{S_{CR}} n_i . \qquad \ldots(1.70)$$

4.1.h. Validity of the QSS approximation

The QSS approximation is based on the fact that the relaxation time of the ground state is greater than that of any of the excited states. Thus as the population density of the ground state changes, the population densities of the excited states respond in a comparatively very short time and remain in equilibrium with the ground state population density, the free electron density, and the ionic density. McWhirter and Hearn (1963) state that such is always the case, even when the plasma is not near its steady state. However, since we assume that n_e and n_i remain constant during the time of establishment of the QSS, the approximation will break down under certain plasma conditions.

According to McWhirter and Hearn (1963), this will occur when the total population density of the discrete excited states is greater than the population density of the ions in the next stage of ionization. Then if a change in the plasma conditions occurs, a large proportion of electrons may pass between the continuum and the bound levels and substantially change the value of n_e or n_i. The QSS approximation for constant n_e and n_i is thus valid if

$$\sum_{p=2}^{\infty} n_p < n_i \quad \text{for} \quad n_1 = 0. \qquad \ldots(1.71)$$

Substituting eq.(1.64) in eq.(1.71), we get

$$n_e \sum_{p=2}^{\infty} Z_p r_p^{(o)} < 1. \qquad \ldots(1.72)$$

Other conditions must also hold for the approximation to be valid:

$$n_{p\neq 1} \ll n_e ; \qquad \ldots(1.73)$$

$$n_{p\neq 1} \ll n_1 . \qquad \ldots(1.74)$$

From eq.(1.73), Bates et al. (1962b) derive the validity condition

$$n_e < 10^{14 + (\log T - 3)/\log 2} \ cm^{-3} \qquad \ldots(1.75)$$

which is satisfied by all but very dense plasmas. Eq.(1.74) holds if the mean thermal energy of the free electrons is much less than the first excitation energy of the ion considered:

$$\frac{1}{2} m v_e^2 < E_{1,2} . \qquad \ldots(1.76)$$

Substituting the average velocity of a Maxwellian velocity distribution of the free electrons

$$\bar{v}_e = \sqrt{\frac{8kT}{\pi m}} \qquad \ldots(1.77)$$

in eq.(1.76), we obtain the condition

$$T < 9100 \; E_{1,2} \; K \qquad \ldots(1.78)$$

where $E_{1,2}$ is in eV. For hydrogenic ions, eq.(1.78) becomes

$$T < 93,000 \; Z^2 \; K \qquad \ldots(1.79)$$

and for lithium-like ions, with the 2p – 3s excitation energy,

$$C \; \underline{IV} : \; T < 260,000 \; K ; \qquad \ldots(1.80)$$

$$N \; \underline{V} : \; T < 420,000 \; K ; \qquad \ldots(1.81)$$

$$O \; \underline{VI} : \; T < 600,000 \; K . \qquad \ldots(1.82)$$

The conditions (1.75) and (1.79) are displayed graphically in Fig.1.4 for a hydrogen plasma. In general, the QSS approximation for constant n_e and n_i will not hold for very dense and very hot plasmas.

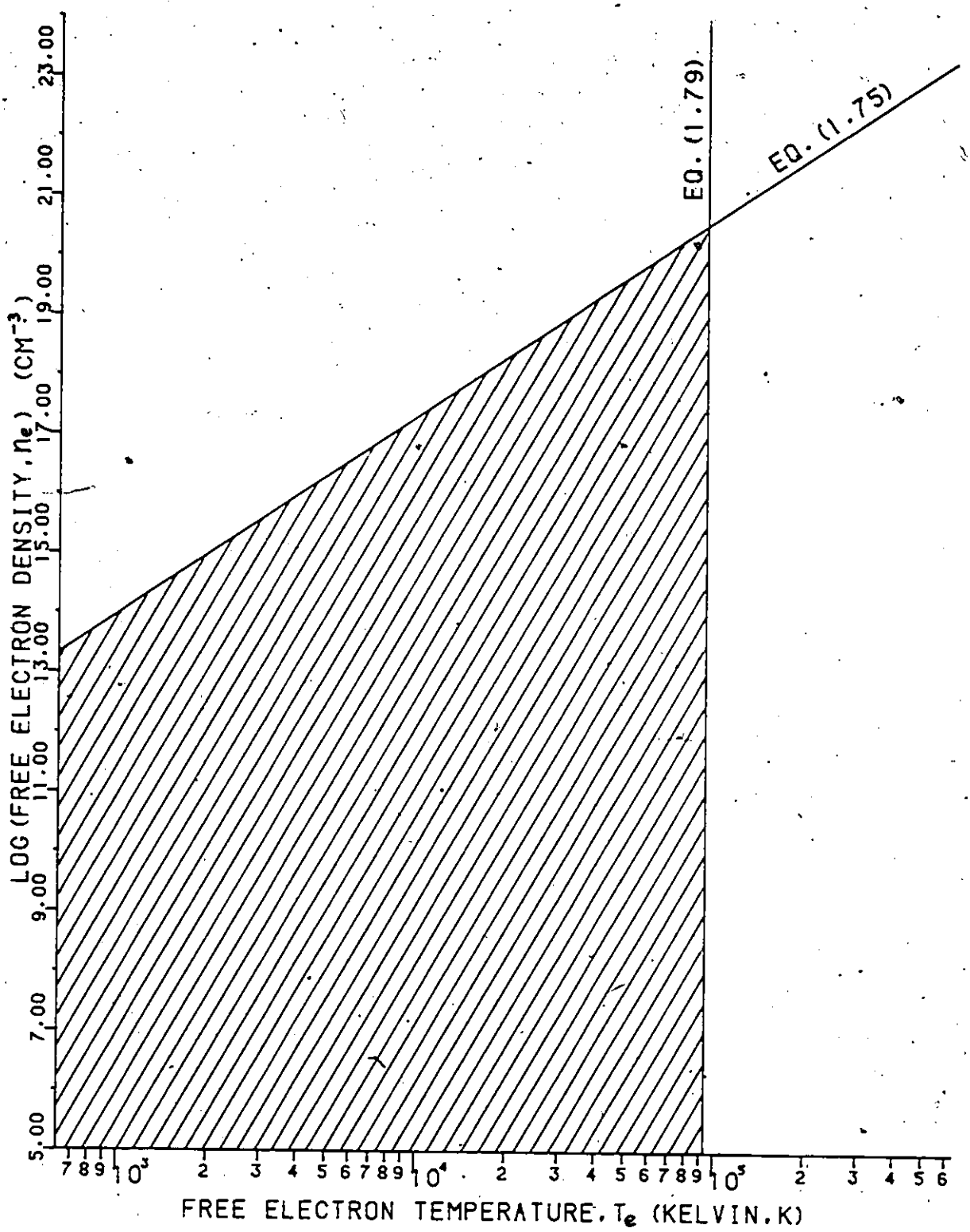

FIGURE 1.4 - APPROXIMATE LIMITS OF APPLICABILITY OF THE QSS APPROXIMATION AT CONSTANT n_e AND n_i FOR HYDROGEN PLASMAS (SHADED REGION).

4.2. Calculation of the ionization equilibrium

4.2.a. The model

The relative population densities of various stages of ionization of a monatomic non-LTE plasma under statistical equilibrium are calculated approximately with the model of House (1964). Even though the calculations are highly simplified, the model provides a first approximation to the ionization equilibrium of monatomic plasmas of hydrogen to iron and a general method of obtaining a consistent set of relative population densities for the ionization stages of these elements.

Since the plasma is not in LTE, the individual physical processes contributing to the ionization equilibrium must be considered. The model is based on the following assumptions: Each stage of ionization of element A consists of only a ground state and a continuum. The monatomic plasma is optically thin. Thus the only processes that control the ionization equilibrium are collisional ionization by electron impact, three-body recombination, and radiative recombination; photoionization is absent. Furthermore, since excited states are not considered, any ionization or recombination process occurring through these states is neglected and, under certain conditions, can restrict the applicability of the model.

4.2.b. Ionization equilibrium equations

Let the rate coefficient for ionization of the X-times ionized atom (ion X) of element A be denoted by $R_{x\to x+1}$ and that for recombination of ion X+1 by $R_{x+1\to x}$. Then under statistical equilibrium, we have

$$n^{(x)} R_{x\to x+1} = n^{(x+1)} R_{x+1\to x} \qquad \ldots(1.83)$$

where $n^{(x)}$ and $n^{(x+1)}$ are the densities of ions X and X+1 respectively. We denote the rate coefficients for the individual processes included in the model as follows:

i. collisional ionization of ion X: $S'_{x\to x+1}$; ...(1.84)

ii. radiative recombination of ion X+1: $\beta'_{x+1\to x}$; ...(1.85)

iii. three-body recombination of ion X+1: $\alpha'_{x+1\to x}$ . ...(1.86)

The prime on these coefficients indicates that they are not defined as those used in the CR model; they are equivalent to the CR model coefficients multiplied by n_e (n_e^2 for $\alpha'_{x+1\to x}$). Substituting the rate coefficients (1.84), (1.85), and (1.86) into eq.(1.83), we get

$$n^{(x)} S'_{x\to x+1} = n^{(x+1)} \left[\beta'_{x+1\to x} + \alpha'_{x+1\to x} \right]. \qquad \ldots(1.87)$$

We use simple but very approximate expressions for the rate coefficients of eq.(1.87). The advantage of such an approach is that general calculations can be performed without considering each ion individually. The collisional ionization rate coefficient is calculated with the following simple approximate formula (Allen, 1961):

$$S'_{x\to x+1} = 1.15 \times 10^{-8} f_{x\to x+1} \frac{\xi_x}{I_x^2} n_e \sqrt{T}\, e^{-I_x/kT} \qquad \ldots(1.88)$$

where ξ_x is the number of electrons in the outer shell of ion X, I_x is the ionization potential of ion X in eV,

$$f_{x\to x+1} = 3.1 - \frac{1.2}{Z_x} + \frac{0.9}{Z_x^2}, \qquad \ldots(1.89)$$

Z_x is the core charge of ion X, and all other symbols have their usual meaning. The three-body recombination rate coefficient is obtained from the collisional ionization rate coefficient since they are inverse processes. Under LTE conditions, we have

$$n_{SAHA}^{(x)} S'_{x\to x+1} = n_{SAHA}^{(x+1)} \alpha'_{x+1\to x}. \qquad \ldots(1.90)$$

Thus

$$\alpha'_{x+1\to x} = \frac{n_{SAHA}^{(x)}}{n_{SAHA}^{(x+1)}} S'_{x\to x+1} \qquad \ldots(1.91)$$

where $n_{SAHA}^{(x)} / n_{SAHA}^{(x+1)}$ is given by eq.(1.15). Using eq.(1.90) insures that when the population densities approach their LTE value, statistical equilibrium is maintained. The radiative recombination rate coefficient, in the hydrogenic approximation, is given by the approximate formula (Elwert, 1952):

$$\beta'_{x+1\to x} = 5.46\times 10^{-14} f_1 \left(\frac{I_H}{kT}\right)^{1/2} \frac{I_x}{I_H} n_{gd}^x n_e G_1\left(\frac{I_x}{kT}\right) g \qquad \ldots(1.92)$$

where I_H is the ionization potential of hydrogen, n_{gd}^x is the quantum number of the ground state of ion X,

$$G_1(x) = x\, e^x\, E_1(x), \qquad \ldots(1.93)$$

$E_1(x)$ is the exponential integral, $f_1 = 0.8$, $g' = 3$ ($g = 4$ for iron), and all other symbols have their usual meaning. The values of f_1 and g come from Allen (1961).

The fraction of the atoms of element A that have been ionized X times is given by $n^{(x)} / \sum_x n^{(x)}$. This quantity is plotted in Fig.1.5 as a function of temperature for carbon at $n_e = 10^{15}$ cm^{-3}. The values of the parameters used in eqs.(1.88) to (1.92) to calculate these curves are given in Tab.1.1.

4.2.c. Validity of the model

House (1964) states that, in general, the calculations should apply to plasmas with

$$n_e \leq 10^{15} \text{ cm}^{-3} \qquad \ldots(1.94)$$

and, in many cases, to values of up to $n_e = 10^{16} - 10^{17}$ cm^{-3}. However, more stringent validity conditions may be necessary due to the assumption that each ionization stage consists only of a ground state and a continuum.

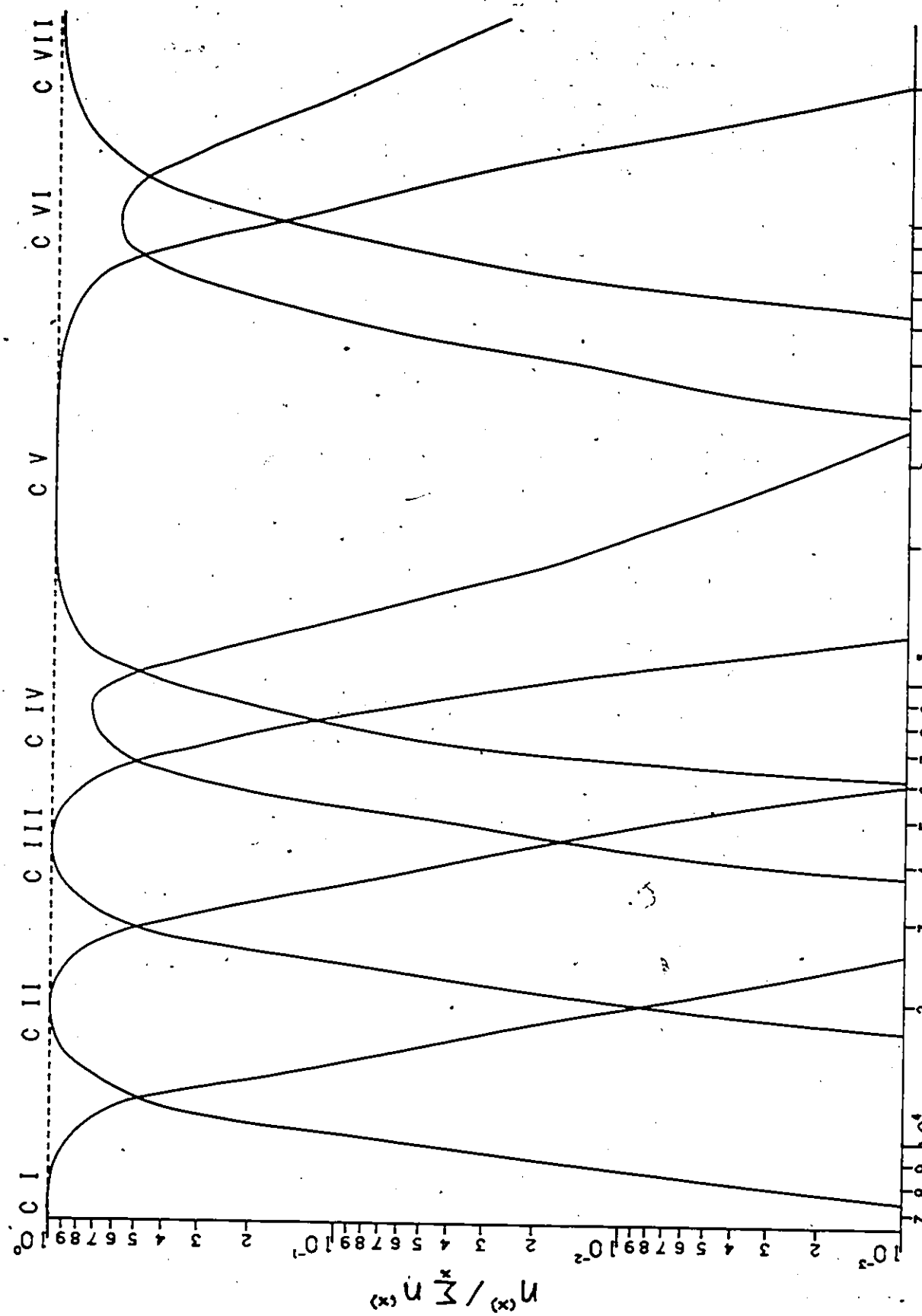

FIGURE 1.5 - IONIZATION EQUILIBRIUM OF CARBON AT $n_e = 10^{15}$ CM^{-3}.

Table 1.1 - Parameters used to calculate the ionization equilibrium of Carbon given in Figure 1.5.

	Ionization stage						
Parameter	C I	C II	C III	C IV	C V	C VI	C VII
I_x(eV)	11.260	24.383	47.887	64.492	392.077	489.981	-
Z_x	1	2	3	4	5	6	7
ξ_x	4	3	2	1	2	1	-
n_{gd}^x	2	2	2	2	1	1	-
$U^{(x)}$	9	6	1	2	1	2	1

An ion can be approximated by a single bound state if the population density of the ground state is much greater than that of any excited state:

$$n_1 \gg n_{p \neq 1} . \qquad \ldots(1.95)$$

As mentioned previously in Section 4.1.h of this Chapter, this will hold if the average kinetic energy of the free electrons is less than the energy separation of levels 1 and 2. The validity of this approximation is thus given by eq.(1.78):

$$T < 9100 \; E_{1,2} \; K$$

where $E_{1,2}$ is in eV. Special cases of this equation for hydrogenic and lithium-like ions are given in eqs.(1.79) to (1.82).

The approximation of a single-state ion also neglects all ionization and recombination processes which occur through an excited state. For example, ionization from the ground state may occur by excitation to state p followed by ionization from state p; recombination into the ground state may occur by recombination into excited state p followed by de-excitation to the ground state. The approximation is thus valid if direct ionization or recombination to the ground state occurs more rapidly than through an excited state. The relaxation time of the one-step processes must thus be much smaller than that of the two-step processes:

$$\tau_1 \ll \tau_{1p} + \tau_p \qquad \ldots(1.96)$$

where τ_p is the relaxation time for an electron to enter or leave state p and τ_{1p} for an electron to make a transition from the ground state to the excited state p or vice versa. Calculating the relaxation times from the corresponding rate coefficients, we find in general that condition (1.96) is valid for all states $p > p_{min}$ where p_{min} is a function of T. For hydrogen, one-step processes occur at least ten times faster than two-step processes,

$$\tau_1 \leq (\tau_{1p} + \tau_p)/10, \qquad \ldots(1.97)$$

above the following values of p_{min}:

T	p_{min}
4000 K	5
32000 K	4
256000 K	3

$\ldots(1.98)$

For levels below p_{min}, the relaxation times become comparable and eventually, two-step processes predominate over one-step processes. However, since the values of the coefficients used in these model calculations are very approximate, the additional complications introduced in the model by including the first few low-lying levels in the calculations are not justified.

Conditions (1.78) and (1.98) are valid if n_e satisfies the validity condition (1.94) given by House (1964). For values of n_e greater than those of eq.(1.94), the recombination of a free electron into an excited state p with a subsequent de-excitation to the ground state occurs

faster than direct recombination into the ground state. The model thus breaks down at high values of n_e. It should also be noted that for lithium-like ions, larger errors may result from the use of the model, due to the small energy separation of the ground and the first excited states.

5. POPULATION INVERSIONS IN PLASMAS COOLED BY ADIABATIC EXPANSION

5.1. Introduction

The possibility of using a recombining plasma as an amplifying medium of electromagnetic radiation was first suggested by Gudzenko and Shelepin (1963). Calculations performed on a hydrogen plasma by Gudzenko and Shelepin (1965) and Gudzenko et al. (1967) subsequently confirmed this suggestion. Since then, elements with more complex electron structures have been investigated: for example, lithium by Gordiets et al. (1968) and argon by Gordiets et al. (1971). Such plasmas are called plasma lasers (Gudzenko et al., 1974).

5.2. Plasma lasers

We consider the basic principles of operation of a plasma laser. As discussed in Appendix A, the mean time between electron collisions determines the rate of establishment of the electron temperature within a plasma. The smallness of the time between elastic collisions in a dense plasma thus makes it possible, in principle, to rapidly reduce the electron temperature of such a plasma (see eq.A.7). For example, in plasma densities of order $n_i \sim n_e \sim 10^{15} - 10^{16}$ cm^{-3}, a single distribution of

the electrons is established in a time of order $\tau \sim 10^{-11} - 10^{-10}$ s (Gudzenko and Shelepin, 1963).

Rapid cooling of a strongly ionized plasma results in rapid recombination of the electrons and the ions into highly excited atomic states. The subsequent relaxation of the electrons to the ground state by spontaneous and non-radiative transitions occurs in a time which, for the estimated values of the plasma parameters used in this work, is larger than 10^{-7} s. At these densities, electron-ion recombination occurs by three-body recombination in a time shorter than 10^{-7} s such that a rapid filling-up of the upper excited levels of the ions occurs. Furthermore, since recombination into highly excited states occurs much more rapidly than into lower states, the establishment of large population inversions is favored.

When large population inversions have been established in the excited levels, the plasma is said to be in a stationary drainage state. It is still substantially ionized. As an example of the times involved, Gudzenko and Shelepin (1965) find that for a dense low temperature plasma ($T_e \sim 1000 - 6000$ K and n_e - bound and free states $\sim 10^{13} - 10^{16}$ cm^{-3}), cooled by a factor of twenty, stationary drainage of the excited discrete levels is established in a time $\sim 10^{-8} - 10^{-7}$ s. Stationary drainage is maintained for a time $\sim 10^{-5}$ s, and is followed by a stage in which the plasma is weakly ionized and the population densities of its levels return to normal. Gudzenko et al. (1967) find that the above conditions can be significantly relaxed; for example, the cooling can be done more slowly or by stages.

5.3. Adiabatic cooling of a plasma

Various mechanisms of free electron cooling can be used. Several of these were first considered by Gordiets et al. (1966): cooling of the free electrons by elastic collisions with heavy particles and by diffusion of the electrons to the container walls. The method of interest to us, rapid cooling of a plasma by adiabatic expansion, was first investigated by Gudzenko et al. (1966) both for magnetized and unmagnetized plasmas.

An example of this cooling mechanism is the adiabatic expansion of a plasma jet in a vacuum. The advantage of this method is that continuous amplification, and thus continuous operation of a laser is possible due to the fact that the different stages of the recombining plasma decay at different times. Thus, as the plasma expands, the stages of the recombination process outlined previously (see Section 5.2 of this Chapter) are spread over space and the de-excited medium is thus removed from the active lasing zone. Experimental evidence of laser action due to the adiabatic expansion of highly ionized hydrogen or hydrogenic plasmas has been given by the following workers: Gol'dfarb et al. (1966), Gol'dfarb et al. (1969), Hoffmann and Bohn (1972), Irons and Peacock (1974), Dewhurst et al. (1976), and Sato et al. (1977).

Under adiabatic expansion conditions, the density n and the temperature T of a gas are related by (Gudzenko et al., 1967)

$$T n^{1-\gamma} = \text{constant} \qquad \ldots(1.99)$$

where $\gamma = c_p / c_v$ $\qquad \ldots(1.100)$

is the ratio of the specific heat at constant pressure c_p and the specific heat at constant volume c_v. For a monatomic gas and for a fully ionized plasma of hydrogen, we use (Gudzenko et al., 1967)

$$\gamma = 5/3. \qquad \ldots(1.101)$$

However, it should be noted that the actual value of γ for a plasma is lower than 5/3. Denoting the initial density and temperature of the plasma by n° and T° respectively, and the final density and temperature by n and T respectively, we characterize the expansion by the factor

$$f_\varepsilon = \frac{n^\circ}{n} > 1 \qquad \ldots(1.102)$$

and the ensuing cooling of the plasma by the factor

$$f_c = \frac{T^\circ}{T} > 1 \qquad \ldots(1.103)$$

Then from eq.(1.99), we have the relation

$$f_c = f_\varepsilon^{\gamma-1} \qquad \ldots(1.104)$$

under adiabatic expansion conditions. In this work, we use $f_c = 5$; then from eqs.(1.104) and (1.101), $f_\varepsilon = 11.2$.

5.4. Model calculations

We consider a monatomic, unmagnetized, stationary and spatially homogeneous plasma characterized initially by a density $n_A^\circ = 10^{14}$ cm^{-3}, a temperature T°, and a free electron density n_e°. Denoting the ionization stage of element A of interest to us by X, we obtain $n_A^{\circ(x)}$ and $n_A^{\circ(x+1)}$ from the ionization equilibrium of element A calculated with the model of House (1964) (see Section 4.2 of this Chapter). Using the simplified notation of eq.(1.16) of Section 3.3 of this Chapter, these can be written as follows:

$$n_A^{\circ(x)} \rightarrow n_1^\circ$$

$$n_A^{\circ(x+1)} \rightarrow n_i^\circ . \qquad \ldots(1.105)$$

The population density of ion X is equivalent to the sum of the population densities of its individual atomic levels p:

$$n^\circ = \sum_{p=1}^{\infty} n_p^\circ . \qquad \ldots(1.106)$$

Under most conditions, the population densities of the excited states are much smaller than that of the ground state:

$$n_1^\circ \gg \sum_{p=2}^{\infty} n_p^\circ . \qquad \ldots(1.107)$$

The conditions under which this expression is valid can be obtained from one of the validity conditions of the CR model, eq.(1.78), and are discussed in Section 4.1.h of this Chapter. If expression (1.107) holds,

$$n^\circ \simeq n_i^\circ \qquad \ldots(1.108)$$

and the calculation of the ionization equilibrium then gives the ionic density n_i° and the ground state population density n_1°.

We then cool the plasma "instantaneously" under adiabatic expansion conditions by a factor of five. This represents a situation in which the cooling occurs in a time shorter than the electron-ion recombination time. The feasibility of this situation has been discussed previously in Section 5.2 of this Chapter. The plasma parameters, after cooling, become

$$T = T^\circ / f_c$$

$$n_e = n_e^\circ / f_E$$

$$n_i = n_i^\circ / f_E$$

$$n_1 = n_1^\circ / f_E$$

$$n_A = n_A^\circ / f_E . \qquad \ldots(1.109)$$

The QSS population densities of the excited states n_p, $p = 2, 3, \ldots$ are then obtained from the set of parameters (1.109) with the CR model by solving eqs.(1.61) and (1.62) for the population coefficients and by using these in eq.(1.64).

This solution holds when stationary drainage has been established in the plasma and it represents the amplifying properties of the plasma. We do not study the time evolution of the population densities of the excited levels a) from the start of the cooling process to the establishment of stationary drainage, and b) from the decay of stationary drainage due to the relaxation of the inversely populated excited levels to the final weakly ionized plasma in which the population of the excited states have returned to normal.

5.5. Analysis of the inversely populated transitions

Many transitions are found to be inversely populated in these calculations. However, only a few of these giving rise to prominent lines in the visible spectrum are studied. We follow the analysis used by Varshni and Lam (1976) on the λ4686 He II 4 -> 3 transition.

The strength of an inversely populated transition q -> p (p < q) can be characterized by the fractional gain per unit distance, α. At the centre of a Doppler-broadened line, it is given by the following expression (Willett, 1974, p.23):

$$\alpha = \sqrt{\frac{\ell n\, 2}{\pi}} \left[\frac{\omega_q A_{q\to p}}{4\pi}\right] \frac{\mathcal{P} \lambda_o^2}{\Delta\nu} \qquad \ldots(1.110)$$

where λ_o is the centre wavelength of the transition, $\Delta\nu$ is the linewidth, ω_q is the statistical weight of level q, $A_{q\to p}$ is the Einstein probability coefficient for spontaneous transition from level q to p, and (Lengyel, 1966)

$$\mathcal{P} = \frac{n_q}{\omega_q} - \frac{n_p}{\omega_p} . \qquad \ldots(1.111)$$

P is a measure of the population inversion and, for laser action to be operative, $P > 0$. α is related to the intensity of a plane wave at λ_0 by the equation

$$I = I_0 e^{\alpha L} \qquad \ldots(1.112)$$

where L is the length over which gain occurs.

To be able to compare various transitions without specifying the linewidth $\Delta\nu$, we define a quantity α' given by

$$\alpha' = \alpha \Delta\nu \qquad \ldots(1.113)$$

where α is given by eq.(1.110). The inversion is displayed on n_e, T_e plots ($n_e - T_e$ diagrams) showing contours of equal α' (equi-α' contours). Fig.9.13 of Chapter IX is a typical $n_e - T_e$ diagram. On a three-dimensional plot with α' as the third axis perpendicular to both the n_e and the T_e axes, the diagram would appear as a triangular pyramidal-shaped mountain with a very steep slope on the high-n_e side, a steep slope on the low-T_e side, and a gradual slope on the low-n_e, high-T_e side. Strong population inversion thus occurs only within a narrow range of values of n_e and T_e, and each transition has its own region of strong population inversion.

Chapter II

HYDROGENIC IONS

1. INTRODUCTION

A hydrogenic ion is composed of a single electron orbiting a nucleus of core charge Z (in units of the electronic charge e). This orbiting electron is called the valence electron. The core charge is the total integral electric charge acting on the valence electron and, for hydrogenic ions, it is equivalent to the nuclear charge Z_N. Thus for H I, neutral hydrogen, Z = 1; for He II, singly-ionized helium, Z = 2; ... .

The energy eigenstates of the valence electron with the same value of the principal quantum number n but with different values of the azimuthal quantum number ℓ are very nearly equal. In this work, we can consider them to be equal without any loss of generality. The ground state quantum number is thus n = 1; the first excited state quantum number, n = 2; ... . The energy eigenstates of the hydrogenic ions are thus degenerate with respect to the ℓ-value splitting of state n and the statistical weight of level n is then given by

$$\omega_n = 2n^2. \qquad \ldots(2.1)$$

The energy eigenvalue of the valence electron in state n is given by

$$\mathcal{E}_n = -E_n \qquad \ldots(2.2)$$

where E_n is greater than zero. For hydrogenic ions,

$$E_n = hcR\frac{Z^2}{n^2} \qquad \ldots(2.3)$$

where h is Planck's constant, c is the velocity of light, and R is the Rydberg constant of the ion that is being considered. It is given by (Herzberg, 1944, p.21)

$$R = R_\infty / \left(1 + \frac{m}{M}\right) \qquad \ldots(2.4)$$

where R_∞ is the Rydberg constant of an infinitely massive nucleus, m is the mass of the electron, and M is the mass of the ion. Each ion then has its own Rydberg constant, but the difference between these for hydrogenic ions is at most only in the fifth significant digit. We thus use for all hydrogenic ions

$$E_n \simeq \frac{Z^2}{n^2} \text{ Rydbergs} \qquad \ldots(2.5)$$

where the Rydberg energy unit is defined by

$$1 \text{ Rydberg} = \frac{e^2}{2a_0} = hcR_\infty. \qquad \ldots(2.6)$$

The energy level diagram of hydrogen (H I) is given in Fig.2.1.

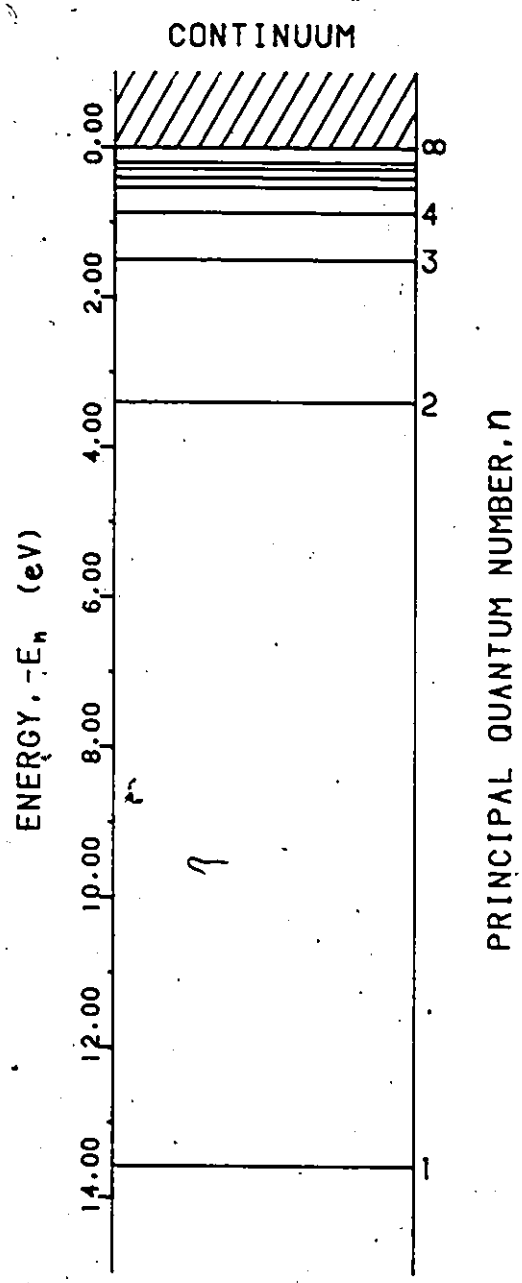

FIGURE 2.1 - ENERGY LEVEL DIAGRAM OF THE HYDROGEN ATOM (H I).

2. RATE COEFFICIENTS

The stationary states of a hydrogenic ion can be described exactly using the methods of quantum mechanics. However, the interaction of a hydrogenic ion and a particle can only be treated approximately. The approximation is particularly good for the interaction of a hydrogenic ion and a photon. Thus reasonably accurate values of the spontaneous transition probabilities and the radiative recombination rate coefficients can be obtained within the physical conditions of interest to us. However, processes occurring by electron impact are very difficult to treat and the approximations used have varying degrees of success depending on the particulars of the collision. A consistent order of magnitude estimate of the electron impact ionization, excitation, de-excitation, and three-body recombination rate coefficients can be obtained from most approximations, but the actual accuracy of a calculation depends on the particular process considered and the particular approximation used.

A very large amount of work has been done on the calculation of hydrogenic rate coefficients. A review of this work is not the aim of our work and is not necessary since certain specific calculations are preferred and used extensively in the literature. In the following sections, we consider those calculations which we use in this work.

3. SPONTANEOUS TRANSITION PROBABILITY

We consider the spontaneous transition of an electron in a hydrogenic ion from an upper state n to a lower state n'. Within the electric

dipole approximation, the Einstein probability coefficient for the transition can be evaluated exactly, and it is given by (Menzel and Pekeris, 1935):

$$A_{n\to n'} = \frac{8\pi^2 e^2}{mc^3}\,\upsilon_{nn'}^2\,\frac{\omega_{n'}}{\omega_n}\,f_{n'\to n} \qquad \ldots(2.7)$$

where ω_n and $\omega_{n'}$ are the statistical weights of levels n and n' respectively, $\upsilon_{nn'}$ is the frequency of the photon emitted as a result of the transition and $f_{n'\to n}$ is the absorption oscillator strength for the n' -> n transition.

The absorption oscillator strength is given by (Menzel and Pekeris, 1935; Green et al., 1957):

$$f_{n'\to n} = \frac{32}{3}\,n^4 n'^2\,\frac{(n-n')^{2n+2n'-4}}{(n+n')^{2n+2n'+3}} \times \left\{\left[{}_2F_1\left(-n', -n+1; 1; -\frac{4nn'}{(n-n')^2}\right)\right]^2 - \left[{}_2\tilde{F}_1\left(-n'+1, -n; 1; -\frac{4nn'}{(n-n')^2}\right)\right]^2\right\} \qquad \ldots(2.8)$$

where

$${}_2F_1(a, b; c; x) = \sum_{k=0}^{\infty} \frac{(a)_k (b)_k}{(c)_k}\,\frac{x^k}{k!} \qquad \ldots(2.9)$$

is the hypergeometric function (Abramowitz and Stegun, 1965, p.555) and

$$(a)_k = \Gamma(a+k) / \Gamma(a). \qquad \ldots(2.10)$$

If a and b are negative integers, the sum (2.9) is terminated and the hypergeometric function is then a polynomial. Let $a = -i$ and $b = -j$ where i and j are positive integers and $i \leq j$; let $x \geq 0$; then eq.(2.9) becomes

$$ {}_2F_1(-i,-j;1;-x) = \sum_{k=0}^{i} (-1)^k \frac{i!}{(i-k)!} \frac{j!}{(j-k)!} \frac{x^k}{[k!]^2} \qquad \ldots(2.11) $$

For large values of n' and n, eq.(2.11) is difficult to evaluate since it is given by a sum of very large terms which alternate in sign and which tend to cancel one another. The value of the sum is then smaller than the magnitude of these very large terms, and significant loss of accuracy can occur. Furthermore, since the two hypergeometric functions of eq.(2.8) are very similar, the difference of the square of these functions becomes very small as n' and n increases. An even greater loss of accuracy can then occur. For large values of n', n, and n-n', we thus use the asymptotic formula (Menzel and Pekeris, 1935):

$$ f_{n' \to n} = \frac{2^6}{3\pi\sqrt{3}} \frac{1}{\omega_{n'}} \left(\frac{1}{n'^2} - \frac{1}{n^2} \right)^{-3} \left| \frac{1}{n'^3} \frac{1}{n^3} \right| g \qquad \ldots(2.12) $$

where g, the Gaunt factor for the n' -> n transition, is of order unity. With g = 1, we obtain a value of $f_{20 \to 21}$ off by ~25% and a value of $f_{20 \to 70}$ off by ~3%. The accuracy of eq.(2.12) can be improved by using a better estimate of the Gaunt factor. In Appendix E, we derive an expression for the Gaunt factor which we use to evaluate the absorption oscillator strengths for moderately high values of n' and n, and

any value of $n-n'$. Eq.(2.12) then gives an accuracy of 3S for $n-n' = 1$ and at least 4S for $n-n' \geq 2$.

Emission oscillator strengths, $f_{n\to n'}$, are also occasionally used. They can be obtained from the absorption oscillator strengths from the relation

$$\omega_n f_{n\to n'} = \omega_{n'} f_{n'\to n}. \qquad \ldots(2.13)$$

4. COLLISIONAL IONIZATION RATE COEFFICIENT

The cross-section for ionization of an atom or ion by removal of an atomic electron from state n by electron impact has been thoroughly investigated by Drawin (1961, 1962, 1963, 1966). He has proposed a semi-empirical expression which gives a good fit to the available experimental data, and which is proportional to $\ln E/E$ for large values of the free electron kinetic energy E as required by quantum mechanics (Massey and Burhop, 1952, p.140).

The cross-section is written as

$$\sigma_n(u_n) = 4\pi a_0^2 \alpha_n |S_n|^2 \frac{I_1^H}{I_n} \frac{u_n - 1}{u_n^2} \ln(1.25\beta_n u_n) \qquad \ldots(2.14)$$

where $I_1^H = E_1^H$ is the ionization energy of the hydrogen atom in its ground state, $I_n = E_n$ is the ionization energy of the atom or ion in state n, $u_n = E/I_n$ is the kinetic energy of the incident electron in units of the threshold energy for ionization from state n,

$$|S_n|^2 = |z_n|^2 / a_o^2 , \qquad \ldots(2.15)$$

$|z_n|$ is the mean dipole length on the z-axis for the discrete-continuous transition, and α_n and β_n are correction factors of order unity. To obtain the correct threshold law, β_n must be larger than 0.8. Drawin suggests that the correction factors be approximated by the following expressions:

$$\alpha_n |S_n|^2 \simeq 0.665 \frac{I_1^H}{I_n} \xi_n \qquad \ldots(2.16)$$

where ξ_n is the number of equivalent electrons in state n and 0.665 is a mean value for low and medium principal quantum numbers;

$$\beta_n = 1 + \frac{Z_{eff} - 1}{Z_{eff} + 2} \qquad \ldots(2.17)$$

where Z_{eff} denotes the effective charge of the nucleus acting on the electrons in state n; for hydrogenic ions, $Z_{eff} = Z$. The cross-section is then written as

$$\sigma_n(u_n) = 2.66 \pi a_o^2 \left(\frac{I_1^H}{I_n}\right)^2 \xi_n \frac{u_n - 1}{u_n^2} \ln (1.25 \beta_n u_n) \qquad \ldots(2.18)$$

which, for hydrogenic ions, becomes

$$\sigma_n(u_n) = 2.66 \pi a_o^2 \left(\frac{n}{Z}\right)^4 \frac{u_n - 1}{u_n^2} \ln (1.25 \beta_n u_n). \qquad \ldots(2.19)$$

The rate coefficient is obtained by integrating the cross-section over the free electron velocity distribution, f(v):

$$S_n(T) = \int_v \sigma_n(v)\, v\, f(v)\, dv \qquad \ldots(2.20)$$

For a Maxwellian velocity distribution of the free electrons, we have

$$f(v)\, dv = \frac{4}{\sqrt{\pi}} \left(\frac{m}{2kT}\right)^{3/2} v^2\, e^{-\frac{mv^2}{2kT}}\, dv \qquad \ldots(2.21)$$

In units of the threshold energy for ionization from state n,

$$u_n = \tfrac{1}{2} m v^2 / I_n , \qquad \ldots(2.22)$$

eq.(2.20) then becomes

$$S_n(T) = 2\sqrt{\frac{2}{\pi m}} \frac{I_n^2}{(kT)^{3/2}} \int_1^\infty \sigma_n(u_n)\, u_n\, e^{-\frac{I_n}{kT} u_n}\, du_n . \qquad \ldots(2.23)$$

Substituting for $\sigma_n(u_n)$ from eq.(2.19), eq.(2.23) can be written as

$$S_n(T) = \frac{3.62}{T^{3/2}} G(\beta_n, \theta_n) \quad cm^3 s^{-1} \qquad \ldots(2.24)$$

where

$$G(\beta_n, \theta_n) = \int_1^\infty \frac{u_n - 1}{u_n} \ln(1.25 \beta_n u_n)\, e^{-\theta_n u_n}\, du_n , \qquad \ldots(2.25)$$

$$\theta_n = I_n / kT = 157,890\, Z^2 / T n^2 , \qquad \ldots(2.26)$$

and T is in Kelvin.

The evaluation of integral (2.25) is not elementary. We rewrite eq.(2.25) by changing the variable u_n to $x = \theta_n u_n$, then

$$G(\beta_n, \theta_n) = \frac{1}{\theta_n} \int_{\theta_n}^{\infty} \left(1 - \frac{\theta_n}{x}\right) \ln\left(\frac{1.25\,\beta_n}{\theta_n} x\right) e^{-x}\, dx. \qquad \ldots(2.27)$$

Expanding the natural logarithm, we obtain

$$\theta_n G(\beta_n, \theta_n) = \ln\left(\frac{1.25\,\beta_n}{\theta_n}\right) \int_{\theta_n}^{\infty} \left(1 - \frac{\theta_n}{x}\right) e^{-x}\, dx + \int_{\theta_n}^{\infty} \left(1 - \frac{\theta_n}{x}\right) \ln x\, e^{-x}\, dx. \qquad \ldots(2.28)$$

The first integral is easily evaluated:

$$\int_{\theta_n}^{\infty} \left(1 - \frac{\theta_n}{x}\right) e^{-x} dx = e^{-\theta_n} - \theta_n E_1(\theta_n) \qquad \ldots(2.29)$$

where $E_1(\theta_n)$ is the exponential integral:

$$E_1(\theta_n) = \int_{\theta_n}^{\infty} \frac{e^{-x}}{x}\, dx. \qquad \ldots(2.30)$$

This is a well known function for which many analytical approximations are available (Abramowitz and Stegun, 1965, p.228). Substituting eq.(2.29) in eq.(2.28), we get

$$\theta_n G(\beta_n, \theta_n) = \ln\left(\frac{1.25\,\beta_n}{\theta_n}\right) \left[e^{-\theta_n} - \theta_n E_1(\theta_n)\right] + \int_{\theta_n}^{\infty} \ln x\, e^{-x}\, dx - \theta_n \int_{\theta_n}^{\infty} \frac{\ln x}{x} e^{-x}\, dx. \qquad \ldots(2.31)$$

These last two integrals are evaluated in Appendix C:

$$\int_{\theta_n}^{\infty} \ln x\, e^{-x} dx = \ln \theta_n\, e^{-\theta_n} + E_1(\theta_n) \qquad \ldots(2.32)$$

$$\int_{\theta_n}^{\infty} \frac{\ln x}{x} e^{-x} dx = \ln \theta_n\, E_1(\theta_n) + \epsilon_1(\theta_n) \qquad \ldots(2.33)$$

where $\epsilon_1(\theta_n) = \int_{\theta_n}^{\infty} \frac{E_1(x)}{x} dx$. $\qquad \ldots(2.34)$

Analytical approximations to function $\epsilon_1(\theta_n)$ are also derived in Appendix C. Substituting for eqs.(2.32) to (2.34) in eq.(2.31), we obtain

$$\theta_n G(\beta_n, \theta_n) = \ln(1.25\beta_n)\left[e^{-\theta_n} - \theta_n E_1(\theta_n)\right] + \left[E_1(\theta_n) - \theta_n \epsilon_1(\theta_n)\right] \qquad \ldots(2.35)$$

which can be evaluated by analytical approximations.

Since the exponential integral $E_1(\theta_n)$ can be evaluated to an accuracy of 14S with approximations given by Cody and Thacher (1968), the accuracy of $G(\beta_n, \theta_n)$ depends on the accuracy of the approximations to $\epsilon_1(\theta_n)$. As given in Appendix C, $\epsilon_1(\theta_n)$ can be evaluated to an accuracy of 4-6S, depending on the value of θ_n. This is thus the minimum accuracy of $G(\beta_n, \theta_n)$. For large values of θ_n, where substantial cancellations may occur in the terms

$$\left[e^{-\theta_n} - \theta_n E_1(\theta_n)\right] \quad \text{and} \quad \left[E_1(\theta_n) - \theta_n \epsilon_1(\theta_n)\right],$$

comparable accuracy can be obtained by evaluating the first term with the asymptotic expansion of $E_1(x)$ (Abramowitz and Stegun, 1965, p.231); then

$$[e^{-\theta_n} - \theta_n E_1(\theta_n)] \propto e^{-\theta_n}\left(\frac{1!}{\theta_n} - \frac{2!}{\theta_n^2} + \frac{3!}{\theta_n^3} - + \cdots\right). \quad \ldots(2.36)$$

Since the second term is of order

$$[E_1(\theta_n) - \theta_n E_1(\theta_n)] \sim \frac{1}{\theta_n}[e^{-\theta_n} - \theta_n E_1(\theta_n)], \quad \ldots(2.37)$$

its effect on the accuracy of $G(\beta_n, \theta_n)$, compared to the first term, is minimal. It can be evaluated asymptotically with the help of eq.(C.60).

The accuracy of the analytical approximations to $G(\beta_n, \theta_n)$ is thus better than 4S for all values of θ_n. The accuracy of the values of the rate coefficients calculated from eq.(2.24) thus depends exclusively on the validity of the Drawin expression for the collisional ionization cross-section, eq.(2.14). By adjusting the correction factors α_n and β_n, this expression can be made to agree closely with experiment (Drawin, 1961, 1962). However, using the average values (2.16) and (2.17) for these factors restricts the accuracy of expression (2.18). For hydrogenic ions, the accuracy should still be better than a factor of 1.5 for all states n.

5. COLLISIONAL EXCITATION RATE COEFFICIENT

The cross-section for excitation of an atomic electron from a lower state n' to an upper state n by electron impact can be evaluated with a semi-empirical expression proposed by Drawin (1963, 1966):

$$\sigma_{n' \to n}(u_{n'n}) = 4\pi \frac{E_i^H}{E_{n'n}} |z_{n'n}|^2 \, g(u_{n'n}) \qquad \ldots(2.38)$$

where $E_{n'n}$ is the excitation energy of the n' -> n transition,

$$u_{n'n} = E / E_{n'n} \qquad \ldots(2.39)$$

is the free electron kinetic energy in units of the threshold energy for excitation of the n' -> n transition, $|z_{n'n}|$ is the dipole length on the z-axis for the n' -> n transition, and $g(u_{n'n})$ is an appropriate function giving the correct asymptotic behavior of the cross-section. The dipole length can be written in terms of $f_{n' \to n}$, the absorption oscillator strength for the n' -> n transition:

$$|z_{n'n}|^2 = a_o^2 \frac{E_i^H}{E_{n'n}} f_{n' \to n} . \qquad \ldots(2.40)$$

With eq.(2.40), eq.(2.38) then becomes

$$\sigma_{n' \to n}(u_{n'n}) = 4\pi a_o^2 \left(\frac{E_i^H}{E_{n'n}}\right)^2 f_{n' \to n} \, g(u_{n'n}). \qquad \ldots(2.41)$$

Drawin proposes that different functions $g(u_{n'n})$ be used for atoms and ions:

$$g_{atom} = \alpha_{n'n} \frac{u_{n'n} - 1}{u_{n'n}^2} \ln (1.25\, \beta_{n'n}\, u_{n'n}) \qquad \ldots(2.42)$$

$$g_{ion} = 0.302, \quad \text{for} \quad 1 \leq u_{n'n} \leq 3.85$$

$$= \frac{u_{n'n} - 1}{u_{n'n}^2} \ln (1.25\, u_{n'n}), \quad \text{for } u_{n'n} \geq 3.85 \qquad \ldots(2.43)$$

where $\alpha_{n'n}$ and $\beta_{n'n}$ are adjustable parameters. Equations (2.42) and (2.43) reflect the fact that at threshold, the excitation cross-section for atoms is zero, whereas for ions, it is finite. Drawin suggests that the following values of the parameters $\alpha_{n'n}$ and $\beta_{n'n}$ be used for atoms:

$$\alpha_{n'n} = 1$$

$$\beta_{n'n} = 2. \qquad \ldots(2.44)$$

The expression (2.43) given for ions implies that

$$\alpha_{n'n} = 1$$

$$\beta_{n'n} = 1 \qquad \ldots(2.45)$$

for ions.

The rate coefficient is obtained by integrating the cross-section over f(v), the free electron velocity distribution:

$$C_{n' \to n}(T) = \int_v \sigma_{n' \to n}(v)\, v\, f(v)\, dv. \qquad \ldots(2.46)$$

Using the Maxwellian velocity distribution, eq.(2.21), and units of the threshold energy for excitation of the n' -> n transition,

$$u_{n'n} = \tfrac{1}{2} m v^2 / E_{n'n}, \qquad \ldots(2.47)$$

eq.(2.46) becomes

$$C_{n'\to n}(T) = 2\sqrt{\frac{2}{\pi m}}\,\frac{E_{n'n}^2}{(kT)^{3/2}}\int_1^\infty \sigma_{n'\to n}(u_{n'n}) \times u_{n'n}\, e^{-\frac{E_{n'n}}{kT}u_{n'n}}\, du_{n'n}. \qquad \ldots(2.48)$$

Substituting for $\sigma_{n'\to n}(u_{n'n})$ from eq.(2.41) in eq.(2.48), we get

$$C_{n'\to n}(T) = \frac{5.45}{T^{3/2}}\, f_{n'\to n}\, G(\alpha_{n'n}, \beta_{n'n}, \theta_{n'n})\ cm^3 s^{-1} \qquad \ldots(2.49)$$

where

$$G(\alpha_{n'n}, \beta_{n'n}, \theta_{n'n}) = \int_1^\infty g(u_{n'n})\, u_{n'n}\, e^{-\theta_{n'n} u_{n'n}}\, du_{n'n}, \qquad \ldots(2.50)$$

$$\theta_{n'n} = \frac{E_{n'n}}{kT} = \frac{157{,}890\, z^2}{T}\,\frac{n^2 - n'^2}{n^2 n'^2}, \qquad \ldots(2.51)$$

and T is in Kelvin.

The integral (2.50) has different forms for atoms and ions:

$$G_{atom} = \alpha_{n'n} \int_1^{\infty} \frac{u_{n'n}-1}{u_{n'n}} \ln(1.25\,\beta_{n'n} u_{n'n})\, e^{-\theta_{n'n} u_{n'n}}\, du_{n'n} \qquad \ldots(2.52)$$

$$G_{ion} = 0.302 \int_1^{3.85} u_{n'n}\, e^{-\theta_{n'n} u_{n'n}}\, du_{n'n}$$

$$+ \int_{3.85}^{\infty} \frac{u_{n'n}-1}{u_{n'n}} \ln(1.25\,\beta_{n'n} u_{n'n})\, e^{-\theta_{n'n} u_{n'n}}\, du_{n'n}. \qquad \ldots(2.53)$$

One of these integrals can be very easily evaluated:

$$\int_1^{3.85} u_{n'n}\, e^{-\theta_{n'n} u_{n'n}}\, du_{n'n} = \frac{1}{\theta_{n'n}^2}\left[(1+\theta_{n'n})\, e^{-\theta_{n'n}}\right.$$

$$\left. -(1+3.85\,\theta_{n'n})\, e^{-3.85\,\theta_{n'n}}\right]. \qquad \ldots(2.54)$$

The other two integrals involve the evaluation of a more general integral:

$$Dr(\beta_{n'n}, \theta_{n'n}, a) = \int_a^{\infty} \frac{u_{n'n}-1}{u_{n'n}} \ln(1.25\,\beta_{n'n} u_{n'n})$$

$$\times\, e^{-\theta_{n'n} u_{n'n}}\, du_{n'n}. \qquad \ldots(2.55)$$

The function $G(\beta_n, \theta_n)$ obtained in the evaluation of the collisional ionization rate coefficient is a special case of this general integral:

$$G(\beta_n, \theta_n) = Dr(\beta_n, \theta_n, 1). \qquad \ldots(2.56)$$

To evaluate the general integral (2.55), we thus follow the method which was used to evaluate eq. (2.56): steps (2.25) to (2.35). We then obtain the general solution

$$\theta_{n'n}\, Dr(\beta_{n'n}, \theta_{n'n}, a) = \ln(1.25 a \beta_{n'n})\left[e^{-a\theta_{n'n}} - \theta_{n'n} E_1(a\theta_{n'n})\right]$$

$$+\left[E_1(a\theta_{n'n}) - \theta_{n'n} \epsilon_1(a\theta_{n'n})\right]. \qquad \ldots(2.57)$$

The functions G_{atom} and G_{ion} are then given by

$$G_{atom} = \alpha_{n'n}\; Dr(\beta_{n'n}, \theta_{n'n}, 1) \qquad \ldots(2.58)$$

$$G_{ion} = \frac{0.302}{\theta_{n'n}^2}\left[(1+\theta_{n'n})e^{-\theta_{n'n}} - (1+3.85\,\theta_{n'n})e^{-3.85\theta_{n'n}}\right]$$

$$+\; Dr(1, \theta_{n'n}, 3.85). \qquad \ldots(2.59)$$

The accuracy of the function $Dr(\beta_{n'n}, \theta_{n'n}, a)$ is the same as that of the function $G(\beta_n, \theta_n)$. An estimate of this accuracy can be obtained from the discussion of the accuracy of $G(\beta_n, \theta_n)$ given in Section 4 of this Chapter. The excitation rate coefficients should also have an accuracy comparable to that of the ionization rate coefficients: better than a factor of two for hydrogenic ions (see Section 4 of this Chapter).

6. INVERSE PROCESSES AND DETAILED BALANCING

The collisional de-excitation and three-body recombination processes are the inverse of the collisional excitation and collisional ionization processes respectively. The rate coefficients of each pair of processes are related by the principle of detailed balancing. This principle

states that under conditions of thermodynamic equilibrium, the differential reaction rates for each microscopic process and for the corresponding inverse process are equal (Mitchner and Kruger, 1973, p.80). If the free electron distribution function is Maxwellian, the rate coefficients are also related by the requirements of detailed balancing (Mitchner and Kruger, 1973, p.435).

As an example of the method, we consider reactions of the type (Seaton, 1958b)

$$A_q + B \rightarrow A_p + B \qquad \ldots(2.60)$$

where A_q and A_p represent particle A in states q and p respectively, and B represents particle B. We denote the particle densities by $n(A_q)$, $n(A_p)$, and $n(B)$, and the rate coefficients in the forward direction by $R_{q\rightarrow p}$ and in the reverse direction by $R_{p\rightarrow q}$. Under thermodynamic equilibrium, these rate coefficients are related by the detailed balance relation,

$$n(A_q)\, n(B)\, R_{q\rightarrow p} = n(A_p)\, n(B)\, R_{p\rightarrow q}. \qquad \ldots(2.61)$$

Combining eq.(2.61) and the Boltzmann relation

$$\frac{n(A_q)}{n(A_p)} = \frac{\omega_q}{\omega_p}\, e^{(E_p - E_q)/kT}, \qquad \ldots(2.62)$$

we obtain the relation

$$R_{p\rightarrow q} = \frac{\omega_q}{\omega_p}\, e^{(E_p - E_q)/kT}\, R_{q\rightarrow p} \qquad \ldots(2.63)$$

between the rate coefficients.

7. THREE-BODY RECOMBINATION RATE COEFFICIENT

The rate coefficient for the recombination of a free electron in an atomic state n with subsequent absorption of the excess energy by a neighbouring electron, $\alpha_n(T)$, is obtained by the principle of detailed balancing from the rate coefficient for the inverse process of ionization by electron impact, $S_n(T)$. The rate coefficients are related by the expression (Drawin, 1963)

$$\alpha_n(T) = \frac{\omega_n}{2u_i} \frac{h^3}{(2\pi m kT)^{3/2}} e^{\theta_n} S_n(T) \qquad \ldots(2.64)$$

where u_i is the partition function of the ion before recombination, ω_n is the statistical weight of the recombined electron in state n, and $\theta_n = I_n / kT$. Recalling the Saha equation (1.17), we can write

$$\alpha_n(T) = Z_n(T)\, S_n(T). \qquad \ldots(2.65)$$

Numerically, for T in Kelvin and $S_n(T)$ in $cm^3 s^{-1}$, we obtain

$$\alpha_n(T) = \frac{2.071 \times 10^{-16}}{T^{3/2}} \frac{\omega_n}{u_i} e^{\theta_n} S_n(T) \ cm^6 s^{-1}. \qquad \ldots(2.66)$$

As θ_n increases, the exponential term e^{θ_n} becomes very large, and the ionization rate coefficient, $S_n(T)$, very small. The product of the two terms remains finite, but on a computer, it gives rise to com-

plications (overflows and underflows) which can be resolved by multiplying the two terms algebraically. Substituting for $S_n(T)$ from eq.(2.24) in eq.(2.66), we get

$$\alpha_n(T) = \frac{7.50 \times 10^{-16}}{T^3} \frac{\omega_n}{u_i} G'(\beta_n, \theta_n) \ cm^6 s^{-1} \qquad \ldots(2.67)$$

where $$G'(\beta_n, \theta_n) = e^{\theta_n} \cdot G(\beta_n, \theta_n). \qquad \ldots(2.68)$$

Substituting for $G(\beta_n, \theta_n)$ from eq.(2.35), we obtain

$$\theta_n G'(\beta_n, \theta_n) = \ln(1.25\beta_n)[1 - \theta_n E_1'(\theta_n)] + [E_1'(\theta_n) - \theta_n \epsilon_1'(\theta_n)] \qquad \ldots(2.69)$$

where $$E_1'(\theta_n) = e^{\theta_n} E_1(\theta_n) \qquad \ldots(2.70)$$

and $$\epsilon_1'(\theta_n) = e^{\theta_n} \epsilon_1(\theta_n). \qquad \ldots(2.71)$$

For large values of θ_n, the functions $E_1'(\theta_n)$ and $\epsilon_1'(\theta_n)$ can be evaluated accurately from their asymptotic expansions. For $E_1'(\theta_n)$, we have (Abramowitz and Stegun, 1965, p.231)

$$E_1'(\theta_n) \simeq \frac{1}{\theta_n}\left[1 - \frac{1!}{\theta_n} + \frac{2!}{\theta_n^2} - + \ldots\right]. \qquad \ldots(2.72)$$

The function $\epsilon_1'(\theta_n)$ for large θ_n can be evaluated from the approximations (C.58) and (C.60) given in Appendix C.

8. COLLISIONAL DE-EXCITATION RATE COEFFICIENT

The rate coefficient for de-excitation of an atomic electron from an upper state n to a lower state n' by electron impact, $F_{n\to n'}(T)$, is obtained by the principle of detailed balancing from the rate coefficient for the inverse process of excitation by electron impact, $C_{n'\to n}(T)$. The rate coefficients are related by the expression (Drawin, 1963)

$$F_{n\to n'}(T) = \frac{\omega_{n'}}{\omega_n} e^{\theta_{n'n}} C_{n'\to n}(T). \qquad \ldots(2.73)$$

For large values of $\theta_{n'n}$, the product $e^{\theta_{n'n}} C_{n'\to n}(T)$ is evaluated algebraically as has been done for the three-body recombination rate coefficient. Using eqs.(2.13) and (2.49), eq.(2.73) becomes

$$F_{n\to n'}(T) = \frac{5.45}{T^{3/2}} f_{n\to n'} G'(\alpha_{n'n}, \beta_{n'n}, \theta_{n'n}) \, cm^3 s^{-1} \qquad \ldots(2.74)$$

where $$G'(\alpha_{n'n}, \beta_{n'n}, \theta_{n'n}) = e^{\theta_{n'n}} G(\alpha_{n'n}, \beta_{n'n}, \theta_{n'n}). \qquad \ldots(2.75)$$

From eqs.(2.58) and (2.59), the function $G'(\alpha_{n'n}, \beta_{n'n}, \theta_{n'n})$ has different forms for atoms and ions:

$$G'_{atom} = \alpha_{n'n} \, Dr'(\beta_{n'n}, \theta_{n'n}, 1) \qquad \ldots(2.76)$$

$$G'_{ion} = \frac{0.302}{\theta_{n'n}^2}\left[1 + \theta_{n'n} - (1 + 3.85\theta_{n'n}) e^{-2.85\theta_{n'n}}\right] + Dr'(1, \theta_{n'n}, 3.85) \qquad \ldots(2.77)$$

where $Dr'(\beta_{n'n}, \theta_{n'n}, a) = e^{\theta_{n'n}} Dr(\beta_{n'n}, \theta_{n'n}, a)$. ...(2.78)

From eq.(2.57),

$$\theta_{n'n} Dr'(\beta_{n'n}, \theta_{n'n}, a) = \ln(1.25 a \beta_{n'n}) \left[e^{-(a-1)\theta_{n'n}} - \theta_{n'n} e^{\theta_{n'n}} E_1(a\theta_{n'n}) \right] + \left[e^{\theta_{n'n}} E_1(a\theta_{n'n}) - \theta_{n'n} e^{\theta_{n'n}} \epsilon_1(a\theta_{n'n}) \right] \quad \ldots(2.79)$$

For large values of $\theta_{n'n}$, $e^{\theta_{n'n}} E_1(a\theta_{n'n})$ and $e^{\theta_{n'n}} \epsilon_1(a\theta_{n'n})$ are finite, and can be evaluated accurately from their asymptotic expansion. $e^{\theta_{n'n}} E_1(a\theta_{n'n})$ is given by (Abramowitz and Stegun, 1965, p.231)

$$e^{\theta_{n'n}} E_1(a\theta_{n'n}) \simeq \frac{1}{a\theta_{n'n}} e^{-(a-1)\theta_{n'n}} \left[1 - \frac{1!}{a\theta_{n'n}} + \frac{2!}{(a\theta_{n'n})^2} - + \cdots \right] \quad \ldots(2.80)$$

$e^{\theta_{n'n}} \epsilon_1(a\theta_{n'n})$ for large $\theta_{n'n}$ can be evaluated from eqs.(C.58) and (C.60) given in Appendix C. From eqs.(2.79) and (2.80), we note that for large $\theta_{n'n}$, eq.(2.77) becomes

$$G'_{ion} = 0.302 \frac{1 + \theta_{n'n}}{\theta_{n'n}^2} . \quad \ldots(2.81)$$

9. RADIATIVE RECOMBINATION RATE COEFFICIENT

The rate coefficient for the recombination of a free electron in a hydrogenic atomic state n with subsequent emission of a photon of fre-

quency υ is calculated from an approximation proposed by Seaton (1959). The rate coefficient is obtained from the photoionization cross-section by the principle of detailed balancing:

$$\beta_n(T) = \frac{1}{c^2}\sqrt{\frac{2}{\pi}}\,\frac{2n^2}{(mkT)^{3/2}}\,e^{I_n/kT} \times \int_{I_n}^{\infty} (h\upsilon)^2\, e^{-\frac{h\upsilon}{kT}}\, a_n(\upsilon)\, d(h\upsilon) \qquad \ldots(2.82)$$

where $a_n(\upsilon)$ is the cross-section for photoionization of a hydrogenic ion in state n and all other symbols are as defined previously. The cross-section is given by

$$a_n(\upsilon) = \frac{2^6 \alpha \pi a_o^2}{3\sqrt{3}}\,\frac{n}{Z^2}\,\frac{g_{II}(n,\epsilon)}{(1+n^2\epsilon)^3} \qquad \ldots(2.83)$$

where α is the fine-structure constant, $Z^2\epsilon$ is the kinetic energy of the ejected electron in Rydbergs, and $g_{II}(n,\epsilon)$ is the Kramers-Gaunt factor; it is of order unity. From the energy conservation condition

$$h\upsilon = Z^2\left(\frac{1}{n^2} + \epsilon\right) \ \text{Rydbergs} \qquad \ldots(2.84)$$

and the relation

$$\theta_n = \frac{I_n}{kT} = \frac{157{,}890}{T}\,\frac{Z^2}{n^2}, \qquad \ldots(2.85)$$

and substituting for $a_n(\upsilon)$ from eq.(2.83), eq.(2.82) becomes

$$\beta_n(T) = \frac{2^6}{3}\sqrt{\frac{\pi}{3}}\,\alpha^4 c\, a_o^2\, Z\, \theta_n^{3/2}\, \mathcal{L}_n(\theta_n) \qquad \ldots(2.86)$$

where $\mathcal{A}_n(\theta_n) = \int_0^\infty \frac{g_{II}(n,\epsilon)}{1+u_n} e^{-\theta_n u_n} du_n$ ...(2.87)

and $u_n = n^2\epsilon = Z^2\epsilon / I_n$ ...(2.88)

is the kinetic energy of the ejected electron in units of the threshold energy for photoionization from state n. Numerically,

$$\beta_n(T) = 5.197 \times 10^{-14} Z \theta_n^{3/2} \mathcal{A}_n(\theta_n) \ cm^3 s^{-1}. \quad ...(2.89)$$

Putting the Kramers-Gaunt factor equal to unity in eq.(2.87) gives rise to errors as large as 20%. The accuracy of $\beta_n(T)$ is improved by using the asymptotic expansion of $g_{II}(n,\epsilon)$ (Menzel and Pekeris, 1935; Burgess, 1958):

$$g_{II}(n,\epsilon) = 1 + \frac{0.1728}{n^{2/3}} \frac{u-1}{(u+1)^{2/3}} - \frac{0.0496}{n^{4/3}} \frac{u^2 + \frac{4}{3}u + 1}{(u+1)^{4/3}} + \cdots . \quad ...(2.90)$$

Substituting eq.(2.90) in eq.(2.87), we get

$$\mathcal{A}_n(\theta_n) = \mathcal{A}_n^{(0)}(\theta_n) + \frac{0.1728}{n^{2/3}} \mathcal{A}_n^{(1)}(\theta_n) - \frac{0.0496}{n^{4/3}} \mathcal{A}_n^{(2)}(\theta_n) + \cdots \quad ...(2.91)$$

where $\mathcal{A}_n^{(0)}(\theta_n) = \int_0^\infty \frac{1}{1+u_n} e^{-\theta_n u_n} du_n$, ...(2.92)

$$\mathcal{A}_n^{(1)}(\theta_n) = \int_0^\infty \frac{u_n - 1}{(u_n+1)^{5/3}} e^{-\theta_n u_n} du_n, \qquad \ldots(2.93)$$

and $$\mathcal{A}_n^{(2)}(\theta_n) = \int_0^\infty \frac{u_n^2 + 4/3\, u_n + 1}{(u_n+1)^{7/3}} e^{-\theta_n u_n} du_n. \qquad \ldots(2.94)$$

These integrals can be expressed in terms of well-known functions:

$$\mathcal{A}_n^{(0)}(\theta_n) = e^{\theta_n} E_1(\theta_n) \qquad \ldots(2.95)$$

$$\mathcal{A}_n^{(1)}(\theta_n) = -3 + (1+3\theta_n)\, \Psi(1; 4/3; \theta_n) \qquad \ldots(2.96)$$

$$\mathcal{A}_n^{(2)}(\theta_n) = -\tfrac{3}{2}(1+\theta_n) + (1 + 2\theta_n + \tfrac{3}{2}\theta_n^2)\, \Psi(1; 5/3; \theta_n) \qquad \ldots(2.97)$$

where $E_1(x)$ is the exponential integral, and $\Psi(a;c;x)$ is the confluent hypergeometric function (Abramowitz and Stegun, 1965, p.503).

$\Psi(1;c;x)$ is evaluated from the relation

$$(c-1)\, \Psi(1;c;x) = \Gamma(c)\, x^{1-c}\, e^x - \Phi(1;c;x) \qquad \ldots(2.98)$$

where the series

$$\Phi(1;c;x) = 1 + \frac{x}{c} + \frac{x^2}{c(c+1)} + \cdots \qquad \ldots(2.99)$$

converges for all finite x. In the limit of large x, the asymptotic expansion

$$\Psi(1;c;x) \simeq \frac{1}{x}\left[1 - \frac{2-c}{x} + \frac{(2-c)(3-c)}{x^2} - \cdots\right] \qquad \ldots(2.100)$$

is used. Eq.(2.98) is accurate for small values of x, and eq.(2.100) for large values of x. For intermediate values of x, both of these equations loose their accuracy: eq.(2.98) because the two terms of the right hand side become very nearly equal as x increases, and eq.(2.100) because the asymptotic expansion becomes less and less accurate as x decreases. For these values of x, we evaluate $\Phi(1;c;x)$ from its integral representation (Abramowitz and Stegun, 1965, p.505)

$$\Phi(1;c;x) = x^{1-c}\int_0^\infty (z+x)^{c-2} e^{-z}\, dz. \qquad \ldots(2.101)$$

The integral is evaluated numerically with Simpson's 1/3 rule. The integration to $z = \infty$ is truncated at $z = 30$, and the mesh is fixed at 1/15 (450 subdivisions of the range $z = 0$ to 30).

The different expressions used to evaluate $\Phi(1;c;x)$ are applied within the following ranges of x: eq.(2.98) for $x \leq 6$, eq.(2.101) for $6 < x < 15$, and eq.(2.100) for $x \geq 15$. These were obtained by evaluating $\Phi(1;4/3;x)$ to an accuracy of 6S. In this way, the accuracy of $\Phi(1;c;x)$ does not affect the accuracy of $\beta_n(T)$. The accuracy of the rate coefficients depends on the value of $g_{II}(n,\epsilon)$ used in eq.(2.87). With the asymptotic expansion (2.90) of $g_{II}(n,\epsilon)$, these are not in error by more than 2% for temperatures of order 10,000 K or less, but the error may be greater for temperatures of order 1,000,000 K. However, since the error in

$$\beta_{TOTAL}(T) = \sum_{n=1}^{\infty} \beta_n(T)$$

is estimated by Seaton to be of about 10% for $(T/Z^2) = 1{,}000{,}000$ K, the error in $\beta_n(T)$ should not be greater than 10% for this value of (T/Z^2).

Chapter III

THE LITHIUM-LIKE IONS C IV, N V, AND Ø VI

1. INTRODUCTION

The Wolf-Rayet stars are known to show strong emission lines of C IV and also of isoelectronic N V and O VI in their spectra. Varshni (1977) has discussed the possibility of laser action in the line C IV λ4650. It was thus of interest to carry out detailed calculations concerning possible laser action in the emission lines of the lithium-like ions C IV, N V, and O VI.

A lithium-like ion consists of three electrons orbiting a nucleus of nuclear charge Z_N (in units of the electronic charge +e). Two of the electrons occupy the closed $1s^2$ shell while the third electron (the valence electron) orbits the helium-like core composed of this closed $1s^2$ shell and of the nucleus. The core thus has a charge $Z = Z_N - 2$. More details are given on the first six lithium-like ions in Tab.3.1. The core-valence electron system is very similar in structure to a hydrogenic ion. The differences that arise between the two kinds of ions stem from the difference in size of the cores: for lithium-like ions, the core has a finite size while for hydrogenic ions, it can be considered as point-like.

Table 3.1 - The first six lithium-like ions.

Notation	Charge	Z_N	Z	Description
Li I	Li^0	3	1	neutral
Be II	Be^+	4	2	singly-ionized
B III	B^{2+}	5	3	doubly-ionized
C IV	C^{3+}	6	4	triply-ionized
N V	N^{4+}	7	5	ionized four times
O VI	O^{5+}	8	6	ionized five times

2. ENERGY EIGENVALUES

The finite size of the core causes a splitting of the energy levels of the lithium-like ions with respect to the orbital angular momentum quantum number ℓ. This is illustrated in Fig.3.1 (Herzberg, 1944, p.61). The reason for this situation is best visualized with the Bohr model of the atom. Classically, a low angular momentum electron passes closer to the core than a high angular momentum electron. Close to the core, the electron experiences an effective potential which is different from the Coulomb potential effective at large distances from the core. Consequently, for a given principal quantum number n, states with different values of the azimuthal quantum number ℓ will have different energy eigenvalues, especially at low values of n and ℓ.

In this work, we thus consider the splitting of the energy levels with respect to the quantum number ℓ, but neglect the splitting with respect to the magnetic quantum number. Then the 2s state is the ground state of the valence electron; the 2p state, the first excited state; the 3s state, the second excited state; and so on, in order of increasing level energy. The statistical weight of level $n\ell$ is given by

$$\omega_{n\ell} = 2(2\ell + 1). \qquad \ldots(3.1)$$

We use the experimentally observed and extrapolated term values of the energy levels compiled by Moore (1949), wherever available.

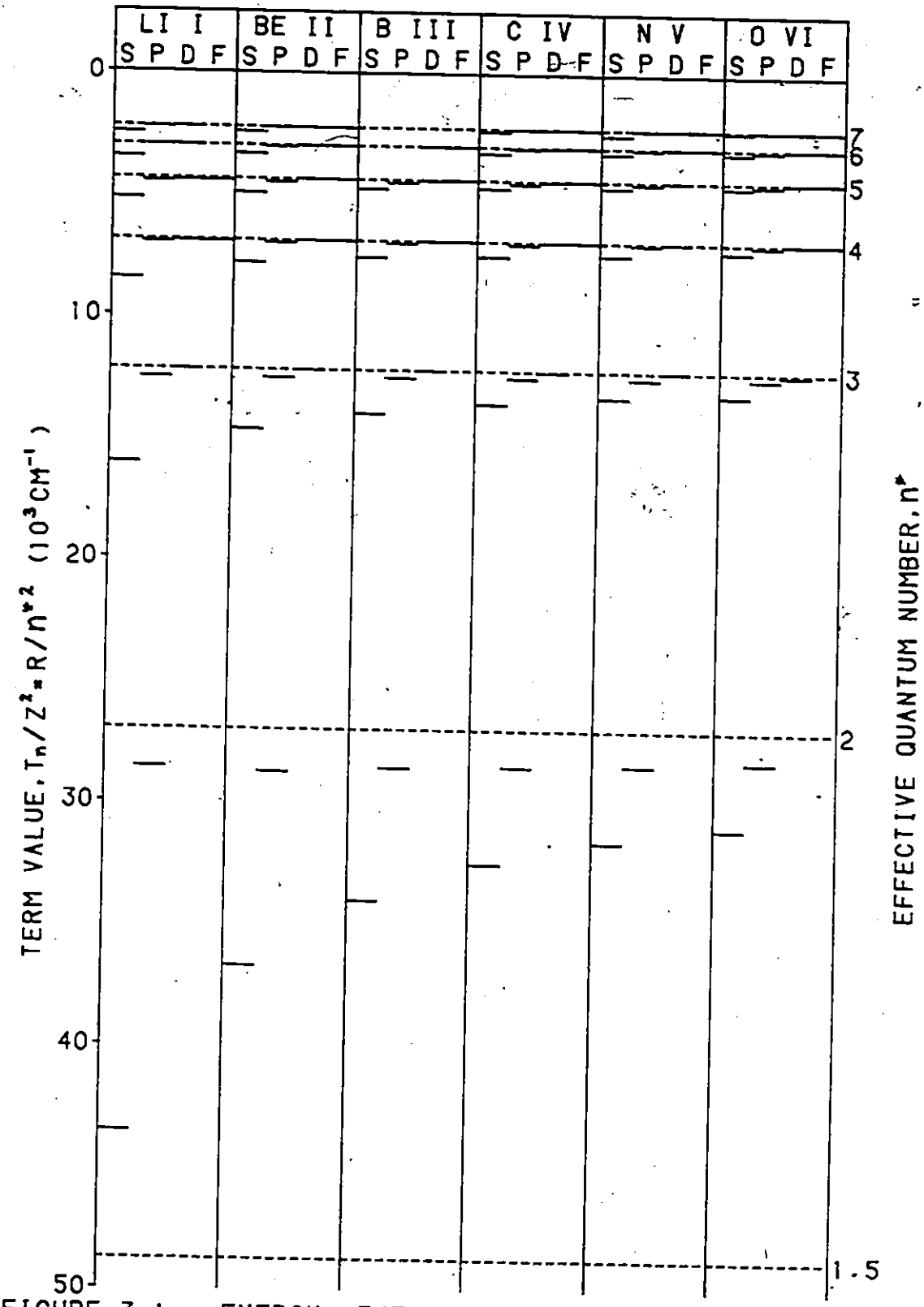

FIGURE 3.1 - ENERGY LEVEL DIAGRAMS OF LITHIUM AND LITHIUM-LIKE IONS UP TO O VI (HERZBERG, 1944, P.61) FROM THE DATA OF MOORE (1949).

3. EFFECTIVE QUANTUM NUMBERS

Since lithium-like ions are similar in structure to hydrogenic ions, their energy eigenvalues can be expressed as follows:

$$E_{n\ell} = hcR\frac{Z^2}{n_\ell^{*2}} \qquad \ldots(3.2)$$

where R is the Rydberg constant of the ion of interest and n_ℓ^* is the effective quantum number of state $n\ell$. The Rydberg constant is calculated with eq.(2.4), using the mass of the most abundant isotope of the ion because the observed spectrum will be that of the most abundant isotope. We thus use the following isotopes in our calculations: $^{12}_{6}$C IV, $^{14}_{7}$N V, and $^{16}_{8}$O VI (abundances: 98.9%, 99.6%, and 99.8% respectively). Using (Taylor et al., 1969)

$$R_\infty = 109,737.312 \pm 0.011 \ cm^{-1}, \qquad \ldots(3.3)$$

we obtain the following Rydberg constants:

$$R_{C\,IV} = 109,732.295 \pm 0.011 \ cm^{-1};$$

$$R_{N\,V} = 109,733.012 \pm 0.011 \ cm^{-1};$$

$$R_{O\,VI} = 109,733.548 \pm 0.011 \ cm^{-1}. \qquad \ldots(3.4)$$

From the Rydberg constants and the values of E_{nl} given by Moore (1949), the effective quantum numbers can be calculated from eq.(3.2). The values for the known levels of C IV, N V, and O VI are given in Tables 3.2, 3.3, and 3.4. In general, the effective quantum numbers are non-integral and lower than the corresponding hydrogenic values. The difference between the hydrogenic integral value and the effective non-integral value of the quantum number is called the quantum defect μ_{nl}:

$$n_l^* = n - \mu_{nl}. \qquad \ldots(3.5)$$

For the ions C IV, N V, and O VI, we have the approximate values

$$\mu_{ns} \sim 0.10 - 0.15$$

$$\mu_{np} \sim 0.03 - 0.04$$

$$\mu_{nd} \sim 0.002 - 0.003$$

$$|\mu_{nf}| < 0.0005. \qquad \ldots(3.6)$$

As can be seen from Tables (3.2), (3.3), and (3.4), Fig.(3.1), and eq.(3.6), the quantum defects are larger at low values of l, n, or Z. As l increases, μ_{nl} tends to zero; as n increases, μ_{nl} tends to a constant value; as Z increases, μ_{nl} tends to zero since the core then becomes point-like.

Table 3.2 - Known effective quantum numbers of the levels of the ion C IV.

	Orbital angular momentum quantum number, ℓ					
n	s	p	d	f	g	h
2	1.8371783	1.9630202	-	-	-	-
3	2.8422841	2.9620656	2.9983746	-	-	-
4	3.843812	3.961775	3.998013	3.999776	-	-
5	4.844427	4.96163	4.99777	4.99961	4.99997	-
6	5.84375	5.96072	5.99757	5.99970	5.99997	6.00000
7	6.84073	6.95973	6.99631	6.99970	6.99998	7.00001
8		7.96067		7.99975	8.00004	8.00004

Table 3.3 - Known effective quantum numbers of the levels of the ion N V.

	Orbital angular momentum quantum number, ℓ					
n	s	p	d	f	g	h
2	1.8640328	1.9671952	-	-	-	-
3	2.868511	2.9666473	2.998514	-	-	-
4	3.869731	3.966310	3.998018		-	-
5	4.870395	4.966108	4.998295			-
6	5.87112	5.96622	5.99841	5.99990	6.00018	6.00022
7	6.87143	6.96564	6.99808	7.00002	7.00033	7.00033
8	7.87172	7.96685	7.99819	8.00015	8.00052	8.00052

Table 3.4 - Known effective quantum numbers of the levels of the ion O VI.

	Orbital angular momentum quantum number, ℓ					
n	s	p	d	f	g	h
2	1.8831220	1.9706202	-	-	-	-
3	2.8870231	2.9702136	2.9986036	-	-	-
4	3.888198	3.9701819	3.9983314	3.9998726	-	-
5	4.888460	4.970159	4.997989			-
6	5.88873	5.96918	5.99760	5.99997	6.00024	6.00027
7	6.88983	6.96771	6.99762	7.00013	7.00044	7.00044
8	7.89011	7.96457	8.0014	8.00036	8.00069	8.00069

The non-integral values of the effective quantum numbers are due to departures of the effective potential acting on the valence electron from a Coulomb potential. The finite size of the core also accounts for the smaller-than-hydrogenic values of the effective quantum numbers. As the valence electron approaches or penetrates the core, it is acted upon by an effective core charge which is larger than Z. Since we elect to keep Z constant, the larger effective core charge becomes, in the context of eq.(3.2), an effective quantum number which is smaller than the actual integral value of the quantum number of the state considered.

It is also possible to explain the variation of $\mu_{n\ell}$ with ℓ, n, or Z by using similar arguments. Valence electrons with low values of ℓ ($\ell = 0, 1$) actually penetrate the core. These states thus have large quantum defects. However, as ℓ increases, the electron does not penetrate the core since, in the classical model of Bohr, its orbit becomes more circular. (In quantum mechanics, the probability of finding the electron within or close to the core becomes very small.) Thus $\mu_{n\ell}$ approaches zero. Similarly, as n increases, the electron's distance from the core increases and $\mu_{n\ell}$ consequently becomes smaller. However, since the extent of the penetration of the electron within the core depends on ℓ, penetration can still occur and $\mu_{n\ell}$ does not approach zero. As Z increases, the core becomes smaller and $\mu_{n\ell}$ decreases. For $Z \rightarrow \infty$, the core becomes point-like and $\mu_{n\ell}$ approaches zero. It should also be noted that even though $\mu_{n\ell}$ tends to a constant value as n increases, $\mu_{n\ell}/n$ tends to zero and the states thus become more hydrogenic as n increases.

4. ENERGY LEVEL SCHEME

In view of these considerations, the simplified energy level scheme depicted in Fig.3.2 is used in this work. For $n \leq 6$, levels with different ℓ values are considered separately. For higher values of n, the data on the required cross-sections are very scarce and the splitting of the energy levels with respect to the ℓ values becomes very small. Consequently, the following simplified scheme is adopted. For $n = 7$, 8, and 9, s states are kept separate, but other ℓ-value states are lumped together into hydrogenic states which we denote by $n\langle \ell \geq 1 \rangle$. For $n \geq 10$, the ℓ-value splitting is neglected altogether and all angular momentum states are combined into hydrogenic levels.

The labelling of the various states, as used in this work, is indicated on the right hand side of the levels in Fig.3.2. The effective quantum numbers are given in Tab.3.5. The hydrogenic states obtained by combining the different ℓ-value states have been assigned integral quantum numbers. The superscripted values of n_ℓ^* have been obtained from various methods of interpolation or extrapolation; a detailed description of these is given in Section 9 of this Chapter. All other effective quantum numbers have been obtained from the tables of term values given by Moore (1949).

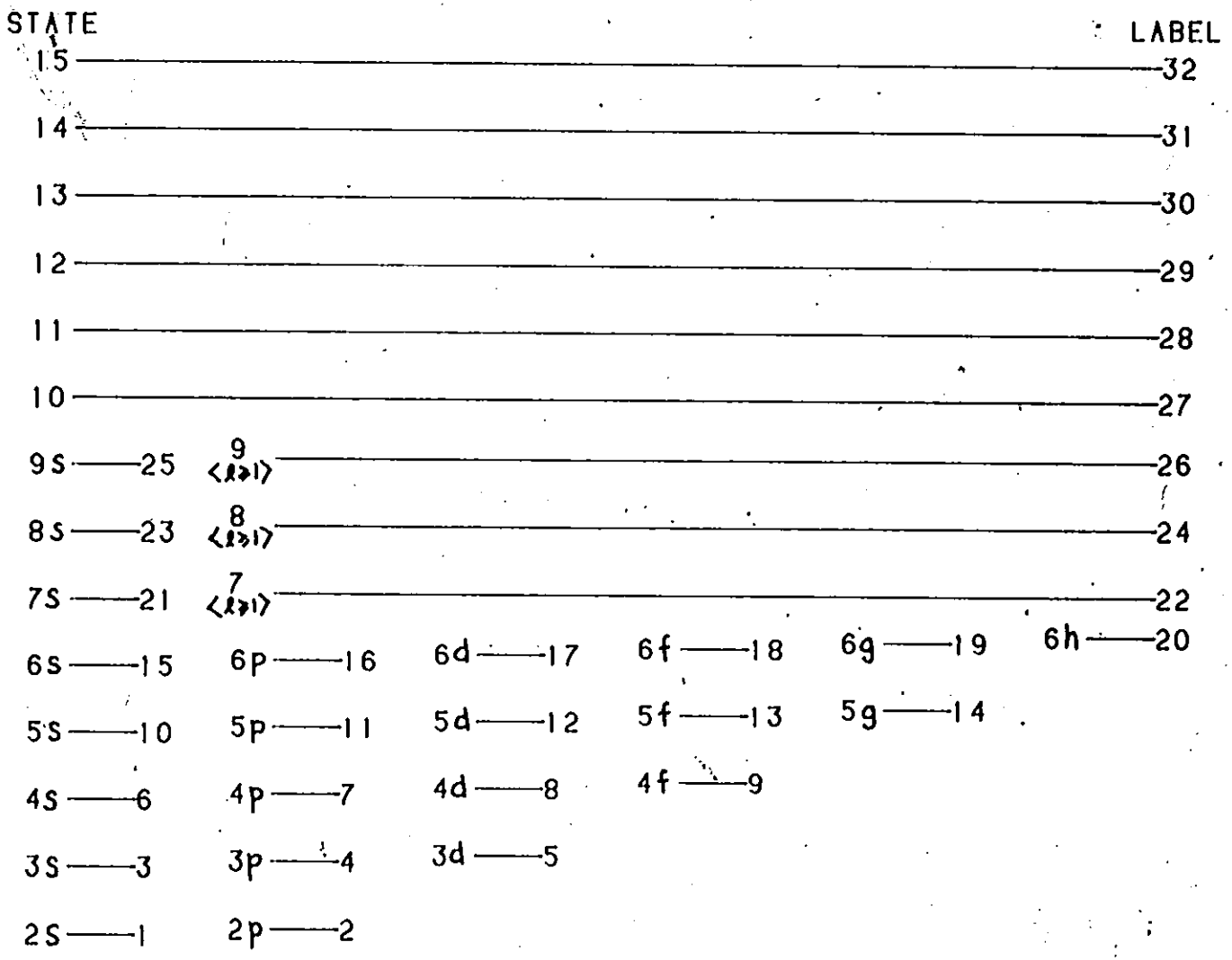

FIGURE 3.2 - LEVEL SCHEME USED IN THIS WORK (NOT TO SCALE).

Table 3.5 - Effective quantum numbers of the ions C IV, N V, and O VI used in this work.

State	C IV	N V	O VI
2s	1.837178	1.864033	1.883122
2p	1.963020	1.967195	1.970620
3s	2.842284	2.868511	2.887023
3p	2.962066	2.966647	2.970214
3d	2.998375	2.998514	2.998604
4s	3.843812	3.869731	3.888198
4p	3.961775	3.966310	3.970182
4d	3.998013	3.998018	3.998331
4f	3.999776	3.99980[b]	3.999873
5s	4.844427	4.87039	4.88846
5p	4.96163	4.96611	4.97016
5d	4.99777	4.99829	4.99799
5f	4.99961	4.99982[b]	4.99990[b]
5g	4.99997	5.00020[c]	5.00028[c]
6s	5.84375	5.87112	5.88873
6p	5.96072	5.96622	5.96918
6d	5.99757	5.99841	5.99760
6f	5.99970	5.99990	5.99997
6g	5.99997	6.00018[c]	6.00024[c]
6h	6.00000	6.00022[c]	6.00027[c]
7s	6.84073	6.87143	6.88983
$7<\ell\geq l>$	7	7	7
8s	7.8438[a]	7.87172	7.89011
$8<\ell\geq l>$	8	8	8
9s	8.8437[a]	8.8718[a]	8.8900[a]
$9<\ell\geq l>$	9	9	9
10	10	10	10
11	11	11	11
12	12	12	12
13	13	13	13
14	14	14	14
15	15	15	15

a, b, c: as explained in the text

5. THE CR MODEL

The CR model must be modified to account for the difference in structure of lithium-like and hydrogenic ions. To simplify the application of the theory developed in Chapter I, the same system of state labelling is used: the ground state (2s) is labelled 1, the first excited state (2p) is labelled 2, the second excited state (3s) is labelled 3, and so on in order of increasing level energy as indicated in Fig.3.2. The derivation of the equations of the CR plasma model for lithium-like ions then parallels that given in Chapter I for hydrogenic ions.

The time evolution of the population density of level p in an optically thin plasma is given by eq.(1.50):

$$\frac{d\rho_p}{dt} = \sum_{q=1}^{p-1} F_{p\to q}\, n_e\, \rho_q$$

$$- \left\{ \left[\sum_{q=1}^{p-1} F_{p\to q} + S_p + \sum_{q=p+1}^{s} C_{p\to q} \right] n_e + \sum_{q=1}^{p-1} A_{p\to q} \right\} \rho_p$$

$$+ \sum_{q=p+1}^{r} \left\{ C_{p\to q}\, n_e + \frac{Z_q}{Z_p} A_{q\to p} \right\} \rho_q + \frac{1}{Z_p} \left\{ \alpha_p\, n_e + \beta_p \right\}$$

$$+ \sum_{q=r+1}^{s} \left\{ C_{p\to q}\, n_e + \frac{Z_q}{Z_p} A_{q\to p} \right\} \qquad \ldots(3.7)$$

where p and q are state labels; p = 1, 2, 3, ..., r; r is some high-lying state above which the levels are in LTE; s is the last bound state of the ion (s > r); n_e is the free electron density; ρ_p is the population density of level p normalized with the Saha equilibrium value of the population density; $C_{q\to p}$ is the electron impact excitation rate coefficient for the q -> p transition; $F_{p\to q}$ is the electron impact

de-excitation rate coefficient for the p -> q transition; $A_{p\to q}$ is the Einstein probability coefficient for the spontaneous radiative transition p -> q; S_p is the electron impact ionization rate coefficient for level p; α_p is the three-body recombination rate coefficient for level p; β_p is the radiative recombination rate coefficient for level p; and Z_p is proportional to the Saha equilibrium population density of level p and is given by eq.(1.17).

The steady state (SS) solution to the set of coupled first order differential equations (3.7) is obtained as in Chapter I, from

$$\dot{\rho}_p^{ss}(t) = 0 \; ; \quad p = 1, 2, \ldots, r \qquad \ldots(3.8)$$

where the dot over ρ_p denotes differentiation with respect to time. However, the quasi-steady state (QSS) solution must be modified to account for the small energy separation of the ground and the first excited states as compared to that of the first and the second excited states. As can be seen in Fig.3.1, this is particularly significant for ions with large values of Z such as C IV, N V, and O VI. As a result of this, the population density of the first excited state (level 2) is very much larger than that of the other excited states, and it may even be comparable to that of the ground state. Then one of the validity conditions of the CR model, condition (1.74), is not valid.

The QSS solution is modified by using a method similar to the one developed by Bates et al. (1962b) to describe hydrogenic plasmas optically thick toward the lines of the Lyman series. The normalized popu-

lation density of level p is expressed as a function of the ground and the first excited state population densities:

$$\rho_p = r_p^{(0)} + r_p^{(1)} \rho_1 + r_p^{(2)} \rho_2 \qquad \ldots(3.9)$$

where $3 \leq p \leq r$ and $r_p^{(0)}$, $r_p^{(1)}$, and $r_p^{(2)}$ are the population coefficients of level p. The QSS solution is obtained when the population densities of the second and higher excited states are in equilibrium with the population densities of the ground and the first excited states which, in general, are not in equilibrium. We then have

$$\dot{\rho}_1 (t) \neq 0$$

$$\dot{\rho}_2 (t) \neq 0$$

$$\dot{\rho}_{p \geq 3} (t) = 0. \qquad \ldots(3.10)$$

Substituting the solution (3.9) in the system of equations (3.7), and using the last of eq.(3.10), we obtain a set of equations of the form

$$a_p + b_p \rho_1 + c_p \rho_2 = 0 \quad ; \; p = 3, 4, \ldots, r. \qquad \ldots(3.11)$$

For arbitrary values of ρ_1 and ρ_2, the general solution of eq.(3.11) is

$$a_p = 0$$

$$b_p = 0$$

$$c_p = 0. \qquad \ldots(3.12)$$

We must also impose the limiting conditions corresponding to the values of p = 1, 2 and p > r on the population coefficients $r_p^{(0)}$, $r_p^{(1)}$, and $r_p^{(2)}$:

$$r_1^{(0)} = 0$$

$$r_1^{(1)} = 1$$

$$r_1^{(2)} = 0 \; ; \qquad \ldots(3.13)$$

$$r_2^{(0)} = 0$$

$$r_2^{(1)} = 0$$

$$r_2^{(2)} = 1 \; ; \qquad \ldots(3.14)$$

$$r_{p>r}^{(0)} = 1$$

$$r_{p>r}^{(1)} = 0$$

$$r_{p>r}^{(2)} = 0. \qquad \ldots(3.15)$$

Eq.(3.15) has already been applied to derive the system of equations (3.7). Using eqs.(3.12), (3.13), and (3.14), we obtain three sets of r−2 equations which are solved for the population coefficients $r_p^{(0)}$, $r_p^{(1)}$, and $r_p^{(2)}$ respectively:

$$\sum_{q=3}^{p-1} \mathcal{A}_{pq}\, r_q^{(0)} - \mathcal{B}_p\, r_p^{(0)} + \sum_{q=p+1}^{r} \mathcal{C}_{pq}\, r_q^{(0)} = -\frac{1}{Z_p}\{\alpha_p n_e + \beta_p\}$$

$$- \sum_{q=r+1}^{s} \{C_{p\to q}\, n_e + \frac{Z_q}{Z_p} A_{q\to p}\}\ ; \qquad \ldots(3.16)$$

$$\sum_{q=3}^{p-1} \mathcal{A}_{pq}\, r_q^{(1)} - \mathcal{B}_p\, r_p^{(1)} + \sum_{q=p+1}^{r} \mathcal{C}_{pq}\, r_q^{(1)}$$

$$= - F_{p\to 1}\, n_e\ ; \qquad \ldots(3.17)$$

$$\sum_{q=3}^{p-1} \mathcal{A}_{pq}\, r_q^{(2)} - \mathcal{B}_p\, r_p^{(2)} + \sum_{q=p+1}^{r} \mathcal{C}_{pq}\, r_q^{(2)}$$

$$= - F_{p\to 2}\, n_e \qquad \ldots(3.18)$$

where

$$\mathcal{A}_{pq} = F_{p\to q}\, n_e\ ; \qquad \ldots(3.19)$$

$$\mathcal{B}_p = \Big[\sum_{q=1}^{p-1} F_{p\to q} + S_p + \sum_{q=p+1}^{s} C_{p\to q}\Big] n_e$$

$$+ \sum_{q=1}^{p-1} A_{p\to q}\ ; \qquad \ldots(3.20)$$

$$\mathcal{C}_{pq} = C_{p\to q}\, n_e + \frac{Z_q}{Z_p} A_{q\to p}\ ;\ p = 3, 4, \ldots, r. \qquad \ldots(3.21)$$

From the population coefficients $r_p^{(0)}$, $r_p^{(1)}$, and $r_p^{(2)}$, the population densities n_p can be calculated for any value of n_1 and n_2 from

$$n_p = Z_p\, n_i\, n_e\, r_p^{(0)} + \frac{Z_p}{Z_1}\, n_1\, r_p^{(1)} + \frac{Z_p}{Z_2}\, n_2\, r_p^{(2)} \quad ; \quad p = 3, 4, \ldots, r \qquad \ldots(3.22)$$

where n_i is the ionic density. The time evolution of the population densities of the ground state and the first excited state, n_1 and n_2 respectively, can be obtained by substituting eq.(3.9) and the population coefficients $r_p^{(0)}$, $r_p^{(1)}$, and $r_p^{(2)}$ into eq.(3.7) with p = 1 and p = 2. We then get the two coupled first order differential equations

$$\dot{n}_1 = -S_1^{CR}\, n_e\, n_1 + M_{21}^{CR}\, n_e\, n_2 + \alpha_1^{CR}\, n_e\, n_i$$

$$\dot{n}_2 = -S_2^{CR}\, n_e\, n_2 + M_{12}^{CR}\, n_e\, n_1 + \alpha_2^{CR}\, n_e\, n_i \qquad \ldots(3.23)$$

where

$$S_1^{CR} = S_1 + \sum_{q=2}^{s} C_{1\to q} - \frac{1}{n_e Z_1} \sum_{q=3}^{s} \left[F_{q\to 1}\, n_e + A_{q\to 1} \right] Z_q\, r_q^{(1)} \; ; \qquad \ldots(3.24)$$

$$S_2^{CR} = S_2 + F_{2\to 1} + \frac{1}{n_e} A_{2\to 1} + \sum_{q=3}^{s} C_{2\to q} - \frac{1}{n_e Z_2} \sum_{q=3}^{s} \left[F_{q\to 2}\, n_e + A_{q\to 2} \right] Z_q\, r_q^{(2)} \; ; \qquad \ldots(3.25)$$

$$\alpha_1^{CR} = \alpha_1 n_e + \beta_1$$

$$+ \sum_{q=3}^{S} \left[F_{q\to 1}\, n_e + A_{q\to 1} \right] Z_q\, r_q^{(0)}; \qquad \ldots(3.26)$$

$$\alpha_2^{CR} = \alpha_2 n_e + \beta_2$$

$$+ \sum_{q=3}^{S} \left[F_{q\to 2}\, n_e + A_{q\to 2} \right] Z_q\, r_q^{(0)}; \qquad \ldots(3.27)$$

$$\tilde{M}_{21}^{CR} = F_{2\to 1} + \frac{1}{n_e} A_{2\to 1}$$

$$+ \frac{1}{n_e Z_2} \sum_{q=3}^{S} \left[F_{q\to 1}\, n_e + A_{q\to 1} \right] Z_q\, r_q^{(2)}; \qquad \ldots(3.28)$$

$$M_{12}^{CR} = C_{1\to 2}$$

$$+ \frac{1}{n_e Z_1} \sum_{q=3}^{S} \left[F_{q\to 2}\, n_e + A_{q\to 2} \right] Z_q\, r_q^{(1)}. \qquad \ldots(3.29)$$

The coefficients S_1^{CR}, S_2^{CR} and α_1^{CR}, α_2^{CR} are similar to the hydrogenic collisional-radiative ionization rate coefficient S_{CR} (eq.1.67) and recombination rate coefficient α_{CR} (eq.1.68) respectively. The coefficients M_{21}^{CR} and M_{12}^{CR} have no hydrogenic counterparts. The collisional-radiative rate coefficient M_{21}^{CR} expresses the recombination which occurs in the ground state due to the neighbouring first excited state and vice versa for the collisional-radiative rate coefficient M_{12}^{CR}.

The general solution of the coupled system of equations (3.23) can be written as

$$n_j(t) = n_j^{ss} + n_j^{(+)} e^{-\lambda^{(+)}t} - n_j^{(-)} e^{-\lambda^{(-)}t} \qquad \ldots(3.30)$$

where j = 1 or 2,

$$\lambda^{(\pm)} = \frac{n_e}{2}\Big[S_1^{CR} + S_2^{CR} \pm \sqrt{(S_1^{CR} - S_2^{CR})^2 + 4 M_{12}^{CR} M_{21}^{CR}}\ \Big], \qquad \ldots(3.31)$$

$$n_j^{ss} = \frac{K_j^{ss}}{\lambda^{(+)}\lambda^{(-)}}, \qquad \ldots(3.32)$$

$$n_j^{(\pm)} = \frac{n_j(t=0)\,\lambda^{(\pm)2} - K_j \lambda^{(\pm)} + K_j^{ss}}{\lambda^{(\pm)}\left(\lambda^{(+)} - \lambda^{(-)}\right)}, \qquad \ldots(3.33)$$

$$K_1^{ss} = n_e^2 n_i \left[\alpha_1^{CR} S_2^{CR} + \alpha_2^{CR} M_{21}^{CR} \right], \qquad \ldots(3.34)$$

$$K_2^{ss} = n_e^2 n_i \left[\alpha_2^{CR} S_1^{CR} + \alpha_1^{CR} M_{12}^{CR} \right], \qquad \ldots(3.35)$$

$$K_1 = n_e \Big[\alpha_1^{CR} n_i + S_2^{CR} n_1(t=0) + M_{21}^{CR} n_2(t=0) \Big], \qquad \ldots(3.36)$$

$$K_2 = n_e \Big[\alpha_2^{CR} n_i + S_1^{CR} n_2(t=0) + M_{12}^{CR} n_1(t=0) \Big]. \qquad \ldots(3.37)$$

The steady state population densities, which are obtained in the limit as $t \to \infty$, are explicitly given by

$$n_1^{ss} = \frac{\alpha_1^{CR} S_2^{CR} + \alpha_2^{CR} M_{21}^{CR}}{S_1^{CR} S_2^{CR} - M_{12}^{CR} M_{21}^{CR}} n_i \qquad \ldots(3.38)$$

$$n_2^{ss} = \frac{S_1^{CR} \alpha_2^{CR} + \alpha_1^{CR} M_{12}^{CR}}{S_1^{CR} S_2^{CR} - M_{12}^{CR} M_{21}^{CR}} n_i . \qquad \ldots(3.39)$$

The validity of the QSS solution is discussed extensively in Section 4.1.h of Chapter I. The conditions derived therein need little modification for lithium-like ions. They will hold provided all terms involving state 1 are replaced by terms involving states 1 and 2; in addition, any discussion of the excited states should not include the first excited state.

6. ADIABATIC COOLING OF THE PLASMA

The adiabatic expansion and subsequent cooling of a lithium-like plasma is described by eqs.(1.99) to (1.104) as derived for hydrogenic ions in Section 5.3 of Chapter I. Due to the similarity of lithium-like and hydrogenic ions, the value of γ (the ~~ratio~~ of the specific heats at constant pressure and volume, eq.1.100) is taken to be

$$\gamma = 5/3 \qquad \ldots(3.40)$$

although, as noted earlier in Section 5.3 of Chapter I, the actual value for a plasma is lower than 5/3. The following parameters are also assigned the same value as in Chapter I: the cooling factor $f_c = 5$; then the expansion factor $f_E = 11.2$; the initial density of element A (C, N, or Ø) before expansion is

$$n_A^\circ \cong 10^{14}\,cm^{-3} \qquad \ldots(3.41)$$

7. MODEL CALCULATIONS

The model calculations describing the adiabatic cooling of a lithium-like plasma must be modified to account for the relatively large population density of the first excited state. Since the population densities of the excited states n_p, $p = 3, 4, \ldots, r$ depend on the population densities of the ground and the first excited states, both n_1 and n_2 must be specified to calculate these. Using the model of House (1964) as done previously for hydrogenic ions in Section 5.4 of Chapter I only yields the sum of n_1 and n_2, not their individual values. To correct for this situation, the model calculations must be carried out as follows.

We assume that the plasma is monatomic, unmagnetized, stationary (except for the expansion), and spatially homogeneous. Initially, it is characterized by a density n_A° given by eq.(3.41), a free electron density n_e°, and a temperature T_e°. We calculate the ionization equilibrium of the plasma with the model of House (1964) and hence obtain n_i°. Assuming that the plasma parameters have been constant for a sufficiently long time, steady state conditions will prevail and the population densities of the levels p will be given by the steady state solution of the system of equations (3.7) obtained from eq.(3.8):

$$n_p^\circ = n_p^{\circ\,ss}(n_e^\circ, T_e^\circ) \qquad \ldots(3.42)$$

At t = ∅, the plasma is "instantaneously" cooled under adiabatic expansion conditions by a factor $f_c = 5$. The validity of this assumption is discussed in Section 5.4 of Chapter I. Immediately after the cooling, the plasma parameters are given by

$$n_e^c = n_e^\circ / f_c$$

$$T_e^c = T_e^\circ / f_c$$

$$n_i^c = n_i^\circ / f_c$$

$$n_p^c = n_p^\circ / f_c . \qquad \ldots(3.43)$$

The plasma then evolves toward the quasi-steady state described by the CR model. This transient state of the plasma is not studied in this work due to its complexity. Once QSS conditions have been established in the plasma, the plasma parameters n_e, T_e, n_i, and n_p are obtained as follows: It is assumed that n_e^c, T_e^c, n_i^c, n_1^c, and n_2^c do not change significantly during the transient stage of the plasma. The validity of this assumption is discussed in Section 4.1.h of Chapter I. Then

$$n_e = n_e^c$$

$$T_e = T_e^c$$

$$n_i = n_i^c$$

$$n_1 = n_1^c$$

$$n_2 = n_2^c . \qquad \ldots(3.44)$$

From these parameters, the population densities of the excited states n_p, p = 3, 4, ..., r can be obtained from the QSS solution of the CR model given by eqs.(3.7) and (3.10) as outlined in Section 5 of this Chapter. The analysis of the inversely populated transitions follows that given in Section 5.5 of Chapter I.

8. THE RATE COEFFICIENTS

8.1. Available data

The rate coefficients used in eq.(3.7) are evaluated from the data available in the literature. However, experimental data are scarce and we must thus rely almost exclusively on theoretical calculations. Quantum mechanical calculations have been carried out on most cross-sections involving the lower states 2s, 2p, 3s, 3p, and 3d, and they should thus provide reliable estimates of the rate coefficients. However, since the degree of sophistication of the quantum mechanical effects included in the calculations varies substantially, the accuracy of the rate coefficients is not uniform. For higher states ($n \geq 4$), very little work has been done and the amount of data that is available depends on the particular physical process considered. The availability of experimental and theoretical data is discussed more extensively for each individual process in the following Chapters.

8.2. General calculations

A very large number of rate coefficients are required in this work and most of them involve states with $n \geq 4$. Due to the lack of available data on these states, it is necessary to use data obtained from less reliable methods of calculation or from relatively simple general formulas when available. However, only those formulas which yield reasonable estimates of the rate coefficients are used in this work.

Radiative processes are easier to deal with than collisional processes. Consequently, general formulas are available for the calculation of optical cross-sections and they provide reliable estimates of these due to the relatively simple structure of lithium-like ions. On the other hand, few general formulas have been developed to calculate the collisional cross-sections. Most of the proposed formulas give unreliable results and they are thus not used. Various methods have been devised in this work to calculate the collisional cross-sections and they are considered in detail in the following Chapters. At large values of n ($n \geq 10$), the rate coefficients should tend to the corresponding hydrogenic values. This provides a mean of estimating the reliability of the methods used.

9. EXTRAPOLATION OF THE QUANTUM DEFECTS

9.1. The Quantum Defect Theory (QDT)

We use the Quantum Defect Theory for two purposes: to calculate the energy levels of high-lying levels and to obtain photoionization cross-sections. Both of these require knowledge of the quantum defect: at

low negative values of the electron's energy for the former, and at positive values of the electron's energy for the latter. The QDT developed by Seaton (1955, 1958a, 1966a, 1966b) provides the best method for extrapolating the known quantum defects to the continuum states of the valence electron. The method should thus also provide reasonable estimates of the quantum defects of high-lying levels since these are situated between the continuum states and the low-lying levels of the valence electron for which experimental values of the quantum defects are available.

According to the Quantum Defect Theory, the effective quantum numbers n^* satisfy the relation

$$Tan(\pi n^*) + R(\epsilon_n) = 0 \qquad \ldots(3.45)$$

where the function $R(\epsilon_n)$ is such that, for bound states,

$$R(\epsilon_n) = A_\ell(\epsilon_n)\, Y(\epsilon_n), \qquad \ldots(3.46)$$

$$A_\ell(\epsilon_n) = 1\,(1 + 1^2\epsilon_n)(1 + 2^2\epsilon_n)\cdots(1 + \ell^2\epsilon_n), \qquad \ldots(3.47)$$

$$\epsilon_n = -1/n^{*2}, \qquad \ldots(3.48)$$

ℓ is the orbital angular momentum quantum number, and $Y(\epsilon_n)$ can be represented by an expansion of the form

$$Y(\epsilon_n) = \frac{\sum_{m=0}^{\infty} \alpha_m \epsilon_n^m}{\sum_{m=0}^{\infty} \beta_m \epsilon_n^m} \qquad \ldots(3.49)$$

where α_m and β_m are fit parameters. It is possible to introduce a function $\mu(\epsilon)$ such that

$$R(\epsilon) = \tan \pi\mu(\epsilon). \qquad \ldots(3.50)$$

$\mu(\epsilon)$ is the quantum defect function; for bound states, we write

$$\mu_n = \mu(\epsilon_n). \qquad \ldots(3.51)$$

The solution of eq.(3.45) can then be written as

$$n^* = n - \mu_n. \qquad \ldots(3.52)$$

For continuum states, ϵ becomes

$$\epsilon = E / Z^2 \qquad \ldots(3.53)$$

where E is the kinetic energy of the free electron. For small values of ϵ, $\mu(\epsilon)$ is related to the phase $\delta(\epsilon)$ of the continuum wave function by

$$\delta(\epsilon) = \pi\mu(\epsilon). \qquad \ldots(3.54)$$

The parameters α_m and β_m, used in eq.(3.49), are determined by fitting them to the available term values. For a given value of ℓ, Seaton (1966b) recommends that we use the following expansion of $Y(\epsilon)$:

$$Y_\ell(\epsilon) = \sum_{i=0}^{p} \alpha_i \epsilon^i \Big/ \left[1 + \sum_{m=1}^{q} \beta_m \epsilon^m\right] \qquad \ldots(3.55)$$

where $q = p + \ell + 1$. $\qquad \ldots(3.56)$

This insures that $Y_\ell(\epsilon)$ remains bounded as $\epsilon \to \infty$ and that it has the asymptotic behavior

$$Y_\ell(\epsilon) \sim \epsilon^{-\ell-1} \qquad \ldots(3.57)$$

required by Seaton (1966b). The known values of ϵ_n are fitted by a least squares method to the expression

$$\tan[\pi \mu_\ell(\epsilon)] = A_\ell(\epsilon)\, Y_\ell(\epsilon) \qquad \ldots(3.58)$$

and the fit parameters α_i and β_m are obtained from the minimization conditions derived in Appendix D.

The extrapolated values of $\mu_\ell(\epsilon)$ are calculated from eq.(3.58) with eqs.(3.55) and (3.47). For bound states, $\mu_{n\ell}$ is obtained by an iterative method: a first approximation $\mu_{n\ell}^{(0)} = 0$ is substituted in the R.H.S. of eq.(3.58) by using eq.(3.48) and a better approximation $\mu_{n\ell}^{(1)}$ is obtained from the L.H.S. of eq.(3.58). The procedure is repeated until sufficient accuracy is obtained. This method is used to obtain the quantum defects of the 8s and 9s states of C IV and the 9s states of N V and O VI. These values are given with superscript "a" in Tab.3.5. For C IV and N V, they are found to be in satisfactory agreement with

those calculated from the extrapolated term values given by Moore (1970, 1971). For continuous states, the calculation of $\mu_\ell(\epsilon)$ as a function of ϵ is obtained from eq.(3.58) in a straightforward manner. $\mu_\ell(\epsilon)$ is used in the calculation of the photoionization cross-sections (see Chapter VIII).

The accuracy of the extrapolated values of $\mu_\ell(\epsilon)$ is restricted by the number of term values that are available to calculate the parameters α_i and β_m. As ℓ increases, more term values are required to obtain a uniform accuracy due to eq.(3.56). Since only five to seven term values are available for each value of ℓ, this extrapolation procedure can only be used for s and p states. The resulting fit parameters are given in Tab.3.6. Using this method for d states produces unreliable results. However, $\mu_d(\epsilon)$ shows little variation for bound states: $0.002 \leq \mu_d(\epsilon) \leq 0.004$. The value $\mu_d \simeq 0.003$ is thus a reasonable approximation for all continuum d states.

The fit parameters of Tab.3.6 reproduce most of the known s-state quantum defects to at least 3-4S. The extrapolated quantum defects of the bound s states can thus be expected to be of comparable accuracy. For p states, the number of parameters equals the number of known term values. This method of estimating the accuracy of the extrapolations thus fails. However, an accuracy of 3-4S can also be expected for the extrapolated quantum defects of the bound p states. As is evident from Tab.3.7, the extrapolated quantum defects of the continuum s and p states show little variation. An accuracy of at least 2-3S can be expected for these extrapolations. In all cases and for all values of ℓ, an error of

$$\Delta\mu_\ell(\epsilon) \leq \pm 0.01 \qquad \ldots(3.59)$$

can be taken as a reasonable estimate of the maximum uncertainty in the extrapolated quantum defects of the continuum states.

9.2. Graphical interpolation

The effective quantum numbers of Tab.3.5 with the superscript "b" have been interpolated graphically from Fig.3.3. Graphical interpolation is used because not enough data is available to use the Quantum Defect Theory. As can be seen in Fig.3.3, an error estimate of

$$\Delta\mu_\ell \simeq \pm 0.00005 \qquad \ldots(3.60)$$

on the interpolated quantum defects is reasonable.

9.3. Approximate methods

In Tab.3.5, the effective quantum numbers of g and h states with a superscript "c" have been obtained from approximate methods due to the lack of data. The interpolation is performed by considering the f, g, and h sublevels of the n = 5 and 6 levels of the ions C IV, N V, and O VI. For C IV, all the term values of the states are known (Moore, 1949). For N V and O VI, Moore (1949) gives the term values of the 6f and the combined 6g+6h levels; the term values of the 5f levels can be obtained by graphical interpolation (see Section 9.2 of this Chapter). We thus have sufficient data to interpolate these states by

applying the relative spacing of the levels observed for C IV to N V and O VI.

In addition, we also separate the 6g and 6h levels and obtain their term values from the term value of the combined 6g+6h level given by Moore (1949). Even though the energy splitting of the 6g and 6h levels is very small, this is done to have as complete a description of the $n \leq 6$ states as possible. The average energy eigenvalue E_n of a combination of levels $n\ell$ is calculated from the individual energy eigenvalues $E_{n\ell}$ according to

$$\omega_n E_n = \sum_{\ell} \omega_{n\ell} E_{n\ell} \qquad \ldots(3.61)$$

where ω_n and $\omega_{n\ell}$ are the statistical weights of levels n and $n\ell$ respectively. For the combined 6g+6h level, we thus have

$$E_{6g+6h} = \frac{9}{20} E_{6g} + \frac{11}{20} E_{6h}. \qquad \ldots(3.62)$$

Since the energy separation of levels 6g and 6h, $\Delta E_{6g,6h}$, is very small compared to E_{6g} and E_{6h} (for example, $\Delta E^{C\,\text{IV}}_{6g,6h} = 0.5\ cm^{-1}$ while $E^{C\,\text{IV}}_{6g+6h} = 48{,}770.1\ cm^{-1}$), we can put

$$E_{6g} \simeq E_{6g+6h} - \frac{1}{2} \Delta E_{6g,6h}$$

$$E_{6h} \simeq E_{6g+6h} + \frac{1}{2} \Delta E_{6g,6h} \qquad \ldots(3.63)$$

Table 3.6 - Fit parameters used in eq.(3.55) for the s and p states of the ions C IV, N V, and O VI.

State	Parameter		C IV	N V	O VI
s	α	α_0	5.354935×10^{-1}	4.246545×10^{-1}	3.598317×10^{-1}
		α_1	3.326334×10^{-10}	1.633376×10^{1}	2.639833×10^{1}
		α_2	-	2.351671×10^{2}	4.848220×10^{2}
	β	β_1	-1.303138×10^{-1}	3.868594×10^{1}	7.350781×10^{1}
		β_2	-2.129844×10^{-2}	5.611321×10^{2}	1.360768×10^{3}
		β_3	-	1.235595×10^{2}	2.971403×10^{2}
p	α	α_0	1.227365×10^{-1}	1.074347×10^{-1}	7.773314×10^{-2}
		α_1	9.836635	9.988464	1.055687×10^{1}
		α_2	2.026329×10^{2}	2.180029×10^{2}	2.030797×10^{2}
	β	β_1	8.124956×10^{1}	9.358949×10^{1}	1.224259×10^{2}
		β_2	1.726849×10^{3}	2.093684×10^{3}	2.439660×10^{3}
		β_3	1.385593×10^{3}	1.477086×10^{3}	3.337748×10^{3}
		β_4	-1.817164×10^{2}	-1.007446×10^{3}	2.861421×10^{3}

Table 3.7 - Values of $\mu(\varepsilon)$ for the s and p continuum of the ions C IV, N V, and O VI.

	ℓ	ε	C IV	N V	O VI
$\mu(\varepsilon)$	s	0.	0.16	0.13	0.110
		1.	0.18	0.11	0.091
	p	0.	0.039	0.034	0.025
		1.	0.045	0.054	0.016

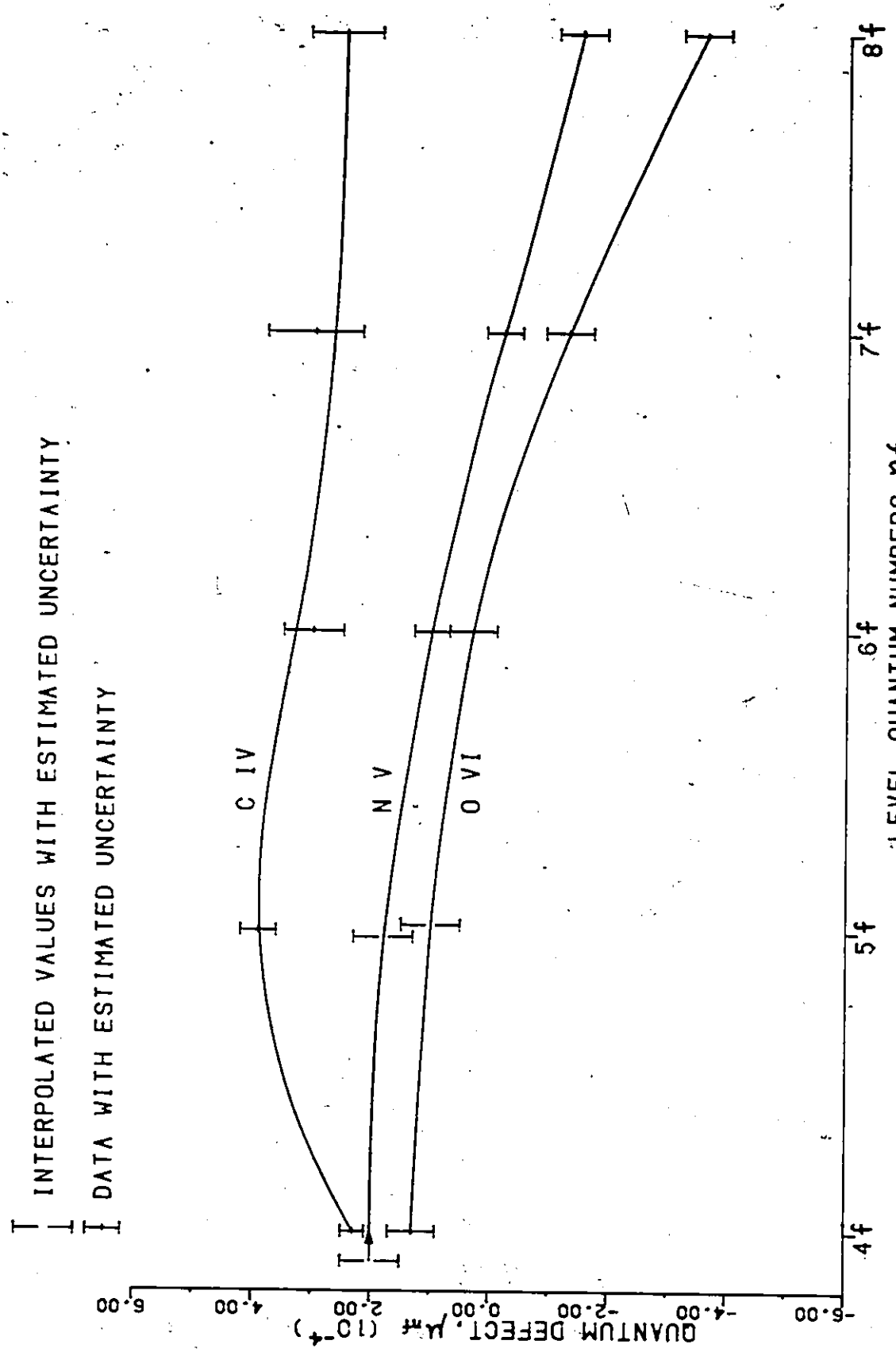

FIGURE 3.3 - INTERPOLATION OF THE f-STATE QUANTUM DEFECTS, μ_{nf}.

We estimate the value of $\Delta E_{6g,6h}$ for N V and O VI by applying the ratio $\Delta E^{C\,IV}_{6g,6h} / E^{C\,IV}_{6g+6h}$ to these ions. We thus obtain

$$\Delta E^{N\,V}_{6g,6h} \simeq 0.8 \ cm^{-1}$$

$$\Delta E^{O\,VI}_{6g,6h} \simeq 1.1 \ cm^{-1} \qquad \ldots(3.64)$$

The effective quantum numbers of the 6g and 6h states of N V and O VI can then be calculated from eqs. (3.64), (3.63), (3.2), and the term values of $E^{N\,V}_{6g+6h}$ and $E^{O\,VI}_{6g+6h}$ given by Moore (1949).

The error on the quantum defects is estimated by comparing the quantum defect of $\Delta\mu_{6g+6h}$ with those of $\Delta\mu_{6g}$ or $\Delta\mu_{6h}$. We find that the error cannot be greater than

$$\Delta\mu_{6g \text{ or } 6h} \simeq \pm 0.00002. \qquad \ldots(3.65)$$

The smallness of this value is due to the small energy separation of levels 6g and 6h. The error on the quantum defects of the 5g levels of N V and O VI calculated by keeping the relative splitting of the C IV, N V, and O VI f, g, and h levels constant is obtained from the uncertainty of the 5f quantum defect:

$$\Delta\mu_{5g} \simeq \pm 0.00005. \qquad \ldots(3.66)$$

The uncertainties also depend on whether the methods used in this Section are appropriate: Comparison of the quantum defects of the f, g,

and h levels of C IV, N V, and O VI with one another and in particular of μ_{sg} and μ_{cg} indicates that the interpolations are reasonable.

Chapter IV

C IV, N V, AND O VI: OSCILLATOR STRENGTHS

1. INTRODUCTION

Most of the data available on oscillator strengths have been obtained from theoretical calculations. A considerable amount of work has been done on the subject and complete bibliographies are available; some of the more recent ones have been published by Glennon and Wiese (1966), Miles and Wiese (1970), and Fuhr and Wiese (1971, 1973). Thus, although a great number of oscillator strengths is needed in our work, we should be able to obtain a reasonably accurate set of f-values.

2. AVAILABLE DATA

The large volume of f-value data available on lithium-like ions has been critically evaluated by Martin and Wiese (1976a). From this, they have compiled tables of oscillator strengths for the 2s -> np, 2p -> ns, nd, 3s -> np, 3p -> ns, nd, 4s -> np, and 4p -> ns, nd ($n \leq 7$) spectral series of the lithium isoelectronic sequence (Martin and Wiese, 1976b).

Several types of systematic trends and fundamental spectroscopic constraints have been applied to the data:

a. Regularities for individual transitions along an isoelectronic sequence. From perturbation theory, the oscillator strength can be

expanded in powers of the inverse nuclear charge Z_N to give (Weiss, 1963; Crossley, 1969)

$$f_{n'\to n} = f^{(0)}_{n'\to n} + f^{(1)}_{n'\to n} Z_N^{-1} + f^{(2)}_{n'\to n} Z_N^{-2} + \cdots . \qquad \ldots(4.1)$$

For lithium-like ions, $f^{(0)}_{n'\to n}$ is simply the known hydrogen f-value; $f^{(1)}_{n'\to n}$ and $f^{(2)}_{n'\to n}$ are parameters that can be found from the data.

b. Regularities for the transitions of a spectral series. For the case of the hydrogen atom, the oscillator strength behaves as

$$f_{n'\ell'\to n\ell'\pm 1} \sim c n^{-3} \qquad \ldots(4.2)$$

along a spectral series. This behavior sets in for fairly small principal quantum numbers, usually before n reaches 10. Since the energy of the highly excited states of the lithium-like ions rapidly approaches the hydrogenic value, the oscillator strengths of the higher members of the lithium-like spectral series can be expected to follow eq.(4.2) for large n, provided n is replaced by the effective quantum number n^* of the state.

c. Requirement of continuity at the ionization limit. The absorption oscillator strength for the n' -> n transition (n' < n) can be written as

$$f_{n'\to n} = \frac{2}{3} \frac{E_{n'n}}{\omega_{n'}} S_{n'\to n} \qquad \ldots(4.3)$$

where $E_{n'n}$ is the energy separation of levels n' and n, $\omega_{n'}$ is the statistical weight of level n', and $S_{n' \to n}$ is the line strength of the n' -> n transition. All quantities are in atomic units. Similarly, for an ionizing transition from a bound state n' to a continuum state of energy E, a differential oscillator strength can be defined as (Burgess and Seaton, 1960)

$$\frac{df_{n'}}{dE} = \frac{2}{3} \frac{I_{n'} + E}{\omega_{n'}} S_{n'}(\epsilon) \qquad \ldots(4.4)$$

where $I_{n'}$ is the ionization potential of state n' and E is the kinetic energy of the ejected electron. The continuity of $df_{n'}/dE$ across the ionization limit has been shown to exist for hydrogen (Marr and Creek, 1968). Marr and Creek also conclude that the assumption of continuity across the ionization limit of the principal series of the alkalies is justified within experimental accuracy. The discrete spectrum and the continuum are connected through the relation (Martin and Wiese, 1976a)

$$\left(\frac{df_{n'}}{dE}\right)_{\text{discrete}} = \frac{n^{*3} f_{n' \to n}}{2Z^2} \qquad \ldots(4.5)$$

where Z is the core charge of the ion. It should be noted here that eq.(4.5) is strictly true only when the quantum defect is constant within a spectral series.

d. f sum rules. In this case, the most useful sum rule is the partial sum rule of Wigner (1931) and Kirkwood (1932) which states that, for one-electron systems, the sum over f of a spectral series

$n'\ell' \rightarrow \ell'\pm 1$ (including its continuum and all downward transitions, as well as the virtual transitions into occupied states) is given by

$$\sum f_{n'\ell' \rightarrow \ell'+1} = \frac{1}{3} \frac{(\ell'+1)(2\ell'+3)}{2\ell'+1} \qquad \ldots(4.6)$$

and

$$\sum f_{n'\ell' \rightarrow \ell'-1} = -\frac{1}{3} \frac{\ell'(2\ell'-1)}{2\ell'+1} \,. \qquad \ldots(4.7)$$

The one-electron model is a close approximation to the valence electron of lithium-like ions. The sum rules (4.6) and (4.7) can thus be expected to be accurate to within a few percent for these ions.

The resulting set of oscillator strengths varies smoothly along the lithium isoelectronic sequence and the spectral series. According to Martin and Wiese, this set of data should be regarded as a highly accurate one.

Additional data can be obtained from the tables of Wiese et al. (1966), an earlier critical data compilation. Many of the f-values given in these tables are the same as the ones given by Martin and Wiese (1976b). However, Wiese et al. (1966) also include oscillator strengths for some $5\ell' \rightarrow 6\ell$, $6\ell' \rightarrow 7\ell$, and $7\ell' \rightarrow 8\ell$ transitions. Since these f-values have been calculated with the Coulomb approximation of Bates and Damgaard (1949), Wiese et al. (1966) estimate their accuracy at 10%.

3. GENERAL CALCULATIONS

3.1. Introduction

It is possible, under certain conditions, to carry out general calculations of oscillator strengths and thus obtain any f-value that is needed. The absorption oscillator strength for the $n'\ell' \rightarrow n\ell$ transition is expressed in terms of the line strength:

$$f_{n'\ell' \rightarrow n\ell} = \frac{2}{3} \frac{m}{\hbar^2 e^2} \frac{E_{n'\ell', n\ell}}{2(2\ell'+1)} S_{n'\ell' \rightarrow n\ell} . \qquad \ldots(4.8)$$

$S_{n'\ell' \rightarrow n\ell}$ is in atomic units $(a_o^2 e^2)$.

If LS-coupling is applicable, and if the transition involves no equivalent electrons, then the line strength can be separated as follows (Bates and Damgaard, 1949; Griem, 1964, p.48):

$$S(\text{core}, n'\ell' S L' J' \rightarrow \text{core}, n\ell S L J)$$

$$= \mathcal{S}(\mathcal{M}) \mathcal{S}(\mathcal{L}) \sigma^2_{n'\ell' \rightarrow n\ell} \qquad \ldots(4.9)$$

where $n'\ell'SL'J'$ and $n\ell SLJ$ are the quantum numbers of the valence electron in its initial and final states respectively, $\mathcal{S}(\mathcal{M}) = \mathcal{S}(\ell' SL' \rightarrow \ell SL)$ represents the strength of the multiplet, and $\mathcal{S}(\mathcal{L}) = \mathcal{S}(SL'J' \rightarrow SLJ)$ the relative strength of the spectral line within the multiplet. The numerical values of these factors may be obtained from tables given by Goldberg (1935, 1936), and White and Eliason (1933) or Russell (1936); their explicit form is given in

Griem (1964, p.48). The evaluation of these factors for hydrogen is greatly simplified if the multiplet splitting is neglected. The line strengths are then summed over J and J', and the following expressions are obtained (Condon and Shortley, 1935, p.239):

$$S_{n'\ell \to n\ell-1} = 2(2\ell+1)\,\ell\,(2\ell-1)\,\sigma^2_{n'\ell\to n\ell-1}$$

$$S_{n'\ell \to n\ell+1} = 2(2\ell+1)(\ell+1)(2\ell+3)\,\sigma^2_{n'\ell\to n\ell+1}. \qquad \ldots(4.10)$$

The same expressions are used to calculate the line strengths of transitions in the lithium-like ions, since multiplet splitting is neglected and since these ions are closely hydrogenic.

The transition integral $\sigma_{n'\ell'\to n\ell}$ is related to the radial matrix element $R^{n\ell}_{n'\ell'}$ by

$$\sigma^2_{n'\ell'\to n\ell} = \frac{1}{4\ell_>^2-1}\left[R^{n\ell}_{n'\ell'}\right]^2 \qquad \ldots(4.11)$$

where

$$\ell_> = \max(\ell',\ell), \qquad \ldots(4.12)$$

$$R^{n\ell}_{n'\ell'} = \int_0^\infty \chi_{n'\ell'}(r)\,\chi_{n\ell}(r)\,r\,dr, \qquad \ldots(4.13)$$

and $\sigma^2_{n'\ell'\to n\ell}$ is in atomic units ($a_0^2 e^2$). $R_{n\ell}(r) = \chi_{n\ell}(r)/r$ is the normalized radial wave function of the valence electron in state $n\ell$ expressed in atomic units. Different methods have been used to evaluate

the wave functions of the lithium-like ions that are needed in eq.(4.13) to calculate $\sigma^2_{n'l' \to nl}$. For example, Varsavsky (1963) uses the screening theory of Layzer (1959), Kelly (1964) uses the Slater approximation to the Hartree-Fock method, and Leibowitz (1972) uses the semi-empirical polarization potential method of Caves and Dalgarno (1972). Unfortunately, these methods are of very limited use since each transition must be treated individually and the calculations rapidly become unmanageable as n increases.

3.2. Coulomb approximation

3.2.a. Method of calculation

A relatively simple method of general applicability is the Coulomb approximation (CA) proposed by Bates and Damgaard (1949). It is based on the fact that for most transitions, the main contribution to the integral (4.13) comes from a region in which the deviation of the potential of an atom or ion from its asymptotic Coulomb form is so small that the deviation can altogether be neglected and the potential replaced by its asymptotic Coulomb form. This method gives remarkably accurate results for simple systems such as a single electron outside a closed shell.

In a central field, the function $\chi_{nl}(r)$ used in integral (4.13) satisfies the differential equation

$$\frac{d^2\chi_{nl}}{dr^2} + \left(2V_{nl} - \frac{l(l+1)}{r^2} - E_{nl} \right) \chi_{nl} = 0 \qquad \ldots(4.14)$$

where V_{nl} is the potential of the atom or ion and E_{nl} is the energy of the state nl. The potential V_{nl} is replaced by its asymptotic Coulomb form

$$V_{nl} \simeq \frac{Z}{r} \qquad \ldots(4.15)$$

where Z is the core charge of the ion. Eq.(4.15) is used in eq.(4.14) to give

$$\frac{d^2\chi_{nl}}{dr^2} + \left(-E_{nl} + \frac{2Z}{r} - \frac{l(l+1)}{r^2}\right)\chi_{nl} = 0. \qquad \ldots(4.16)$$

Using the effective quantum number defined by

$$n^* = \frac{Z}{\sqrt{E_{nl}}}, \qquad \ldots(4.17)$$

the solution of eq.(4.16) can be written as

$$\chi_{nl} \propto W_{n^*, l+\frac{1}{2}}\left(\frac{2Zr}{n^*}\right) \qquad \ldots(4.18)$$

where $W_{a,b}(x)$ is the Whittaker function, a particular confluent hypergeometric function. For integral values of n^*, the normalization factor of function (4.18) is given by

$$\sqrt{\frac{Z}{n^{*2}\,\Gamma(n^*+l+1)\,\Gamma(n^*-l)}}\,. \qquad \ldots(4.19)$$

Expression (4.19) provides an excellent approximation to the normalization factor of function (4.18) for large, non-integral values of n^*; however, for lower non-integral values of n^*, a correction factor of order unity given by Seaton (1966b) in his Quantum Defect Theory (see Section 3 of Chapter VIII) should multiply expression (4.19). We will not include this correction factor in our work since we use the CA for transitions with large values of n^*.

The asymptotic behavior of the Whittaker function (4.18) is

$$W_{n^*,\ell+\frac{1}{2}}\left(\frac{2Zr}{n^*}\right) \sim \left(\frac{2Zr}{n^*}\right)^{n^*} e^{-\frac{Zr}{n^*}} \sum_{t=0}^{\infty} \frac{a_t}{r^t}$$

where

$$a_0 = 1$$

$$a_1 = \frac{n^*}{2Z}\left[\ell(\ell+1) - n^*(n^*-1)\right]$$

$$a_t = a_{t-1}\frac{n^*}{2tZ}\left[\ell(\ell+1) - (n^*-t+1)(n^*-t)\right]. \quad \ldots(4.20)$$

Combining eqs.(4.18), (4.19), and (4.20), we can then write

$$\chi_{n\ell}(r) \simeq \sqrt{\frac{Z}{n^{*2}\,\Gamma(n^*+\ell+1)\,\Gamma(n^*-\ell)}}\, e^{-\frac{Zr}{n^*}} \sum_{t=0}^{\infty} b_t \left(\frac{2Zr}{n^*}\right)^{n^*-t}$$

where $b_0 = 1$

$$b_t = \frac{1}{t!}\prod_{j=1}^{t}\left[\ell(\ell+1) - (n^*-j+1)(n^*-j)\right]. \quad \ldots(4.21)$$

Eq.(4.21) is finally rewritten in the form

$$\chi_{n\ell}(r) \simeq \sum_{t=0}^{\infty} C_t(n^*,\ell)\sqrt{z}\,(zr)^{n^*-t}\,e^{-\frac{zr}{n^*}}$$

where

$$C_t(n^*,\ell) = \frac{b_t}{\sqrt{n^{*2}\,\Gamma(n^*+\ell+1)\,\Gamma(n^*-\ell)}}\left(\frac{2}{n^*}\right)^{n^*-t} . \qquad \ldots(4.22)$$

A similar expression for the initial state radial wavefunction is obtained upon replacing n, ℓ, and t by n', ℓ', and s respectively.

The radial matrix element given by eq.(4.13) thus becomes

$$R^{n\ell}_{n'\ell'} \simeq \frac{1}{z}\sum_{s=0}^{\infty}\sum_{t=0}^{\infty} C_s(n'^*,\ell')\,C_t(n^*,\ell)$$
$$\times \int_0^{\infty} (zr)^{n'^*+n^*+1-s-t}\; e^{-zr\left(\frac{n'^*+n^*}{n'^*n^*}\right)}\, d(zr). \qquad \ldots(4.23)$$

This last integral is easily evaluated from the general formula (Spiegel, 1968, p.98)

$$\int_0^{\infty} x^n e^{-ax}\,dx = \frac{\Gamma(n+1)}{a^{n+1}} . \qquad \ldots(4.24)$$

Thus eq.(4.23) becomes

$$R^{n\ell}_{n'\ell'} \simeq \frac{1}{z}\sum_{s=0}^{\infty}\sum_{t=0}^{\infty} C_s(n'^*,\ell')\,C_t(n^*,\ell)$$
$$\times \Gamma(n'^*+n^*+2-s-t)\left(\frac{n'^*n^*}{n'^*+n^*}\right)^{n'^*+n^*+2-s-t} . \qquad \ldots(4.25)$$

This sum can be evaluated in such a way that each successive term decreases until a minimum term is reached, after which each successive term increases indefinitely. This is the characteristic behavior of a certain type of asymptotic expansion. In the case of expansion (4.25), the sum is terminated with the term preceding the minimun one; we label this term P. The error in the sum is then numerically smaller than the magnitude of the first neglected term of the sum, the minimum term P+1 (Olver, 1974, p.2; Rainville, 1960, p.35).

On the other hand, Bates and Damgaard (1949) terminate the sum (4.25) by using a physical argument. In the sum over the integral of eq.(4.23), we neglect those terms for which the powers of Zr are less than 2, because the main contribution from these terms comes from regions close to the origin where the CA does not necessarily hold and where the use of asymptotic expansions is not valid. We thus neglect those terms of eq.(4.25) for which

$$s + t > n'^{*} + n^{*} - 1 . \qquad \ldots(4.26)$$

The range of allowed values of s+t is thus

$$0 \leq s+t \leq P_{BD} \qquad \ldots(4.27)$$

where $$P_{BD} = Int\left[n'^{*} + n^{*} - 1 \right], \qquad \ldots(4.28)$$

the integer part of $(n'^{*}+n^{*}-1)$.

Interestingly enough, we find that the limit P_{BD} either corresponds exactly to the limit P or is very close to it. In all cases, we have

$$0 \leq P - P_{BD} \leq 2. \qquad \ldots(4.29)$$

In our work, we will use the limit P obtained by terminating the asymptotic expansion mathematically because the sum evaluated in this manner is more accurate, and the error in the value of $R^{nl}_{n'l'}$ is also obtained.

The summation of eq.(4.25)

$$\sum_{\substack{s=0 \\ 0 \leq s+t \leq P}}^{\infty} \sum_{t=0}^{\infty} A(s,t) \qquad \ldots(4.30)$$

is now simplified by making use of the following transformation (Rainville, 1960, p.56):

$$\sum_{t=0}^{\infty} \sum_{s=0}^{\infty} A(s,t) = \sum_{t=0}^{\infty} \sum_{s=0}^{t} A(s, t-s). \qquad \ldots(4.31)$$

Expression (4.30) thus becomes

$$\sum_{\substack{s=0 \\ 0 \leq s+t \leq P}}^{\infty} \sum_{t=0}^{\infty} A(s,t) = \sum_{\substack{t=0 \\ 0 \leq t \leq P}}^{\infty} \sum_{s=0}^{t} A(s, t-s)$$

$$= \sum_{t=0}^{P} \sum_{s=0}^{t} A(s, t-s). \qquad \ldots(4.32)$$

Equation (4.25) can thus finally be rewritten as

$$R^{n\ell}_{n'\ell'} \simeq \frac{1}{Z} K(n'^*\ell', n^*\ell) \sum_{t=0}^{p} (-1)^t W_t(n'^*\ell', n^*\ell)\, \Gamma(n'^*+n^*+2-t) \left(\frac{n'^*+n^*}{2n'^*}\right)^t \quad \ldots(4.33)$$

where

$$K(n'^*\ell', n^*\ell) = \frac{1}{4} \frac{(n'^*)^{n'^*+1}}{\sqrt{\Gamma(n'^*+\ell'+1)\,\Gamma(n'^*-\ell')}} \times \frac{(n^*)^{n^*+1}}{\sqrt{\Gamma(n^*+\ell-1)\,\Gamma(n^*-\ell)}} \left(\frac{2}{n'^*+n^*}\right)^{n'^*+n^*+2}, \quad \ldots(4.34)$$

$$W_t(n'^*\ell', n^*\ell) = \sum_{s=0}^{t} \frac{1}{s!\,(t-s)!} \left(\frac{n'^*}{n^*}\right)^s \times \prod_{i=1}^{s} P_i(n'^*\ell') \prod_{j=1}^{t-s} P_j(n^*\ell), \quad \ldots(4.35)$$

$$P_i(n'^*\ell') = (n'^*-i+1)(n'^*-i) - \ell'(\ell'+1), \quad \ldots(4.36)$$

$$P_j(n^*\ell) = (n^*-j+1)(n^*-j) - \ell(\ell+1). \quad \ldots(4.37)$$

We use eqs.(4.33) to (4.37) to evaluate the oscillator strengths of the transitions that are not covered in the tables of Martin and Wiese (1976b) or Wiese et al. (1966).

3.2.b. Accuracy

The error in the oscillator strengths calculated with the Coulomb approximation is usually estimated to be ~10% for simple transitions with low values of n (Wiese et al., 1966; Crossley, 1969). However, since highly accurate values of the oscillator strengths of the lithium-

like ions are available for low values of n (Martin and Wiese, 1976b), it is possible to compare these with the f-values calculated from the CA to obtain a better estimate of the accuracy of the method as used in this work. Except for a few cases, all oscillator strengths calculated with the CA are found to be systematically lower than the corresponding values of Martin and Wiese (1976b). In most cases, for $n \leq 7$, the difference between the two sets of f-values is less than 15% for s-p transitions, with a maximum value of ~25%, and less than 5% for p-d transitions.

At larger values of n, the error in the oscillator strengths increases due to the fact that $f_{n' \to n}$ is proportional to both the transition integral $\sigma_{n' \to n}$ and the energy separation $E_{n'n}$ of the states n' and n, and both these quantities then have far greater uncertainties than at low values of n. The error in $\sigma^2_{n' \to n}$ increases because the CA becomes less accurate due to the large number of operations that must be performed to evaluate eq.(4.33) and due to the resulting loss of significant digits through truncation. This situation is further complicated by the fact that the positive and negative parts of the transition integral $\sigma_{n' \to n}$ almost exactly cancel each other. The energy eigenvalues of the higher states are not known and they must thus be extrapolated from the data available on lower states (see Section 9 of Chapter III). Consequently, the error in $E_{n'n}$ is much larger for transitions involving high-lying quantum states, especially if the energy separation of states n' and n is small.

Since the error in the oscillator strengths of the transitions to $n \geq 8$ states is thus dependent on individual transitions, no simple numerical estimate of the error can be given. However, after this work was completed, tables of oscillator strengths were published by Lindgård and Nielsen (1977) with which the f-values calculated from the CA can be compared. The calculations of Lindgård and Nielsen (1977) were carried out with a numerical Coulomb approximation (NCA) in which the wave functions used in eq.(4.13) are evaluated numerically from eq.(4.14). The CA and NCA results agree to within 25% for s-p transitions, 5% for p-d transitions, with a maximum of $\sim$25% for smaller values, and a few percent for d-f transitions, with a maximum of $\sim$5% for smaller values.

The differences between the oscillator strengths of $\Delta n = n - n' = 0$ transitions calculated with the CA and the NCA are however much larger; the f-values may differ by as much as a factor of three. However, Bates and Damgaard (1949) mention that the CA gives reliable results for very small Δn transitions, for which very little cancellation of the positive and negative parts of the integral $\sigma_{n' \to n}$ occurs. The large differences between the f-values must thus be due almost entirely to the uncertainty in the energy of these states, especially since the energy separation between them is very small. That this is indeed the case can be shown by calculating the oscillator strengths of the $\Delta n = 0$ transitions with a method different from the CA. Equation (4.43), which is derived further on in this Chapter, is independent of the CA; the only extrapolated quantity on which it depends is the energy separation of the states. The f-values calculated from it are in close agreement with those obtained from eq.(4.33) of the CA. The uncertainties in the

energy eigenvalues of high-lying quantum states thus significantly affect the oscillator strengths of transitions etween states of small energy separation.

As a general rule, we observe that the oscillator strengths of transitions involving s states calculated with the CA have much larger uncertainties than those involving p, d, and higher ℓ-value states. The reason for this behavior is that the wave functions of s states have an antinode close to the origin, whereas the wavefunctions of $\ell \geq$ p states are quite unimportant at small radial distances (Bates and Damgaard, 1949). Since the CA includes only contributions to the transition integral $\sigma_{n' \to n}$ coming from the wave functions at large radial distances, the finite value of the s state wavefunctions close to the origin is neglected and the resulting oscillator strengths thus have greater uncertainties.

3.3. Hydrogenic values

3.3.a. Method of calculation

As ℓ increases, the lithium-like states become more hydrogenic and the oscillator strengths tend to the hydrogenic values, as can be seen in Fig.4.1, 4.2, and 4.3. Consequently, for transitions from states with $\ell' \geq$ f, the oscillator strengths are calculated with the simpler hydrogenic expression (Green et al., 1957):

$$f_{n'\ell' \to n\ell} = \frac{1}{3}\left(\frac{Z^2}{n'^2} - \frac{Z^2}{n^2}\right)\frac{\ell_>}{2\ell'+1}\left(R_{n'\ell'}^{n\ell}\right)^2 \qquad \ldots(4.38)$$

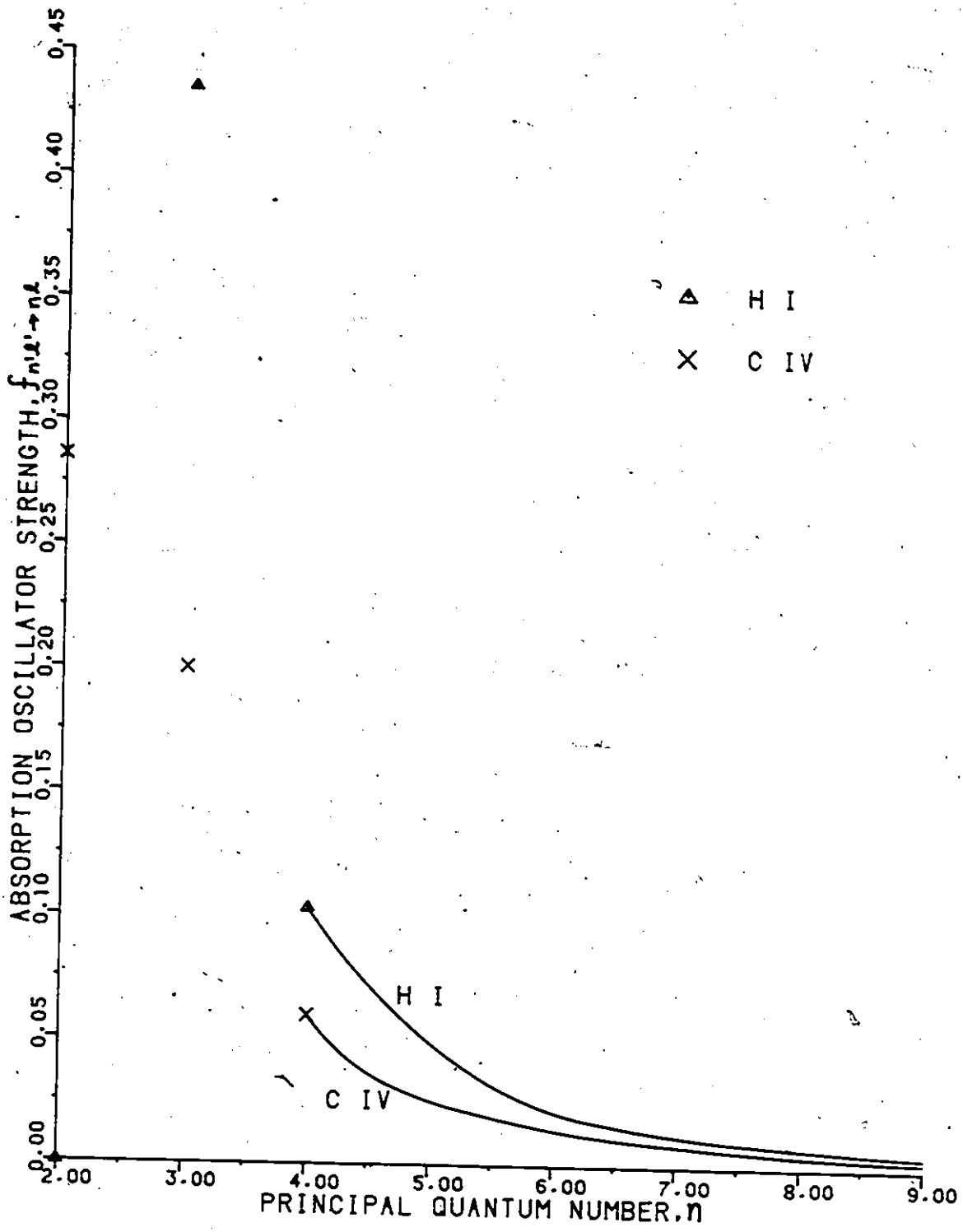

FIGURE 4.1 - ABSORPTION OSCILLATOR STRENGTHS OF THE 2S→np TRANSITIONS OF C IV AND HYDROGEN.

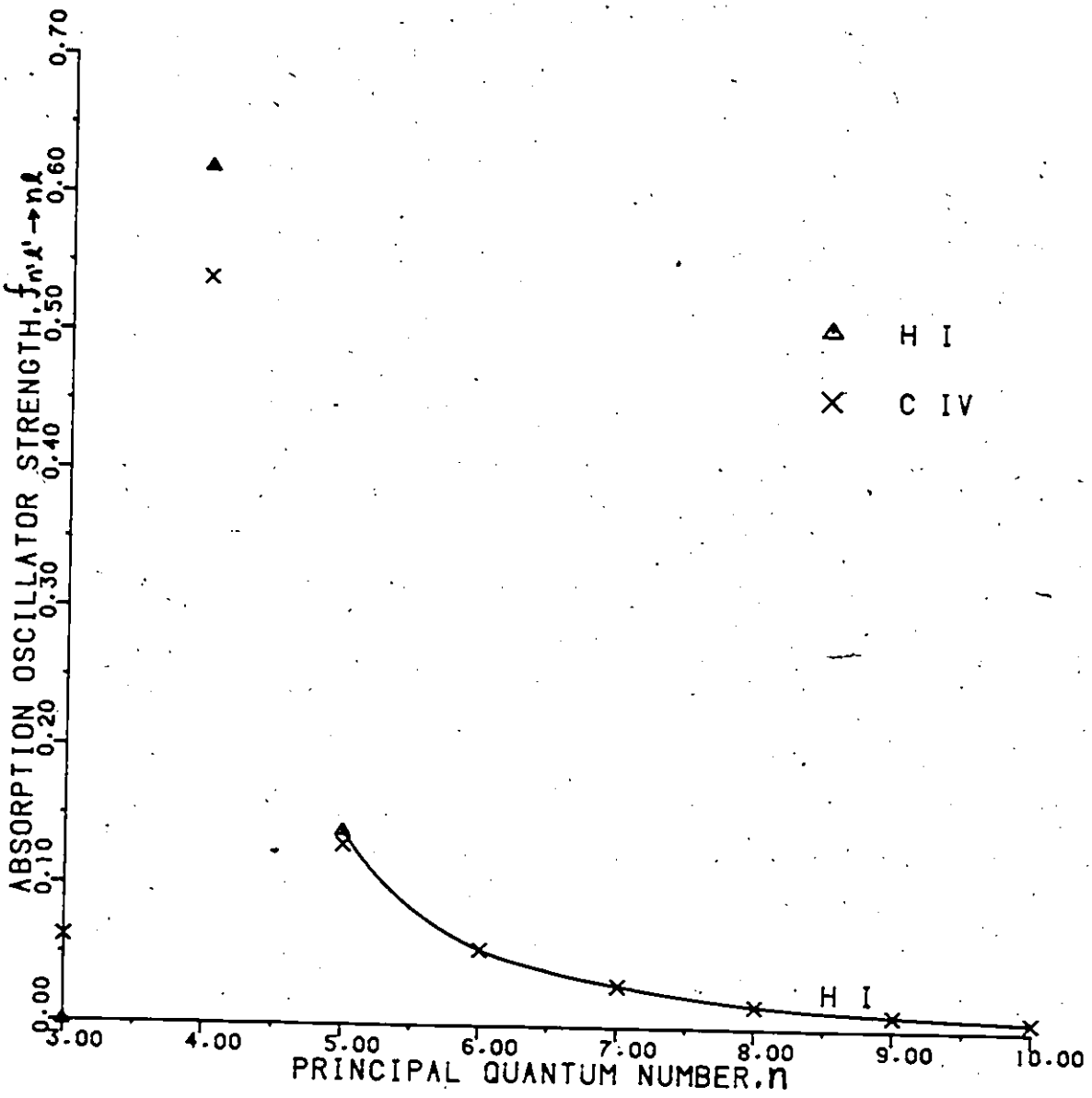

FIGURE 4.2 - ABSORPTION OSCILLATOR STRENGTHS OF THE $3p\to nd$ TRANSITIONS OF C IV AND HYDROGEN.

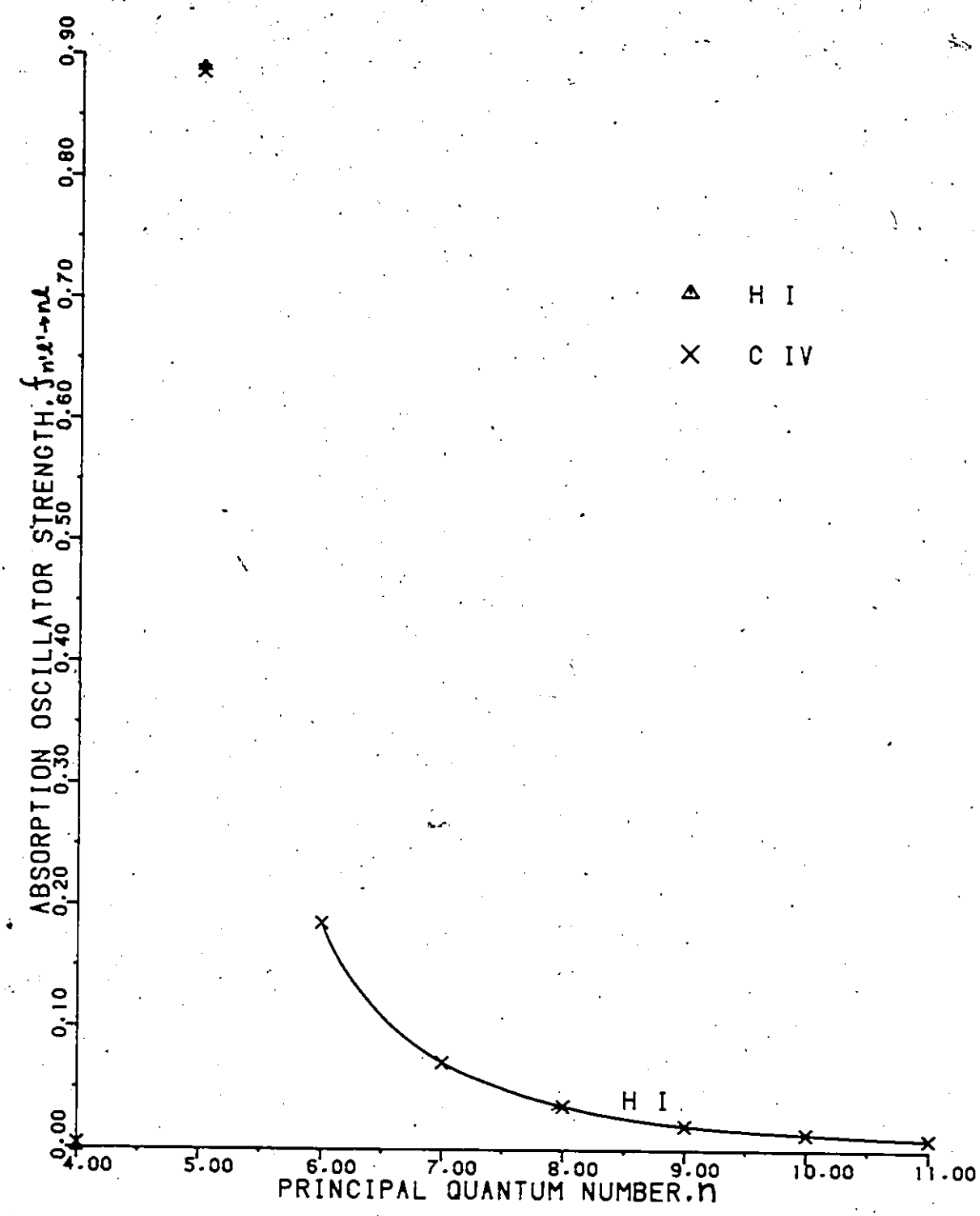

FIGURE 4.3 - ABSORPTION OSCILLATOR STRENGTHS OF THE 4d→nf TRANSITIONS OF C IV AND HYDROGEN.

where $R^{n\ell}_{n'\ell'}$ is given by eq.(4.13), Z is the core charge, and $\ell_>$ is the maximum value of ℓ' and ℓ. Since the hydrogenic radial wavefunctions are known exactly, the integral (4.13) can readily be evaluated and, in the general case, is given by the closed expression (Gordon, 1929):

$$\left\{R^{n'\ell-1}_{n\ell}\right\}^2 = \left\{\frac{(-1)^{n'-\ell}}{4Z(2\ell-1)!}\ \frac{(n+\ell)!\,(n'+\ell-1)!}{(n-\ell-1)!\,(n'-\ell)!}\right.$$

$$\times \frac{(4nn')^{\ell+1}\ (n-n')^{n+n'-2\ell-2}}{(n+n')^{n+n'}}$$

$$\times \left[{}_2F_1\left(-n+\ell+1\,,-n'+\ell\,;2\ell\,;\frac{-4nn'}{(n-n')^2}\right)\right.$$

$$\left.\left.-\left(\frac{n-n'}{n+n'}\right)^2 {}_2F_1\left(-n+\ell-1,-n'+\ell\,;\,2\ell\,;\frac{-4nn'}{(n-n')^2}\right)\right]\right\}^2 \qquad \ldots(4.39)$$

where ${}_2F_1(a,b;c;x)$ is the hypergeometric function

$${}_2F_1(a,b;c;x) = 1 + \frac{a\cdot b}{c}\frac{x}{1!} + \frac{a(a-1)b(b-1)}{c(c-1)}\ \frac{x^2}{2!} + \cdots \qquad \ldots(4.40)$$

and the quantum number n is associated with the state with the largest ℓ-value (in eq.4.39 only).

For $\Delta n = 0$ transitions, a different expression is used to calculate $\left\{R^{n\ell}_{n'\ell'}\right\}^2$ (Bethe and Salpeter, 1957, p.263):

$$\left\{R^{n\ell}_{n\ell'}\right\}^2 = \frac{9}{4}\ \frac{n^2}{Z^2}\ (n^2-\ell_>^2). \qquad \ldots(4.41)$$

The oscillator strength is then given by

$$f_{n\ell'\to n\ell} = \frac{3}{4}\left(\frac{1}{n_{p'}^2}-\frac{1}{n_\ell^2}\right)\frac{\ell_>}{2\ell'+1}\ n^2(n^2-\ell_>^2) \qquad \ldots(4.42)$$

where $n_{\ell'}$ and n_{ℓ} are the principal quantum numbers associated with the $n\ell'$ and $n\ell$ states respectively and the expression $(1/n_{\ell'}^2 - 1/n_{\ell}^2)$ is related to the energy separation between the two states. For hydrogen, this energy separation is theoretically zero and the corresponding oscillator strength is also zero. However, the energy separation of the $n\ell'$ and $n\ell$ states of lithium-like ions is finite and the oscillator strength of the transition thus has a non-zero value. The actual f-value can be evaluated from eq.(4.42) provided $n_{\ell'}$ and n_{ℓ} are replaced by their corresponding effective quantum numbers $n_{\ell'}^*$ and n_{ℓ}^* respectively. We then have

$$f_{n\ell'\to n\ell} = \frac{3}{4}\,\frac{\ell_>}{2\ell'+1}\,n^2(n^2-\ell_>^2)\left(\frac{1}{n_{\ell'}^{*2}} - \frac{1}{n_{\ell}^{*2}}\right). \qquad \ldots(4.43)$$

We use this expression to estimate the oscillator strengths of the $n\ell'$ -> $n\ell$, $\ell' \geq$ f transitions of C IV, N V, and O VI.

3.3.b. Accuracy

In Tab.4.1, the oscillator strengths of some $\Delta n = 0$ s -> p and p -> d transitions with low values of n calculated from eq.(4.43) are compared with the critically evaluated values of Martin and Wiese (1976b). In most cases, the results agree to better than 10%; eq.(4.43), when applied to $n\ell'$ -> $n\ell$, $\ell' \geq$ f transitions, can thus be expected to be more accurate than this value if the effective quantum numbers of the states are well known. Otherwise, as mentioned previously, the accuracy of these f-values is limited by the accuracy with which the energy separation of the two states is known.

Table 4.1 - Comparison of the oscillator strengths of some $\Delta n=0$ transitions calculated from eq.(4.43) with the values given by Martin and Wiese (1976b).

Transition	Ion			
	C IV	N V	O VI	H I
2s→2p	0.286 0.331	0.235 0.264	0.199 0.220	0
3s→3p	0.481 0.529	0.393 0.427	0.335 0.357	0
4s→4p	0.68 0.71	0.54 0.58	0.45 0.49	0
3p→3d	0.0623 0.0619	0.0544 0.0541	0.0481 0.0483	0
4p→4d	0.117 0.111	0.103 0.096	0.091 0.086	0

Top value: from Martin and Wiese (1976b)
Bottom value: calculated from eq.(4.43)

On the other hand, the accuracy of the oscillator strengths of the $n'\ell' \rightarrow n\ell$ transitions obtained from the corresponding hydrogenic values with eqs.(4.38) and (4.39) depends on how close to hydrogenic the $n'\ell'$ and $n\ell$ states are. For the $\ell' \geq$ f states, this is a reasonably good approximation and an accuracy of 2-3S can be expected in the oscillator strengths involving these states.

4. TRANSITIONS INVOLVING AVERAGE STATES

The oscillator strengths of transitions involving average states can be obtained from the oscillator strengths of transitions between individual states by using summation rules. These are derived from the fact that the line strength of a group of lines equals the sum of the line strengths of the individual lines comprising the group (Wiese et al., 1966):

$$S_{n' \rightarrow n} = \sum_{\ell' \ell} S_{n'\ell' \rightarrow n\ell} . \qquad \ldots(4.44)$$

The relation between the oscillator strength and the line strength of an absorption line is

$$S_{n\ell' \rightarrow n\ell} = \frac{1}{C'} \frac{\omega_{n'\ell'}}{\nu_{n'\ell' \rightarrow n\ell}} f_{n'\ell' \rightarrow n\ell} \qquad \ldots(4.45)$$

where $$C' = \frac{8\pi^2 m}{3he^2} , \qquad \ldots(4.46)$$

$\omega_{n'\ell'}$ is the statistical weight of level $n'\ell'$, $\nu_{n'\ell' \rightarrow n\ell}$ is the frequency of the line emitted during the $n'\ell' \rightarrow n\ell$ transition, and the other

symbols have their usual meaning. In most cases, if the splitting of the levels due to the different ℓ-values is not too large, we can put

$$\upsilon_{n'\ell' \to n\ell} \simeq \upsilon_{n'\ell' \to n} \simeq \upsilon_{n' \to n} . \qquad \ldots(4.47)$$

Consider a $n'\ell'$ -> n transition. From eq.(4.45), we can write

$$S_{n'\ell' \to n} = \frac{1}{C'} \frac{\omega_{n'\ell'}}{\upsilon_{n'\ell' \to n}} f_{n'\ell' \to n} \qquad \ldots(4.48)$$

which, from eq.(4.44), also equals

$$S_{n'\ell' \to n} = \sum_{\ell} S_{n'\ell' \to n\ell} \; ; \qquad \ldots(4.49)$$

substituting from eq.(4.45), eq.(4.49) becomes

$$S_{n'\ell' \to n} = \frac{1}{C'} \sum_{\ell} \frac{\omega_{n'\ell'}}{\upsilon_{n'\ell' \to n\ell}} f_{n'\ell' \to n\ell} . \qquad \ldots(4.50)$$

Thus if we equate relations (4.48) and (4.50), we get the summation rule

$$f_{n'\ell' \to n} = \sum_{\ell} \frac{\upsilon_{n'\ell' \to n}}{\upsilon_{n'\ell' \to n\ell}} f_{n'\ell' \to n\ell} \qquad \ldots(4.51)$$

and using eq.(4.47), we obtain

$$f_{n'\ell' \to n} \simeq \sum_{\ell} f_{n'\ell' \to n\ell} . \qquad \ldots(4.52)$$

Similarly, for the n' -> nℓ transitions, we obtain

$$f_{n'\to nl} = \sum_{l'} \frac{\omega_{n'l'}}{\omega_{n'}} \frac{\upsilon_{n'\to nl}}{\upsilon_{n'l'\to nl}} f_{n'l'\to nl} \quad \ldots(4.53)$$

$$\simeq \sum_{l'} \frac{\omega_{n'l'}}{\omega_{n'}} f_{n'l'\to nl} \quad \ldots(4.54)$$

and, for the n' -> n transitions,

$$f_{n'\to n} = \sum_{l'} \frac{\omega_{n'l'}}{\omega_{n'}} \frac{\upsilon_{n'\to n}}{\upsilon_{n'l'\to n}} f_{n'l'\to n} \quad \ldots(4.55)$$

$$\simeq \sum_{l'} \frac{\omega_{n'l'}}{\omega_{n'}} f_{n'l'\to n} \quad \ldots(4.56)$$

or

$$f_{n'\to n} = \sum_{l} \frac{\upsilon_{n'\to n}}{\upsilon_{n'\to nl}} f_{n'\to nl} \quad \ldots(4.57)$$

$$\simeq \sum_{l} f_{n'\to nl} . \quad \ldots(4.58)$$

5. RESULTS

The final set of oscillator strengths for all allowed transitions possible between all levels which are relevant to this work is given in Tables 4.2, 4.3, and 4.4 for the lithium-like ions C IV, N V, and O VI respectively, and in Tab.4.5.

Table 4.2 - Oscillator strengths of the ion C IV used in this work.

		n'→n transition							
		final state n							
		2p	3p	4p	5p	6p	7<ℓ≥1>	8<ℓ≥1>	9<ℓ≥1>
initial state n'	2s	0.286	0.197	0.610 (-1)	0.290 (-1)	0.156 (-1)	0.92 (-2)	0.557 (-2)	0.365 (-2)
	3s	-0.113	0.481	0.240	0.76 (-1)	0.344 (-1)	0.193 (-1)	0.103 (-1)	0.686 (-2)
	4s	-0.207 (-1)	-0.249	0.68	0.278	0.86 (-1)	0.40 (-1)	0.189 (-1)	0.119 (-1)
	5s	-0.90 (-2)	-0.456 (-1)	-0.387	0.833	0.237	0.768 (-1)	0.364 (-1)	0.208 (-1)
	6s	-0.45 (-2)	-0.180 (-1)	-0.759 (-1)	-0.528	1.01	0.258	0.814 (-1)	0.390 (-1)
	7s	-0.258 (-2)	-0.93 (-2)	-0.297 (-1)	-0.103	-0.680	1.20	0.255	0.846 (-1)
	8s	-0.141 (-2)	-0.524 (-2)	-0.147 (-1)	-0.397 (-1)	-0.129	-0.809	1.35	0.282
	9s	-0.863 (-3)	-0.337 (-2)	-0.869 (-2)	-0.204 (-1)	-0.506 (-1)	-0.156	-0.960	1.53

Power of ten is given in parenthesis

Table 4.2 - continued

n'→n transition :

initial state n'	final state n: 7⟨ℓ≥1⟩	8⟨ℓ≥1⟩	9⟨ℓ≥1⟩	3d	4d	5d	6d
2p	0.139 (-1)	0.838 (-2)	0.566 (-2)	0.654	0.124	0.472 (-1)	0.234 (-1)
3p	0.290 (-1)	0.173 (-1)	0.112 (-1)	0.623 (-1)	0.545	0.134	0.555 (-1)
4p	0.594 (-1)	0.319 (-1)	0.196 (-1)	-0.280 (-1)	0.117	0.518	0.137
5p	0.141	0.622 (-1)	0.342 (-1)	-0.540 (-2)	-0.753 (-1)	0.155	0.516
6p	0.527	0.145	0.652 (-1)	-0.206 (-2)	-0.137 (-1)	-0.117	0.199
7 ⟨ℓ≥1⟩		1.62	0.260	-0.268 (-2)	-0.771 (-2)	-0.214 (-1)	-0.945 (-1)
8 ⟨ℓ≥1⟩	-1.23		1.81	-0.116 (-2)	-0.299 (-2)	-0.674 (-2)	-0.175 (-1)
9 ⟨ℓ≥1⟩	-0.156	-1.43		-0.576 (-3)	-0.139 (-2)	-0.279 (-2)	-0.581 (-2)

Power of ten is given in parenthesis

Table 4.2 - continued

n'→n transition

initial state n'	final state n: 4f	5f	6f	5g	6g	6h
7<ℓ≥1>	-0.843 (-2)	-0.334 (-1)	-0.164	-0.373 (-1)	-0.277	-0.451
8<ℓ≥1>	-0.294 (-2)	-0.943 (-2)	-0.277 (-1)	-0.848 (-2)	-0.378 (-1)	-0.375 (-1)
9<ℓ≥1>	-0.128 (-2)	-0.366 (-2)	-0.864 (-2)	-0.290 (-2)	-0.105 (-1)	-0.816 (-2)
3d	1.02	0.157	0.542 (-1)			
4d	0.279 (-2)	0.995	0.186			
5d	-0.128 (-1)	0.533 (-2)	0.837			
6d	-0.228 (-2)	-0.334 (-1)	0.863 (-2)			
4f				1.35	0.182	
5f				0.617 (-3)	1.19	
6f				-0.949 (-2)	0.857 (-3)	
5g	-1.05	-0.480 (-3)	0.738 (-2)			1.68
6g	-0.142	-0.925	-0.667 (-3)			0.12 (-3)
6h				-1.37	0.10 (-3)	

Power of ten is given in parenthesis

Table 4.2 - continued

n'→n transition

initial state n'	final state n = 10	11	12	13	14	15
2s	0.262 (-2)	0.195 (-2)	0.148 (-2)	0.116 (-2)	0.922 (-3)	0.746 (-3)
3s	0.482 (-2)	0.352 (-2)	0.266 (-2)	0.206 (-2)	0.163 (-2)	0.131 (-2)
4s	0.806 (-2)	0.574 (-2)	0.425 (-2)	0.324 (-2)	0.253 (-2)	0.202 (-2)
5s	0.133 (-1)	0.907 (-2)	0.652 (-2)	0.487 (-2)	0.374 (-2)	0.295 (-2)
6s	0.225 (-1)	0.144 (-1)	0.993 (-2)	0.718 (-2)	0.539 (-2)	0.417 (-2)
7s	0.409 (-1)	0.237 (-1)	0.153 (-1)	0.106 (-1)	0.767 (-2)	0.579 (-2)
8s	0.929 (-1)	0.447 (-1)	0.259 (-1)	0.167 (-1)	0.116 (-1)	0.844 (-2)
9s	0.301	0.988 (-1)	0.475 (-1)	0.275 (-1)	0.178 (-1)	0.124 (-1)
2p	0.422 (-2)	0.311 (-2)	0.235 (-2)	0.182 (-2)	0.145 (-2)	0.118 (-2)
3p	0.855 (-2)	0.618 (-2)	0.463 (-2)	0.355 (-2)	0.280 (-2)	0.225 (-2)
4p	0.149 (-1)	0.104 (-1)	0.763 (-2)	0.578 (-2)	0.449 (-2)	0.356 (-2)
5p	0.254 (-1)	0.170 (-1)	0.121 (-1)	0.886 (-2)	0.676 (-2)	0.528 (-2)
6p	0.449 (-1)	0.279 (-1)	0.188 (-1)	0.134 (-1)	0.995 (-2)	0.762 (-2)
7<ℓ≥1>	0.927 (-1)	0.448 (-1)	0.252 (-1)	0.162 (-1)	0.111 (-1)	0.794 (-2)
8<ℓ≥1>	0.290	0.101	0.483 (-1)	0.273 (-1)	0.175 (-1)	0.119 (-1)
9<ℓ≥1>	2.03	0.316	0.109	0.518 (-1)	0.294 (-1)	0.185 (-1)

Power of ten is given in parenthesis

Table 4.3 - Oscillator strengths of the ion N V used in this work.

n'→n transition

initial state n'	final state n: 2p	3p	4p	5p	6p	7<ℓ≥1>	8<ℓ≥1>	9<ℓ≥1>
2s	0.235	0.233	0.696 (-1)	0.322 (-1)	0.170 (-1)	0.102 (-1)	0.607 (-2)	0.418 (-2)
3s	-0.966 (-1)	0.393	0.277	0.83 (-1)	0.376 (-1)	0.209 (-1)	0.114 (-1)	0.762 (-2)
4s	-0.186 (-1)	-0.219	0.54	0.319	0.97 (-1)	0.45 (-1)	0.212 (-1)	0.134 (-1)
5s	-0.84 (-2)	-0.408 (-1)	-0.336	0.685	0.284	0.894 (-1)	0.416 (-1)	0.237 (-1)
6s	-0.42 (-2)	-0.165 (-1)	-0.672 (-1)	-0.459	0.825	0.318	0.963 (-1)	0.456 (-1)
7s	-0.234 (-2)	-0.84 (-2)	-0.267 (-1)	-0.917 (-1)	-0.588	0.960	0.348	0.105
8s	-0.127 (-2)	-0.476 (-2)	-0.134 (-1)	-0.363 (-1)	-0.117	-0.711	1.11	0.363
9s	-0.858 (-3)	-0.307 (-2)	-0.797 (-2)	-0.188 (-1)	-0.467 (-1)	-0.143	-0.848	1.24

Power of ten is given in parenthesis

Table 4.3 - continued

$n' \rightarrow n$ transition

initial state n'	final state n: $7\langle \ell \geq 1 \rangle$	$8\langle \ell \geq 1 \rangle$	$9\langle \ell \geq 1 \rangle$	3d	4d	5d	6d
2p	0.136 (-1)	0.833 (-2)	0.562 (-2)	0.658	0.124	0.469 (-1)	0.230 (-1)
3p	0.289 (-1)	0.173 (-1)	0.113 (-1)	0.544 (-1)	0.548	0.134	0.555 (-1)
4p	0.597 (-1)	0.321 (-1)	0.196 (-1)	-0.267 (-1)	0.103	0.527	0.136
5p	0.142	0.628 (-1)	0.345 (-1)	-0.518 (-2)	-0.651 (-1)	0.137	0.524
6p	0.543	0.148	0.661 (-1)	-0.196 (-2)	-0.131 (-1)	-0.110	0.174
$7\langle \ell \geq 1 \rangle$		1.62	0.260	-0.269 (-2)	-0.770 (-2)	-0.214 (-1)	-0.944 (-1)
$8\langle \ell \geq 1 \rangle$	-1.23		1.81	-0.116 (-2)	-0.298 (-2)	-0.673 (-2)	-0.174 (-1)
$9\langle \ell \geq 1 \rangle$	-0.156	-1.43		-0.576 (-3)	-0.139 (-2)	-0.278 (-2)	-0.580 (-2)

Power of ten is given in parenthesis

Table 4.3 - continued

n'→n transition

initial state n'	final state n: 4f	5f	6f	5g	6g	6h
$7<\ell\geq 1>$	-0.843 (-2)	-0.333 (-1)	-0.164	-0.373 (-1)	-0.277	-0.451
$8<\ell\geq 1>$	-0.293 (-2)	-0.943 (-2)	-0.278 (-1)	-0.848 (-2)	-0.378 (-1)	-0.375 (-1)
$9<\ell\geq 1>$	-0.127 (-2)	-0.366 (-2)	-0.864 (-2)	-0.290 (-2)	-0.105 (-1)	-0.816 (-2)
3d	1.02	0.157	0.542 (-1)			
4d	0.281 (-2)	0.886	0.186			
5d	-0.127 (-1)	0.440 (-2)	0.839			
6d	-0.226 (-2)	-0.332 (-1)	0.606 (-2)			
4f				1.35	0.182	
5f				0.463 (-3)	1.19	
6f				-0.949 (-2)	0.857 (-3)	
5g	-1.05	-0.360 (-3)	0.738 (-2)			1.68
6g	-0.142	-0.925	-0.667 (-3)			0.6 (-4)
6h				-1.37	-0.5 (-4)	

Power of ten is given in parenthesis

Table 4.3 - continued

n'→n transition

initial state n'	final state n = 10	11	12	13	14	15
2s	0.300 (-2)	0.223 (-2)	0.170 (-2)	0.133 (-2)	0.106 (-2)	0.857 (-3)
3s	0.534 (-2)	0.390 (-2)	0.294 (-2)	0.227 (-2)	0.179 (-2)	0.144 (-2)
4s	0.901 (-2)	0.640 (-2)	0.473 (-2)	0.360 (-2)	0.281 (-2)	0.224 (-2)
5s	0.150 (-1)	0.102 (-1)	0.733 (-2)	0.546 (-2)	0.419 (-2)	0.330 (-2)
6s	0.260 (-1)	0.166 (-1)	0.114 (-1)	0.819 (-2)	0.613 (-2)	0.473 (-2)
7s	0.494 (-1)	0.282 (-1)	0.180 (-1)	0.124 (-1)	0.898 (-2)	0.676 (-2)
8s	0.113	0.531 (-1)	0.304 (-1)	0.195 (-1)	0.134 (-1)	0.974 (-2)
9s	0.388	0.120	0.565 (-1)	0.324 (-1)	0.208 (-1)	0.143 (-1)
2p	0.419 (-2)	0.309 (-2)	0.234 (-2)	0.182 (-2)	0.144 (-2)	0.117 (-2)
3p	0.848 (-2)	0.613 (-2)	0.459 (-2)	0.353 (-2)	0.278 (-2)	0.222 (-2)
4p	0.147 (-1)	0.104 (-1)	0.758 (-2)	0.573 (-2)	0.445 (-2)	0.354 (-2)
5p	0.252 (-1)	0.169 (-1)	0.119 (-1)	0.880 (-2)	0.671 (-2)	0.524 (-2)
6p	0.447 (-1)	0.278 (-1)	0.187 (-1)	0.133 (-1)	0.990 (-2)	0.759 (-2)
$7<\ell\geq 1>$	0.925 (-1)	0.446 (-1)	0.252 (-1)	0.161 (-1)	0.110 (-1)	0.792 (-2)
$8<\ell\geq 1>$	0.290	0.101	0.483 (-1)	0.273 (-1)	0.175 (-1)	0.118 (-1)
$9<\ell\geq 1>$	2.03	0.316	0.109	0.518 (-1)	0.294 (-1)	0.185 (-1)

Power of ten is given in parenthesis

Table 4.4 - Oscillator strengths of the ion O VI used in this work.

n'→n transition

initial state n'	final state n: 2p	3p	4p	5p	6p	7<ℓ≥1>	8<ℓ≥1>	9<ℓ≥1>
2s	0.199	0.257	0.766 (-1)	0.343 (-1)	0.181 (-1)	0.107 (-1)	0.655 (-2)	0.442 (-2)
3s	-0.861 (-1)	0.335	0.305	0.88 (-1)	0.397 (-1)	0.219 (-1)	0.127 (-1)	0.826 (-2)
4s	-0.168 (-1)	-0.195	0.45	0.349	0.105	0.47 (-1)	0.236 (-1)	0.144 (-1)
5s	-0.78 (-2)	-0.375 (-1)	-0.297	0.587	0.327	0.999 (-1)	0.470 (-1)	0.257 (-1)
6s	-0.39 (-2)	-0.153 (-1)	-0.615 (-1)	-0.420	0.701	0.370	0.111	0.498 (-1)
7s	-0.219 (-2)	-0.78 (-2)	-0.246 (-1)	-0.857 (-1)	-0.534	0.797	0.429	0.117
8s	-0.118 (-2)	-0.456 (-2)	-0.126 (-1)	-0.341 (-1)	-0.109	-0.648	0.874	0.419
9s	-0.799 (-3)	-0.296 (-2)	-0.751 (-2)	-0.178 (-1)	-0.438 (-1)	-0.133	-0.746	1.06

Power of ten is given in parenthesis.

Table 4.4 - continued

$n' \rightarrow n$ transition

initial state n'	final state n: $7\langle \ell \geq 1 \rangle$	$8\langle \ell \geq 1 \rangle$	$9\langle \ell \geq 1 \rangle$	3d	4d	5d	6d
2p	0.135 (-1)	0.832 (-2)	0.557 (-2)	0.662	0.123	0.466 (-1)	0.229 (-1)
3p	0.289 (-1)	0.173 (-1)	0.112 (-1)	0.481 (-1)	0.555	0.135	0.555 (-1)
4p	0.600 (-1)	0.321 (-1)	0.197 (-1)	-0.257 (-1)	0.91 (-1)	0.536	0.136
5p	0.144	0.629 (-1)	0.349 (-1)	-0.499 (-2)	-0.627 (-1)	0.119	0.539
6p	0.556	0.148	0.669 (-1)	-0.190 (-2)	-0.128 (-1)	-0.107	0.153
7 $\langle \ell \geq 1 \rangle$		1.63	0.260	-0.268 (-2)	-0.769 (-2)	-0.213 (-1)	-0.938 (-1)
8 $\langle \ell \geq 1 \rangle$	-1.24		1.81	-0.116 (-2)	-0.299 (-2)	-0.673 (-2)	-0.174 (-1)
9 $\langle \ell \geq 1 \rangle$	-0.156	-1.43		-0.577 (-3)	-0.139 (-2)	-0.278 (-2)	-0.578 (-2)

Power of ten is given in parenthesis

Table 4.4 - continued

n'→n transition

initial state n'	final state n: 4f	5f	6f	5g	6g	6h
$7<\ell\geq 1>$	-0.843 (-2)	-0.333 (-1)	-0.164	-0.373 (-1)	-0.277	-0.451
$8<\ell\geq 1>$	-0.293 (-2)	-0.942 (-2)	-0.277 (-1)	-0.848 (-2)	-0.378 (-1)	-0.375 (-1)
$9<\ell\geq 1>$	-0.127 (-2)	-0.366 (-2)	-0.873 (-2)	-0.290 (-2)	-0.105 (-1)	-0.816 (-2)
3d	1.02	0.157	0.542 (-1)			
4d	0.245 (-2)	0.886	0.186			
5d	-0.127 (-1)	0.552 (-2)	0.838			
6d	-0.228 (-2)	-0.335 (-1)	0.965 (-2)			
4f				1.35	0.182	
5f				0.309 (-3)	1.19	
6f				-0.949 (-2)	0.857 (-3)	
5g	-1.05	-0.240 (-3)	0.738 (-2)			1.68
6g	-0.142	-0.925	-0.667 (-3)			0.3 (-4)
6h				-1.37	-0.2 (-4)	

Power of ten is given in parenthesis

Table 4.4 - continued

$n' \rightarrow n$ transition

initial state n'	final state n = 10	11	12	13	14	15
2s	0.317 (-2)	0.235 (-2)	0.180 (-2)	0.140 (-2)	0.112 (-2)	0.904 (-3)
3s	0.569 (-2)	0.415 (-2)	0.312 (-2)	0.241 (-2)	0.191 (-2)	0.153 (-2)
4s	0.968 (-2)	0.686 (-2)	0.506 (-2)	0.385 (-2)	0.301 (-2)	0.240 (-2)
5s	0.162 (-1)	0.110 (-1)	0.788 (-2)	0.586 (-2)	0.449 (-2)	0.353 (-2)
6s	0.282 (-1)	0.179 (-1)	0.122 (-1)	0.880 (-2)	0.659 (-2)	0.508 (-2)
7s	0.543 (-1)	0.308 (-1)	0.196 (-1)	0.135 (-1)	0.972 (-2)	0.730 (-2)
8s	0.126	0.585 (-1)	0.332 (-1)	0.212 (-1)	0.146 (-1)	0.106 (-1)
9s	0.448	0.134	0.623 (-1)	0.355 (-1)	0.226 (-1)	0.156 (-1)
2p	0.414 (-2)	0.305 (-2)	0.231 (-2)	0.179 (-2)	0.143 (-2)	0.115 (-2)
3p	0.844 (-2)	0.609 (-2)	0.456 (-2)	0.350 (-2)	0.275 (-2)	0.221 (-2)
4p	0.147 (-1)	0.103 (-1)	0.755 (-2)	0.572 (-2)	0.444 (-2)	0.352 (-2)
5p	0.252 (-1)	0.168 (-1)	0.119 (-1)	0.879 (-2)	0.670 (-2)	0.524 (-2)
6p	0.446 (-1)	0.277 (-1)	0.187 (-1)	0.133 (-1)	0.987 (-2)	0.756 (-2)
$7<\ell\geq 1>$	0.925 (-1)	0.446 (-1)	0.252 (-1)	0.161 (-1)	0.110 (-1)	0.792 (-2)
$8<\ell\geq 1>$	0.290	0.101	0.483 (-1)	0.273 (-1)	0.175 (-1)	0.118 (-1)
$9<\ell\geq 1>$	2.03	0.316	0.109	0.516 (-1)	0.294 (-1)	0.184 (-1)

Power of ten is given in parenthesis

Table 4.5 - Oscillator strengths of the ions C IV, N V, and O VI used in this work.

n'→n transition

initial state n'	final state n = 10	11	12	13	14	15
3d	0.629 (-2)	0.446 (-2)	0.329 (-2)	0.250 (-2)	0.195 (-2)	0.155 (-2)
4d	0.145 (-1)	0.100 (-1)	0.721 (-2)	0.540 (-2)	0.415 (-2)	0.328 (-2)
5d	0.273 (-1)	0.179 (-1)	0.124 (-1)	0.912 (-2)	0.690 (-2)	0.536 (-2)
6d	0.504 (-1)	0.307 (-1)	0.204 (-1)	0.144 (-1)	0.106 (-1)	0.807 (-2)
4f	0.908 (-2)	0.605 (-2)	0.426 (-2)	0.314 (-2)	0.238 (-2)	0.185 (-2)
5f	0.244 (-1)	0.155 (-1)	0.106 (-1)	0.758 (-2)	0.565 (-2)	0.433 (-2)
6f	0.515 (-1)	0.305 (-1)	0.198 (-1)	0.137 (-1)	0.997 (-2)	0.751 (-2)
5g	0.139 (-1)	0.833 (-2)	0.546 (-2)	0.380 (-2)	0.276 (-2)	0.209 (-2)
6g	0.446 (-1)	0.250 (-1)	0.156 (-1)	0.105 (-1)	0.744 (-2)	0.550 (-2)
6h	0.247 (-1)	0.126 (-1)	0.737 (-2)	0.472 (-2)	0.323 (-2)	0.232 (-2)
10		2.19	0.341	0.117	0.551 (-1)	0.311 (-1)
11	-1.81		2.38	0.367	0.125	0.587 (-1)
12	-0.237	-2.00		2.57	0.394	0.133
13	-0.692 (-1)	-0.263	-2.19		2.76	0.420
14	-0.281 (-1)	-0.772 (-1)	-0.289	-2.38		2.95
15	-0.138 (-1)	-0.316 (-1)	-0.851 (-1)	-0.315	-2.57	

Power of ten is given in parenthesis

Chapter V

C IV, N V, AND O VI: COLLISIONAL IONIZATION RATE COEFFICIENTS

1. INTRODUCTION

A very limited amount of data is available on the collisional ionization cross-sections or rate coefficients of the lithium-like ions C IV, N V, and O VI. Cross-section data are given in

Trefftz (1963): 2s state of O VI,

Lotz (1967, 1968): 2s state of C IV, N V, and O VI,

and rate coefficients are discussed in

Kulander (1970): 2s state of N V and O VI,

Kunze (1971): 2s state of C IV, N V, and O VI, 2p state of O VI.

Most of the work has been done on the ground state; very little attention has been given to the excited states. Furthermore, there is no simple general method of obtaining reliable estimates of the rate coefficients needed in this work.

2. CROSS-SECTION DATA

Trefftz (1963) calculates the electron impact ionization cross-section of the 2s state of O VI with the Coulomb-Born approximation, with and without exchange. The inclusion of exchange between the scattered and the ejected electrons reduces the cross-section to less than 60% of the non-exchange cross-section at maximum.

Lotz (1967, 1968) proposes an empirical expression for single ionization of atoms and ions from the ground state that approximates experimentally determined cross-sections within the experimental error and, in most cases, within 10% over the energy range from the threshold to 10 keV. The formula cannot reproduce the fine structures observed in the cross-section curves, but it has the advantage that it applies to all elements.

Lotz's formula for the total cross-section for single ionization from the ground state is written in the general form

$$\sigma(E) = \sum_{i=1}^{N} a_i \xi_i \ln(E/P_i)\,(E P_i)^{-1} \times \left\{1 - b_i e^{-c_i (E/P_i - 1)}\right\} \qquad \ldots(5.1)$$

where i is the subshell from which ionization occurs and N is the total number of subshells which contribute to the cross-section; N is usually small. The subshells are counted inwards, starting from the outermost one for which i = 1. ξ_i is the number of equivalent electrons in subshell i and a_i, b_i, and c_i are constants which are adjusted to the available data. P_i is the binding energy of the electrons in subshell i and E is the kinetic energy of the impacting electron; the condition $E \geq P_i$ holds for ionization from the i^{th} subshell. Formula (5.1) gives the correct theoretical energy-dependence both for small and large energies of the impacting electron; for small energies, we have (Burgess, 1961; Geltman et al., 1963)

$$\sigma(E) \sim \frac{E}{P_1} - 1 \quad \text{for } E \sim P_1, \qquad \ldots(5.2)$$

and for large energies (Massey and Burhop, 1952, p.140)

$$\sigma(E) \sim \frac{\ln E}{E} \quad \text{for} \quad E \gg P_i . \qquad \ldots(5.3)$$

For four times and higher ionized atoms, Lotz assumes

$$a_i = 4.5 \times 10^{-14} \ \text{cm}^2 \ \text{eV}^2$$

$$b_i = 0. \qquad \ldots(5.4)$$

This assumption gives results which agree within a few percent with theoretical calculations of Rudge and Schwartz (1966) for a hydrogen-like ion with high nuclear charge Z_N in the Born-exchange approximation. For lithium-like ions, we neglect inner shell ionization which occurs only at high values of E; then N = 1. We also have, for the valence electron, $\xi_1 = 1$ and $P_1 = I_{2s}$, the ionization potential of the ground state. Expressing the energy of the impacting electron in units of the threshold energy for ionization

$$u = E / I_{2s} , \qquad \ldots(5.5)$$

we can write the ground state collisional ionization cross-section of the ions C IV, N V, and O VI as

$$\sigma_{2s}(u) = \frac{a_{2s}}{I_{2s}^2} \frac{\ln u}{u} \qquad \ldots(5.6)$$

where $a_{2s} = 4.5 \times 10^{-14}$ cm^{2}eV^2 and I_{2s} is in eV. In Fig.5.1, we compare the cross-section of the 2s state of O VI as calculated by Lotz's formula with that given by Trefftz. It is seen that the results obtained with Lotz's eq.(5.6) are in approximate agreement with the values of the cross-section with exchange calculated by Trefftz.

Integrating eq.(5.6) over a Maxwellian energy distribution function

$$\frac{dn}{n} = \frac{2}{kT}\sqrt{\frac{E}{\pi kT}}\, e^{-\frac{E}{kT}}\, dE, \qquad \ldots(5.7)$$

we obtain the rate coefficient for electron impact ionization of the ground state of the ions C IV, N V, and O VI:

$$S_{2s}(T) = 6.7 \times 10^{7}\, \frac{a_{2s}}{I_{2s}\sqrt{T}}\, E_1\left(\frac{I_{2s}}{T}\right) \text{cm}^3\text{s}^{-1} \qquad \ldots(5.8)$$

where $E_1(x)$ is the exponential integral and I_{2s} and T are in eV. For T in K and I_{2s} in Rydbergs, eq.(5.8) becomes

$$S_{2s}(T) = \frac{2.4 \times 10^{-5}}{I_{2s}\sqrt{T}}\, E_1\left(157{,}890\, \frac{I_{2s}}{T}\right) \text{cm}^3\text{s}^{-1} \qquad \ldots(5.9)$$

3. RATE COEFFICIENT DATA

3.1. Ground state

Kulander (1970) compares the collisional ionization rate coefficients of the ground state of N V and O VI calculated with an empirical and a semi-empirical expression, various classical approximations, and the formula of Lotz (1967, 1968). The coefficients are found to agree with each other within a factor of two.

Kunze (1971) has experimentally measured the collisional ionization rate coefficients of the 2s state of the ions C IV, N V, and O VI. The experimental rate coefficients he obtains are only about 60% of theoretical rates calculated with a semi-empirical expression which he proposes (eq.5.10). However, this is within the experimental accuracy estimate of a factor of two or better quoted by Kunze, and these results are thus in agreement with theory. Kunze also mentions possible systematic errors in his measurements which would tend to yield values of the rate coefficients which are too low.

The semi-empirical formula proposed by Kunze is

$$S_{nl}(T) \simeq 7.5 \times 10^{-5} \frac{\xi_{nl}}{I_{nl}} \left[\left(\ln \frac{40kT}{I_{nl}} \right)^3 + 40 \right] \times \frac{\sqrt{kT}}{I_{nl} + 3kT} e^{-\frac{I_{nl}}{kT}} \; cm^{3} s^{-1}. \qquad \ldots(5.10)$$

This equation gives a ~10% fit in the temperature range $I_{nl}/10 \leq kT \leq 10\, I_{nl}$ to the rate coefficients derived for hydrogenic ions by Rudge and Schwartz (1966) with the Born-exchange approximation. The rate coefficients calculated with eq.(5.10) are also in agreement

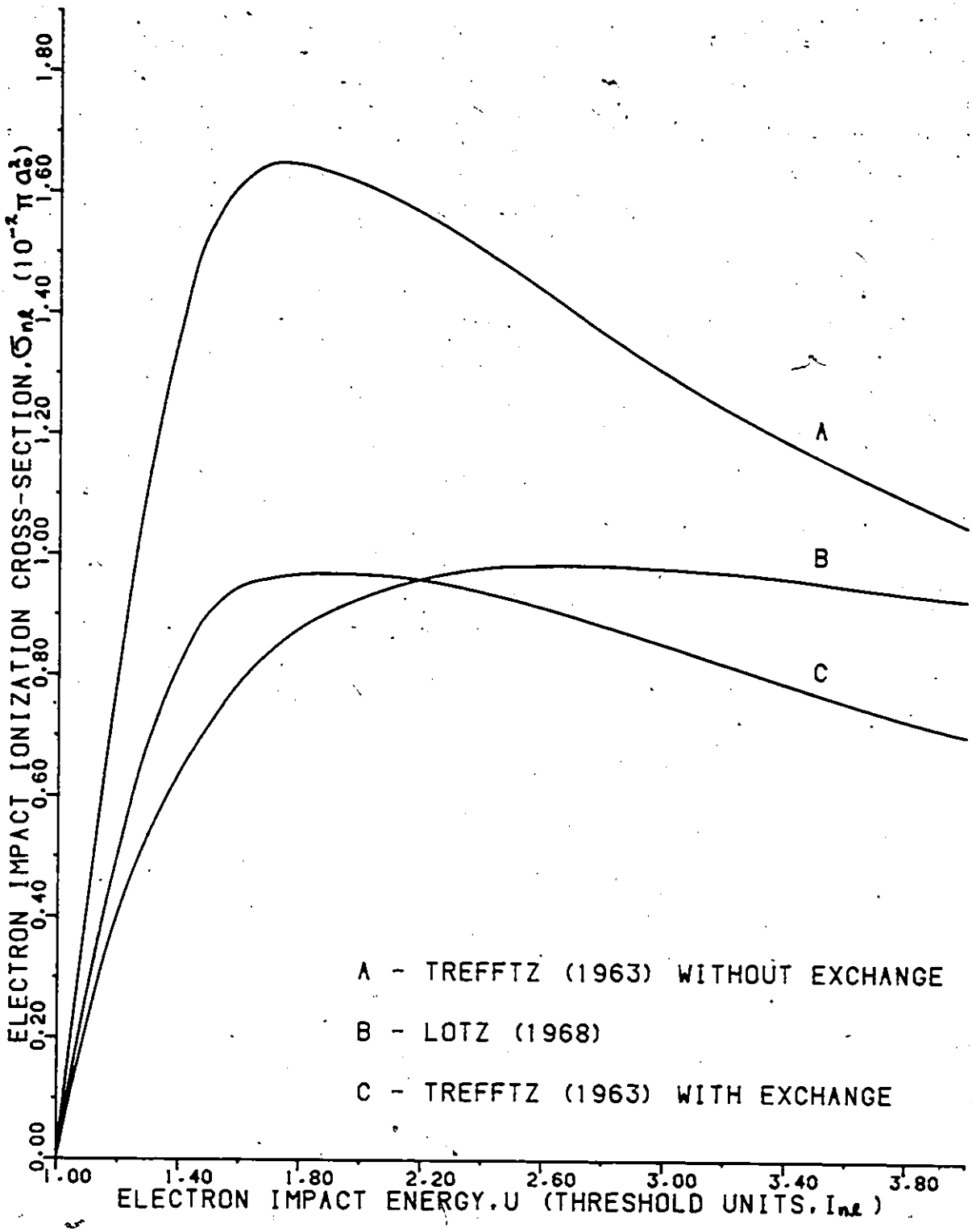

FIGURE 5.1 - ELECTRON IMPACT IONIZATION CROSS-SECTION OF THE 2S STATE OF O VI.

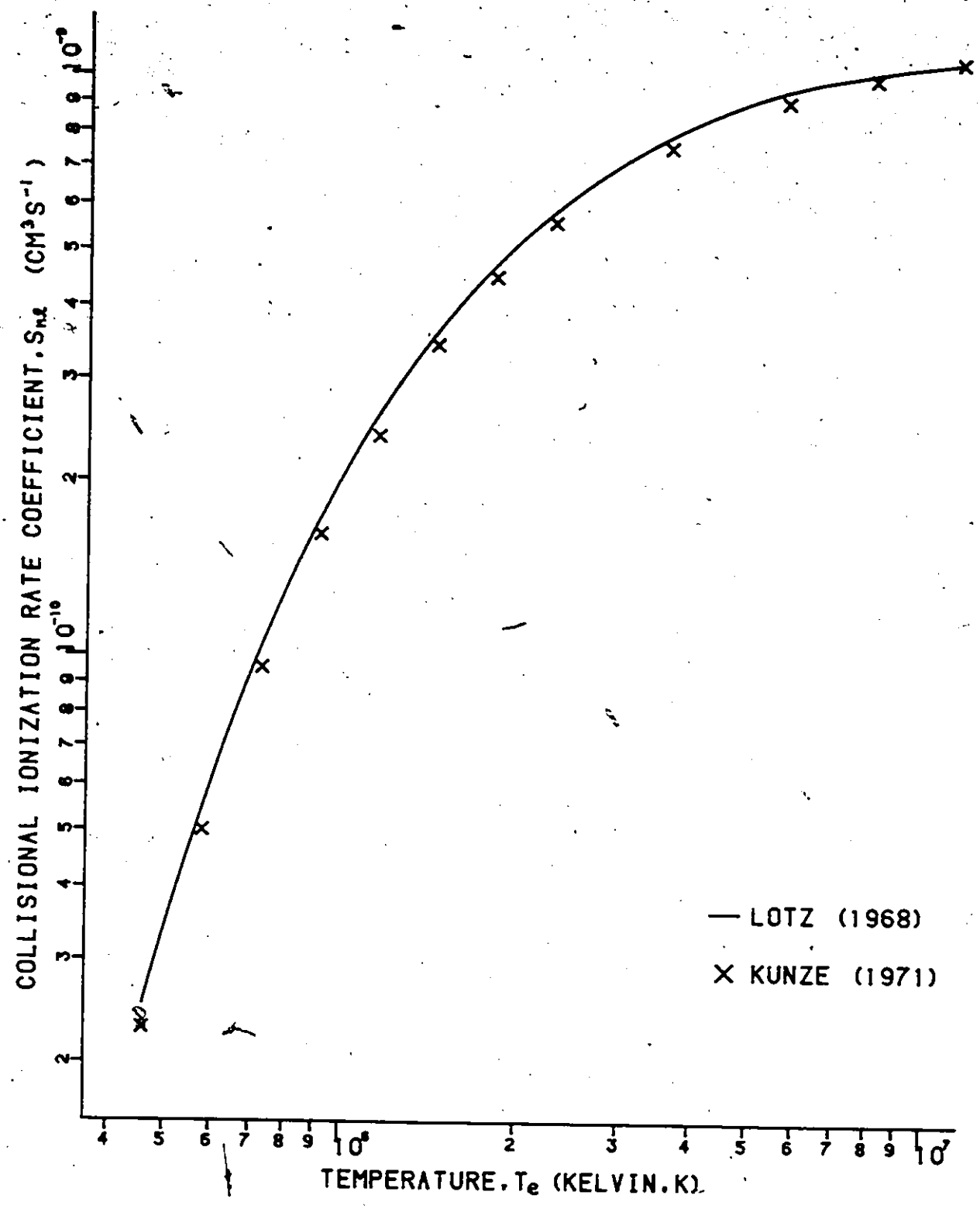

FIGURE 5.2 - COLLISIONAL IONIZATION RATE COEFFICIENT OF THE 2S STATE OF O VI.

with results obtained from Lotz's formula (5.9) to within 15% as shown in Fig.5.2, and with unpublished calculations of Schwartz (1971), mentioned by Kunze, to within ~10%.

3.2. Excited states

According to Kunze, eq.(5.10) is also applicable to excited states; results of Schwartz (1971) on the 2p state of O VI can be approximated to within ~20% with eq.(5.10). However, it should be noted that as n increases, I_{nl} decreases and the range of validity of this equation is accordingly reduced.

4. RATE COEFFICIENTS OF THE EXCITED STATES

The applicability of Kunze's semi-empirical expression to excited states suggests that Lotz's formula (5.9) may also be used to calculate the collisional ionization rate coefficients of the excited states of the ions C IV, N V, and O VI. Assuming that the parameter a_{2s} is a constant for all states nl, it is then possible to generalize eq.(5.9) to excited states as follows:

$$S_{nl}(T) = \frac{2.4 \times 10^{-5}}{I_{nl}\sqrt{T}} E_1\left(157{,}890 \frac{I_{nl}}{T}\right) cm^3 s^{-1} \quad \ldots(5.11)$$

where I_{nl}, the ionization potential of the electron in state nl, is in Rydbergs and T in K. In Fig.5.3, we compare the rate coefficients of the 2p state of O VI and the 5d state of N V as calculated with Kunze's eq.(5.10) and Lotz's eq.(5.11). The results are in close agreement; Lotz's rate coefficients are slightly greater than the ones calculated

with Kunze's equation, except at very high values of T ($kT > \sim 10\, I_{n\ell}$) where the coefficients diverge substantially.

The reason for this agreement becomes evident when a detailed investigation of equations (5.10) and (5.11) is carried out. The collisional ionization rate coefficient of state $n\ell$ can be written as

$$S_{n\ell}(\theta) = \frac{3.0 \times 10^{-6}}{I_{n\ell}^{3/2}\sqrt{\theta}}\, e^{-\theta} f(\theta) \qquad \ldots(5.12)$$

where $\theta = I_{n\ell}/kT$ and $f(\theta)$ is a factor which has different analytical forms in Lotz's and Kunze's work: in Lotz's eq.(5.11), we have

$$f_L(\theta) = \theta e^{\theta} E_1(\theta)$$

$$\simeq 1 - \frac{1!}{\theta} + \frac{2!}{\theta^2} - + \cdots, \quad \theta \gg 1; \qquad \ldots(5.13)$$

Kunze's eq.(5.10) requires

$$f_K(\theta) = \frac{1 + \frac{1}{40}\left(\ln \frac{40}{\theta}\right)^3}{1 + \frac{3}{\theta}}. \qquad \ldots(5.14)$$

$f_L(\theta)$ is well-behaved for all values of θ, whereas $f_K(\theta)$ becomes negative for $\theta > \sim 1220$ ($kT < \sim I_{n\ell}/1220$). However, as can be seen in Fig.5.4 where we compare $f_L(\theta)$ with the positive part of $f_K(\theta)$, the two functions agree to within 20% in the region

$$\frac{1}{100} \leq \theta \leq 300$$

$$\left(\frac{I_{n\ell}}{300} \leq kT \leq 100\, I_{n\ell}\right). \qquad \ldots(5.15)$$

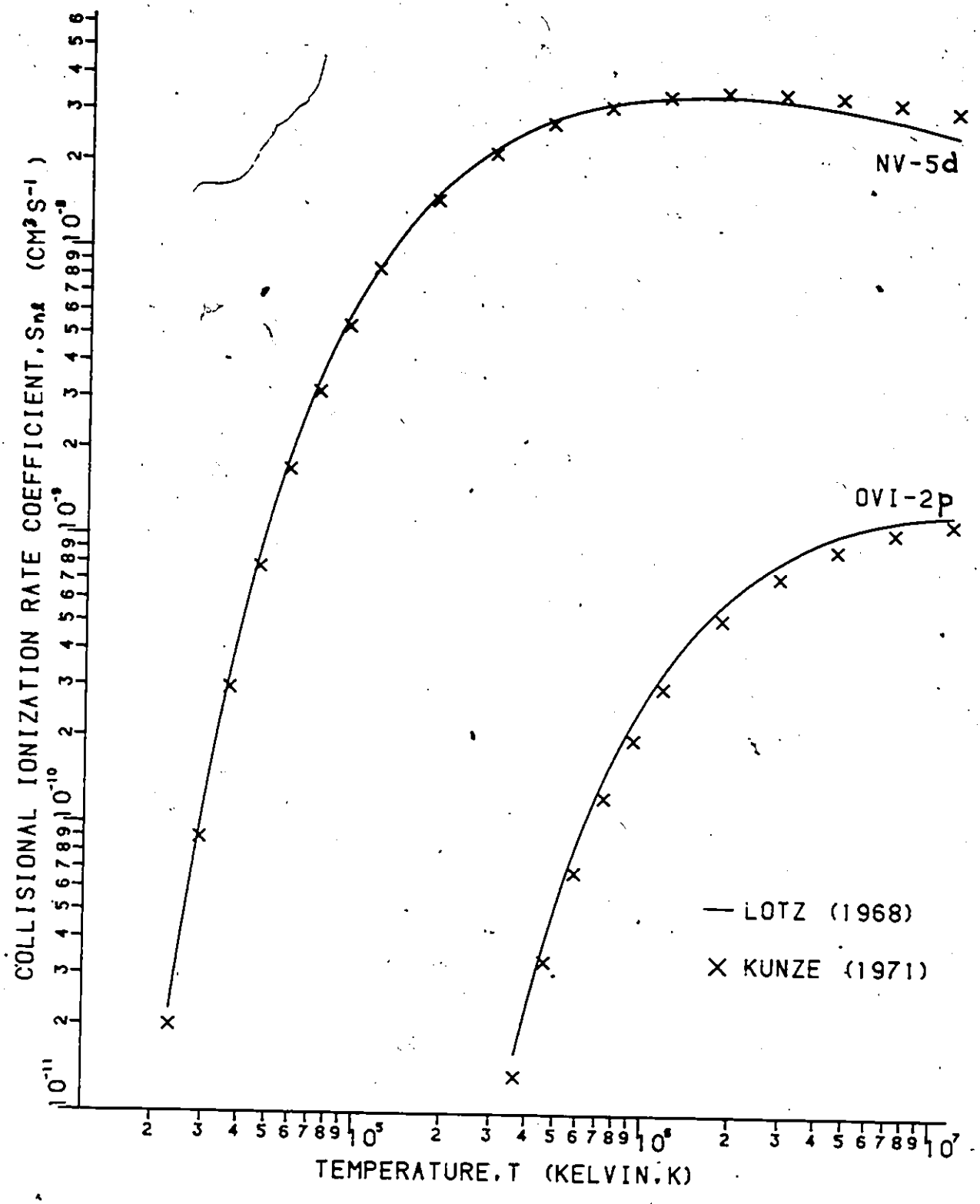

FIGURE 5.3 - COLLISIONAL IONIZATION RATE COEFFICIENTS OF THE 2p STATE OF O VI AND 5d STATE OF N V.

This is the region where equations (5.10) and (5.11) are usually applied. Kunze's estimated range of validity of eq.(5.10), viz.

$$\frac{I_{nl}}{10} \leq kT \leq 10\, I_{nl},$$

is well within the limits (5.15).

Lotz's semi-empirical formula (5.11) will be used in this work. There are many reasons which support this choice:

1. Lotz's formula is derived from a semi-empirical expression with three adjustable parameters which can be chosen such that all available exprerimental data can be reproduced. On the other hand, Kunze introduces an empirical correction factor

$$A(T) \sim \left(\ln \frac{40\,kT}{I_{nl}}\right)^3 + 40 \qquad \ldots(5.16)$$

in the rate coefficient which is not based on any known behavior of the cross-section or the rate coefficient.

2. Kunze's eq.(5.10) breaks down at low values of T; Lotz's formula remains well-behaved for all T.

3. The form of Lotz's equation is simpler and more aesthetic. The evaluation of the exponential integral poses no serious problem since well-known rational approximations to this function are available (Abramowitz and Stegun, 1965, p.231; Cody and Thacher, 1968).

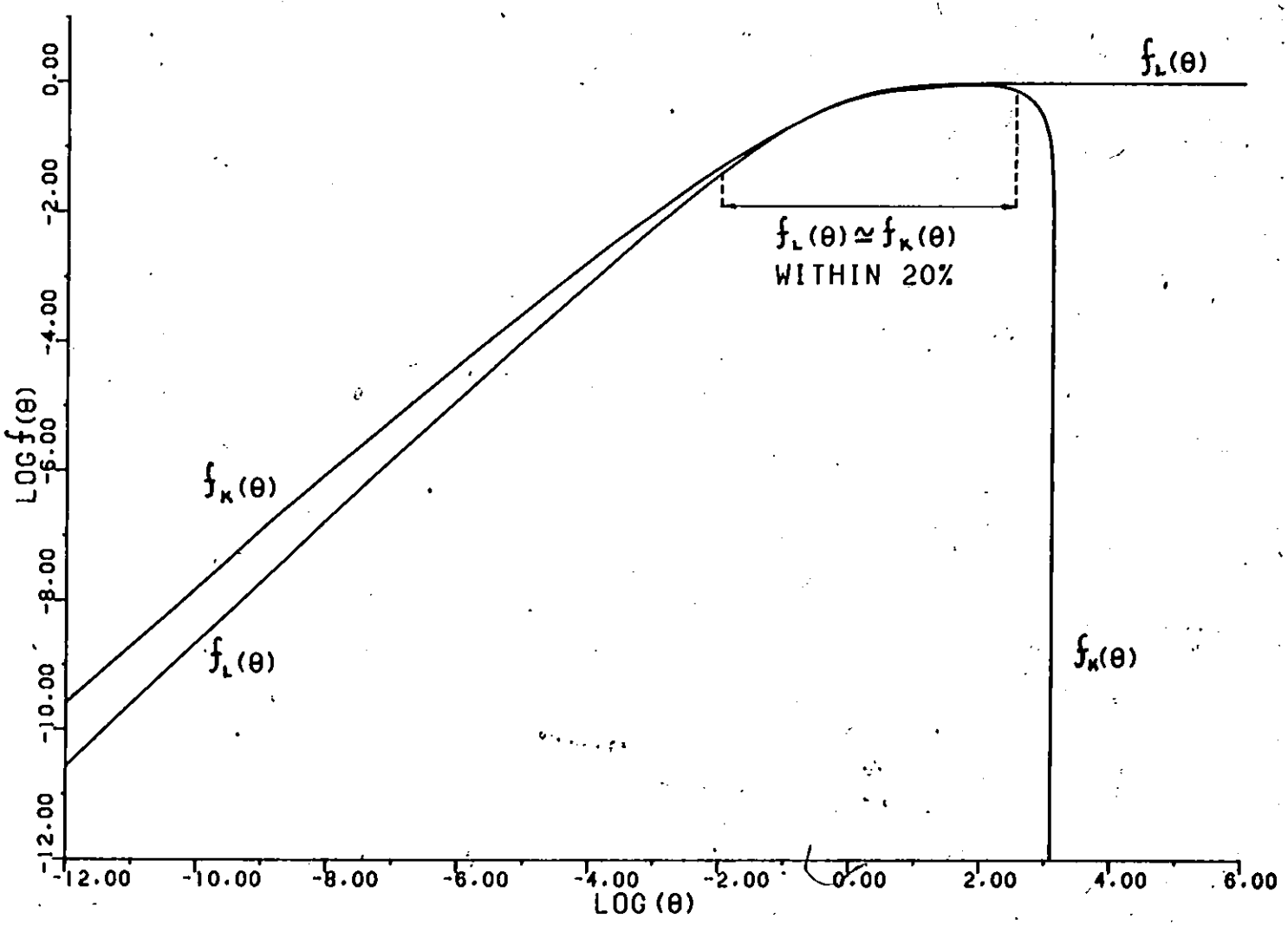

FIGURE 5.4 - COMPARISON OF THE POSITIVE PART OF THE FUNCTIONS $f_L(\theta)$ AND $f_K(\theta)$.

5. COMPARISON WITH HYDROGENIC VALUES

The rate coefficients of the average states n are obtained from the rate coefficients of the individual $n\ell$ states as follows. The cross-section of the average state n is computed with (Moiseiwitsch and Smith, 1968)

$$\sigma_n = \sum_{\ell} \frac{\omega_{n\ell}}{\omega_n} \sigma_{n\ell} \qquad \ldots(5.17)$$

where $\omega_{n\ell}$ and ω_n are the statistical weights of levels $n\ell$ and n respectively. Substituting for $\omega_{n\ell}$ and ω_n in eq.(5.17), we obtain

$$\sigma_n = \sum_{\ell} \frac{2\ell+1}{n^2} \sigma_{n\ell} . \qquad \ldots(5.18)$$

Since the rate coefficient is obtained from the cross-section by a straightforward integration over a Maxwellian energy distribution function, we then have

$$S_n(T) = \sum_{\ell} \frac{2\ell+1}{n^2} S_{n\ell}(T). \qquad \ldots(5.19)$$

In Fig.5.5, we compare the values of $S_n(T)$ for the lithium-like ion C IV calculated using eq.(5.19) with the values for a hydrogenic ion with Z = 4 calculated with a semi-empirical formula due to Drawin (1961, 1962, 1963, 1966) (see Section 4 of Chapter II). The lithium-like rate coefficients are observed to be closely hydrogenic. However, the dif-

ferences between the two coefficients are more pronounced at low temperatures and small n.

6. ACCURACY OF THE RATE COEFFICIENTS

Lotz (1968)[6] estimates the error on the ground state cross-sections calculated with eq.(5.1) to be not higher than $^{+40}_{-30}$ %. The rate coefficients of the excited states calculated with eq.(5.11) should also be reasonably good estimates of the actual coefficients due to the close agreement between the calculations of Lotz and Kunze for $I_{n\ell}/300 \leq kT \leq 100\ I_{n\ell}$. Furthermore, the lithium-like rate coefficients are within a factor of 1.5 of the corresponding hydrogenic values for $T \geq 4000$ K. Accordingly, we estimate the rate coefficients of the excited states of lithium-like ions calculated with eq.(5.11) to be within a factor of two or better of the actual coefficients provided that inner shell ionization is negligible. According to Kunze (1971), this should be the case for $kT \leq 10\ I_{n\ell}$.

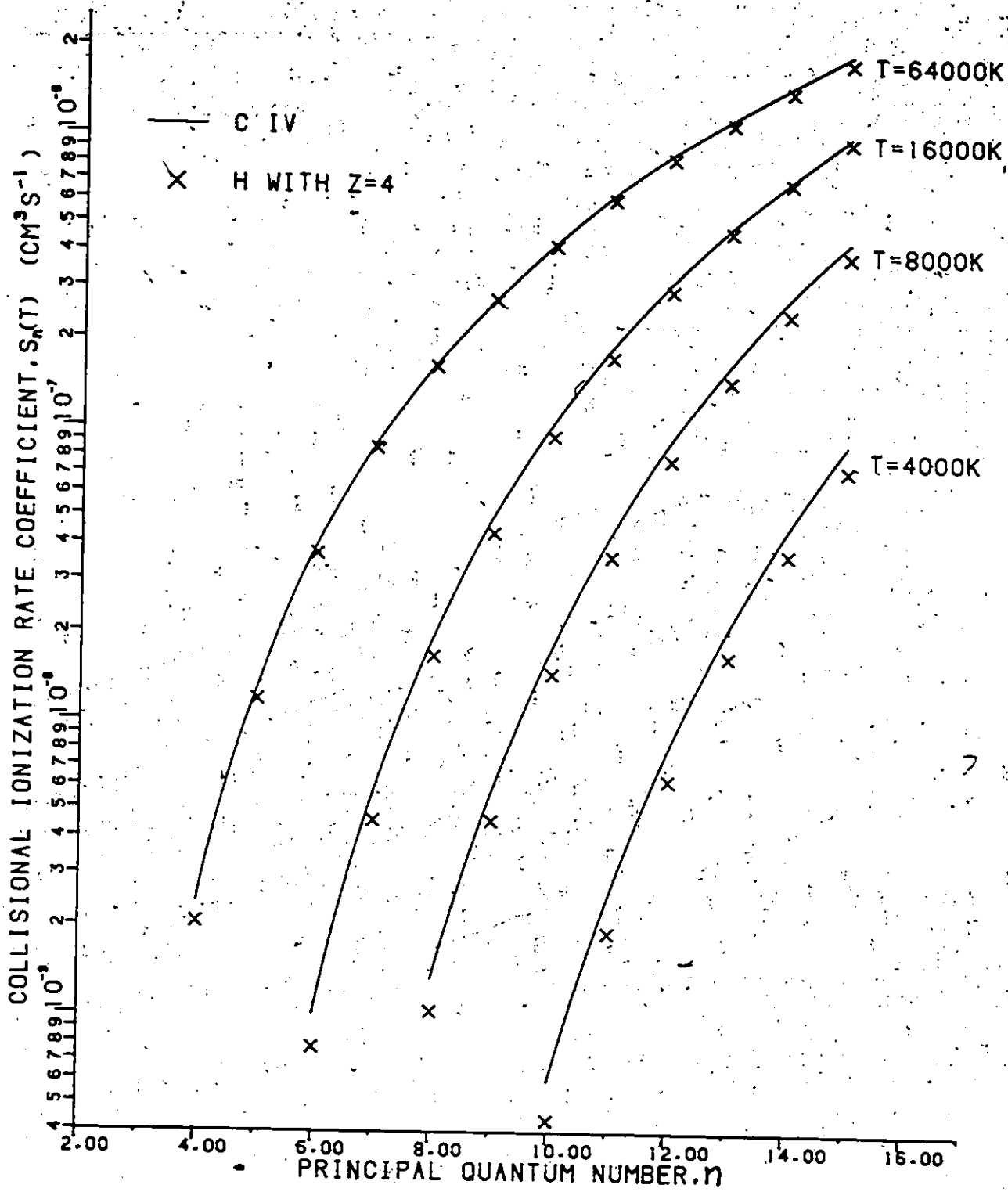

FIGURE 5.5 - COMPARISON OF THE COLLISIONAL IONIZATION RATE COEFFICIENTS OF THE LITHIUM-LIKE ION C IV AND A HYDROGENIC ION WITH Z=4.

Chapter VI

C IV, N V, AND O VI: COLLISIONAL EXCITATION RATE COEFFICIENTS

1. INTRODUCTION

A very large number of excitation cross-sections is required in this work. The cross-sections must be known as a function of the kinetic energy of the impacting electron for each of the 496 transitions possible between the 32 states considered in our calculations. Unfortunately, the available data are but a very small fraction of the required cross-sections.

A good number of approximations have been devised to calculate excitation cross-sections (Moiseiwitsch and Smith, 1968). Consequently, the degree of accuracy of the available data is not uniform; it depends on the approximation that is used. Some of the more important references on the electron impact excitation of the lithium-like ions C IV, N V, and O VI are given below:

Bely (1962): O VI - 2s -> 2p, 3p;

Bely (1965): Li isoelectronic sequence (Iso) - 2s -> np;

Burke et al. (1966): N V - 2s -> 2p, 3s, 3p, 3d;
2p -> 3s, 3p, 3d;
3s -> 3p, 3d; 3p -> 3d;

Bely (1966a): Iso - 2s -> np;

Bely (1966b): Iso - 2s -> ns, nd;

Moiseiwitsch and Smith (1968): review article;

Bely and Van Regemorter (1970): review article;

Davis and Morin (1970): N V - 5p -> 6s; 6s -> 7p; 6p -> 7s, 7d;

Boland et al. (1970): N V - 2s -> 2p, 3s, 3p, 3d, 4p;

Bely and Petrini (1970): Iso - 2p -> ns, np, nd;

Kunze and Johnston (1971): N V - 2s -> 2p, 3s, 3p, 3d, 4s, 4p, 4d;

O VI - 2s -> 2p, 3s, 3p, 3d, 4s, 4p, 4d;

Flower (1971): N V - 2s -> 2p, 3s, 3p, 3d;

2p -> 3s, 3p, 3d;

Petrini (1972): Iso - 2s -> nf;

Bradbury et al. (1973): N V - 2s -> 2p;

Henry (1974): N V - 2s -> 3s, 3p, 3d;

Hayes (1975): N V - 2s -> 2p, 3s, 3p, 3d;

Presnyakov and Urnov (1975): O VI - 2s -> 3s; 2p -> 3s.

Most calculations have been carried out on the excitations from the ground state and the first excited state. Excitations from higher excited states have been neglected.

2. AVAILABLE DATA

2.1. Theoretical calculations

The most general work available on the excitation of the 2s and 2p states has been done by Bely with the relatively simple Coulomb-Born approximation. His work can be extrapolated to all values of n of the 2s -> ns, np, nd, nf and 2p -> ns, np, nd transitions of all lithium-like ions by a simple method (Bely, 1966a). Although Bely's calculations may not be as accurate as more sophisticated ones, the fact that a uniform set of cross-sections is obtained is a definite advantage espe-

cially since the actual values of the cross-sections are not known exactly.

Calculations on the excitation from higher excited states are very scarce. Burke et al. (1966) have carried out Coulomb-Born calculations on the 3s -> 3p, 3d and 3p -> 3d transitions of N V while Davis and Morin (1970), using a semiclassical approximation, have done calculations on the 5p -> 6s, 6s -> 7p, and 6p -> 7s, 7d transitions of N V. Both calculations should be used with caution.

Some of Burke's cross-sections for excitation from the 2s and 2p states have been shown to be in error: Norcross (1969) has found that all strong coupling calculations performed prior to 1969 can be expected to have large uncertainties; Burke carries out a strong coupling calculation for the 2s -> 3p transition. Bely and Petrini (1970) mention that Burke's cross-sections for the 2p -> 3p, 3d transitions are wrong due to a mistake in the final calculations; however, the results for the 2p -> 3s transition are correct. We should thus be careful when using the 3s -> 3p, 3d and 3p -> 3d cross-sections calculated by Burke et al.

The calculations of Davis and Morin, performed with a semiclassical approximation, will probably not have the same accuracy as cross-sections calculated with the Coulomb-Born approximation. However, Davis and Morin claim that their results should be in reasonable agreement with experiment.

Since 1970, calculations have been performed only on a few selected transitions from the 2s and 2p states; not even approximate calculations

for excitations from higher excited states have been made. The accuracy of the excitation cross-sections has been improved by including more sophisticated quantum mechanical effects in the approximations used. The resulting data are however less useful for our purposes since the cross-section values are calculated only for a very limited number of incident electron energies. Consequently, we will use the Coulomb-Born calculations of Bely and Petrini (Bely, 1966a, b; Bely and Petrini, 1970; Petrini, 1972) for excitation from the 2s and 2p states, especially since, as can be seen in Fig.6.1 and 6.2, the more sophisticated approximations do not affect the cross-sections significantly.

2.2. General calculations

Due to the lack of data, a general method of calculating excitation cross-sections with reasonable accuracy would be most useful. Unfortunately, the general formulas available are highly inaccurate and unreliable.

One of the best known approximation was obtained by Seaton (1962) by treating the collisional excitation as a radiative process. The semi-empirical formula obtained in this manner is applicable only to optically allowed transitions and is proportional to the absorption oscillator strength of the corresponding optical transition. Unfortunately, the formula is also proportional to an effective Gaunt factor $\bar{g}$ which has to be calculated for each individual transition and which is a function of the incident electron energy. Van Regemorter (1962) proposed using an average value $\bar{g} \sim 0.2$ for excitation of positive ions at low energies.

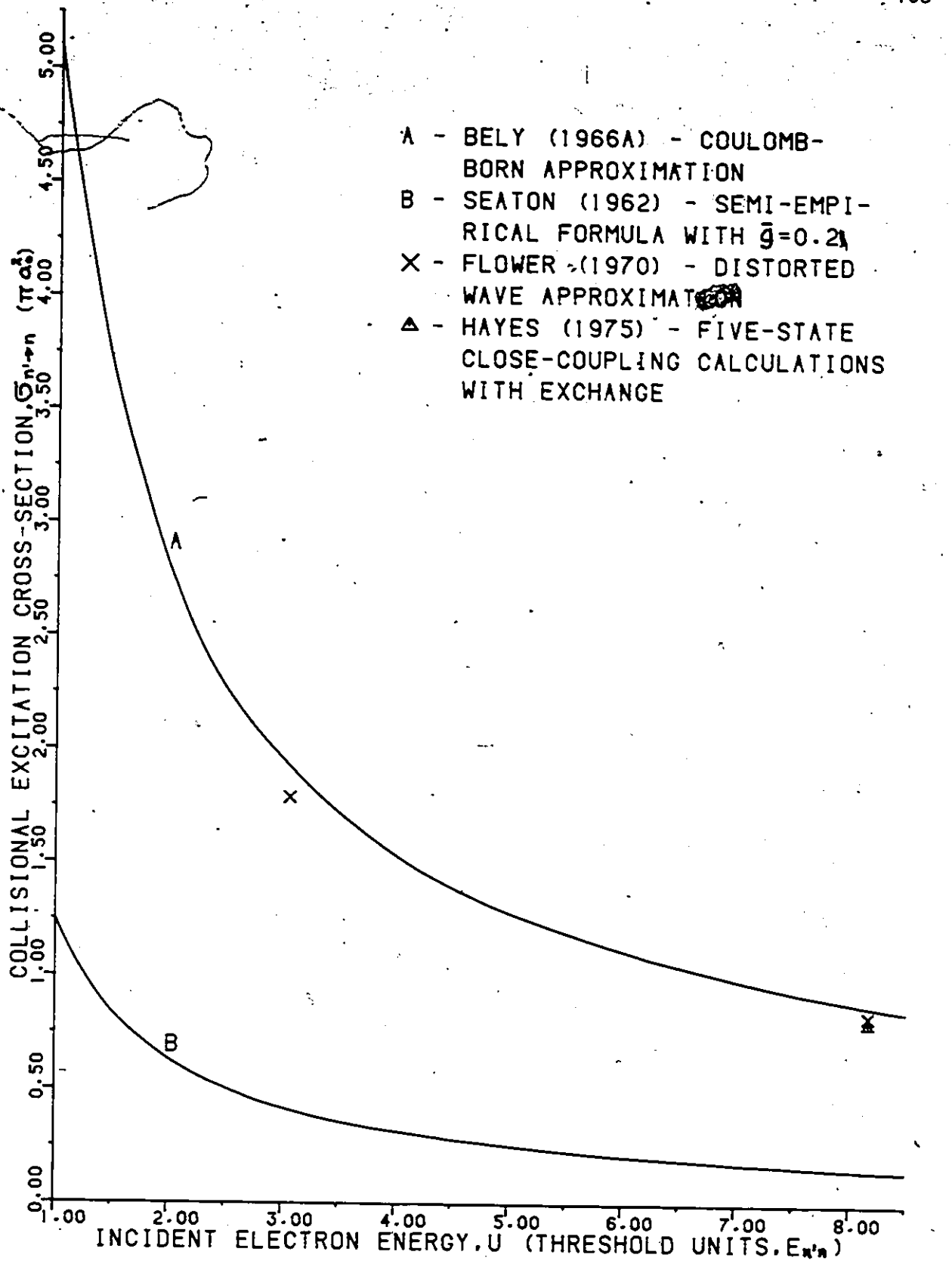

FIGURE 6.1 - ELECTRON IMPACT EXCITATION CROSS-SECTION OF THE 2s→2p TRANSITION IN N V AS CALCULATED WITH DIFFERENT APPROXIMATIONS.

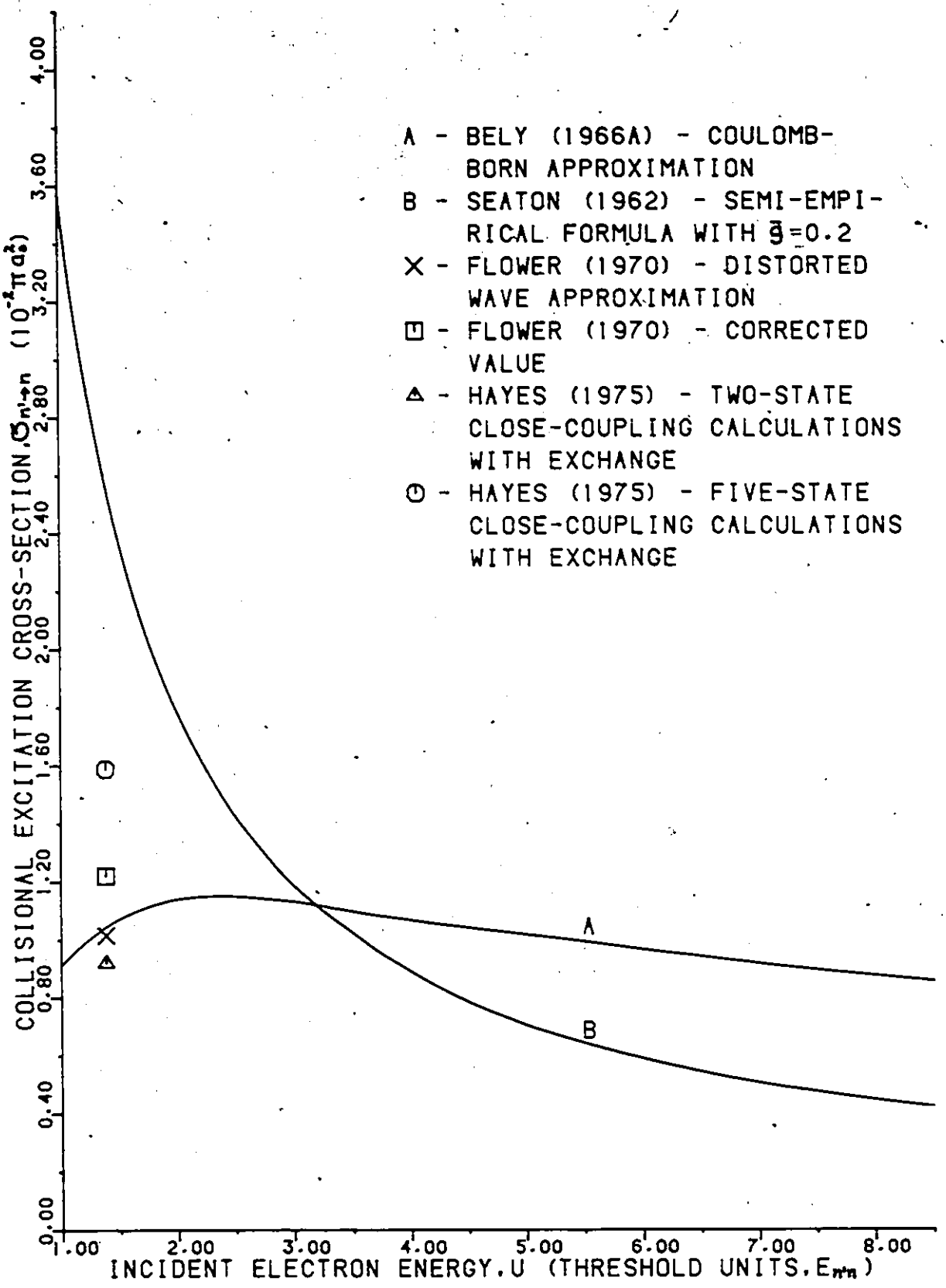

FIGURE 6.2 - ELECTRON IMPACT EXCITATION CROSS-SECTION OF THE 2s→3p TRANSITION IN N V AS CALCULATED WITH DIFFERENT APPROXIMATIONS.

In Fig.6.1 and 6.2, we compare the cross-sections for the 2s -> 2p and 2s -> 3p transitions of N V as calculated from Seaton's formula by putting $\bar{g} = 0.2$ with the values calculated by Bely (1966a) from the Coulomb-Born approximation. We see that Seaton's formula should be used with caution; results from it may be in considerable error (Bely and Van Regemorter, 1970). We also note that the asymptotic behavior of Seaton's formula is 1/E, which differs from the theoretically expected $\ell n E/E$ behavior (Massey and Burhop, 1952, p.140). The formula also has the disadvantage that it applies only to optically allowed transitions.

2.3. Hydrogenic values

The cross-sections for excitation from high-lying lithium-like quantum states could be estimated by using the corresponding hydrogenic cross-sections. However, this method can introduce large errors in the cross-sections. Bely (1966b) finds that optically forbidden transitions play an important role in lithium-like ions. For example, at low energy, the transitions from the 2s state of N V are dominated by the $\Delta\ell = 2$ forbidden transiion; the cross-section for the $\Delta\ell = 0$ forbidden transition is also close to the $\Delta\ell = 1$ optically allowed transition as is seen in Fig.6.3. On the other hand, the hydrogen cross-sections are dominated by the optically allowed transitions. This shows a fundamental difference between lithium-like and hydrogenic electron impact excitation cross-sections which indicates that straightforward application of hydrogenic cross-sections to high-lying lithium-like quantum states in not justified.

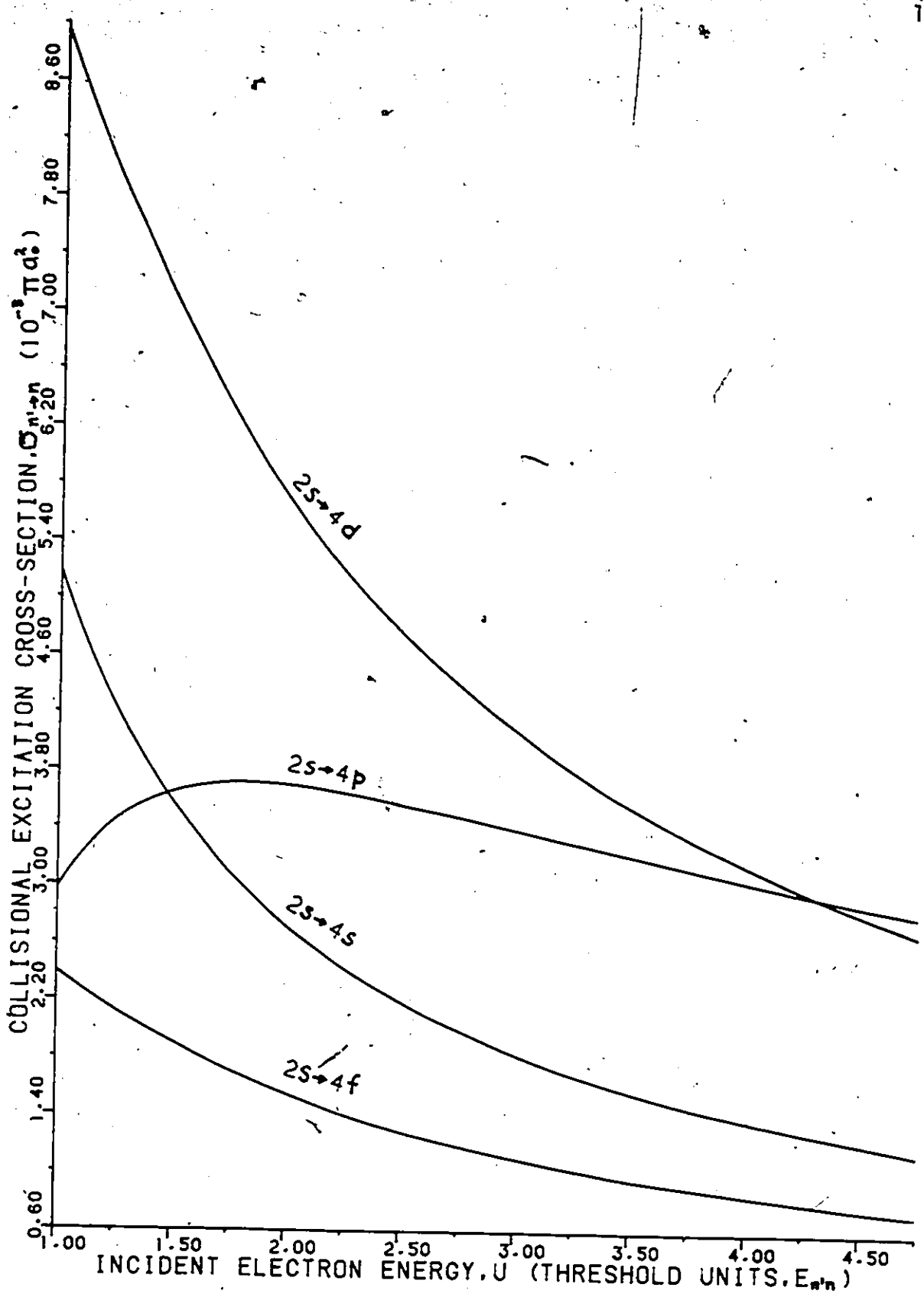

FIGURE 6.3 - ELECTRON IMPACT EXCITATION CROSS-SECTIONS OF THE 2s→4ℓ TRANSITIONS IN N V CALCULATED BY BELY (1966A,B) AND PETRINI (1972) WITH THE COULOMB-BORN APPROXIMATION.

2.4. Experimental measurements

Some experimental work on collisional excitation from the ground state of lithium-like ions has been done by Boland et al. (1970), Kunze and Johnston (1971), and Bradbury et al. (1973).

Bradbury et al. (1973) have studied the 2s -> 2p cross-section of N V in the energy range 125 to 400 eV. They found the measured cross-section to be consistently larger than the theoretical values of Bely (1966a) and Burke (1966) by an amount somewhat larger than the estimated theoretical error. However, there is a possibility of systematic errors and cascade effects.

Boland et al. (1970) have studied the rate coefficients of the 2s -> 2p, 3s, 3p, 3d, 4p transitions of N V at a temperature of 210,000 K. Their results agree within the experimental uncertainty of ~20% for relative values and 50% for absolute values with the results of Burke et al. (1966) and Taylor and Lewis (1965). There is also a possibility of errors that would tend to reduce the rate coefficients by a factor of up to two.

Kunze and Johnston (1971) have studied the rate coefficients of the 2s -> 2p, 3s, 3p, 3d, 4s, 4p, 4d transitions of N V and O VI at several temperatures. They estimate the maximum error in individual rate coefficients to be a factor of two for excitation to the n = 2 and 3 levels, and less than a factor of 2.5 for excitation to the n = 4 levels. The standard deviation of the experimental values from the theoretical ones

of Bely (1966a, b) averaged over N V, O VI, and Ne VIII is found to be less than 30% for excitation to the n = 2 and 3 levels, and less than 40% for excitation to the 4s level. The experimental rate coefficients for excitation to the 4p and 4d levels are consistently ~40% below the theoretical ones.

Some of the experimental rate coefficients are compared with the theoretical values of Bely (1966a, b) in Fig.6.4, 6.5, and 6.6. Within the experimental uncertainties, the results of Kunze and Johnston, and Boland et al. support the theoretical rate coefficients obtained in the Coulomb-Born approximation.

3. FIT OF THE DATA

Numerous empirical and semi-empirical formulas have been proposed to represent electron impact excitation cross-sections. For example, Mewe (1972) proposes a four parameter formula and tabulates the parameters for ground state excitation of the lithium and other isoelectronic sequences.

However, we will use modified forms of semi-empirical formulas proposed by Drawin (1963, 1964, 1966). There are several reasons for this choice:

1. Drawin did an extensive review of the work done in the field before proposing his formulas (Drawin, 1963, 1966).

2. His formulas have been found to be quite successful in representing known cross-sections.

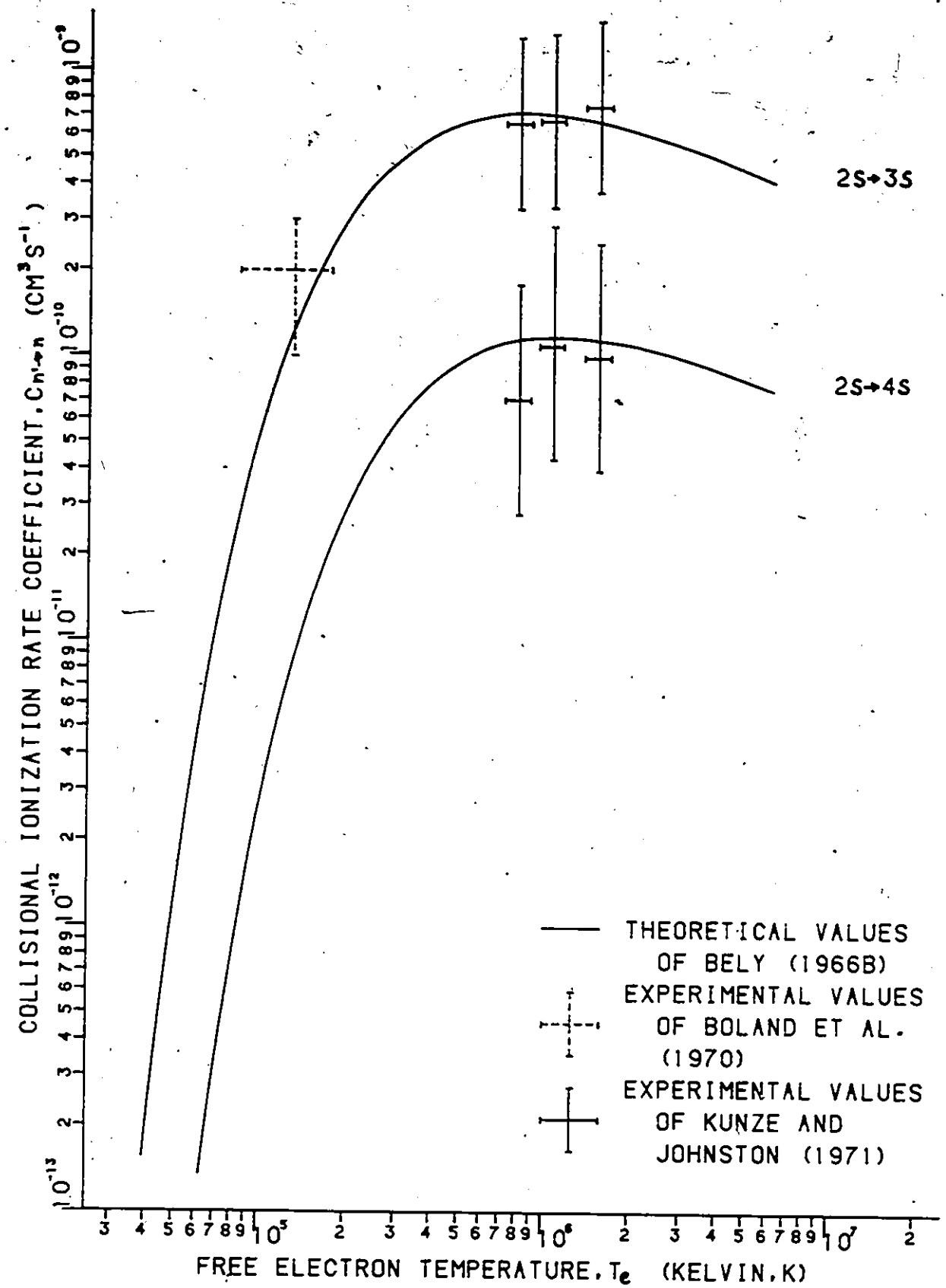

FIGURE 6.4 - ELECTRON IMPACT EXCITATION RATE COEFFICIENTS OF THE 2s→ns (n=3,4) TRANSITIONS OF N V.

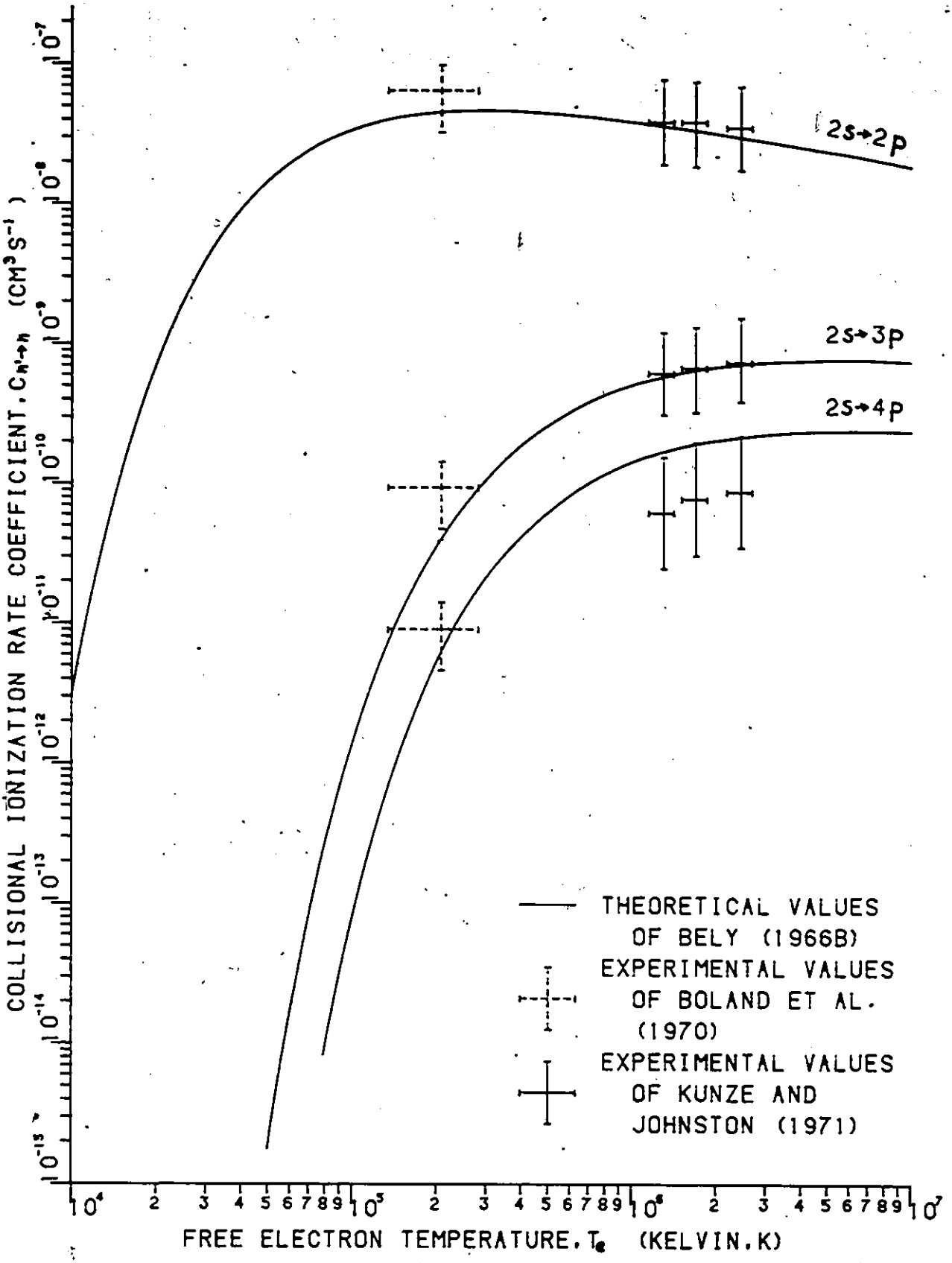

FIGURE 6.5 - ELECTRON IMPACT EXCITATION RATE COEFFICIENTS OF THE 2S→np (n=2,3,4) TRANSITIONS OF N V.

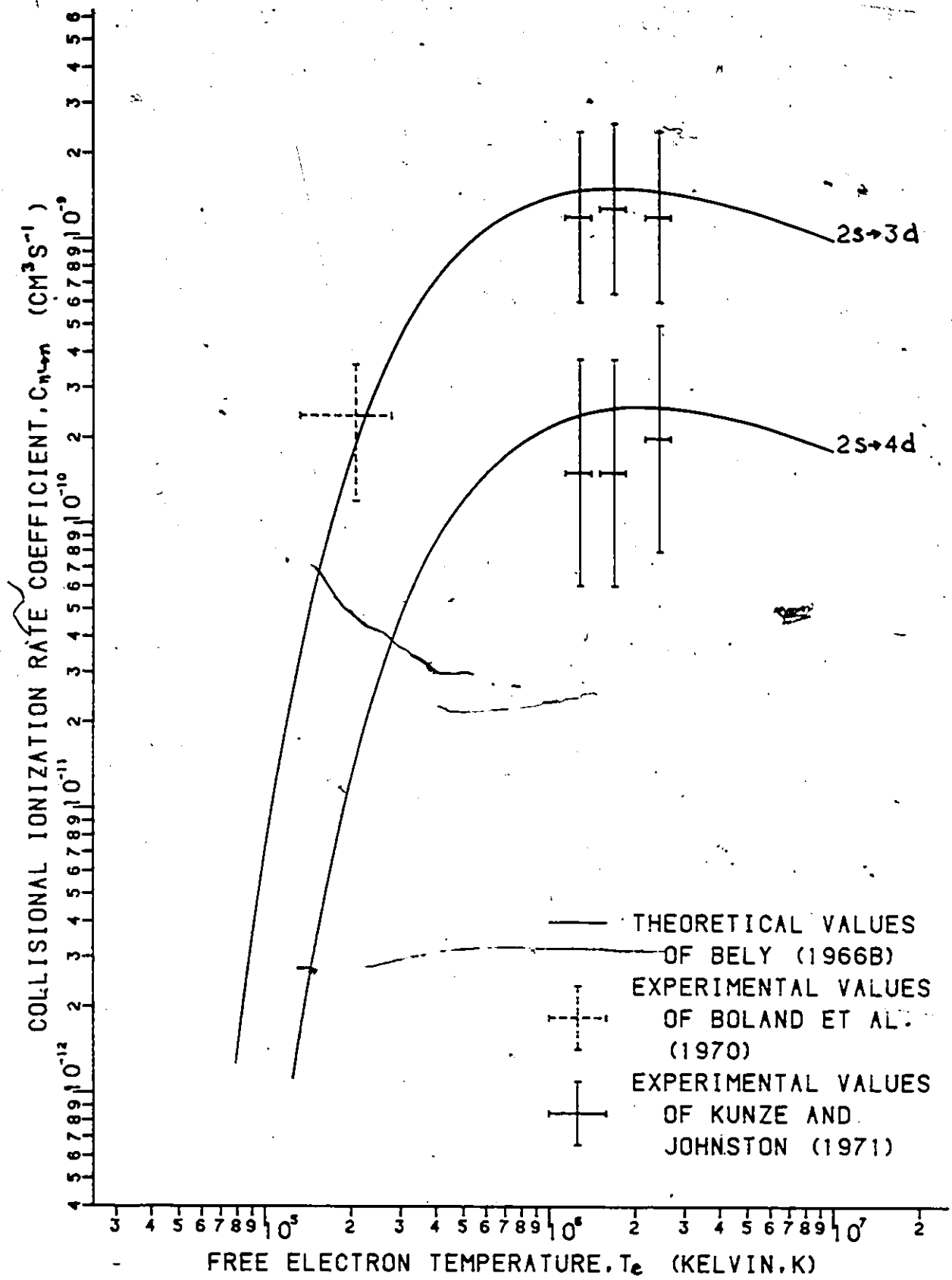

FIGURE 6.6 - ELECTRON IMPACT EXCITATION RATE COEFFICIENTS OF THE 2s→nd (n=3,4) TRANSITIONS OF N V.

3. Since his formulas have already been used for hydrogen, it will be easier to compare the lithium-like cross-sections with the corresponding hydrogenic values.

4. The parameters are not totally unknown since their hydrogenic values are known.

5. The integrals arising from the integration of this cross-section over a Maxwellian energy distribution to obtain the rate coefficient have already been evaluated.

Different formulas are used for optically allowed and forbidden transitions.

3.1. Optically allowed transitions

Drawin (1963, 1966) writes the cross-section for excitation of the n' -> n transition by electron impact as

$$\sigma_{n'\to n}(u) = 4\pi a_0^2 \frac{f_{n'\to n}}{E_{n'n}} g_{n'n}(u) \qquad \ldots(6.1)$$

where $E_{n'n}$ is the threshold energy for the excitation of the n' -> n transition in Rydbergs, $u = E/E_{n'n}$ is the energy of the impacting electron E in threshold units, $f_{n'\to n}$ is the absorption oscillator strength for the n' -> n transition, and a_0 is the Bohr radius. Drawin proposes the functions

$$g_{n'n}(u) = \alpha_{n'n} \frac{u-1}{u^2} \ln(1.25\beta u) \qquad \ldots(6.2)$$

for atoms, and

$$g_{n'n}(u) = \frac{\alpha_{n'n}}{u_{max}-2}\left(\frac{u_{max}-1}{u_{max}}\right)^2 \quad , 1 \leq u \leq u_{max}$$

$$= \alpha_{n'n}\frac{u-1}{u^2}\ln(1.25\beta u), \; u \geq u_{max} \qquad \ldots(6.3)$$

for ions since the cross-section for excitation of ions is observed to be finite at threshold. $\alpha_{n'n}$ and $\beta_{n'n}$ are parameters that are adjusted to the known data and u_{max} is the value of U at which $g_{n'n}(u)$ is maximum. The functions (6.2) and (6.3) are given in Fig.6.7 for $\alpha_{n'n} = 1$ and $\beta_{n'n} = 1$.

The actual behavior of the function $g_{n'n}(u)$ for ions is shown in Fig.6.8, with curves a, b, and c. Drawin's function (6.3), given by curve d, is seen to be a very crude approximation to the actual function at low energies. To improve the situation, we introduce a third adjustable parameter $\phi_{n'n}$ in the function $g_{n'n}(u)$ to account for the finite value of the cross-section at threshold. Fig.6.9 suggests how $\phi_{n'n}$ may be introduced in eq.(6.2): $\phi_{n'n}$ is the value of U at which the cross-section would be 0 if U could take values less than 1. We thus have

$$\phi_{n'n} < 1 \qquad \ldots(6.4)$$

and the function $g_{n'n}(u)$ becomes

$$g_{n'n}(u) = \alpha_{n'n}\frac{u-\phi_{n'n}}{u^2}\ln(1.25\beta_{n'n}u). \qquad \ldots(6.5)$$

The function $g_{n'n}(u)$ for atoms, eq.(6.2), which is 0 at threshold, is then a special case of eq.(6.5) with $\phi_{n'n} = 1$.

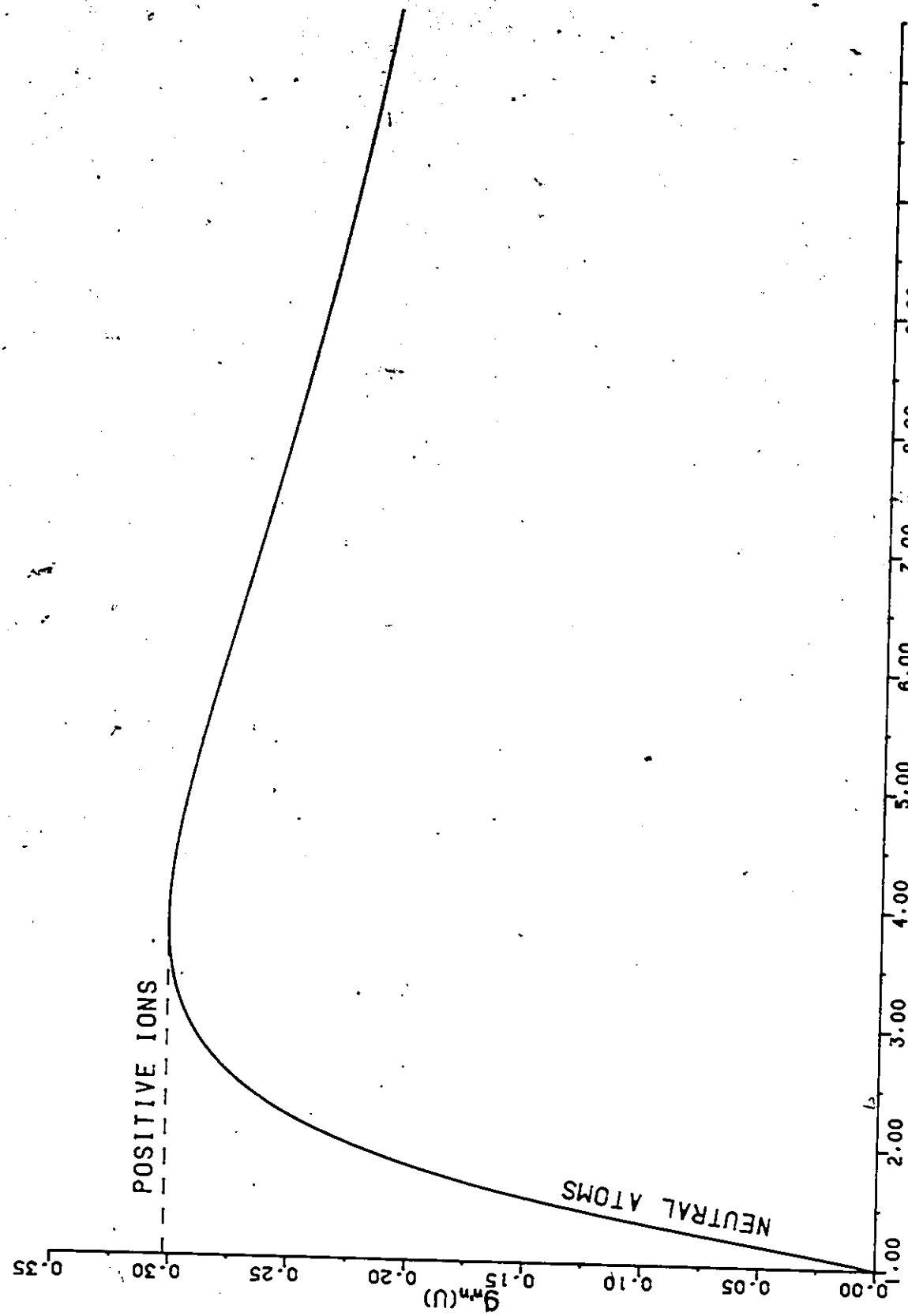

FIGURE 6.7 - DRAWIN'S FUNCTION $g_{n'n}(U)$ WITH $\alpha_{n'n}=1$ AND $\beta_{n'n}=1$.

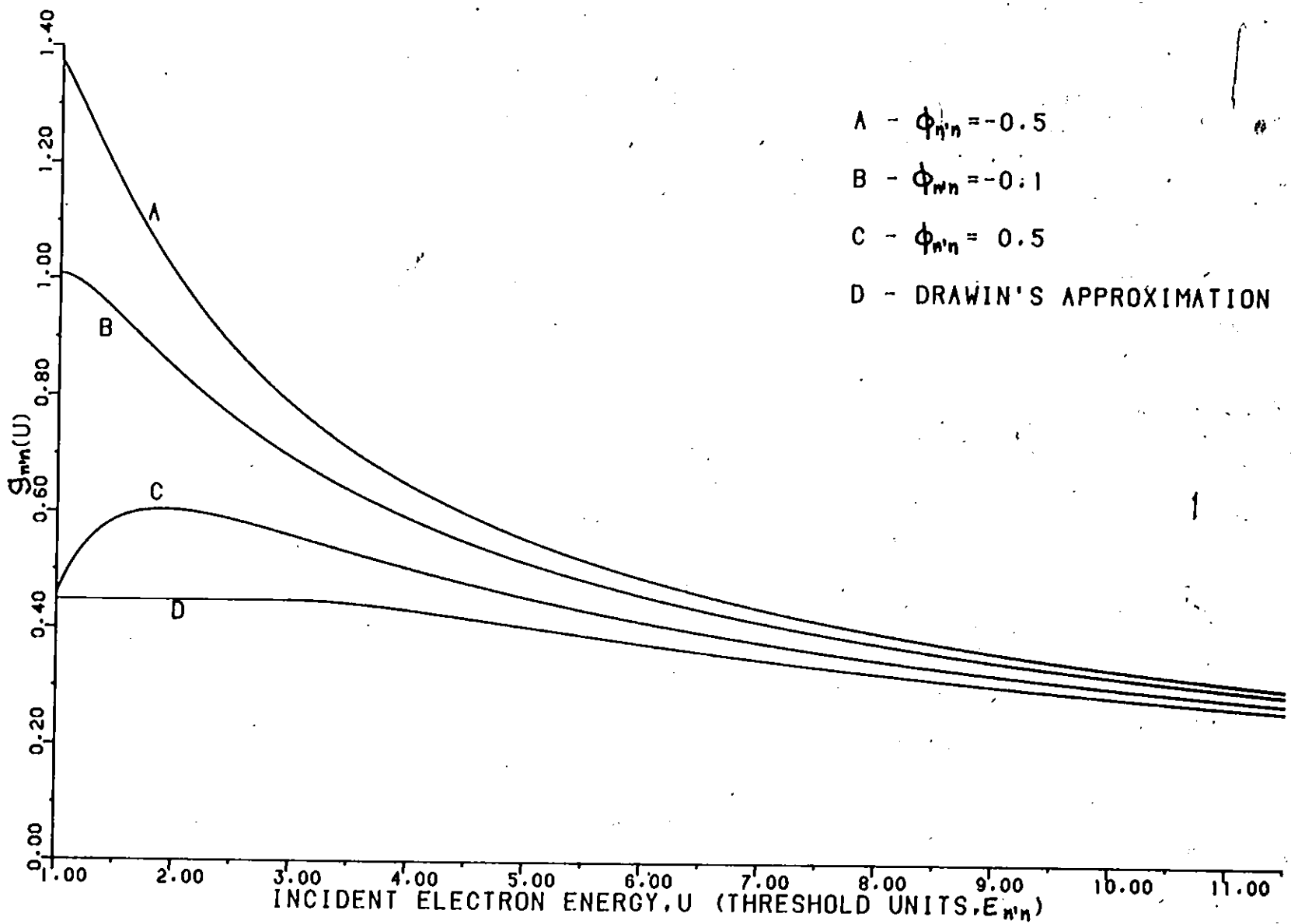

FIGURE 6.8 - COMPARISON OF THE FUNCTION $g_{n'n}(U)$ FOR $\alpha_{n'n}=1$, $\beta_{n'n}=2$, AND VARIOUS VALUES OF $\phi_{n'n}$ WITH THE DRAWIN APPROXIMATION TO $g_{n'n}(U)$ FOR POSITIVE IONS.

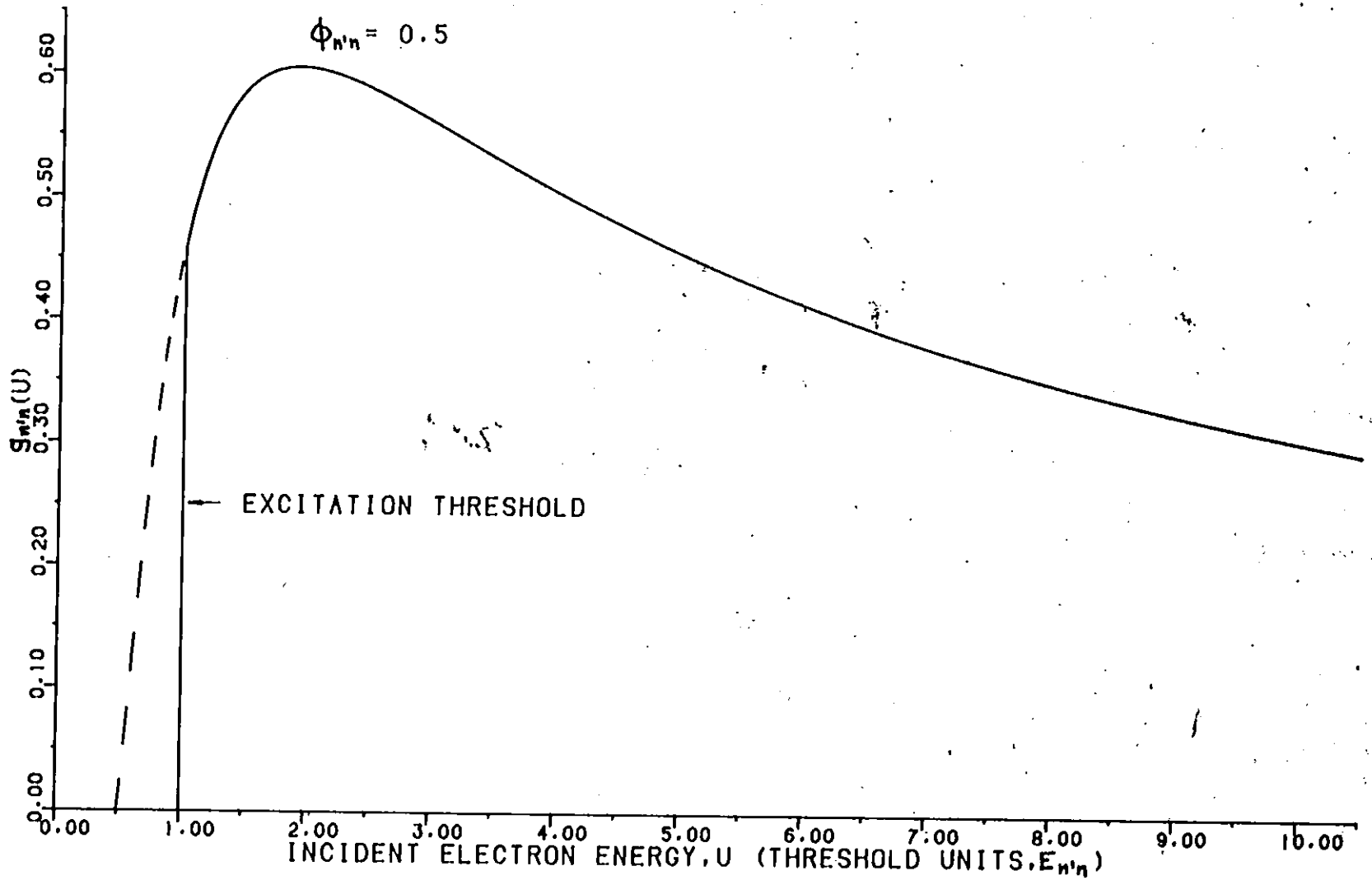

FIGURE 6.9 - BASIS FOR THE INTRODUCTION OF THE PARAMETER $\phi_{n'n}$ IN EQ. (6.2).

For the sake of simplicity in writing down the equations, we now drop the suffixes on the parameters $\alpha_{n'n}$, $\beta_{n'n}$, and $\phi_{n'n}$; however, it should be understood that there is a different set of parameters for each transition. The cross-section for excitation of the optically allowed transition n' -> n by electron impact can then be written as

$$\sigma_{n'\to n}(u) = 4\pi a_o^2 \frac{f_{n'\to n}}{E_{n'n}^2} \alpha \frac{u-\phi}{u^2} \ln(1.25\beta u) \quad \ldots(6.6)$$

where $E_{n'n}$ is in Rydbergs.

3.2. Forbidden transitions

Drawin (1963, 1964, 1966) has proposed the following expression for the cross-section for electron impact excitation of the optically forbidden transition n' -> n in which no change of multiplicity occurs:

$$\sigma_{n'\to n}(u) = 4\pi a_o^2 \, Q_{n'n} \frac{u-1}{u^2} . \quad \ldots(6.7)$$

An obvious generalization of this equation to cross-sections which are finite at threshold is

$$\sigma_{n'\to n}(u) = 4\pi a_o^2 \, Q_{n'n} \frac{u-\phi_{n'n}}{u^2} . \quad \ldots(6.8)$$

The parameter $Q_{n'n}$ shows large variations in value.

We wish to obtain a slowly varying parameter $\alpha_{n'n}$ from $Q_{n'n}$ by factoring out its highly varying part. For allowed transitions, one has

$$Q_{n'n}^{\text{allowed}} = \frac{f_{n'\to n}}{E_{n'n}^2} \alpha_{n'n} . \quad \ldots(6.9)$$

By looking at the values of $Q_{n'n}$ for the forbidden transitions of the hydrogen atom calculated by Kingston and Lauer (1966a, b), and by analogy with eq.(6.9), we find that if, for forbidden transitions, we take

$$Q_{n'n}^{\text{forbidden}} = \frac{1}{E_{n'n}^2} \left(\frac{n'}{n}\right)^3 \alpha_{n'n}, \qquad \ldots(6.10)$$

the parameter $\alpha_{n'n}$ then varies slowly.

Dropping the suffixes on the parameters $\alpha_{n'n}$ and $\phi_{n'n}$, we can then write the cross-section for electron impact excitation of the forbidden transition n' -> n in which no change of multiplicity occurs as

$$\sigma_{n'\to n}(u) = 4\pi a_o^2 \left(\frac{n'}{n}\right)^3 \frac{\alpha}{E_{n'n}^2} \frac{u-\phi}{u^2} \qquad \ldots(6.11)$$

where $E_{n'n}$ is in Rydbergs.

3.3. Fitting procedure

The adjustable parameters of eqs.(6.6) and (6.11) are determined by fitting the available data to these expressions with a least squares method (see Appendix D). The sum of the square of the relative differences between the actual and the fit values of the cross-sections is minimized with respect to the fit parameters. The resulting minimization conditions are non-linear equations in the parameters α, β, and ϕ for eq.(6.6), and α and ϕ for eq.(6.11). These equations are solved by an iterative procedure.

3.4. Fit parameters

The fit parameters obtained for the forbidden transitions 2s -> ns, nd, nf and 2p -> np of the ion N V are given in Fig.6.10 and 6.11. The fit parameters of the allowed transitions 2s -> np and 2p -> ns, nd of the ion N V are given in Fig.6.12, 6.13, and 6.14.

In general, a smooth variation of the parameters is observed as n increases. For forbidden transitions, α has a highly regular behavior, whereas the values of ϕ are more scattered; this is especially evident for those parameters which have been obtained from cross-sections extrapolated with Bely's method. The parameters α, β, and ϕ for allowed transitions also exhibit a regular behavior; however, the 2p -> nd parameters show some degree of scattering.

Based on Fig.6.10 to 6.14, we can expect that, as a general rule, the parameters within a spectral series will vary smoothly as n changes. Some of the parameters of the above transitions have accordingly been corrected. Most of the parameters which need correction come from cross-sections which have been obtained with Bely's extrapolation procedure. In most cases, the parameters which have been obtained directly from Bely's calculations need very little correction. However, it should be noted that since Bely gives only a few cross-section values at low values of U close to the threshold, some scattering of the parameters is to be expected; this is due to the fact that a small variation in the cross-sections will cause a large variation in the parameters.

The final values of the parameters of the ions C IV, N V, and O VI after correction are given in Tables 6.1, 6.2, and 6.3 for forbidden transitions, and in Tables 6.4, 6.5, and 6.6 for allowed transitions.

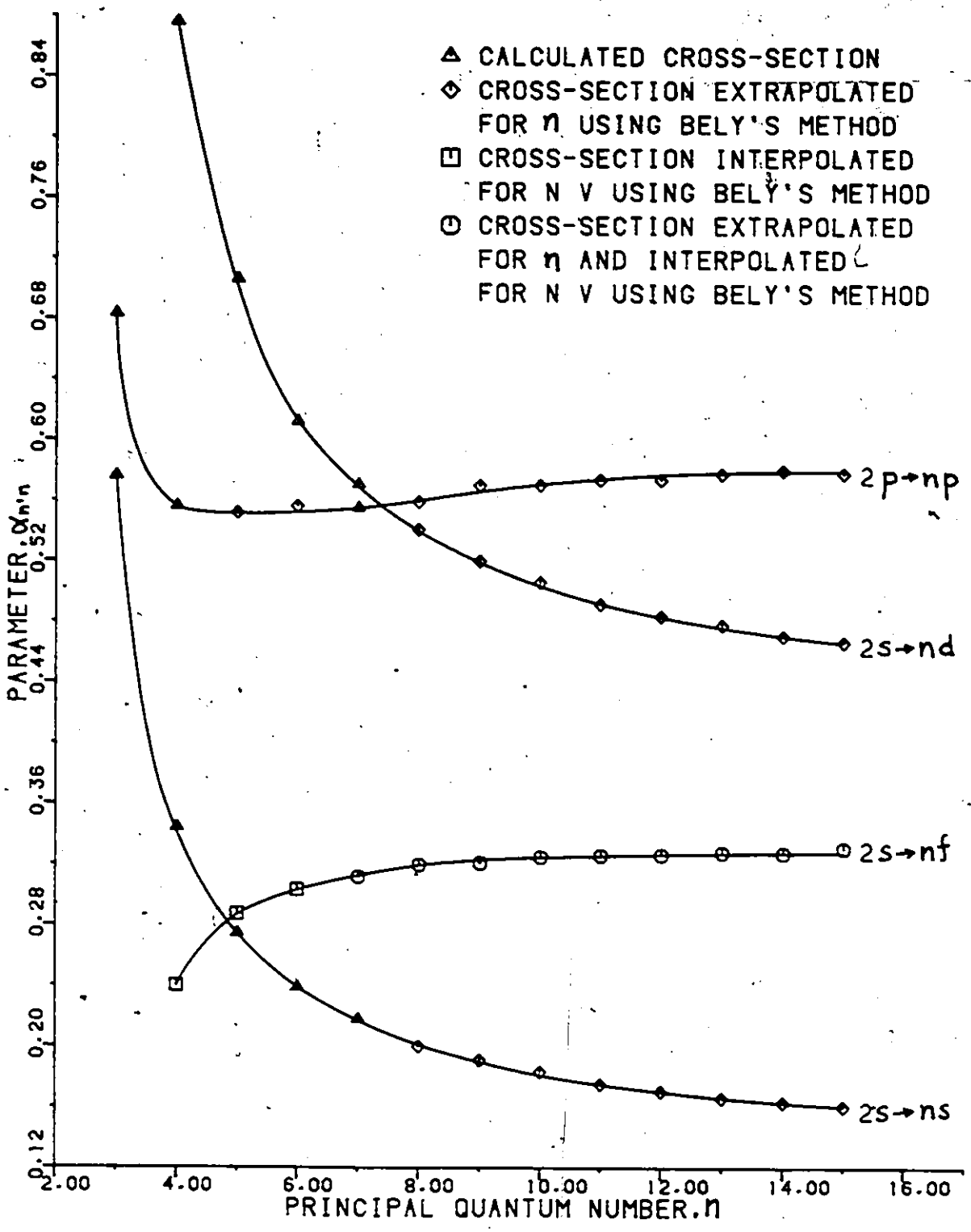

FIGURE 6.10 - KNOWN VALUES OF THE PARAMETER $\alpha_{n'n}$ FOR THE FORBIDDEN TRANSITIONS OF N V FROM THE WORKS OF BELY (1966B), BELY AND PETRINI (1970), AND PETRINI (1972).

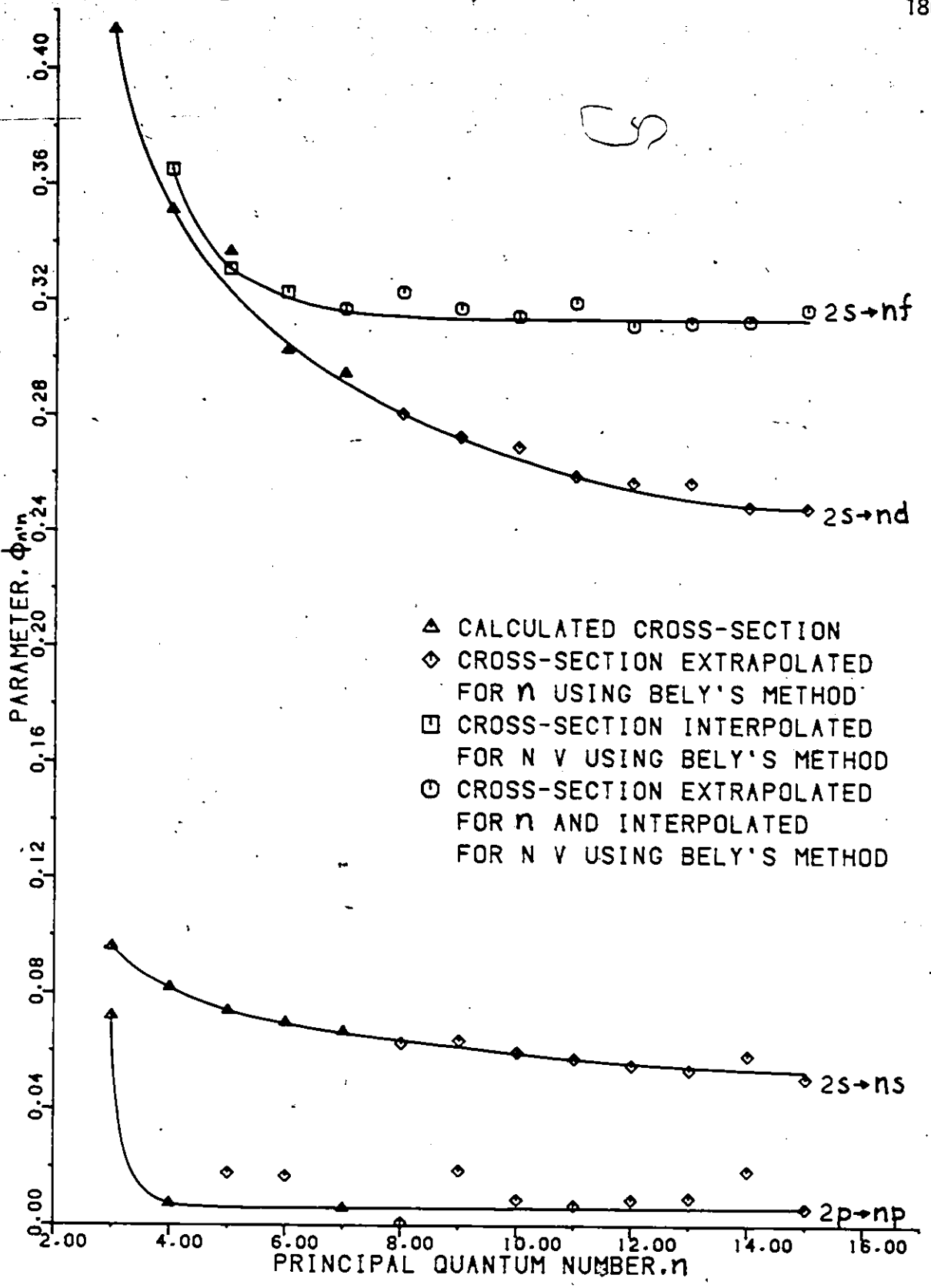

FIGURE 6.11 - KNOWN VALUES OF THE PARAMETER $\phi_{n'n}$ FOR THE FORBIDDEN TRANSITIONS OF N V FROM THE WORKS OF BELY (1966B), BELY AND PETRINI (1970), AND PETRINI (1972).

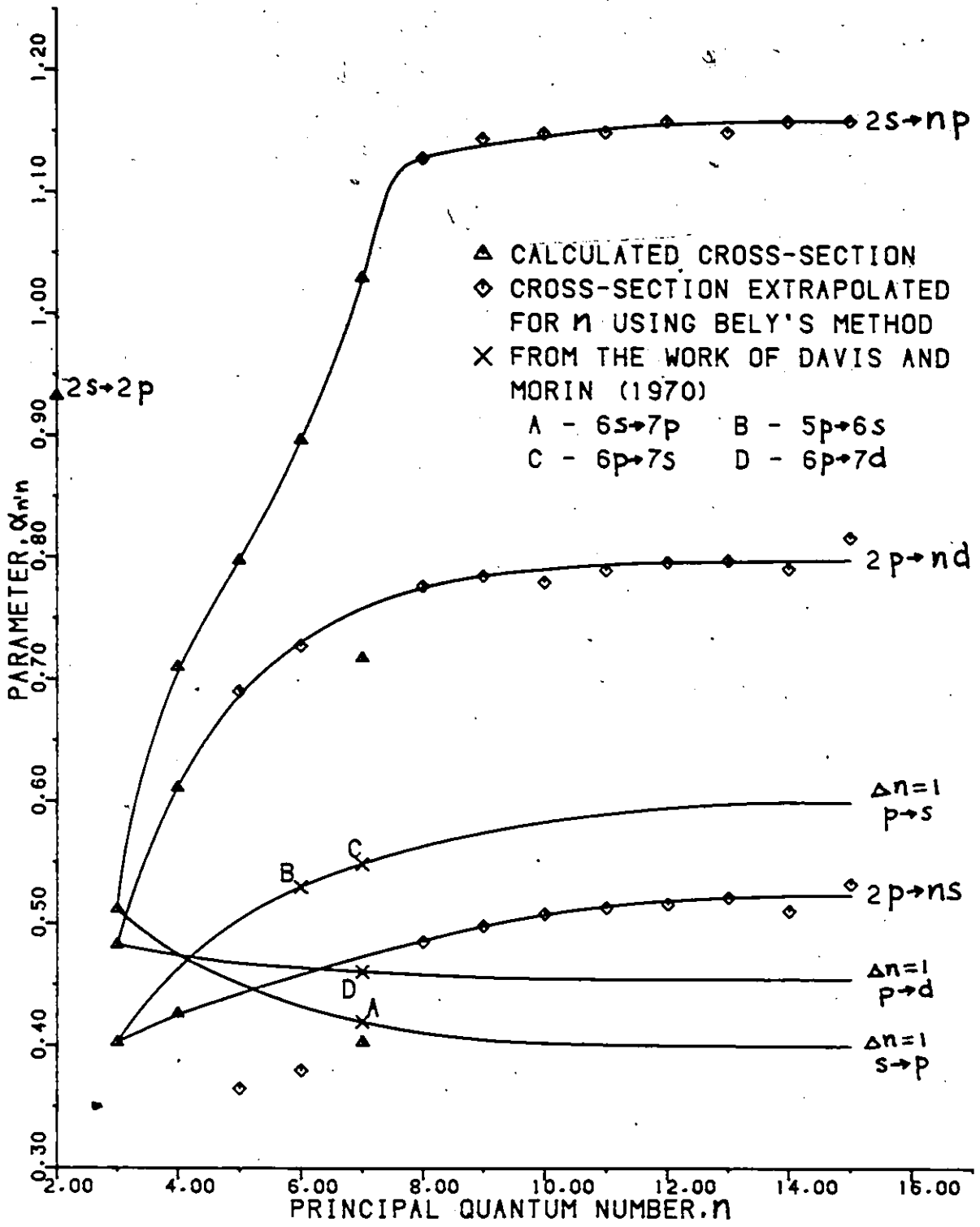

FIGURE 6.12 - KNOWN VALUES OF THE PARAMETER $\alpha_{n'n}$ FOR THE ALLOWED TRANSITIONS OF N V FROM THE WORKS OF BELY (1966A) AND BELY AND PETRINI (1970).

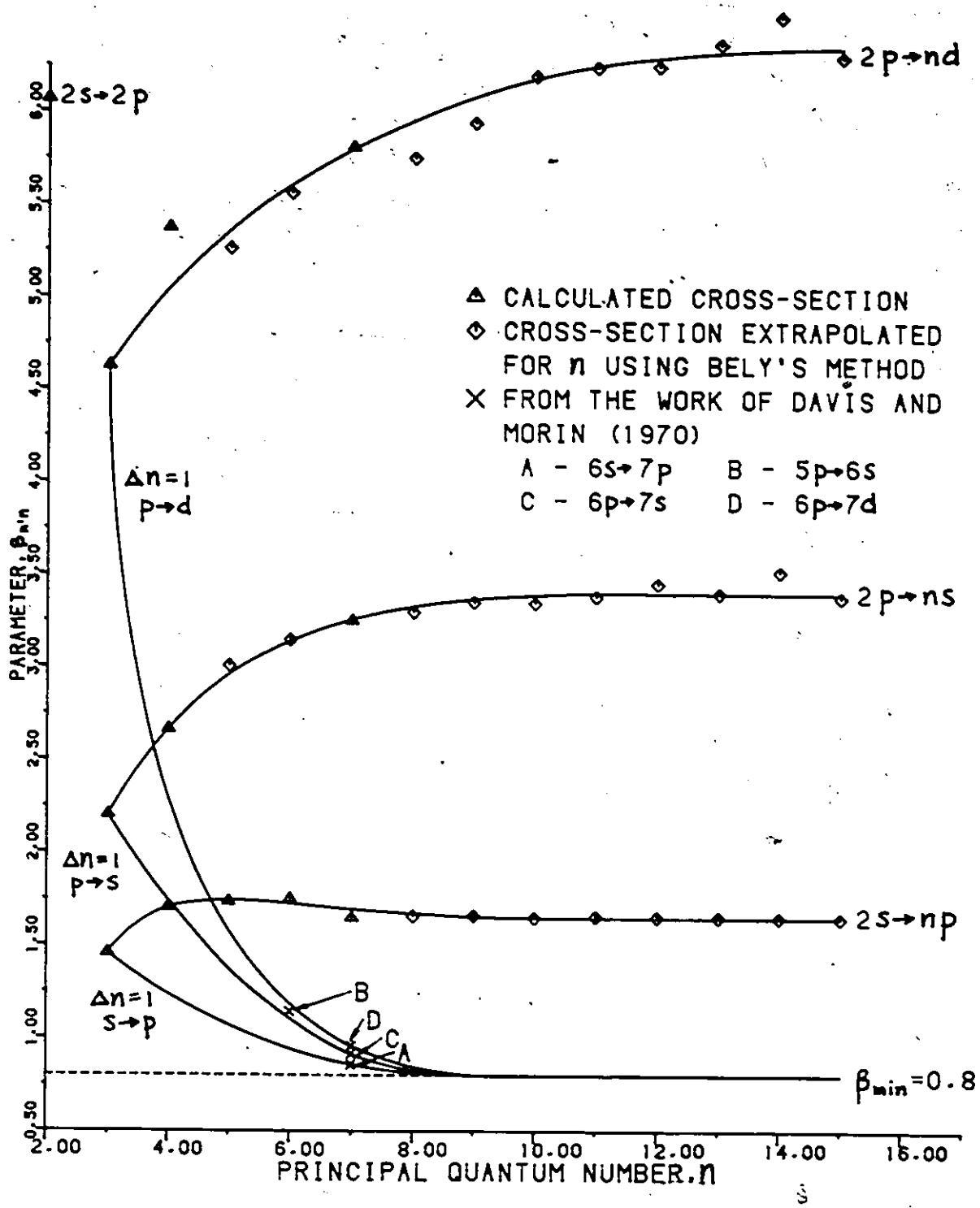

FIGURE 6.13 - KNOWN VALUES OF THE PARAMETER $\beta_{n'n}$ FOR THE ALLOWED TRANSITIONS OF N V FROM THE WORKS OF BELY (1966A) AND BELY AND PETRINI (1970).

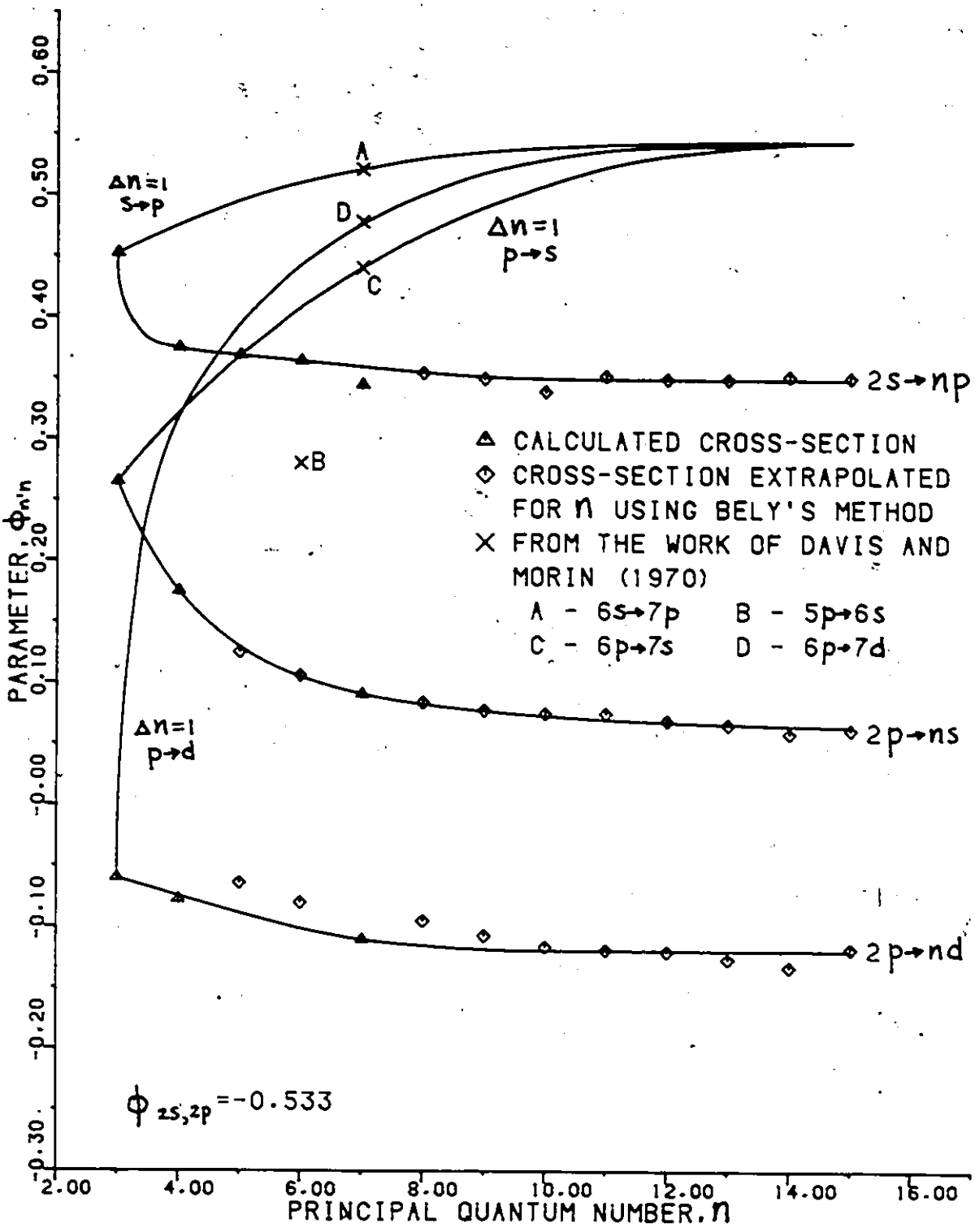

FIGURE 6.14 - KNOWN VALUES OF THE PARAMETER $\Phi_{n'n}$ FOR THE ALLOWED TRANSITIONS OF N V FROM THE WORKS OF BELY (1966A) AND BELY AND PETRINI (1970).

Table 6.1 - Fit parameters for the collisional excitation of the 2s→ns, nd, nf and 2p→np forbidden transitions of the ion C IV.

n	2s→ns		2s→nd		2s→nf		2p→np	
	α	ϕ	α	ϕ	α	ϕ	α	ϕ
3	4.48	0.113	2.45	0.469	-	-	1.84	0.959 (-1)
4	2.64	0.105	1.41	0.387	0.247	0.393	1.52	0.230 (-1)
5	2.12	0.100	1.15	0.363	0.299	0.357	1.54	0.177 (-1)
6	1.84	0.938 (-1)	1.00	0.340	0.317	0.343	1.55	0.126 (-1)
7	1.66	0.972 (-1)	0.928	0.323	0.327	0.337	1.57	0.108 (-1)
8	1.55	0.847 (-1)	0.871	0.307	0.333	0.334	1.58	0.176 (-2)
9	1.47	0.807 (-1)	0.830	0.293	0.337	0.333	1.59	0.115 (-1)
10	1.41	0.777 (-1)	0.800	0.280	0.339	0.332	1.60	0.391 (-2)
11	1.37	0.753 (-1)	0.777	0.272	0.341	0.332	1.61	-0.239 (-3)
12	1.34	0.735 (-1)	0.759	0.265	0.342	0.332	1.62	0.994 (-2)
13	1.31	0.723 (-1)	0.747	0.259	0.344	0.332	1.63	0.111 (-1)
14	1.29	0.710 (-1)	0.734	0.254	0.344	0.332	1.63	0.109 (-1)
15	1.28	0.719 (-1)	0.727	0.252	0.345	0.332	1.64	0.104 (-1)

Power of ten is given in parenthesis

Table 6.2 - Fit parameters for the collisional excitation of the 2s→ns, nd, nf and 2p→np forbidden transitions of the ion N^{+4}.

n	2s→ns		2s→nd		2s→nf		2p→np	
	α	φ	α	φ	α	φ	α	φ
3	4.61	0.964 (-1)	2.51	0.414	-	-	1.82	0.720 (-1)
4	2.76	0.821 (-1)	1.40	0.352	0.274	0.366	1.48	0.734 (-2)
5	2.20	0.742 (-1)	1.13	0.323	0.328	0.331	1.47	0.59 (-2)
6	1.91	0.699 (-1)	0.981	0.306	0.347	0.321	1.47	0.59 (-2)
7	1.74	0.671 (-1)	0.914	0.292	0.357	0.316	1.48	0.584 (-2)
8	1.61	0.645 (-1)	0.865	0.281	0.363	0.313	1.49	0.58 (-2)
9	1.53	0.624 (-1)	0.832	0.273	0.367	0.312	1.51	0.58 (-2)
10	1.46	0.600 (-1)	0.809	0.266	0.371	0.312	1.52	0.58 (-2)
11	1.40	0.582 (-1)	0.787	0.260	0.373	0.311	1.53	0.58 (-2)
12	1.37	0.564 (-1)	0.775	0.255	0.374	0.311	1.54	0.58 (-2)
13	1.33	0.550 (-1)	0.765	0.252	0.375	0.311	1.54	0.58 (-2)
14	1.31	0.540 (-1)	0.754	0.249	0.376	0.311	1.55	0.58 (-2)
15	1.29	0.530 (-1)	0.747	0.249	0.376	0.311	1.55	0.58 (-2)

Power of ten is given in parenthesis

Table 6.3 - Fit parameters for the collisional excitation of the 2s→ns, nd, nf and 2p→np forbidden transitions of the ion O VI.

n	2s→ns		2s→nd		2s→nf		2p→np	
	α	ϕ	α	ϕ	α	ϕ	α	ϕ
3	4.68	0.748 (-1)	2.54	0.376	-	-	1.83	0.700 (-1)
4	2.84	0.670 (-1)	1.39	0.325	0.297	0.341	1.44	0.347 (-2)
5	2.26	0.598 (-1)	1.12	0.302	0.348	0.309	1.42	0.970 (-3)
6	1.97	0.533 (-1)	0.963	0.283	0.368	0.302	1.41	0.3 (-3)
7	1.80	0.469 (-1)	0.896	0.269	0.378	0.299	1.41	0.317 (-3)
8	1.67	0.420 (-1)	0.848	0.255	0.385	0.297	1.41	0.2 (-3)
9	1.58	0.370 (-1)	0.812	0.244	0.390	0.296	1.42	0.2 (-3)
10	1.52	0.323 (-1)	0.789	0.237	0.394	0.295	1.44	0.2 (-3)
11	1.47	0.274 (-1)	0.768	0.232	0.396	0.295	1.45	0.2 (-3)
12	1.43	0.235 (-1)	0.754	0.228	0.398	0.295	1.45	0.2 (-3)
13	1.40	0.200 (-1)	0.744	0.226	0.399	0.295	1.45	0.2 (-3)
14	1.37	0.170 (-1)	0.739	0.225	0.400	0.295	1.45	0.2 (-3)
15	1.35	0.172 (-1)	0.728	0.224	0.401	0.295	1.45	0.2 (-3)

Power of ten is given in parenthesis

Table 6.4 - Fit parameters for the collisional excitation of the 2s→np, 2p→ns, and 2p→nd allowed transitions of the ion C IV.

n	2s→np			2p→ns			2p→nd		
	α	β	φ	α	β	φ	α	β	φ
2	0.919	5.71	-0.493	-	-	-	-	-	-
3	0.511	1.41	0.473	0.413	2.26	0.252	0.478	4.53	-0.589 (-1)
4	0.759	1.58	0.432	0.421	2.57	0.192	0.372	8.45	-0.257
5	0.858	1.61	0.427	0.429	2.64	0.180	0.528	6.44	-0.158
6	0.931	1.66	0.423	0.438	2.67	0.175	0.628	5.98	-0.975 (-1)
7	1.13	1.52	0.417	0.454	2.68	0.174	0.706	5.79	-0.050
8	1.21	1.54	0.413	0.530	2.68	0.174	0.760	7.04	-0.015
9	1.22	1.56	0.411	0.617	2.68	0.174	0.791	7.57	0.011
10	1.23	1.55	0.410	0.650	2.68	0.174	0.808	8.00	0.031
11	1.24	1.53	0.410	0.655	2.68	0.174	0.822	8.36	0.459 (-1)
12	1.25	1.54	0.410	0.655	2.68	0.174	0.834	8.70	0.575 (-1)
13	1.24	1.57	0.410	0.655	2.68	0.174	0.845	9.02	0.069
14	1.25	1.54	0.410	0.655	2.68	0.174	0.854	9.28	0.758 (-1)
15	1.25	1.55	0.410	0.655	2.68	0.174	0.860	9.47	0.082

Power of ten is given in parenthesis

Table 6.5 - Fit parameters for the collisional excitation of the 2s→np, 2p→ns, and 2p→nd allowed transitions of the ion N V.

	2s→np			2p→ns			2p→nd		
n	α	β	ϕ	α	β	ϕ	α	β	ϕ
2	0.932	6.07	-0.533	—	-	-	-	-	-
3	0.512	1.45	0.452	0.402	2.21	0.264	0.483	4.63	-0.596 (-1)
4	0.710	1.70	0.374	0.426	2.67	0.177	0.611	5.05	-0.723 (-1)
5	0.798	1.73	0.369	0.443	2.97	0.125	0.691	5.36	-0.088
6	0.897	1.76	0.373	0.458	3.14	0.106	0.728	5.61	-0.101
7	1.03	1.64	0.360	0.473	3.24	0.909 (-1)	0.753	5.81	-0.110
8	1.13	1.66	0.355	0.486	3.30	0.835 (-1)	0.776	5.96	-0.115
9	1.14	1.66	0.350	0.498	3.35	0.078	0.785	6.08	-0.118
10	1.15	1.64	0.350	0.509	3.39	0.074	0.790	6.19	-0.118
11	1.15	1.66	0.350	0.513	3.39	0.070	0.795	6.24	-0.118
12	1.16	1.66	0.350	0.517	3.39	0.677 (-1)	0.797	6.29	-0.118
13	1.15	1.66	0.350	0.522	3.39	0.664 (-1)	0.799	6.32	-0.118
14	1.16	1.66	0.350	0.524	3.39	0.065	0.798	6.34	-0.118
15	1.16	1.66	0.350	0.524	3.39	0.064	0.798	6.34	-0.118

Power of ten is given in parenthesis

Table 6.6 - Fit parameters for the collisional excitation of the 2s→np, 2p→ns, and 2p→nd allowed transitions of the ion O VI.

n	2s→np			2p→ns			2p→nd		
	α	β	φ	α	β	φ	α	β	φ
2	0.934	6.49	-0.550	-	-	-	-	-	-
3	0.521	1.48	0.425	0.380	2.24	0.259	0.477	4.91	-0.620 (-1)
4	0.671	1.81	0.336	0.436	2.78	0.155	0.530	2.45	-1.56
5	0.765	1.84	0.333	0.462	3.28	0.872 (-1)	0.583	2.82	-0.917
6	0.851	1.88	0.331	0.453	3.68	0.433 (-1)	0.645	5.75	-0.192
7	0.986	1.74	0.325	0.432	4.06	0.980 (-2)	0.721	5.88	-0.116
8	1.05	1.76	0.320	0.419	4.37	-0.014	0.833	5.11	-0.068
9	1.07	1.77	0.316	0.413	4.58	-0.320 (-1)	0.888	4.72	-0.402 (-1)
10	1.08	1.77	0.312	0.408	4.75	-0.045	0.935	4.45	-0.204 (-1)
11	1.09	1.75	0.312	0.405	4.90	-0.056	0.964	4.30	-0.010
12	1.09	1.78	0.312	0.404	4.97	-0.664 (-1)	0.982	4.20	-0.157 (-2)
13	1.10	1.75	0.312	0.404	5.00	-0.073	0.988	4.15	0.241 (-2)
14	1.10	1.75	0.312	0.404	5.01	-0.077	0.989	4.13	0.476 (-2)
15	1.10	1.77	0.312	0.404	5.01	-0.788 (-1)	0.988	4.13	0.005

Power of ten is given in parenthesis

4. EXTRAPOLATION OF THE FIT PARAMETERS

The simplest extrapolation procedure possible is to assume constant values of the parameters for all unknown allowed or forbidden transitions. Unfortunately, the parameters which are known show substantial variations and such an extrapolation procedure will be far less accurate than one based on the known trends of the parameters at low values of n' and on the corresponding hydrogenic values. We carry out the extrapolation of the parameters of N V from which those of C IV and O VI can be obtained.

4.1. Constraints on the parameters

The fact that the excitation cross-section must be positive

$$\sigma_{n' \to n}(u) \geq 0 \qquad \ldots(6.12)$$

imposes certain conditions on the parameters which restrict their range of values. These conditions are obtained by demanding that each parameter be allowed only such values that will satisfy eq.(6.12). From equations (6.6) and (6.11), we thus have the conditions

$$\alpha \geq 0$$

$$u - \phi \geq 0$$

$$\ln(1.25\,\beta u) \geq 0 \qquad \ldots(6.13)$$

or

$$\left.\begin{aligned} &\alpha \geq 0 \\ &\phi \leq U_{min} \\ &\beta \geq \frac{1}{1.25\, U_{min}} \end{aligned}\right\} \quad \ldots(6.14)$$

where U_{min} is the minimum value of U. The smallest possible value of U is 1. We thus obtain the constraints

$$\left.\begin{aligned} &\alpha \geq 0 \\ &\phi \leq 1 \\ &\beta \geq 0.8 \end{aligned}\right\} \quad \ldots(6.15)$$

for optically allowed and forbidden transitions.

The value of U at which the cross-section is a maximum, U_{max}, is given by the relation

$$\ln(1.25\,\beta\, U_{max}) = \frac{U_{max} - \phi}{U_{max} - 2\phi} \quad \ldots(6.16)$$

for allowed transitions and

$$U_{max} = 2\phi \quad \ldots(6.17)$$

for forbidden transitions. The value of U_{max} is not known exactly for every transition. However, it is usually small, less than ~5. It

should also be noted that values of U_{max} less than 1 are also possible, as can be seen from curve a in Fig.6.8. Relation (6.16) or (6.17) can thus be used to establish whether a set of parameters gives a reasonable value of U_{max}.

4.2. Allowed transitions

4.2.a. $\Delta n \geq 1$ transitions

The $\Delta n = 1$ s -> p, p -> s, and p -> d transitions can be extrapolated with reasonable accuracy, due to the work of Davis and Morin (1970) on the 5p -> 6s, 6s -> 7p, 6p -> 7s, and 6p -> 7d transitions of N V. In Fig.6.12, 6.13, and 6.14, we show the position of the parameters of these transitions in relation to the parameters of the transitions from the 2s and 2p states of N V. We also show possible extrapolation curves for the $\Delta n = 1$ s -> p, p -> s and p -> d transitions. The corresponding values of the parameters are given in Tab.6.7. An estimate of the errors in these parameters and a discussion of their effect on the cross-sections is given in Section 4.5 of this Chapter.

To obtain estimates of the parameters of the $\Delta n \geq 2$ s -> p, p -> s, and p -> d transitions, the following extrapolation procedure is used. We take as example the extrapolation of the $\alpha_{n's \to np}$ parameters. We assume that these parameters vary continuously as n' and n are varied. We then take the curves $\alpha_{2s \to np}$ and $\alpha_{\Delta n = 1}$ as envelopes of a family of curves $\alpha_{n's \to np}$ and $\alpha_{\Delta n \geq 2}$ as shown in Fig.6.15. The intersection of the two sets of curves at integer values of n gives estimates of the parameters $\alpha_{n's \to np}$. This extrapolation procedure can be justified by the fact that for all allowed transitions of hydrogen, $\alpha = 1$, and it

Table 6.7 - Extrapolated parameters for the collisional excitation of the $\Delta n=1$ s→p, p→s, and p→d allowed transitions of the ion N V.

Tran-sition	s→p			p→s			p→d		
	α	β	ϕ	α	β	ϕ	α	β	ϕ
2→3	0.512†	1.45†	0.452†	0.402†	2.21†	0.264†	0.483†	4.63†	-0.596 (-1)†
3→4	0.45	1.2	0.48	0.45	1.75	0.3	0.48	2	0.3
4→5	0.45	1.1	0.5	0.5	1.4	0.4	0.47	1.6	0.4
5→6	0.4	0.95	0.51	0.530*	1.14*	0.281*	0.47	1.2	0.45
6→7	0.420*	0.869*	0.521*	0.550*	0.916*	0.442*	0.463*	0.962*	0.479*
7→8	0.4	0.8	0.55	0.6	0.8	0.5	0.45	0.8	0.5
8→9	0.4	0.8	0.55	0.6	0.8	0.5	0.45	0.8	0.5
9→10	0.4	0.8	0.55	0.6	0.8	0.5	0.45	0.8	0.5
10→11	0.4	0.8	0.55	0.6	0.8	0.5	0.45	0.8	0.5
11→12	0.4	0.8	0.55	0.6	0.8	0.5	0.45	0.8	0.5
12→13	0.4	0.8	0.55	0.6	0.8	0.5	0.45	0.8	0.5
13→14	0.4	0.8	0.55	0.6	0.8	0.5	0.45	0.8	0.5
14→15	0.4	0.8	0.55	0.6	0.8	0.5	0.45	0.8	0.5

† from the work of Bely
* from Davis and Morin (1970)
Power of ten is given in parenthesis

Table 6.8 - Extrapolated parameters for the collisional excitation of the $\Delta n \geq 2$ s↔p, p↔s, and p↔d allowed transitions of the ion N V.

		n'	n=n'+2	n=n'+3	n=n'+4	n=n'+5	n≥n'+6
s↔p	α	≥3	0.7	0.8	0.9	1.0	1
	β	≥3	1.35	1.35	1.35	1.35	1.35
	φ	3	0.4	0.4	0.4	0.4	0.4
		4	0.5	0.4	0.4	0.4	0.4
		≥5	0.5	0.5	0.5	0.5	0.5
p↔d	α	≥3	0.6	0.7	0.7	0.7	0.7
	β	3	2.5	3	3	3	3
		4	2	2	2.5	2.5	2.5
		5	2	2	2	2	2
		6	1	1	2	2	2
		≥7	1	1	1	2	2
	φ	3	0.3	0.3	0.3	0.3	0.3
		4	0.4	0.4	0.4	0.4	0.4
		5	0.45	0.45	0.45	0.45	0.45
		≥6 ≤8	0.5	0.5	0.5	0.5	0.5
		≥9	0.55	0.55	0.55	0.55	0.55

		n'	n=n'+2	n=n'+3	n=n'+4	n=n'+5	n≥n'+6
s↔d	α	3	0.5	0.5	0.5	0.5	0.5
		4	0.5	0.5	0.5	0.5	0.5
		5	0.55	0.55	0.55	0.55	0.55
		≥6	0.6	0.6	0.6	0.6	0.6
	β	3	2	2.5	3	3	3
		4	2	2	2.5	2.5	2.5
		5	1.5	2	2	2	2
		6	1	2	2	2	2
		≥7	1	1	2	2	2
	φ	3	0.2	0.2	0.2	0.2	0.2
		4	0.3	0.2	0.2	0.2	0.2
		5	0.3	0.3	0.3	0.3	0.3
		6	0.4	0.3	0.3	0.3	0.3
		7	0.4	0.4	0.3	0.3	0.3
		8	0.4	0.4	0.4	0.4	0.4
		≥9	0.5	0.4	0.4	0.4	0.4

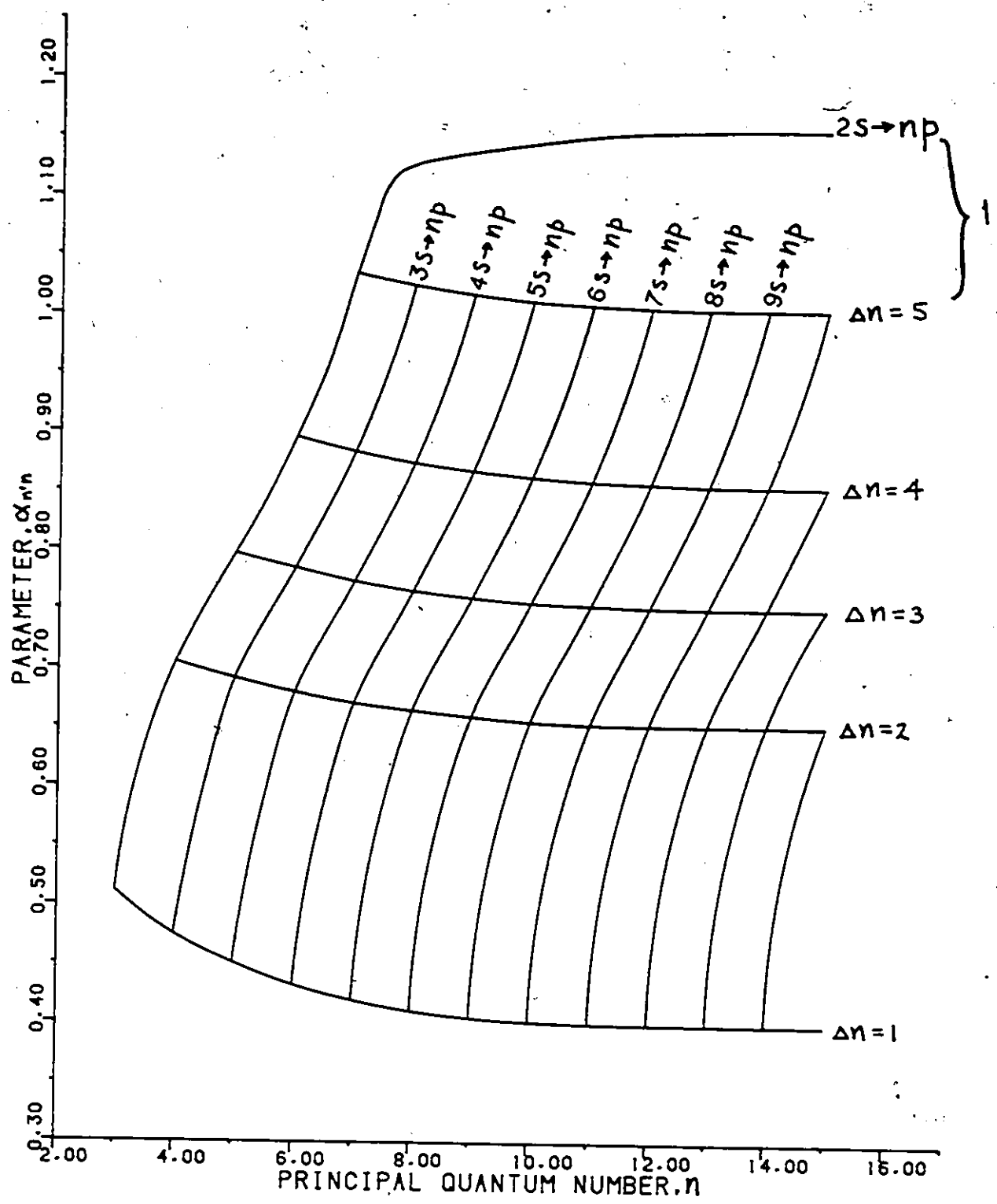

FIGURE 6.15 - EXTRAPOLATION OF THE PARAMETER $\alpha_{n'n}$ FOR THE n's→np TRANSITIONS OF N V.

thus seems reasonable to expect that for all allowed transitions of N V, $0.4 \leq \alpha \leq 1.2$, as is observed for the curves $\alpha_{2s \to np}$ and $\alpha_{\Delta n=1}$. The sets of parameters for the $\Delta n \geq 2$ s -> p, p -> s, and p -> d transitions shown in Tab.6.8 are obtained in this manner.

The parameters of the other allowed transitions from d, f, and higher ℓ-value states are difficult to extrapolate, since no data are available for these transitions in lithium-like ions. These parameters will be estimated by taking into account the behavior of the parameters of s -> p, p -> s, and p -> d transitions of N V and the behavior of the corresponding hydrogen parameters which can be obtained from the works of McCoyd and Milford (1963) and Kingston and Lauer (1966a, b).

i. Behavior of α

The value of α for hydrogen is found to be $\alpha = 1$. For the s -> p, p -> s, and p -> d transitions of N V, $0.4 \leq \alpha \leq 1.2$, with an average value of ~ 0.6. Since α is constant for hydrogen, this suggests that α may be expected to be relatively constant for N V. Consequently, we take rough averages of the values of $\alpha_{\Delta n=1}$, $\alpha_{\Delta n=2}$, ... of the s -> p, p -> s, and p -> d transitions, and use these for all allowed transitions with $\ell' \geq$ d and $\Delta\ell = \pm 1$. The values of α obtained in this way are found to increase slightly with n, as is also the case for the transitions from the 2s and 2p states. The values of α for the $\Delta n \geq 1$, $\ell' \geq$ d transitions are given in Tab.6.9.

ii. Behavior of β

Although the numerical values of β are different for hydrogen and N V, we can however expect the overall behavior of these parameters to be similar. In hydrogen, for $\Delta\ell = \pm 1$,

Table 6.9 - Extrapolated parameters for the collisional excitation of the $\Delta n \geq 1$, $\ell' \geq d$ allowed transitions of the ion N V.

	$\Delta n=1$			$\Delta n=2$			$\Delta n=3$			$\Delta n=4$			$\Delta n \geq 5$		
n'	α	β	ϕ	α	β	ϕ	α	β	ϕ	α	β	ϕ	α	β	ϕ
3	0.5	2	0.3	0.6	3	0.3	0.7	3	0.3	0.7	3	0.3	0.7	3	0.3
4	0.5	1.7	0.4	0.6	2	0.4	0.7	2	0.4	0.7	2.5	0.4	0.7	2.5	0.4
5	0.5	1.2	0.45	0.6	2	0.4	0.7	2	0.4	0.7	2	0.4	0.7	2	0.4
6	0.5	1.0	0.5	0.6	1	0.5	0.7	1.5	0.5	0.7	2	0.5	0.7	2	0.5
7	0.5	0.8	0.5	0.6	1	0.5	0.7	1	0.5	0.7	1.5	0.5	0.7	2	0.5
8	0.5	0.8	0.5	0.6	1	0.5	0.7	1	0.5	0.7	1.5	0.5	0.7	2	0.5
≥9	0.5	0.8	0.55	0.6	1	0.5	0.7	1	0.5	0.7	1.5	0.5	0.7	2	0.5

1. for constant n' and ℓ', β increases as Δn increases;

2. for constant n' and Δn, β increases as ℓ' increases;

3. for constant ℓ' and Δn, β decreases as n' increases;

(Rule 1). The change in β is found to be quite rapid at low values of the variables, but becomes very small as n', ℓ', and Δn increase (Rule 2). This is observed for $\beta_{\ell'}$ and $\beta_{n'}$ of hydrogen. However, the hydrogen values of β have been calculated only for small Δn. But Rule 2 can also be inferred for $\beta_{\Delta n}$ since it holds for the 2s -> np and 2p -> ns, nd transitions of N V. We also find that $\beta_{\Delta\ell=-1}$ is slightly greater than $\beta_{\Delta\ell=1}$; the difference between the two is less than a factor of two in most cases (Rule 3).

As can be seen from Fig.6.13 and Tab.6.8, the values of β for the s -> p, p -> s, and p -> d transitions of N V obey Rules 1, 2, and 3. We thus use these rules to estimate the values of β for all $\Delta n \geq 1$, $\ell' \geq$ d allowed transitions. Assuming $\beta_{\Delta\ell=-1} \simeq \beta_{\Delta\ell=1}$ and $\beta_{\ell'=d} \simeq \beta_{\ell'=f} \simeq \cdots$, and starting from the values of β for the s -> p, p -> s, and p -> d transitions, the parameters shown in Tab.6.9 are obtained.

iii. Behavior of ϕ

The parameter ϕ, for neutral hydrogen, has the value $\phi = 1$ since the cross-section is 0 at threshold. For the excitation of positive ions, values of ϕ are difficult to obtain since ϕ only affects the excitation cross-sections at low values of U.

We thus have to estimate the parameters ϕ for the $\Delta n \geq 1$, $\ell' \geq$ d allowed transitions from the behavior of ϕ for the s -> p, p -> s, and

p -> d transitions. For these transitions, ϕ is relatively constant and, in most cases, $0.2 \leq \phi \leq 0.6$. However, larger variations in the values of ϕ are observed for the transitions from the low-lying 2s and 2p states. The estimated values of ϕ are restricted to the range $0.2 \leq \phi \leq 0.6$ and are based on a rough average of the parameters for the s -> p, p -> s, and p -> d transitions. The behavior observed in Fig.6.14 is also taken into account. The resulting parameters are given in Tab.6.9.

4.2.b. $\Delta n = 0$ transitions

Very little data are available on transitions of the kind $n\ell' \rightarrow n\ell'\pm1$ in which only the angular momentum of the bound electron changes by an amount $\Delta\ell = \pm1$: Bely (1966a) has looked at the 2s -> 2p transition and Burke et al. (1966), the 3s -> 3p and 3p -> 3d transitions. As is evident from Fig.6.12, 6.13, and 6.14, the behavior of the parameters of the 2s -> 2p transition is very different from that of the $\Delta n \geq 1$ transitions 2s -> np. As will be seen later on, this is a peculiarity of $\Delta n = 0$ transitions.

Bely (1966a) states that the Coulomb-Born approximation gives results for the 2s -> 2p transition which are accurate to within a few percents. Tully and Petrini (1974) find that the Born and the Coulomb-Born approximations tend to the same results at high kinetic energy of the incident electron. This suggests that we use the simpler Born approximation for $\Delta n = 0$ transitions to obtain estimates of the parameters α and β; values of ϕ can then be estimated from the cross-sections given by Bely (1966a) and Burke et al. (1966).

The excitation cross-section, in the Born approximation, has the form (Massey and Burhop, 1952, p.140)

$$\sigma_{n'\to n}(E) = \frac{4\pi m e^4}{\hbar^2 E} |z_{n'\to n}|^2 \cdot \frac{1}{2} \ln\left(4\frac{E}{E_{n'n}}\right) \qquad \ldots(6.21)$$

where $|z_{n'\to n}|$ is the mean dipole length on the z axis for the n' -> n transition and the other symbols have their usual meaning. One has

$$z_{n'\to n} = \int \psi_{n'}\, z\, \psi_n^*\, d\tau \qquad \ldots(6.22)$$

where $\psi_{n'}$ and ψ_n are the wave functions of the initial and final states respectively; $d\tau$ is a volume element. Drawin (1963) puts

$$|z_{n'\to n}|^2 = \frac{f_{n'\to n}}{E_{n'n}} a_o^2 \qquad \ldots(6.23)$$

where $f_{n'\to n}$ is the absorption oscillator strength of the n' -> n transition and $E_{n'n}$ is in Rydbergs. Using eq.(6.23) in eq.(6.21) and expressing the energy of the incident electron in threshold units, we get

$$\sigma_{n'\to n}(u) = 4\pi a_o^2 \frac{f_{n'\to n}}{E_{n'n}^2} \frac{\ln(4u)}{u}. \qquad \ldots(6.24)$$

By comparing this equation with eq.(6.6), we obtain the parameters

$$\alpha = 1$$

$$\beta = 3.2$$

$$\phi = 0. \qquad \ldots(6.25)$$

As can be seen in Fig.6.16 and 6.17, these parameters underestimate the actual cross-section at low values of U. However, using $\phi = -1$ gives a good fit to the 2s -> 2p and 3s -> 3p cross-sections. The fit for the 3p -> 3d transition is within a factor of 1.5 of the results of Burke et al. (1966) at low and intermediate values of U. We will thus use the set of parameters

$$\left.\begin{aligned} \alpha &= 1 \\ \beta &= 3.2 \\ \phi &= -1 \end{aligned}\right\} \qquad \ldots(6.26)$$

for $\Delta n = 0$ allowed transitions.

4.3. Optically forbidden transitions

4.3.a. $\Delta n \geq 1$ transitions

i. Extrapolation of α

The parameters α are estimated by comparing their lithium-like values with the ones obtained from the cross-sections of the forbidden transitions of hydrogen calculated by Kingston and Lauer (1966a, b) for $\Delta n = 1$ and 2. In Fig.6.18 to 6.20, the values of α for hydrogen are

plotted as a function of n for most of the $\Delta n = 1$ forbidden transitions from the s, p, and d states.

Several characteristic behaviors of the parameter α emerge from this comparison. Broadly speaking, for constant Δn and n', α is greatest for the $\Delta l = 2$ transition; the other parameters are ordered as follows: $\alpha_{\Delta l=2} > \alpha_{\Delta l=0} > \alpha_{\Delta l=3} > \alpha_{\Delta l=4} \cdots$. However, as Δn and n' increase, $\alpha_{\Delta l=2}$ approaches the value of $\alpha_{\Delta l=0}$. We also observe that $\alpha_{\Delta l<0} \ll \alpha_{\Delta l>0}$. If Δl and n' are constant, the values of α decrease as Δn increases. This decrease is particularly drastic for very low values of Δn, but as Δn increases, α approaches a constant value as is observed in Fig.6.10 for the 2s -> ns, nd, nf and 2p -> np transitions of N V. For constant Δl and Δn, α tends to a more or less constant value as n' increases; however, it should be noted that α is larger for the first few values of n'.

In Tab.6.10, the known values of α for the ions C IV, N V, and O VI are compared with the corresponding hydrogen values. We observe that for a given transition, the lithium-like and hydrogen values of α are approximately equal. Furthermore, the hydrogen parameter is seen to be the limiting value of the C IV, N V, and O VI parameters, as Z increases. The values of α for N V can thus be estimated by taking rough averages of the hydrogen values. The resulting parameters are given in Tab.6.11.

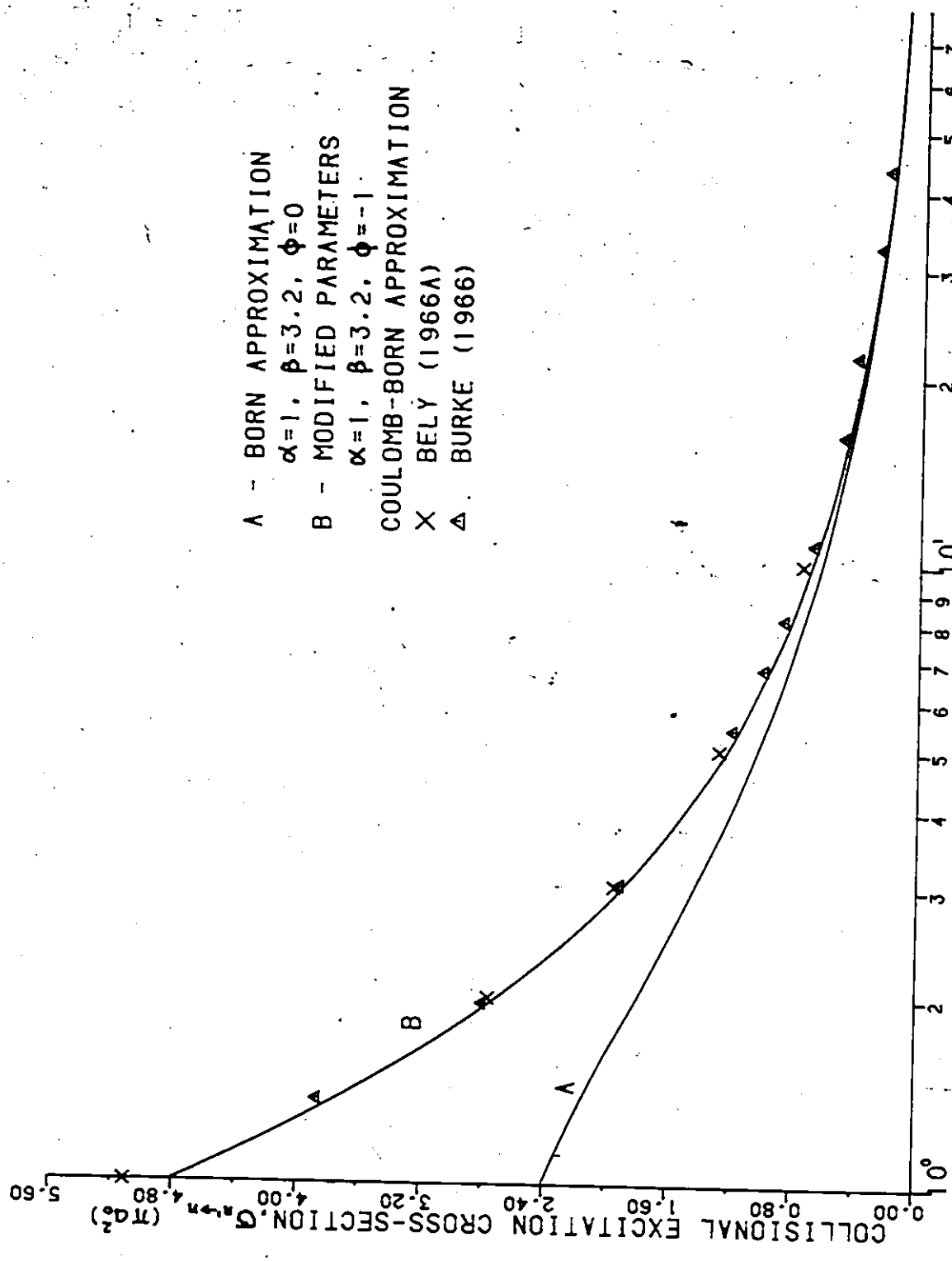

FIGURE 6.16 - ELECTRON IMPACT EXCITATIONCROSS-SECTION FOR THE 2S→2P TRANSITION OF N V.

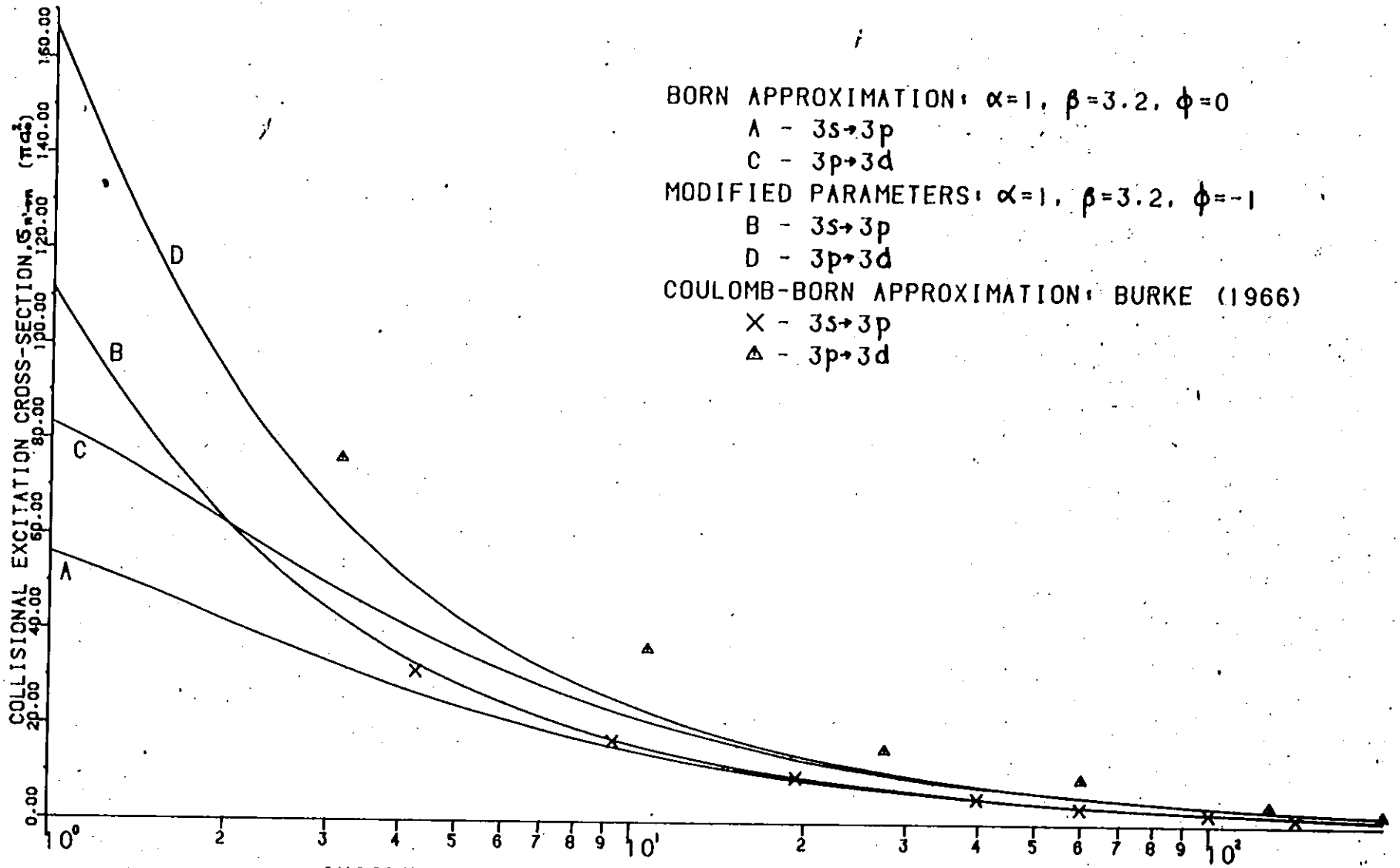

FIGURE 6.17 - ELECTRON IMPACT EXCITATION CROSS-SECTION FOR THE 3s→3p AND 3p→3d TRANSITIONS OF N V.

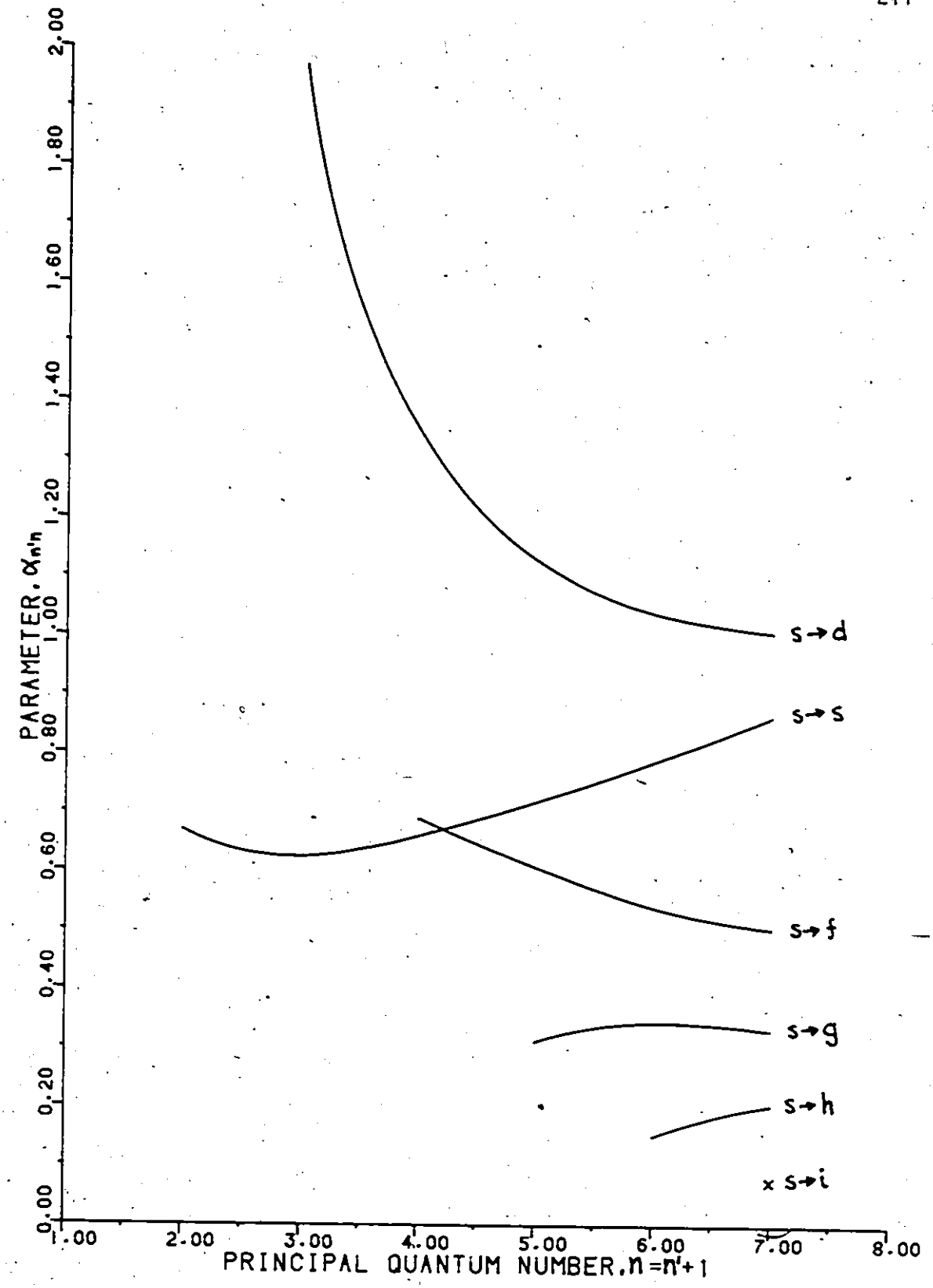

FIGURE 6.18 - VALUES OF THE PARAMETER $\alpha_{n'n}$ FOR THE $\Delta n = 1$ FORBIDDEN TRANSITIONS OF HYDROGEN FROM THE WORKS OF KINGSTON AND LAUER (1966A,B).

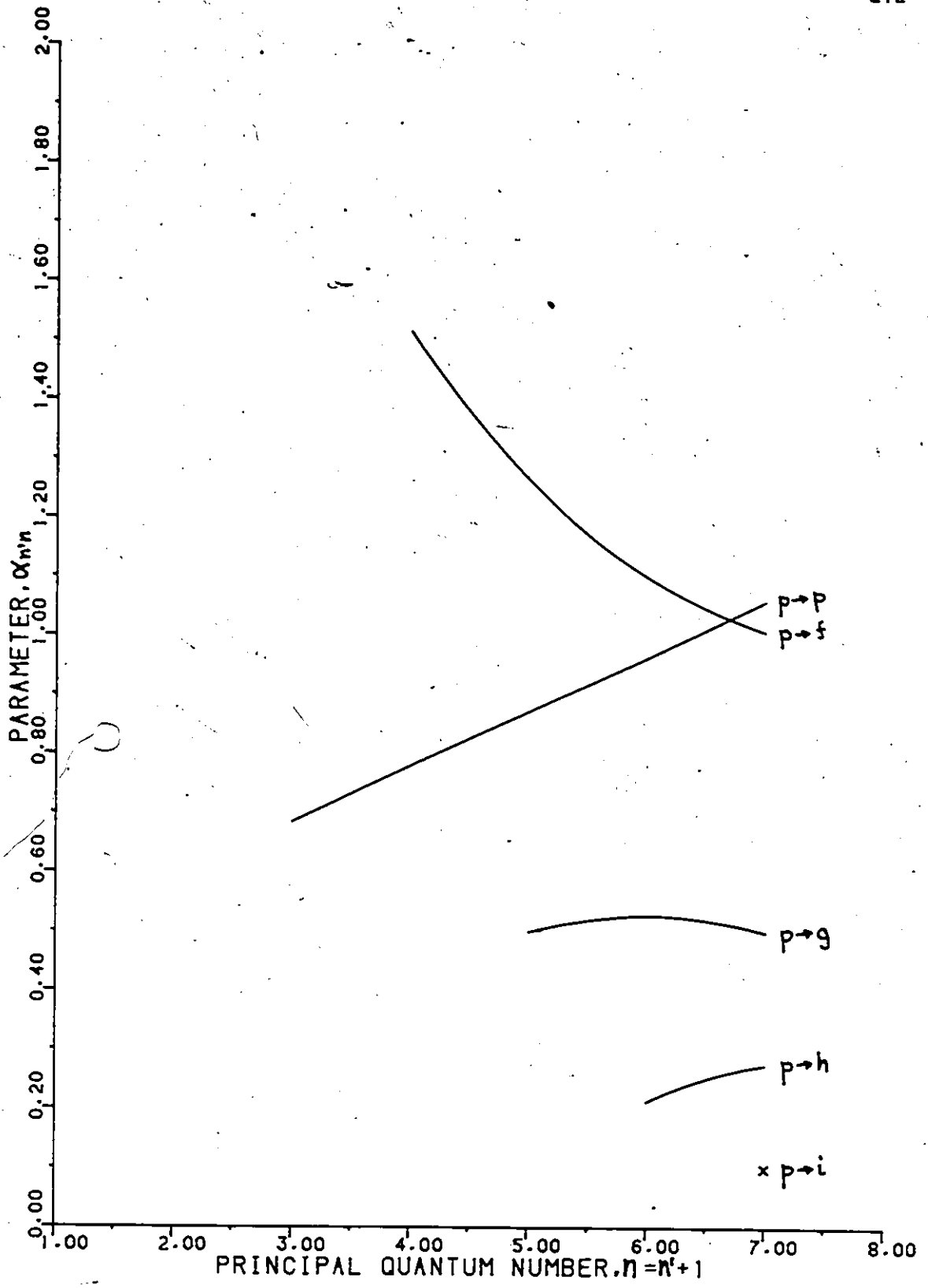

FIGURE 6.19 - VALUES OF THE PARAMETER $\alpha_{n'n}$ FOR THE $\Delta n = 1$ FORBIDDEN TRANSITIONS OF HYDROGEN FROM THE WORKS OF KINGSTON AND LAUER (1966A,B).

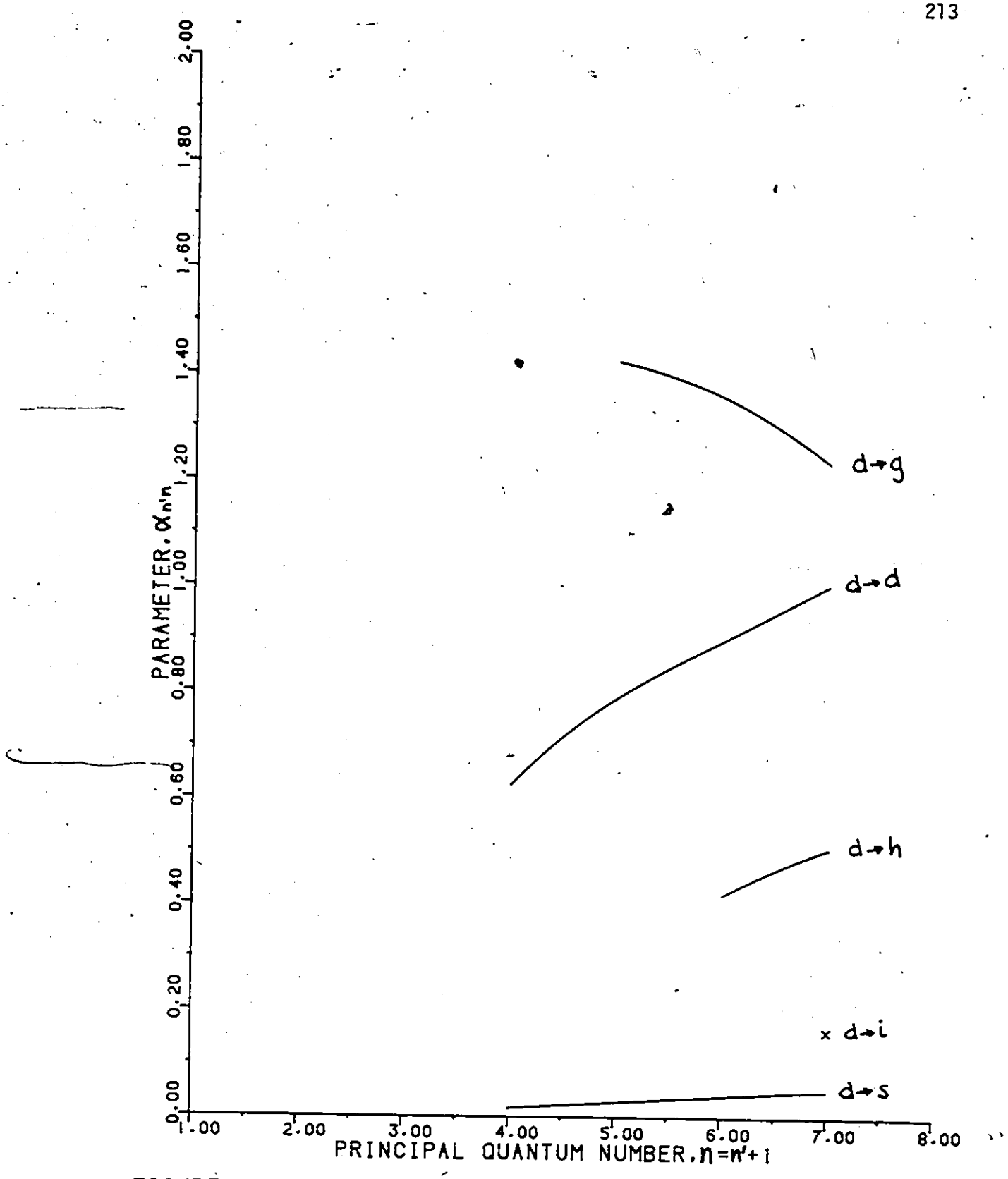

FIGURE 6.20 - VALUES OF THE PARAMETER $\alpha_{n'n}$ FOR THE $\Delta n = 1$ FORBIDDEN TRANSITIONS OF HYDROGEN FROM THE WORKS OF KINGSTON AND LAUER (1966A,B).

Table 6.10 - Comparison of the fit parameters α for the collisional excitation of some forbidden transitions of the ion N V and of Hydrogen.

	α				α/α_H		
Transition	C IV	N V	O VI	H	C IV	N V	O VI
2s→3s	0.560	0.576	0.585	0.624	0.90	0.92	0.94
2s→4s	0.330	0.345	0.355	0.388	0.85	0.89	0.92
2s→3d	1.53	1.57	1.59	1.97	0.78	0.80	0.81
2s→4d	0.881	0.875	0.869	0.788	1.12	1.11	1.10
2s→4f	0.216	0.240	0.260	0.412	0.53	0.58	0.63
2p→3p	0.690	0.683	0.686	0.684	1.01	1.00	1.00
2p→4p	0.570	0.555	0.540	0.428	1.33	1.30	1.26

Table 6.11 - Extrapolated values of the parameter α for the collisional excitation of the $\Delta n \geq 1$ forbidden transitions of the ion N V.

$\Delta\ell$	$\Delta n=1$	$\Delta n=2$	$\Delta n \geq 3$
5	0.2±0.1	Lowest n': 0.3±0.1 Others : 0.08±0.04	Lowest n': 0.1±0.1 Others : 0.04±0.04
4	0.3±0.1	Lowest n': 0.4±0.1 Others : 0.12±0.06	Lowest n': 0.2±0.1 Others : 0.07±0.07
3	0.5±0.2	Lowest n': 0.5±0.2 Others : 0.2±0.1	Lowest n': 0.25±0.20 Others : 0.1±0.1
2	Two lowest n': 1.4±0.5 Others : 1.0±0.4	Lowest n': 0.7±0.3 Others : 0.4±0.2	Lowest n': 0.5±0.3 Others : 0.3±0.2
0	1.0±0.4	0.4±0.2	0.3±0.2
-2	0.05±0.03	0.03±0.01	0.02±0.01
-3	0.01±0.01	0.01±0.01	0.01±0.01

ii. Extrapolation of ϕ

Since no hydrogen values are available for this parameter, the values of ϕ for N V will be estimated by using the behaviors exhibited in Fig.6.11 by the parameters of the 2s -> ns, nd, nf and 2p -> np transitions of N V.

The parameter ϕ is very small for the $\Delta l = 0$ forbidden transitions from the ground state; as Δl increases, ϕ also increases, but it seems to tend to a constant value. The value of ϕ for the 2p -> np transitions is also observed to be very small, being of the order 0. Based on these considerations, the following parameters will be used for $\Delta n \geq 1$ forbidden transitions:

$$\phi_{\Delta l=0} = 0.0$$

$$\phi_{\Delta l=2} = 0.25$$

$$\phi_{\Delta l=3} = 0.3$$

$$\phi_{\Delta l\geq 4} = 0.4. \qquad \ldots(6.27)$$

No data are available at all on the $\Delta l < 0$ forbidden transitions. In the case of allowed transitions, we observe that the values of ϕ for l -> l' transitions are about half the values of the corresponding l' -> l transitions. Accordingly, we will use

$$\phi_{\Delta l=-2} = 0.1$$

$$\phi_{\Delta l \leq -3} = 0.2 \qquad \ldots(6.28)$$

as an estimate of the parameters of the $\Delta n \geq 1$ $\Delta l < 0$ forbidden transitions.

4.3.b. $\Delta n = 0$ transitions

The work of Burke (1966) on the 3s -> 3d transition of N V provides the only data available on $\Delta n = 0$ forbidden transitions. The parameters of this transition are $\alpha = 0.138$ and $\phi = -0.342$. The 3s -> 3d cross-section is found to be about twenty times smaller than the 3s -> 3p one. This is surprising, especially since the $\Delta l = 2$ forbidden transitions dominate all other transitions in the $\Delta n \geq 1$ case. However, the $\Delta n = 0$ transitions are dominated by the optically allowed transitions (Bely and Van Regemorter, 1970). We use this fact to estimate the parameters α of $\Delta n = 0$ forbidden transitions.

The 3s -> 3p excitation cross-section is proportional to

$$K'_{3s\to 3p} = \frac{4\pi a_o^2}{E^2_{3s,3p}} f_{3s\to 3p}\, \alpha_{3s,3p} \qquad \ldots(6.29)$$

and the 3s -> 3d cross-section to

$$K'_{3s\to 3d} = \frac{4\pi a_o^2}{E^2_{3s,3d}} \alpha_{3s,3d}. \qquad \ldots(6.30)$$

Here $E_{3s,3p}$ and $E_{3s,3d}$ are in Rydbergs. The ratio of eq.(6.30) to eq.(6.29) for N V is found to be

$$\frac{K'_{3s\to 3d}}{K'_{3s\to 3p}} = 0.2 \qquad \ldots(6.31)$$

We find that for a $n\ell' \to n\,\ell'+1$ transition, the absorption oscillator strengths show large variations as ℓ' increases. For example, the $10\ell' \to 10\,\ell'+1$ transitions in N V have the following oscillator strengths (Lindgård and Nielsen, 1977):

$$f_{10s\to 10p} = 1.4$$

$$f_{10p\to 10d} = 0.27$$

$$f_{10d\to 10f} = 0.046$$

$$f_{10f\to 10g} = 0.0013. \qquad \ldots(6.32)$$

This causes large variations in the values of K' for allowed transitions which are not present in the values of K' for forbidden transitions since the latter has no quantity equivalent to the former's oscillator strength. If the optically allowed transitions are to dominate the forbidden transitions in the $\Delta n = 0$ case, the values of α for $\Delta n = 0$ forbidden transitions will have to exhibit variations of the kind seen in the oscillator strengths (6.32).

One way of achieving this is to use the ratio

$$\frac{K'_{n\ell'\to n\ell\neq\ell'+1}}{K'_{n\ell'\to n\ell'+1}} \simeq 0.2 \pm 0.2 \qquad \ldots(6.33)$$

for all $\Delta n = 0$ transitions. Using the definitions of K' and the fact that $E_{nl' \to nl \neq l'+1} \simeq E_{nl' \to nl'+1}$, we obtain

$$\frac{\alpha_{nl', nl \neq l'+1}}{f_{nl' \to nl'+1} \; \alpha_{nl', nl'+1}} \simeq 0.2 \pm 0.2 \qquad \ldots(6.34)$$

and since $\alpha_{nl', nl'+1} \simeq 1$ (eq.6.26), we finally get

$$\alpha_{nl', nl \neq l'+1} \simeq (0.2 \pm 0.2) \cdot f_{nl' \to nl'+1}. \qquad \ldots(6.35)$$

This relation provides crude estimates of the parameters α for $\Delta n = 0$ forbidden transitions. These are given in Tab.6.12.

We estimate the parameters ϕ as follows: since $\phi = -0.342$ for the 3s -> 3d transition, and since $\phi \simeq -1$ for all $\Delta n = 0$ allowed transitions, an average value of $\phi \simeq -0.5$ is used for all $\Delta n = 0$ forbidden transitions.

4.4. Parameters of the ions C IV and O VI

The parameters for the transitions for the 2s and 2p states of the ions C IV and O VI are known and are given in Tables 6.1 to 6.6. The parameters for all the other transitions for which no data are available, are obtained from the parameters of the ion N V by the following method.

The quantity $Z^4 \sigma_{n' \to n}(u)$ is independent of Z for hydrogenic ions in the Born approximation (Tully, 1973). Tully and Petrini (1974) mention that at sufficiently high impact energies, the Coulomb-Born approx-

Table 6.12 - Extrapolated values of the parameter α for the collisional excitation of the $\Delta n=0$ forbidden transitions of the ion N V.

Transition	Parameter
4s→4d	0.1
4s→4f	0.1
4p→4f	0.02
5s→5d	0.1
5s→5f	0.1
5s→5g	0.1
5p→5f	0.03
5p→5g	0.03
5d→5g	0.001
6s→6d	0.2
6s→6f	0.2
6s→6g	0.2
6s→6h	0.2
6p→6f	0.03
6p→6g	0.03
6p→6h	0.03
6d→6g	0.001
6d→6h	0.001
6f→6h	0.0002

imation reduces to the Born approximation: for the 2s -> np transitions in lithium-like ions, the two approximations differ by less than 10% for $U \gtrsim 8$. Since the excited states of the lithium-like ions are closely hydrogenic, we can expect that the quantity $Z^4 \sigma_{n' \to n}(u)$ will also be approximately independent of Z for these ions.

The cross-section for electron impact excitation of allowed transitions is given by eq.(6.6), viz.

$$\sigma_{n' \to n}(u) = 4\pi a_o^2 \frac{f_{n' \to n}}{E_{n'n}^2} \propto \frac{u - \phi}{u^2} \ln(1.25 \beta u)$$

where $E_{n'n}$ is in Rydbergs. For large U, the Coulomb-Born approximation applies and we then have

$$Z^4 \sigma^{(Z)}_{n' \to n}(u) \simeq Z^4 \, 4\pi a_o^2 \frac{f^{(Z)}_{n' \to n}}{\{E^{(Z)}_{n'n}\}^2} \times \alpha_Z \frac{\ln(1.25 \beta_Z u)}{u} . \qquad \ldots(6.36)$$

Given that $Z^4 \sigma^{(Z)}_{n' \to n}(u)$ is approximately independent of the ion considered, we get

$$5^4 \frac{f^{(NV)}_{n' \to n}}{\{E^{(NV)}_{n'n}\}^2} \alpha_{NV} \ln(1.25 \beta_{NV} u) \simeq Z^4 \frac{f^{(Z)}_{n' \to n}}{\{E^{(Z)}_{n'n}\}^2} \alpha_Z \ln(1.25 \beta_Z u). \qquad \ldots(6.37)$$

Since β_Z is relatively independent of Z, and since $\ln(1.25 \beta_Z u)$ is a slowly varying function of β_Z, we can drop the terms containing β_Z out of eq.(6.37) and write

$$\alpha_{n'n}^{(Z)} \simeq \left(\frac{5}{Z}\right)^4 \frac{f_{n'\to n}^{(NI)}}{f_{n'\to n}^{(Z)}} \left(\frac{E_{n'n}^{(Z)}}{E_{n'n}^{(NI)}}\right)^2 \alpha_{n'n}^{(NI)} . \qquad \ldots(6.38)$$

For hydrogenic ions, the oscillator strength is independent of Z and, as a first approximation, we can use for lithium-like ions

$$f_{n'\to n}^{(Z)} \simeq f_{n'\to n}^{(NI)} \qquad \ldots(6.39)$$

to simplify the calculations. We thus obtain

$$\alpha_{n'n}^{(Z)} \simeq \left(\frac{5}{Z}\right)^4 \left(\frac{E_{n'n}^{(Z)}}{E_{n'n}^{(NI)}}\right)^2 \alpha_{n'n}^{(NI)} . \qquad \ldots(6.40)$$

In Tab.6.13, we compare the results obtained from eqs.(6.38) and (6.40) for the 2s -> 5p transition with the values obtained from Bely's (1966a) calculations. Although eq.(6.40) is more approximate than eq.(6.38), it gives better results. This shows the approximate nature of this method. We will thus use

$$\alpha_{n'n}^{(CIV)} \simeq 2.44 \left(\frac{E_{n'n}^{(CIV)}}{E_{n'n}^{(NI)}}\right)^2 \alpha_{n'n}^{(NI)} \qquad \ldots(6.41)$$

and

$$\alpha_{n'n}^{(OVI)} \simeq \frac{1}{2.07} \left(\frac{E_{n'n}^{(OVI)}}{E_{n'n}^{(NI)}}\right)^2 \alpha_{n'n}^{(NI)} \qquad \ldots(6.42)$$

to calculate the values of α for the allowed and forbidden transitions of the ions C IV and O VI for which no data are available.

Table 6.13 - Value of the parameter α for the 2s→5p transition of C IV and O VI as calculated from various equations.

	C IV	N V	O VI
Z	4	5	6
$E_{n'n}$	4.09 Rydbergs	6.18 Rydbergs	8.69 Rydbergs
$f_{n'\rightarrow n}$	0.0290	0.0322	0.0343
$\alpha_{n'n}$	0.858	0.798	0.765
Eq.(6.38)	0.947	-	0.714
Eq.(6.40)	0.853	-	0.761

The values of the parameters β and ϕ for these transitions will be set equal to the parameters of the corresponding transitions in N V. There are several reasons which justify this choice of parameters: The extrapolated values of β and ϕ for N V have large uncertainties, and since the known values of these parameters for the ions C IV, N V and O VI are all quite close, we can expect that the unknown parameters of C IV and O VI will fall within the range of uncertainty associated with the parameters of N V. Since ϕ affects the cross-section only at low values of U, and since the cross-section depends on the natural logarithm of β, the cross-section will be less affected by large uncertainties in β and ϕ than by corresponding uncertainties in α. This is more fully discussed in the following Section.

4.5. Estimated errors in the extrapolated parameters

The errors in the extrapolated parameters are difficult to evaluate. Reasonable estimates of the uncertainties associated with them can however be obtained and are given below.

a. The error in the extrapolated values of α is estimated to be less than a factor of two in most cases, based on the fact that the parameters α show little variation and that hydrogen values are used as guidelines in the extrapolation procedure. Since α has a constant value for the allowed transitions of hydrogen, the allowed transition parameters can be expected to be more accurate than the forbidden transition parameters. It should also be noted that this error estimate does not hold for $\Delta n = 0$ forbidden transitions; these, as explained previously, have large uncertainties which cannot be estimated. How-

ever, the overall effect of these large errors is negligible since $\Delta n = 0$ transitions are strongly dominated by the optically allowed transitions.

b. An error of ± 0.5 is assigned to ϕ. Since in most cases, $0 \leq \phi \leq 1$ for $\Delta n \geq 1$ transitions, such an error estimate is reasonable. For $\Delta n = 0$ transitions, $-1 \leq \phi \leq 0$, and again, the error estimate is compatible with the range of values of ϕ.

c. The error in the extrapolated values of β is very difficult to estimate due to the wide range of values which the parameter can take. However, we estimate this error to be a factor of about four in most cases. Since the minimum value of β is 0.8, this error estimate sets the regular range of β to $0.8 \leq \beta \leq 12.8$, with a geometric mean of 3.2, the value of β obtained from the Born approximation.

The error estimates in the extrapolated parameters may be summarized as follows:

$$\frac{\Delta\alpha}{\alpha} = 2^{\pm 1}$$

$$\log\left(\frac{\Delta\alpha}{\alpha}\right) = \pm 0.3$$

$$\frac{\Delta\beta}{\beta} = 4^{\pm 1}$$

$$\log\left(\frac{\Delta\beta}{\beta}\right) = \pm 0.6$$

$$\Delta\phi = \pm 0.5 \qquad \ldots(6.43)$$

The effect of these uncertainties on the cross-sections depends on the parameter considered. The following relations are derived from eqs.(6.6) and (6.11):

$$\frac{\Delta\sigma}{\sigma} = \frac{\Delta\alpha}{\alpha}$$

$$\frac{\Delta\sigma}{\sigma} = \frac{1}{\ln(1.25\beta u)} \frac{\Delta\beta}{\beta}$$

$$\frac{\Delta\sigma}{\sigma} = \frac{\Delta\phi}{u-\phi} \qquad \ldots(6.44)$$

We see that the error in the parameter α dominates the error in the cross-section because the errors in the parameters β and ϕ are decreased by a factor $\ln(1.25\beta u)$ and $(U-\phi)$ respectively. This is due to the fact that α is a factor which determines the magnitude of the cross-section whereas ϕ is related to the value of the cross-section at threshold, and β to the width of the peak observed in the cross-section.

5. CROSS-SECTIONS INVOLVING AVERAGE STATES

The cross-sections of average states can be obtained from the individual cross-sections with the summation rules (Moiseiwitsch and Smith, 1968)

$$\sigma_{n'l'\to n}(u) = \sum_{l} \sigma_{n'l'\to nl}(u) \qquad \ldots(6.45)$$

and

$$\sigma_{n' \to n}(u) = \sum_{l'} \frac{\omega_{n'l'}}{\omega_{n'}} \sigma_{n'l' \to n}(u) \qquad \ldots(6.46)$$

where $\omega_{n'l'}$ and $\omega_{n'}$ are the statistical weights of levels $n'l'$ and n' respectively. With $\omega_{n'l'} = 2(2l'+1)$ and $\omega_{n'} = n'^2$, we get

$$\sigma_{n' \to n}(u) = \sum_{l'} \frac{2l'+1}{n'^2} \sigma_{n'l' \to n}(u). \qquad \ldots(6.47)$$

5.1. $n'l' \to n$ transitions

The cross-sections of these transitions are calculated from a simplified form of eq.(6.45):

$$\sigma_{n'l' \to n}(u) \simeq \sum_{l=l'}^{l'+s} \sigma_{n'l' \to nl}(u). \qquad \ldots(6.48)$$

This simplification is possible because of the following observed behaviors of the individual cross-sections.

Since the $\Delta l < 0$ cross-sections are very much smaller than the $\Delta l \geq 0$ cross-sections, they can be deleted from the sum (6.45). We further neglect the $\Delta l \geq 6$ cross-sections due to the following characteristics of $\Delta l \geq 0$ transitions:

i. large Δn: For large Δn transitions, the $n'l' \to n$ cross-sections are dominated by the $n'l' \to nl$ cross-sections with very low positive values of Δl. This is due to the fact that at low values of U, the average cross-section is dominated by the $\Delta l = 2$ cross-section, and at high values of U, by the $\Delta l = 1$ cross-section due to its logarithmic dependence on U.

ii. small Δn : The average cross-section is still dominated by the $\Delta\ell = 2$ cross-section at low values of U and by the $\Delta\ell = 1$ cross-section at high values of U. However, the contribution from cross-sections with higher positive values of $\Delta\ell$ increases.

iii. $\Delta n = 0$: The average cross-section is dominated by the $\Delta\ell = 1$ allowed transition; the contributions of forbidden transitions are almost negligible.

The cross-sections obtained for the $n'\ell' \rightarrow n$ transitions by applying the summation rule (6.48) are fitted to eq.(6.6). The resulting sets of parameters for the transitions used in this work are then averaged as follows:

i. $\Delta n = 0$ transitions, $ns \rightarrow n\langle \ell \geq 1 \rangle$: The average of the available sets of parameters gives

$$\alpha = 1.9 \pm 0.0$$

$$\beta = 3.5 \pm 0.0$$

$$\phi = -1.0 \pm 0.0 \qquad \ldots(6.49)$$

where the errors given are the standard deviations of the averaged data.

ii. $\Delta n \geq 1$ transitions, $n'\ell' \rightarrow n\langle \ell \geq 1 \rangle$ and $n'\ell' \rightarrow n$: The same set of parameters is obtained for the $n'\ell' \rightarrow n\langle \ell \geq 1 \rangle$ and $n'\ell' \rightarrow n$ transitions because the $n'\ell' \rightarrow ns$ transition contributes very little to the $n'\ell' \rightarrow n$ cross-section.

Almost all values of β are found to lie within the range $1.40 \leq \beta \leq 1.50$; the average value of β is

$$\beta = 1.45 \pm 0.06 \qquad \ldots(6.50)$$

where the error is the standard deviation of the data. The values of α and ϕ show more variation; however, since a more or less constant value of β is obtained for these transitions, constant values of α and ϕ should also be expected. We thus average those values of α and ϕ for which the corresponding value of β lies within one standard deviation of the average (6.50): $1.39 \leq \beta \leq 1.51$. We obtain

$$\alpha = 1.5 \pm 0.4$$

$$\phi = -2.7 \pm 0.5 \qquad \ldots(6.51)$$

where the errors are the standard deviations of the data.

In conclusion, the following sets of parameters are used for the $n'\ell' \rightarrow n$ transitions:

i. $\Delta n = 0$ transitions, $ns \rightarrow n\langle \ell \geq 1 \rangle$

$$\alpha = 1.9$$
$$\beta = 3.5$$
$$\phi = -1.0 \qquad \ldots(6.52)$$

ii. $\Delta n \geq 1$ transitions, $n'\ell' \rightarrow n\langle \ell \geq 1 \rangle$ and $n'\ell' \rightarrow n$

$$\alpha = 1.5$$

$$\beta = 1.45$$

$$\phi = -2.7. \qquad \ldots(6.53)$$

5.2. $n' \rightarrow n$ transitions

Using the summation rule (6.46), viz.

$$\sigma_{n' \rightarrow n}(u) = \sum_{l'} \frac{\omega_{n'l'}}{\omega_{n'}} \sigma_{n'l' \rightarrow n}(u),$$

and eq.(6.6) to represent the cross-section for the $n'l' \rightarrow n$ transition, we get

$$\sigma_{n' \rightarrow n}(u) = 4\pi a_0^2 \left[\sum_{l'} \frac{\omega_{n'l'}}{\omega_{n'}} \frac{f_{n'l' \rightarrow n}}{E^2_{n'l',n}}\right] \alpha \frac{u-\phi}{u^2} \ln(1.25\beta u) \ldots(6.54)$$

where α, β, and ϕ are constants given by relations (6.53) and $E_{n'l',n}$ is in Rydbergs. Since the values of α, β, and ϕ are approximate, we can put $E_{n'l',n}$ independent of l' to simplify the evaluation of the quantity in square brackets: $E_{n'l',n} \simeq E_{n'n}$. Then we have

$$\sum_{l'} \frac{\omega_{n'l'}}{\omega_{n'}} \frac{f_{n'l' \rightarrow n}}{E^2_{n'l',n}} \simeq \frac{1}{\omega_{n'} E^2_{n'n}} \sum_{l'} \omega_{n'l'} f_{n'l' \rightarrow n}. \qquad \ldots(6.55)$$

Since (see Section 4 of Chapter IV)

$$\sum_{\ell'} \omega_{n'\ell'} f_{n'\ell' \to n} \simeq \omega_{n'} f_{n' \to n}$$

eq. (6.55) becomes

$$\sum_{\ell'} \frac{\omega_{n'\ell'}}{\omega_{n'}} \frac{f_{n'\ell' \to n}}{E^2_{n'\ell', n}} \simeq \frac{f_{n' \to n}}{E^2_{n'n}} . \qquad \ldots(6.56)$$

To a good approximation, the equation

$$\sigma_{n' \to n}(u) = 4\pi a_0^2 \frac{f_{n' \to n}}{E^2_{n'n}} \propto \frac{u - \phi}{u^2} \ln(1.25 \beta u) \qquad \ldots(6.57)$$

where

$$\alpha = 1.5$$
$$\beta = 1.45$$
$$\phi = -2.7 \qquad \ldots(6.58)$$

thus holds for the n' -> n transitions.

5.3. $n'\langle \ell' \geq 1 \rangle$ -> ns transitions

A few transitions of this kind occur in the configuration of levels used in this work. Summing over the final states and averaging over the initial states (Moiseiwitsch and Smith, 1968), we obtain the summation rule

$$\sigma_{n'\langle \ell' \geq 1 \rangle \to ns}(u) = \sum_{\ell' \neq s} \frac{\omega_{n'\ell'}}{\omega_{n'\langle \ell' \geq 1 \rangle}} \sigma_{n'\ell' \to ns}(u) . \qquad \ldots(6.59)$$

We use eq.(6.59) to add the individual cross-sections and we fit the resulting data to eq.(6.6). The following set of parameters approximates the $n' \langle \ell' \gtrless 1 \rangle \rightarrow ns$ cross-sections:

$$\alpha = 0.03$$

$$\beta = 1.5$$

$$\phi = 0.2 \qquad \ldots(6.60)$$

As expected for $\Delta\ell < 0$ transitions, α is very small.

6. COLLISIONAL EXCITATION RATE COEFFICIENTS

The rate coefficient for collisional excitation of the $n' \rightarrow n$ transition by electron impact is given by (Drawin, 1966)

$$C_{n' \rightarrow n}(T) = \int_v \sigma_{n' \rightarrow n}(v)\, v\, f(v)\, dv \qquad \ldots(6.61)$$

where v is the velocity and f(v) the velocity distribution of the incident electrons. Here n' and n represent all the quantum numbers of the states considered. Using the Maxwellian velocity distribution

$$\frac{dn_e}{n_e} = f(v)\, dv = \frac{4v^2}{\sqrt{\pi}\,(2kT/m)^{3/2}}\, e^{-\frac{mv^2}{2kT}}\, dv \qquad \ldots(6.62)$$

and expressing eqs.(6.61) and (6.62) in terms of the kinetic energy E of the incident electron, we obtain

$$C_{n' \rightarrow n}(T) = \frac{1}{\sqrt{\pi m}} \left(\frac{2}{kT}\right)^{3/2} \int_E \sigma_{n' \rightarrow n}(E)\, E\, e^{-\frac{E}{kT}}\, dE. \qquad \ldots(6.63)$$

With threshold energy units $U = E/E_{n'n}$, eq.(6.63) becomes

$$C_{n'\to n}(T) = \sqrt{\frac{8}{\pi m k^3}} \frac{E_{n'n}^2}{T^{3/2}} \times \int_1^\infty \sigma_{n'\to n}(u)\, e^{-\frac{E_{n'n}}{kT}u}\, u\, du. \qquad \ldots(6.64)$$

We write the cross-section as

$$\sigma_{n'\to n}(u) = 4\pi a_0^2 \frac{\mathcal{F}_{n'\to n}}{E_{n'n}^2} g_{n'n}(u) \qquad \ldots(6.65)$$

where

$$\mathcal{F}_{n'\to n} = f_{n'\to n}$$

$$g_{n'n}(u) = \alpha_{n'n} \frac{u - \phi_{n'n}}{u^2} \ln(1.25 + \beta_{n'n} u) \qquad \ldots(6.66)$$

for allowed transitions, and

$$\mathcal{F}_{n'\to n} = \left(\frac{n'}{n}\right)^3$$

$$g_{n'n}(u) = \alpha_{n'n} \frac{u - \phi_{n'n}}{u^2} \qquad \ldots(6.67)$$

for forbidden transitions. With $E_{n'n}$ in Rydbergs and T in K, we have

$$C_{n'\to n}(T) = 5.45 \frac{\mathcal{F}_{n'\to n}}{T^{3/2}} D_{n'\to n}(\theta)\ cm^3 s^{-1} \qquad \ldots(6.68)$$

where

$$D_{n'\to n}(\theta) = \int_1^\infty g_{n'n}(u)\, u\, e^{-\theta u}\, du \qquad \ldots(6.69)$$

and $$\theta = .157\,890\,\frac{E_{n'n}}{T}\,. \qquad \ldots(6.70)$$

In particular, we define the functions

$$D_{n'\to n}(\theta) = D_a(\alpha, \beta, \phi; \theta)$$

$$= \alpha \int_1^\infty \frac{u-\phi}{u} \ln(1.25\beta u)\, e^{-\theta u}\, du \qquad \ldots(6.71)$$

for allowed transitions, and

$$D_{n'\to n}(\theta) = D_f(\alpha, \phi; \theta)$$

$$= \alpha \int_1^\infty \frac{u-\phi}{u}\, e^{-\theta u}\, du \qquad \ldots(6.72)$$

for forbidden transitions.

7. EVALUATION OF THE INTEGRALS

We first evaluate the simpler integral $D_f(\alpha, \phi; \theta)$. With the substitution $x = \theta u$ in eq.(6.72), we obtain the integral

$$D_f(\alpha, \phi; \theta) = \frac{\alpha}{\theta} \int_\theta^\infty \left(1 - \frac{\phi\theta}{x}\right) e^{-x}\, dx \qquad \ldots(6.73)$$

which is easily evaluated:

$$D_f(\alpha, \phi; \theta) = \frac{\alpha}{\theta}\left[e^{-\theta} - \phi\,\theta\, E_1(\theta)\right]. \qquad \ldots(6.74)$$

$E_1(\theta)$ is the exponential integral,

$$E_1(\theta) = \int_\theta^\infty \frac{e^{-x}}{x}\, dx \qquad \ldots(6.75)$$

The integral $D_a(\alpha, \beta, \phi; \theta)$ is evaluated by putting $x = \theta U$ in eq.(6.71). We get

$$D_a(\alpha, \beta, \phi; \theta) = \frac{\alpha}{\theta}\int_\theta^\infty \left(1 - \frac{\phi\theta}{x}\right) \ln\left(\frac{1.25\beta}{\theta} x\right) e^{-x} dx. \qquad \ldots(6.76)$$

Expanding the logarithmic term, eq.(6.76) becomes

$$D_a(\alpha, \beta, \phi; \theta) = \frac{\alpha}{\theta} \ln\left(\frac{1.25\beta}{\theta}\right) \int_\theta^\infty \left(1 - \frac{\phi\theta}{x}\right) e^{-x} dx$$

$$+ \frac{\alpha}{\theta}\int_\theta^\infty \left(1 - \frac{\phi\theta}{x}\right) \ln x\, e^{-x} dx \qquad \ldots(6.77)$$

$$= \ln\left(\frac{1.25\beta}{\theta}\right) D_f(\alpha, \phi; \theta)$$

$$+ \frac{\alpha}{\theta}\int_\theta^\infty \ln x\, e^{-x} dx - \alpha\phi \int_\theta^\infty \frac{\ln x}{x}\, e^{-x} dx. \qquad \ldots(6.78)$$

The integrals of eq.(6.78) have already been evaluated for hydrogen in Appendix C. They are

$$\int_\theta^\infty \ln x\, e^{-x} dx = \ln\theta\, e^{-\theta} + E_1(\theta) \qquad \ldots(6.79)$$

$$\int_\theta^\infty \frac{\ln x}{x}\, e^{-x} dx = \ln\theta\, E_1(\theta) + \epsilon_1(\theta) \qquad \ldots(6.80)$$

where $\epsilon_1(\theta) = \int_\theta^\infty \frac{E_1(x)}{x}\, dx.$ ...(6.81)

Analytical approximations to this function are given in Appendix C. Using eqs.(6.79) and (6.80) in eq.(6.78), we obtain

$$D_a^+(\alpha, \beta, \phi; \theta) = \ln\left(\frac{1.25\beta}{\theta}\right) D_f(\alpha, \phi; \theta) + \frac{\alpha}{\theta}\left[\ln\theta\, e^{-\theta} + E_1(\theta)\right] - \alpha\phi\left[\ln\theta\, E_1(\theta) + \epsilon_1(\theta)\right] \quad ...(6.82)$$

which can be rearranged in terms of $D_f(\alpha, \phi; \theta)$ to give

$$D_a(\alpha, \beta, \phi; \theta) = \ln(1.25\beta)\, D_f(\alpha, \phi; \theta) + \frac{\alpha}{\theta}\left[E_1(\theta) - \phi\theta\,\epsilon_1(\theta)\right]. \quad ...(6.83)$$

8. COMPARISON WITH HYDROGENIC VALUES

We wish to compare the lithium-like and hydrogenic collisional excitation rate coefficients of the transitions between the average states n' and n of these ions. The average rate coefficients of the n' -> n transitions are obtained from the individual $n'l'$ -> nl rate coefficients by summation rules which we now derive.

The excitation cross-sections obey the summation rules (6.45) and (6.46), viz.

$$\bar{\sigma}_{n'l' \to n}(v) = \sum_{l} \sigma_{n'l' \to nl}(v)$$

$$\sigma_{n' \to n}(v) = \sum_{l'} \frac{\omega_{n'l'}}{\omega_{n'}} \sigma_{n'l' \to n}(v).$$

Integrating these expressions over a free electron velocity distribution f(v), we obtain

$$\int_v \sigma_{n'l' \to n}(v)\, v\, f(v)\, dv = \int_v \sum_{l} \sigma_{n'l' \to nl}(v)\, v\, f(v)\, dv$$

$$= \sum_{l} \int_v \sigma_{n'l' \to nl}(v)\, v\, f(v)\, dv \qquad \ldots(6.84)$$

and

$$\int_v \sigma_{n' \to n}(v)\, v\, f(v)\, dv = \int_v \sum_{l'} \frac{\omega_{n'l'}}{\omega_{n'}} \sigma_{n'l' \to n}(v)\, v\, f(v)\, dv$$

$$= \sum_{l'} \frac{\omega_{n'l'}}{\omega_{n'}} \int_v \sigma_{n'l' \to n}(v)\, v\, f(v)\, dv \qquad \ldots(6.85)$$

From the definition of the collisional excitation rate coefficient, eq.(6.61), we thus have the summation rules

$$C_{n'l' \to n}(T) = \sum_{l} C_{n'l' \to nl}(T) \qquad \ldots(6.86)$$

and

$$C_{n'\to n}(T) = \sum_{l'} \frac{\omega_{n'l'}}{\omega_{n'}} C_{n'l'\to n}(T). \qquad \ldots(6.87)$$

A satisfactory comparison of the hydrogenic and lithium-like rate coefficients is difficult since the average rate coefficients for excitation of hydrogenic ions are obtained by neglecting the forbidden transitions. On the other hand, the lithium-like rate coefficients $C_{n'\to n}(T)$ obtained from eqs.(6.86) and (6.87) include all transitions and thus they cannot be compared directly with the hydrogenic values calculated from the work of Drawin (1963, 1964, 1966) (see Section 5 of Chapter II). However, we will compare the hydrogenic values of $C_{n'\to n}(T)$ with the lithium-like values obtained by carrying out the summations (6.86) and (6.87) over allowed transitions only, and also over all transitions (allowed + forbidden). We will thus be able to compare directly all transitions with $n \leq 6$; for transitions to states $n \geq 7$, direct comparison is not possible since the contribution of the forbidden transitions to the average rate coefficients of the lithium-like ions is not known.

In Fig.6.21 and 6.22, the rate coefficients for excitation from the states $n' = 2, 3, 4,$ and 5 to all states $n \leq 11$ of N V and a hydrogenic ion with $Z = 5$ are given at temperatures of 16,000 K and 256,000 K. The average rate coefficients of the lithium-like ion N V summed over allowed and forbidden transitions are found to be greater than the corresponding hydrogenic rate coefficients by a factor of up to ten. This is partly due to a significant contribution of forbidden transitions. However, we also observe that the lithium-like average rate coefficients

summed over allowed transitions only are larger than their hydrogenic counterparts at large Δn by a factor of up to three, whereas, for lower values of Δn, they are of comparable magnitude. Since Drawin's hydrogenic rate coefficients are also approximate, the agreement between the lithium-like and the hydrogenic rate coefficients summed over allowed transitions only is quite reasonable, especially when uncertainties are taken into consideration. Drawin's results should be good to within a factor of two, and the lithium-like coefficients to a factor of four or more (see Section 9 of this Chapter). These give possible errors of a factor of eight or more which is well over the factor of three mentioned above.

9. ACCURACY OF THE RATE COEFFICIENTS

The accuracy of the excitation rate coefficients depends on how good the available cross-sections and the extrapolated parameters are.

The accuracy of the cross-sections of the 2s -> ns, np, nd, nf and 2p -> ns, np, nd transitions is discussed by Bely (1966a, b) and Bely and Petrini (1970). The 2s -> 2p cross-section is accurate to within a few percent ; the cross-sections of the other transitions are reliable to within a factor of two for the first few ions of the lithium isoelectronic sequence. However, as Z increases, the Coulomb-Born approximation gives better results and the accuracy of the cross-sections becomes better than a factor of two. The rate coefficients for excitation of the 2s and 2p states of C IV, N V, and O VI are thus within less than a factor of two of the actual ones.

For the excitation of the 3s and higher states of C IV, N V, and O VI, the accuracy of the cross-sections depends on how reliable the extrapolated parameters of these transitions are. As eq.(6.44) shows, the error in the cross-section will thus be dominated by the error in the parameter α. α is reliable to better than a factor of two; however the errors in β and ϕ will increase the error estimate of the cross-section to a bit higher than a factor of two. Since the parameters are extrapolated from the data on the excitation of the 2s and 2p states, and since these data are in error by less than a factor of two, the extrapolated cross-sections should approximate the actual ones to within a factor of $\sim$4 in most cases. The rate coefficients for excitation of the 3s and higher states of C IV, N V, and O VI will thus be, in most cases, within a factor of $\sim$4 of the actual ones, with a possible maximum error of a factor of ten because the lithium-like rate coefficients are within a factor of ten of the corresponding hydrogenic coefficients as seen in Fig.6.23.

This error estimate applies to all transitions with the exception of the $\Delta n = 0$ transitions. The uncertainty in the rate coefficients of $\Delta n = 0$ allowed transitions must be increased because of the large error in the oscillator strengths associated with these transitions (see Section 3.3.b of Chapter IV). Furthermore, the parameters of the $\Delta n = 0$ forbidden transitions have been obtained by a very crude method, and no estimate whatsoever of the resulting errors can be given. Fortunately, $\Delta n = 0$ forbidden transitions contribute very little to $\Delta n = 0$ transitions and their effect is thus quite negligible. It is to be understood that the error analysis given in this Chapter is correct as long as no excitation of the inner shell electrons occurs.

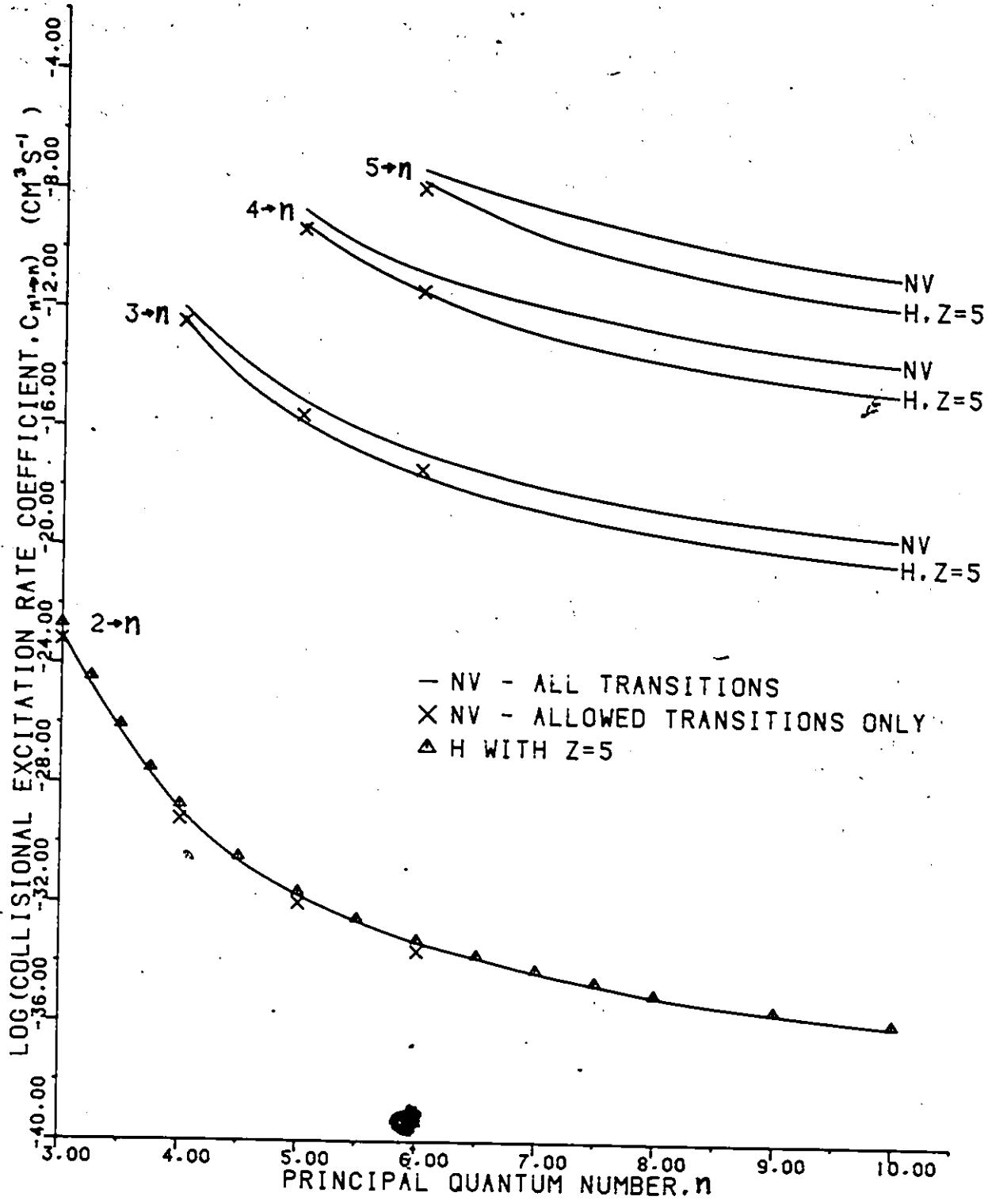

FIGURE 6.21 - ELECTRON IMPACT EXCITATION RATE COEFFICIENT OF N V AND OF A HYDROGENIC ION WITH Z=5 AT T=16000K.

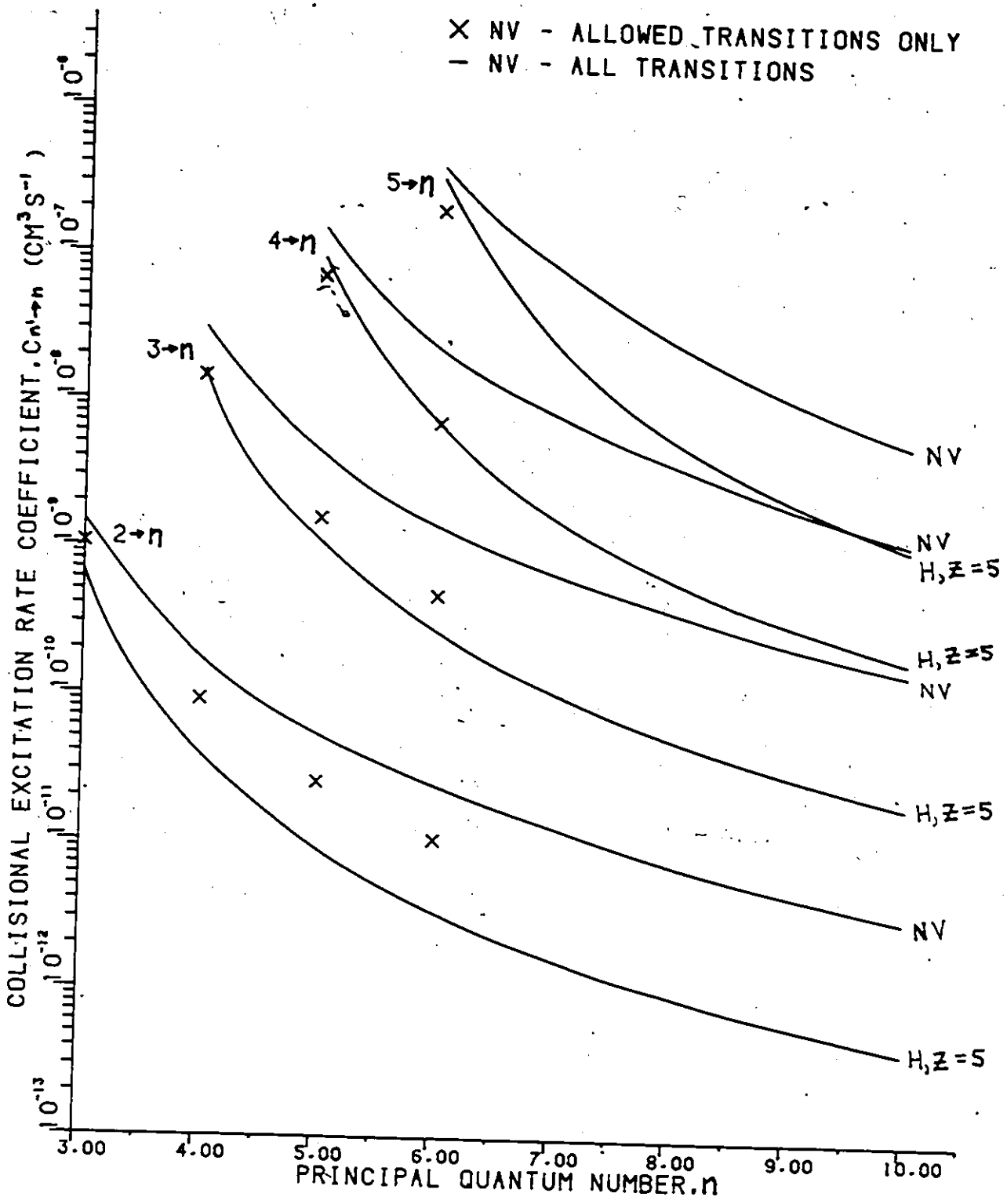

FIGURE 6.22 - ELECTRON IMPACT EXCITATION RATE COEFFICIENT OF N V AND OF A HYDROGENIC ION WITH Z=5 AT T=256000K.

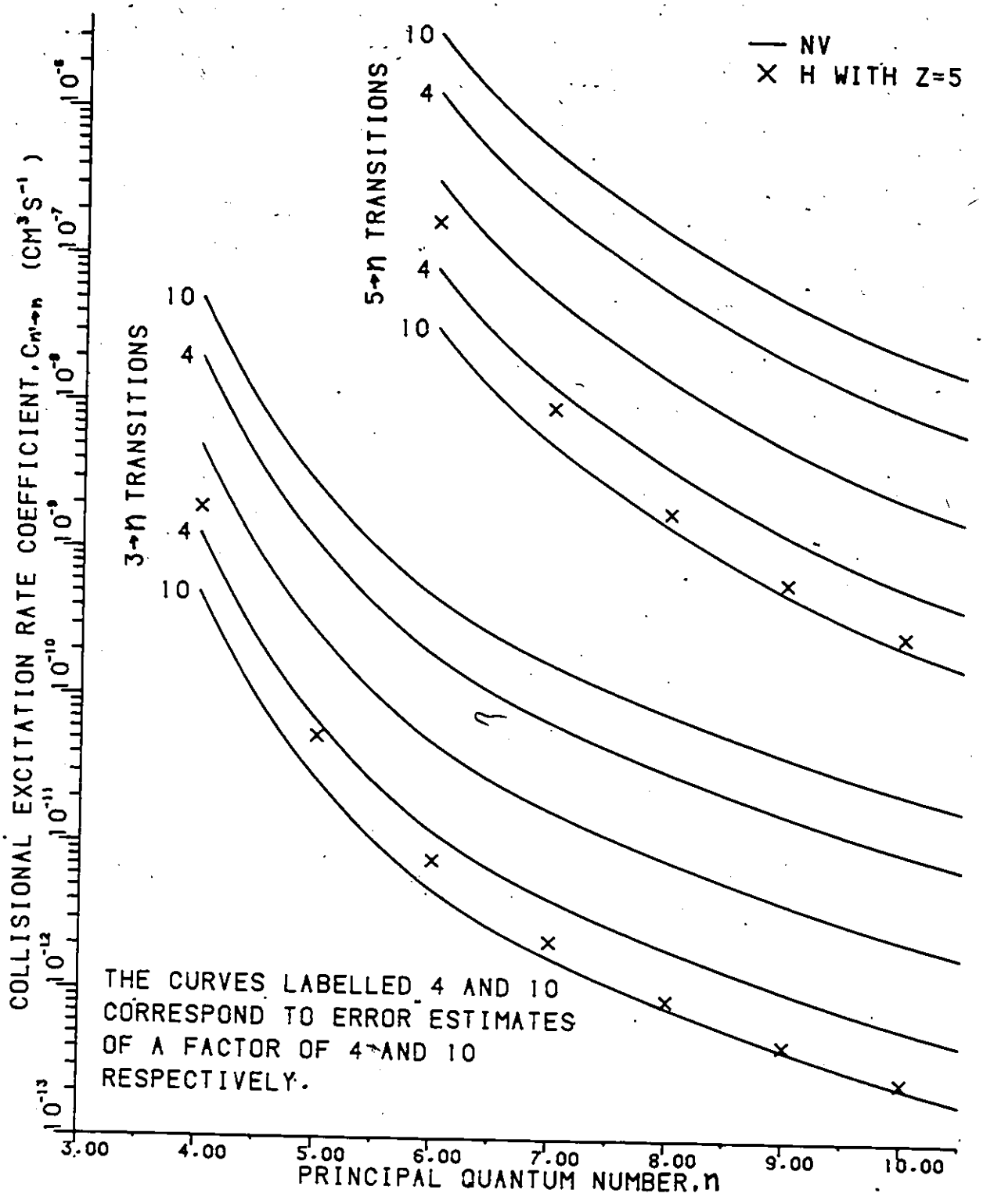

FIGURE 6.23 - ELECTRON IMPACT EXCITATION RATE COEFFICIENT OF N V AND OF A HYDROGENIC ION WITH Z=5 AT T=64000K.

Chapter VII

C IV, N V, AND O VI: COLLISIONAL DE-EXCITATION RATE COEFFICIENTS AND THREE-BODY RECOMBINATION RATE COEFFICIENTS

1. INTRODUCTION

The rate coefficients for the collisional de-excitation of an ion by electron impact and for three-body recombination are related to the rate coefficients of the inverse processes of electron impact excitation and ionization respectively by the principle of detailed balancing (see Section 6 of Chapter II).

2. THREE-BODY RECOMBINATION RATE COEFFICIENT

The rate for three-body recombination of a free electron into state n of an atom or ion is given by (Drawin, 1963)

$$\alpha_n(T) = \frac{h^3}{(2\pi m k T)^{3/2}} \frac{\omega_n}{2u_i} e^{\theta_n} S_n(T) \qquad \ldots(7.1)$$

where u_i is the partition function of the ion before recombination, ω_n is the statistical weight of the recombined electron in state n, $\theta_n = I_n / kT$, I_n is the ionization potential of level n, and $S_n(T)$ is the collisional ionization rate coefficient. Numerically, for T in Kelvin and $S_n(T)$ in cm^3/s,

$$\alpha_n(T) = \frac{2.071 \times 10^{-16}}{T^{3/2}} \frac{\omega_n}{u_i} e^{\theta_n} S_n(T) \ cm^6 s^{-1}. \qquad \ldots(7.2)$$

Substituting for $S_n(T)$ from eq.(5.11),

$$\alpha_n(T) = \frac{5.0 \times 10^{-21}}{I_n T^2} \frac{\omega_n}{u_{i_R}} E_1'(\theta_n) \quad cm^6 s^{-1} \qquad \ldots(7.3)$$

where I_n is in Rydbergs. Alternatively,

$$\alpha_n(T) = \frac{7.8 \times 10^{-16}}{T^3} \frac{\omega_n}{u_i} \frac{E_1'(\theta_n)}{\theta_n} \quad cm^6 s^{-1} \qquad \ldots(7.4)$$

where $$E_1'(\theta_n) = e^{\theta_n} E_1(\theta_n) \qquad \ldots(7.5)$$

and $E_1(\theta_n)$ is the exponential integral. For large values of θ_n, eq.(7.5) can be evaluated with eq.(2.72). The accuracy of the rate coefficients calculated with eq.(7.4) is comparable to that of the collisional ionization rate coefficient $S_n(T)$ used in eq.(7.2) and is discussed in Section 6 of Chapter V.

The rate coefficient for recombination of an electron into an average state n can be obtained from the rate coefficients for recombination into the individual $n\ell$ states of n from the following summation rule. From eq.(5.19), the summation rule for collisional ionization rate coefficients is

$$S_n(T) = \sum_{\ell} \frac{\omega_{n\ell}}{\omega_n} S_{n\ell}(T) \qquad \ldots(7.6)$$

where $\omega_{n\ell}$ and ω_n are the statistical weights of level $n\ell$ and of the average level n respectively. From the principle of detailed balancing, $S_n(T)$ is related to $\alpha_n(T)$ by eq.(7.1):

$$S_n(T) = K \frac{u_i}{\omega_n} e^{-\theta_n} \alpha_n(T) \qquad \ldots(7.7)$$

where $K = \dfrac{2(2\pi m k T)^{3/2}}{h^3}$.

Substituting for $S_{n\ell}(T)$ and $S_n(T)$ into eq.(7.6) from eq.(7.7), we obtain

$$K \frac{u_i}{\omega_n} e^{-\theta_n} \alpha_n(T) = \sum_{\ell} \frac{\omega_{n\ell}}{\omega_n} K \frac{u_i}{\omega_{n\ell}} e^{-\theta_{n\ell}} \alpha_{n\ell}(T) \qquad \ldots(7.8)$$

which becomes

$$\alpha_n(T) = \sum_{\ell} e^{\theta_n - \theta_{n\ell}} \alpha_{n\ell}(T). \qquad \ldots(7.9)$$

As n increases, $\theta_n \simeq \theta_{n\ell}$, and

$$\alpha_n(T) \simeq \sum_{\ell} \alpha_{n\ell}(T). \qquad \ldots(7.10)$$

3. COLLISIONAL DE-EXCITATION RATE COEFFICIENT

The rate coefficient for de-excitation of a bound electron from state n to n' by electron impact is given by (Drawin, 1963)

$$F_{n \to n'}(T) = \frac{\omega_{n'}}{\omega_n} e^{\theta_{n'n}} C_{n' \to n}(T) \qquad \ldots(7.11)$$

where $\omega_{n'}$ and ω_n are the statistical weights of states n' and n respectively, $\theta_{n'n} = E_{n'n} / kT$, $E_{n'n}$ is the energy separation of levels n' and n, and $C_{n' \to n}(T)$ is the collisional excitation rate coefficient. Substituting for $C_{n' \to n}(T)$ from eq.(6.68), eq.(7.11) becomes

$$F_{n\to n'}(T) = \frac{5.45}{T^{3/2}} \frac{\omega_{n'}}{\omega_n} \mathcal{J}_{n'\to n} D'_{n'\to n}(T) \quad cm^3 s^{-1} \qquad \ldots(7.12)$$

where

$$D'_{n'\to n}(T) = e^{\theta_{n'n}} D_{n'\to n}(T). \qquad \ldots(7.13)$$

For forbidden transitions,

$$\mathcal{J}_{n'\to n} = \left(\frac{n'}{n}\right)^3 \qquad \ldots(7.14)$$

$$D_{n'\to n}(T) = D_f(\alpha, \phi; \theta)$$

$$= \frac{\alpha}{\theta}\left[e^{-\theta} - \phi\theta E_1(\theta)\right] \qquad \ldots(7.15)$$

and for allowed transitions,

$$\mathcal{J}_{n'\to n} = f_{n'\to n} \qquad \ldots(7.16)$$

$$D_{n'\to n}(T) = D_a(\alpha, \beta, \phi; \theta)$$

$$= \ln(1.25\beta)\, D_f(\alpha, \phi; \theta)$$

$$+ \frac{\alpha}{\theta}\left[E_1(\theta) - \phi\theta \in_1(\theta)\right] \qquad \ldots(7.17)$$

where $f_{n'\to n}$ is the absorption oscillator strength for the n' -> n transition,

$$\epsilon_1(\theta) = \int_\theta^\infty \frac{E_1(x)}{x}\,dx \qquad \ldots(7.18)$$

and all other quantities are as defined in Chapter VI. The evaluation of eq.(7.18) is discussed in Appendix C. It should be noted that the parameters α, β, ϕ, and θ are equivalent to the subscripted parameters $\alpha_{n'n}$, $\beta_{n'n}$, $\phi_{n'n}$, and $\theta_{n'n}$ respectively. For large values of θ, eq.(7.15) and (7.17) are written as

$$D_f'(\alpha,\phi;\theta) = e^\theta D_f(\alpha,\phi;\theta)$$

$$= \frac{\alpha}{\theta}\left[1-\phi\theta E_1'(\theta)\right] \qquad \ldots(7.19)$$

and

$$D_a'(\alpha,\beta,\phi;\theta) = e^\theta D_a(\alpha,\beta,\phi;\theta)$$

$$= \ln(1.25\beta)\, D_f'(\alpha,\phi;\theta)$$

$$+ \frac{\alpha}{\theta}\left[E_1'(\theta) - \phi\theta\epsilon_1'(\theta)\right] \qquad \ldots(7.20)$$

where $E_1'(\theta) = e^\theta E_1(\theta)$ is evaluated with eq.(2.72) and $\epsilon_1'(\theta) = e^\theta \epsilon_1(\theta)$ is evaluated in Appendix C. The accuracy of eq.(7.12) is comparable to that of the collisional excitation rate coef-

ficients from which it is evaluated. A discussion of this accuracy is given in Section 9 of Chapter VI.

Chapter VIII

C IV, N V, AND O VI: RADIATIVE RECOMBINATION RATE COEFFICIENTS

1. INTRODUCTION

The radiative recombination rate coefficients of a large number of states of the lithium-like ions C IV, N V, and O VI are required in this work. Some calculations of photoionization cross-sections, from which the radiative recombination rate coefficients can be obtained by the application of the principle of detailed balancing (see Section 6 of Chapter II), are available. But only a limited number of states are covered by these calculations. However, more general methods, from which approximate values of the cross-sections can be obtained, are available.

2. AVAILABLE DATA

The lower quantum states have been well investigated by several workers and with various methods. The following is a list of the more important papers:

Varsavsky (1963): 2s, 2p, 3s, 3p, 3d, 4s, 4p states of O VI;

Ivanova (1964): 2s, 2p, 3s, 5s states of N V and O VI;

Hidalgo (1968): 2s, 2p, 3s states of C IV;
2s, 2p states of N V;

Leibowitz (1972): 2s, 2p, 3s, 3p, 4s, 4p, 5s, 5p,
6s, 6p, 7s, 7p states of C IV;

Missavage and Manson (1972): 2s state of O VI;

John and Morgan (1973): 2s state of C IV;

Tiwari et al. (1975): 2s state of C IV, N V, and O VI.

Most of the calculations have been performed on the ground and the first few excited states; some higher excited states have been investigated, but in general, as n increases, the data become scarcer.

There is good agreement between the various calculations except at and close to the threshold of ionization where some values of the cross-sections differ by as much as a factor of two. However, the results of Tiwari et al. (1975) are systematically lower than the others by a factor of ~ 2 for C IV and ~ 1.5 for N V but there is good agreement for O VI. Fig.8.1 shows the photoionization cross-section of the 2s state of C IV as calculated by various methods.

3. CALCULATED DATA

The photoionization cross-sections of lithium-like quantum states with low values of ℓ can be calculated from a method which is an extension to bound-free transitions of the Coulomb approximation (Bates and Damgaard, 1949) used in the calculation of bound-bound transition probabilities (see Section 3.2 of Chapter IV). In this context, it is usually referred to as the quantum defect method (QDM). It was first developed by Burgess and Seaton (1958, 1960) and later improved and extended by Peach (1967).

We shall use Rydberg energy units throughout. Let $I_{n\ell}$ be the ionization potential of an electron in state $n\ell$, bound to an ion of core charge Z; $h\upsilon$ the energy of the absorbed photon; k'^2 the energy of the ejected electron. The energy conservation condition is then

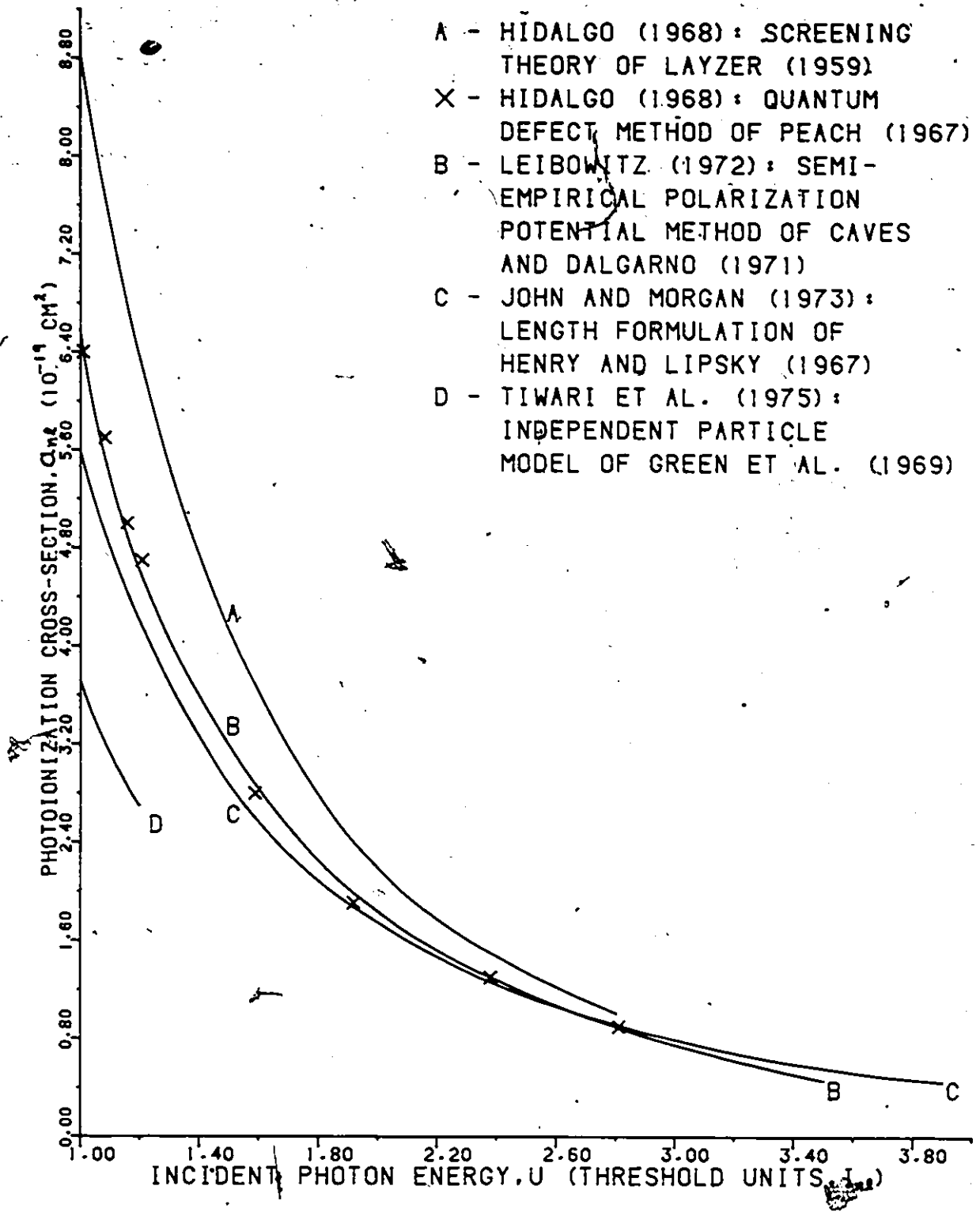

FIGURE 8.1 - COMPARISON OF THE PHOTOIONIZATION CROSS-SECTION OF THE 2S STATE OF C IV CALCULATED WITH VARIOUS METHODS

$$h\nu = I_{n\ell} + k'^2 \qquad \ldots(8.1)$$

and the photoionization cross-section (Burgess and Seaton, 1958)

$$a_{n\ell}(k'^2) = \frac{4\pi\alpha a_o^2}{3} \frac{I_{n\ell} + k'^2}{I_{n\ell}^2} \times \sum_{\ell'=\ell\pm1} C_{\ell'} |g(n^*\ell;\epsilon'\ell')|^2 \qquad \ldots(8.2)$$

where $4\pi\alpha a_o^2/3 = 8.5594 \times 10^{-19}$ cm^2, $C_{\ell'} = \ell_>/(2\ell+1)$ for hydrogenic and lithium-like ions,

$$g(n^*\ell;\epsilon'\ell') = I_{n\ell}\int_0^\infty P_{n\ell}(r)\, r\, F_{\epsilon'\ell'}(r)\, dr; \qquad \ldots(8.3)$$

n^* is the effective quantum number of state $n\ell$ defined by $I_{n\ell} = Z^2/n^{*2}$, and the other constants have their usual meaning. $P_{n\ell}(r)$ and $F_{\epsilon'\ell'}(r)$ denote respectively the initial state bound radial function and the final state continuum function of the ejected electron. ϵ' obeys the relation $k'^2 = Z^2\epsilon'$ and corresponds to the ϵ used by Seaton (1958a, 1966a, b) in his quantum defect theory (QDT) (see Section 9.1 of Chapter III).

It is possible to write $g(n^*\ell;\epsilon'\ell')$ as follows:

$$g(n^*\ell;\epsilon'\ell') = \frac{B(n^*\ell;\epsilon'\ell')}{\sqrt{\mathcal{C}(n^*\ell)}} \times \cos\pi[n^* + \mu_{\ell'}(\epsilon') + \chi(n^*\ell;\epsilon'\ell')] \qquad \ldots(8.4)$$

where

$$\zeta(n^*\ell) = 1 + \frac{2}{n^{*3}} \frac{\partial \mu_\ell(\epsilon)}{\partial \epsilon} \qquad \ldots(8.5)$$

is the correction factor to the normalization constant of the wavefunctions (expressed as Whittaker functions) used in the Coulomb approximation and is given by Seaton (1966b). $\mu_{\ell'}(\epsilon')$ is the quantum defect function extrapolated to positive values of the valence electron energy by using Seaton's (1966b) quantum defect theory (see Section 9.1 of Chapter III). $\chi(n^*\ell;\epsilon'\ell')$ and a function $G(n^*\ell;\epsilon'\ell')$ defined by

$$G(n^*\ell;\epsilon'\ell') = \sqrt{\frac{\pi}{2n^*}}\,(1+n^{*2}\epsilon')^2\, B(n^*\ell;\epsilon'\ell') \qquad \ldots(8.6)$$

are tabulated by Peach (1967).

These tables were interpolated with a parabolic formula to obtain the photoionization cross-sections of ns ($2 \leq n \leq 9$) and np ($2 \leq n \leq 6$) states of C IV, N V and O VI. As seen in Fig.8.2, the cross-sections are in close agreement with the works previously mentioned which also include values calculated with the quantum defect method. In view of this and of the need for a consistent set of data, we will use the photoionization cross-sections calculated with the quantum defect method for the s and p states of the ions C IV, N V, and O VI.

Since d and higher ℓ-value states of lithium-like ions are closely hydrogenic, the photoionization cross-sections of these states can be obtained from tables of hydrogenic values calculated by Burgess (1964)

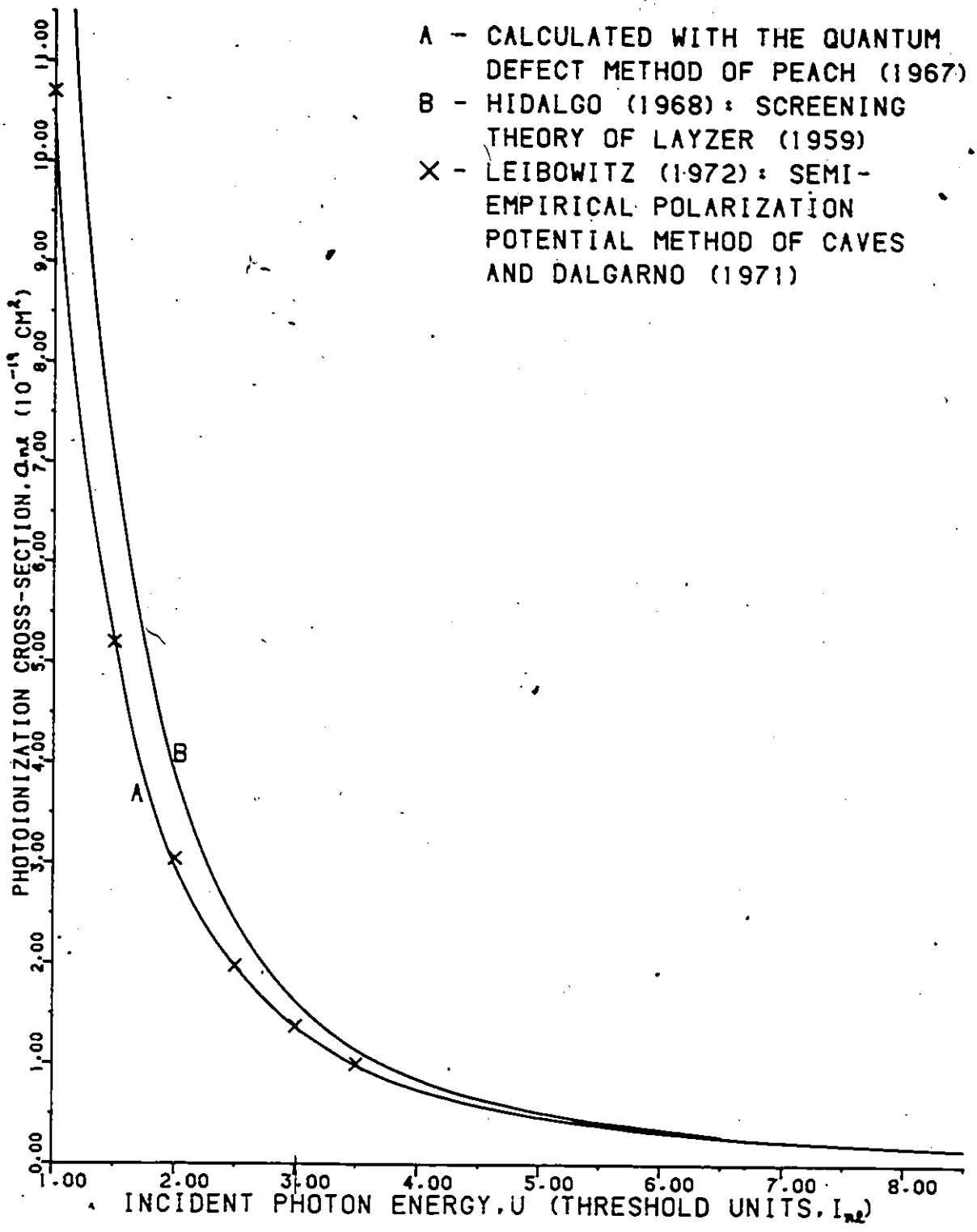

FIGURE 8.2 - COMPARISON OF THE PHOTOIONIZATION CROSS-SECTION OF THE 3S STATE OF C IV CALCULATED WITH THE QUANTUM DEFECT AND OTHER METHODS

where a quantity $\Theta(n\ell; K'\ell')$ is tabulated and is related to eq.(8.2) by the relation

$$|g(n\ell;\epsilon'\ell')|^2 = \frac{\Theta(n\ell;K'\ell')}{1+n^2K'^2} \qquad \ldots(8.7)$$

where $K'^2 = \epsilon'$. Fig.8.3 compares the cross-sections obtained from Burgess' and Peach's tables for the 3d state of O VI. We see that the hydrogenic approximation is indeed justified for d, and thus also for higher ℓ-value states of lithium-like ions.

For those states n which have been averaged over the individual states $n\ell$, the method proposed by Seaton (1959) will be used to obtain the radiative recombination rate coefficients directly. This method, applicable to average hydrogenic states, is based on the asymptotic expansion of the Gaunt factor derived by Menzel and Pekeris (1935) (see Section 9 of Chapter II).

4. FIT OF THE DATA

The calculation of the radiative recombination rate coefficients from the photoionization data requires that the latter be fitted to some simple empirical algebraic expression.

We write the cross-section as a function of the energy of the incident photon in units of the threshold energy. From the energy conservation relation (8.1), viz.

$$h\nu = I_{n\ell} + k'^2,$$

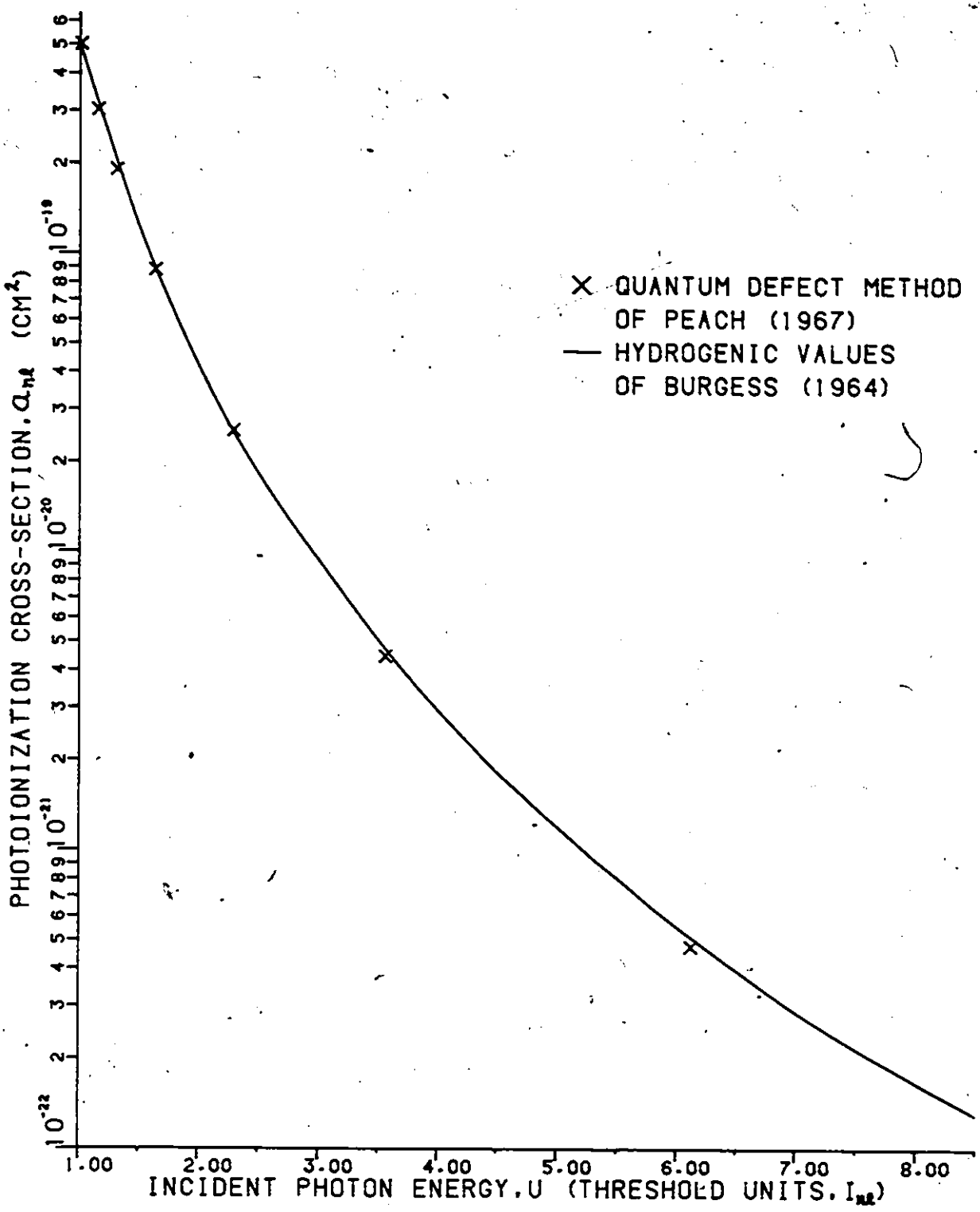

FIGURE 8.3 - COMPARISON OF THE PHOTOIONIZATION CROSS-SECTION OF THE 3d STATE OF O VI CALCULATED WITH THE QUANTUM DEFECT METHOD AND THE CORRESPONDING HYDROGENIC VALUE.

the threshold energy is

$$h\omega_o = \mathcal{I}_{nl} \qquad \ldots(8.8)$$

and the energy of the incident photon in threshold energy units is

$$u = h\omega / h\omega_o \qquad \ldots(8.9)$$

The asymptotic behavior of the photoionization cross-section is known to be (Ivanova, 1964; Fano and Cooper, 1968)

$$a(u) \sim u^{-p} \qquad \ldots(8.10)$$

This suggests using a semi-empirical function of the form

$$a(u) = \frac{C}{u^p}\left[1 + \frac{b_1}{u} + \frac{b_2}{u^2} + \ldots + \frac{b_m}{u^m}\right] \qquad \ldots(8.11)$$

where C and b_k, k = 1, ..., m are fit parameters. A similar expression has been proposed by Seaton (1958b) but he includes only the terms of order 0 and 1 in the sum. Since the rate coefficient is calculated by integrating the cross-section over a Maxwellian energy distribution function, the parameter p is assigned integral or half-integral values to facilitate the evaluation of these integrals; the same restriction has been used by Henry (1970). Furthermore, p and m are restricted to the range of values $0 \leq p \leq 5$ and $1 \leq m \leq 9$ to simplify the evaluation and improve the accuracy of the integrals; this is more fully explained in the following pages.

The function (8.11) is fitted to the cross-section data of state $n\ell$ by using a least squares method in which the sum of the squares of the relative differences between the fit and the actual values of the cross-section is minimized. This procedure provides a uniform fit for all values of the cross-section, large or small (see Appendix D).

The set of parameters which best fits the cross-section of state $n\ell$ is then derived as follows: suitable values of p and of m are chosen; the ensuing conditions imposed on the parameters C and b_k, k = 1, ..., m by the fitting procedure result in a set of linear equations which is solved numerically for the unknowns C and b_k, k = 1, ..., m. This is repeated for all allowed values of p and m, and the resulting sets of parameters are analysed and a best set chosen. Several factors affect this choice.

i. We define a relative deviation

$$R_D = \sqrt{\frac{1}{N}\sum_{i=1}^{N}\left(\frac{\Delta x_i}{x_i}\right)^2} \qquad \ldots(8.12)$$

where x_i is the i^{th} value of the cross-section for photoionization from state $n\ell$; N such values corresponding to different values of the energy U are available. Δx_i is the difference between x_i and the fit value $\bar{x}_i$: $\Delta x_i = x_i - \bar{x}_i$. (The standard deviation is defined as (Kenney and Keeping, 1954, p.77)

$$S_D = \sqrt{\frac{1}{N}\sum_{i=1}^{N}(\Delta x_i)^2}\,. \qquad \ldots(8.13)$$

Evidently, R_D should be as small as possible; for $R_D \leq 0.180 \times 10^{-2}$, the difference between the actual rate coefficients of hydrogenic ions given by Burgess (1964) and the values calculated by integrating eq.(8.11) is about 0.2% at temperatures of 1,000,000 K and 0.02% at 500,000 K provided the following criteria are also satisfied.

ii. We define a quantity

$$R_T = \sum_{k=1}^{m} b_k \,/\, (b_k)_{max} \qquad \ldots(8.14)$$

where b_k, $k = 1, \ldots, m$ are the fit parameters. The value of R_T should be as large as possible. The reason for this is that the terms in the sum $\sum_{k=1}^{m} b_k / u^k$ are usually arranged in pairs in which the terms alternate in sign and are of comparable magnitude; this causes significant cancellations in the sum and thus loss of significant digits. For $R_T \geq 0.5$, the evaluation of the sum will not increase the error estimate quoted previously in factor i.

iii. The rate coefficient is obtained by integrating the cross-section over an exponential function of negative argument. As is seen in Fig.8.4, the largest contribution to the rate coefficient comes from the region of low values of U; emphasis should therefore be put on those parameters which provide a good fit at low values of U.

iv. The smaller the values of p and m are, the easier the rate coefficient is to evaluate. The smaller number of operations done further minimizes the loss of significant digits due to truncation errors.

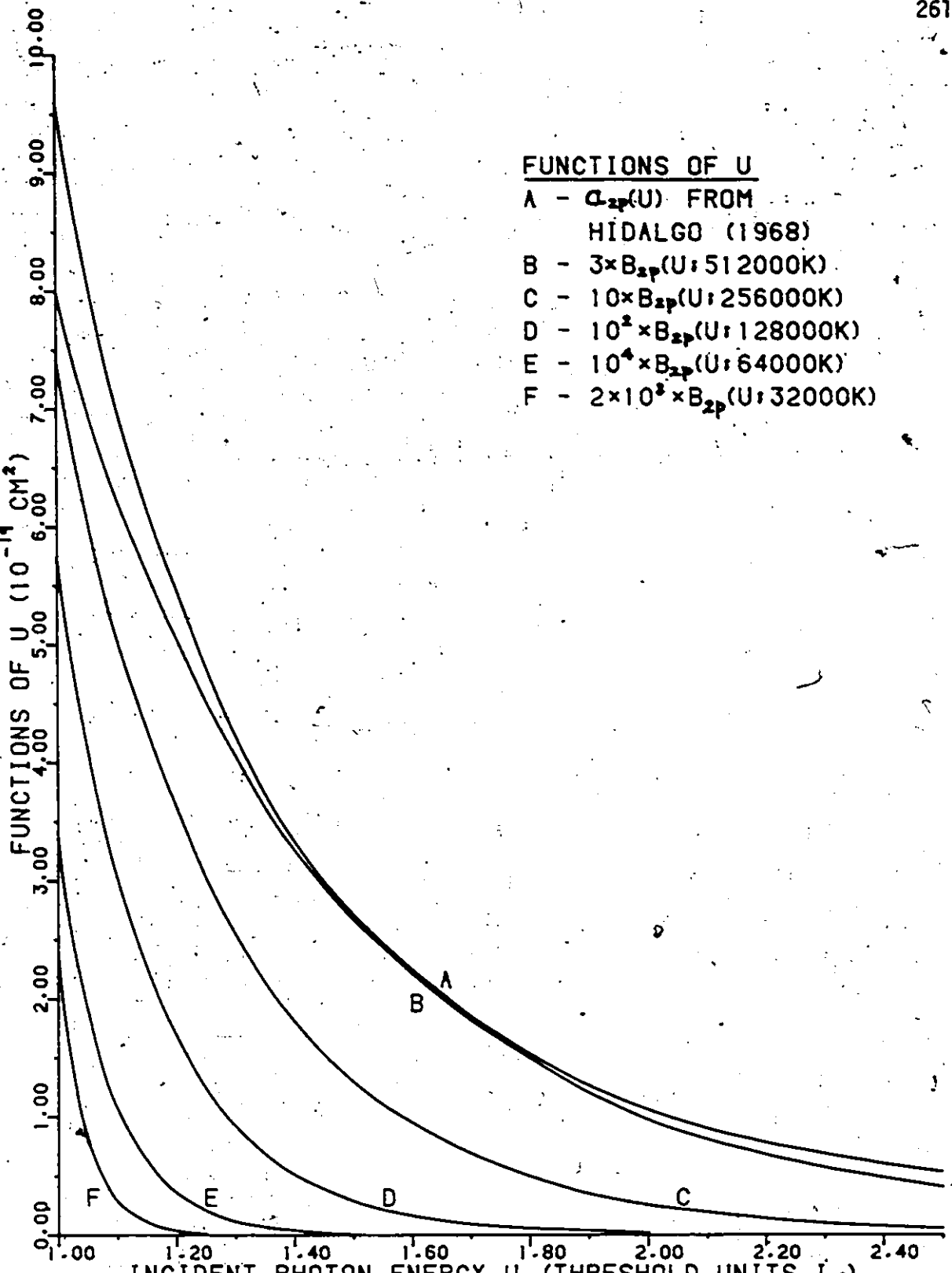

FIGURE 8.4 - COMPARISON OF THE PHOTOIONIZATION CROSS-SECTION, $\alpha_{n\ell}(U)$, AND THE INTEGRAND OF THE RADIATIVE RECOMBINATION RATE COEFFICIENT, $B_{n\ell}(U;T)$, FOR THE 2p STATE OF C IV.

These criteria may not all be satisfied simultaneously; it then becomes necessary to compromise between them to obtain the best set of parameters. Under these circumstances, the following order of decreasing importance was assigned to the factors: ii, i, iii, iv. Tables 8.1, 8.2, and 8.3 give the best sets of fit parameters adopted for the states of the ions C IV, N V, and O VI respectively.

5. RADIATIVE RECOMBINATION RATE COEFFICIENT

The radiative recombination rate coefficient is obtained from the photoionization cross-section by applying the principle of detailed balancing. The rate coefficient is then given by (Seaton, 1958b)

$$\beta_{n\ell}(T) = D_{n\ell}(T) \int_{I_{n\ell}}^{\infty} (h\nu)^2 a_{n\ell}(\nu)\, e^{-\frac{h\nu}{kT}}\, d(h\nu) \qquad \ldots(8.15)$$

where

$$D_{n\ell}(T) = \frac{1}{c^2}\sqrt{\frac{2}{\pi}}\,(mkT)^{-3/2}\,\frac{\omega_{n\ell}}{\omega_i}\, e^{\frac{I_{n\ell}}{kT}}, \qquad \ldots(8.16)$$

T is the free electron temperature, $\omega_{n\ell}$ the statistical weight of level $n\ell$, ω_i the statistical weight of the final ion, and the other symbols have their usual meaning. Using threshold energy units, eq.(8.15) becomes

$$\beta_{n\ell}(T) = D_{n\ell}(T)\, I_{n\ell}^3 \int_1^{\infty} u^2 a_{n\ell}(u)\, e^{-\theta_{n\ell} u}\, du \qquad \ldots(8.17)$$

Table 8.1 - Fit parameters for the radiative recombination of the ion C IV.

State	p	C	m	b_1	b_2	b_3	b_4	b_5	b_6	b_7
2s	0	5.469389 (-3)	3	-2.001679 (1)	1.974840 (2)	-6.123286 (1)	-	-	-	-
3s	0	7.363442 (-4)	3	-7.102934 (1)	2.052092 (3)	-5.543171 (2)	-	-	-	-
4s	0	7.258259 (-4)	4	-6.792716 (1)	2.861367 (3)	-7.522800 (2)	6.934579 (1)	-	-	-
5s	0	3.991404 (-4)	4	-1.015340 (2)	6.556362 (3)	-1.748978 (3)	3.805916 (2)	-	-	-
6s	0	2.194877 (-4)	4	-1.496587 (2)	1.426823 (4)	-3.396205 (3)	1.094031 (3)	-	-	-
7s	0	1.534585 (-4)	5	-1.900494 (2)	2.408986 (4)	-8.936741 (3)	1.189996 (4)	-6.421519 (3)	-	-
8s	0	1.088988 (-4)	5	-2.402563 (2)	3.886555 (4)	-1.058482 (4)	1.705943 (4)	-9.761384 (3)	-	-
9s	0	6.958584 (-5)	5	-3.216595 (2)	6.810101 (4)	-1.382067 (4)	3.221370 (4)	-2.103325 (4)	-	-
2p	2.5	1.837581 (-1)	4	7.164568	-2.751168	-1.470054	1.304527	-	-	-
3p	0.5	7.879000 (-3)	4	-2.481890 (1)	2.835475 (2)	-6.881929	-3.172871 (1)	-	-	-
4p	0.5	4.429038 (-3)	5	-4.472702 (1)	9.047825 (2)	-1.532634 (2)	-3.286811 (2)	2.032432 (2)	-	-

Power of ten is given in parenthesis

Table 8.1 - Continued

State	p	C	m	b_1	b_2	b_3	b_4	b_5	b_6	b_7
5p	0.5	3.274106 (-3)	5	-6.728545 (1)	2.052114 (3)	-1.514690 (3)	7.158093 (2)	-1.203247 (2)	-	-
6p	0.5	1.752858 (-3)	4	-1.071001 (2)	5.237153 (3)	-4.517368 (3)	1.947574 (3)	-	-	-
3d	1	-4.381001 (-5)	6	-9.358114 (1)	3.230994 (3)	-5.647993 (4)	3.592929 (4)	-6.084330 (3)	-2.294838 (3)	-
4d	0.5	-1.378110 (-4)	6	-9.080874 (1)	2.920390 (3)	-4.214640 (4)	2.957122 (4)	-3.233687 (3)	-3.239672 (3)	-
5d	0	-1.834370 (-4)	6	-8.822469 (1)	2.660686 (3)	-3.278500 (4)	2.073906 (3)	2.188639 (4)	-1.197448 (4)	-
6d	0	-2.168550 (-4)	5	-9.837691 (1)	3.548735 (3)	-5.733432 (4)	5.199802 (4)	-1.880275 (4)	-	-
4f	0	7.717375 (-6)	6	-8.877817 (1)	2.735603 (3)	-3.792017 (4)	2.414505 (5)	-3.076407 (4)	-2.105889 (4)	-
5f	1	-2.332035 (-4)	6	-8.855610 (1)	2.692853 (3)	-3.396777 (4)	2.573611 (4)	-1.487663 (3)	-3.884909 (3)	-
6f	0.5	-3.331436 (-4)	6	-8.645421 (1)	2.495874 (3)	-2.787871 (4)	7.102947 (3)	1.714989 (4)	-1.869723 (4)	-
5g	0.5	9.863948 (-6)	6	-8.849532 (1)	2.705931 (3)	-3.675688 (4)	2.215534 (5)	-7.483397 (4)	-1.726800 (3)	-
6g	0	2.316309 (-5)	7	-8.918292 (1)	2.755907 (3)	-3.765646 (4)	2.189032 (5)	2.107522 (4)	-1.720200 (5)	7.873840 (4)
6h	0	3.207363 (-7)	6	-5.322241 (1)	-4.028913 (2)	5.724023 (4)	-1.011832 (6)	6.487351 (6)	-2.680018 (6)	-

Table 8.2 - Fit parameters for the radiative recombination of the ion N V.

State	p	C	m	b_1	b_2	b_3	b_4	b_5	b_6	b_7
2s	0	2.965115 (-3)	3	-2.621039 (1)	2.439374 (2)	-6.605878 (1)	-	-	-	-
3s	0	6.088024 (-4)	3	-7.196029 (1)	1.670806 (3)	-3.775046 (2)	-	-	-	-
4s	0	4.226620 (-4)	4	-8.652678 (1)	3.227192 (3)	-5.287099 (2)	-4.652529 (1)	-	-	-
5s	0	2.830883 (-4)	4	-1.128661 (2)	6.130606 (3)	-1.021152 (3)	1.279606 (2)	-	-	-
6s	0	1.552278 (-4)	3	-1.683449 (2)	1.336107 (4)	-1.158127 (3)	-	-	-	-
7s	0	9.724251 (-5)	4	-2.295038 (2)	2.487246 (4)	-2.173381 (2)	-6.012132 (2)	-	-	-
8s	0	6.749471 (-5)	4	-2.922757 (2)	4.104385 (4)	3.084455 (3)	-2.476554 (3)	-	-	-
9s	1	-1.254618 (-2)	4	-2.461172 (2)	-2.389927 (1)	-5.914341 (1)	6.545147 (1)	-	-	-
2p	1.5	-1.599791 (-2)	4	-1.504863 (1)	-2.435150 (1)	-1.333341 (1)	1.421462 (1)	-	-	-
3p	0.5	4.124305 (-3)	4	-2.649678 (1)	3.066531 (2)	7.356662 (1)	-8.827260 (1)	-	-	-
4p	0.5	2.591313 (-3)	5	-4.657693 (1)	9.246727 (2)	2.169996 (1)	-5.648812 (2)	2.960090 (2)	-	-

Power of ten is given in parenthesis

Table 8.2 - Continued

State	p	C	m	b_1	b_2	b_3	b_4	b_5	b_6	b_7
5p	0.5	1.987629 (-3)	5	-6.928633 (1)	2.054643 (3)	-1.189018 (3)	1.886965 (2)	1.334079 (2)	-	-
6p	0.5	1.247970 (-3)	4	-1.038560 (2)	4.625348 (3)	-3.839683 (3)	1.617880 (3)	-	-	-
3d	1	-2.804147 (-5)	6	-9.358114 (1)	3.230994 (3)	-5.647993 (4)	3.592929 (4)	-6.084330 (3)	-2.294838 (3)	-
4d	0.5	-8.820069 (-5)	6	-9.080874 (1)	2.920390 (3)	-4.214640 (4)	2.957122 (4)	-3.233687 (3)	-3.239672 (3)	-
5d	0	-1.174262 (-4)	6	-8.822469 (1)	2.660686 (3)	-3.278500 (4)	2.073907 (3)	2.188639 (4)	-1.197448 (4)	-
6d	0	-1.388283 (-4)	5	-9.837691 (1)	3.548735 (3)	-5.733432 (4)	5.199802 (4)	-1.880275 (4)	-	-
4f	0	4.939261 (-6)	6	-8.877817 (1)	2.735603 (3)	-3.792017 (4)	2.414505 (5)	-3.076406 (4)	-2.105889 (4)	-
5f	1	-1.492652 (-4)	6	-8.855610 (1)	2.692853 (3)	-3.396777 (4)	2.573611 (4)	-1.487663 (3)	-3.884909 (3)	-
6f	0.5	-2.132296 (-4)	6	-8.645421 (1)	2.495874 (3)	-2.787871 (4)	7.102947 (3)	1.714989 (4)	-1.069723 (4)	-
5g	0.5	6.313609 (-6)	6	-8.849532 (1)	2.705931 (3)	-3.675688 (4)	2.215535 (5)	-7.483394 (4)	-1.726825 (3)	-
6g	0	1.482579 (-5)	7	-8.918294 (1)	2.755909 (3)	-3.765650 (4)	2.189034 (5)	2.107721 (4)	-1.720229 (5)	7.873961 (4)
6h	0	2.052689 (-7)	6	-5.321934 (1)	-4.031647 (2)	5.724865 (4)	-1.011947 (6)	6.488030 (6)	-2.680302 (6)	-

Table 8.3 - Fit parameters for the radiative recombination of the ion O VI.

State	p	C	m	b_1	b_2	b_3	b_4	b_5	b_6	b_7
2s	0	1.612578 (-3)	4	-2.111403 (1)	2.518619 (2)	1.819679 (1)	-4.742574 (1)	-	-	-
3s	0	8.209290 (-4)	4	-3.648990 (1)	8.290160 (2)	-7.002833 (1)	-6.774941 (1)	-	-	-
4s	0	4.988185 (-4)	4	-5.315522 (1)	1.878058 (3)	-1.196176 (2)	-1.417544 (2)	-	-	-
5s	0	2.586279 (-4)	5	-8.147655 (1)	4.503355 (3)	4.346171 (2)	-1.467113 (3)	6.755431 (2)	-	-
6s	0	1.693280 (-4)	5	-1.108887 (2)	8.402231 (3)	1.009480 (3)	-2.411324 (3)	1.099067 (3)	-	-
7s	0	1.119745 (-4)	5	-1.478229 (2)	1.492469 (4)	1.178105 (3)	-5.349044 (3)	2.416161 (3)	-	-
8s	0	7.774888 (-5)	5	-1.898684 (2)	2.468550 (4)	7.901756 (3)	-1.162230 (4)	5.282879 (3)	-	-
9s	0	5.550624 (-5)	5	-2.383859 (2)	3.899928 (4)	1.752615 (4)	-2.544994 (4)	1.235716 (4)	-	-
2p	1.5	-1.928285 (-2)	4	-1.322001 (1)	5.885091	-4.140622 (1)	2.788515 (1)	-	-	-
3p	0.5	2.934388 (-3)	4	-2.626015 (1)	2.932335 (2)	8.146185 (1)	-9.710450 (1)	-	-	-
4p	0.5	1.960180 (-3)	5	-4.524812 (1)	8.537037 (2)	-4.057282 (1)	-4.171757 (2)	2.203381 (2)	-	-

Power of ten is given in parenthesis

Table 8.3 - Continued

State	p	C	m	b_1	b_2	b_3	b_4	b_5	b_6	b_7
5p	0.5	1.452912 (-3)	5	-6.794601 (1)	1.934984 (3)	-1.159682 (3)	2.860572 (2)	5.996161 (1)	-	-
6p	0.5	8.890334 (-4)	4	-1.025495 (2)	4.443527 (3)	-3.641824 (3)	1.528882 (3)	-	-	-
3d	1	-1.947409 (-5)	6	-9.358114 (1)	3.230994 (3)	-5.647993 (4)	3.592929 (4)	-6.084330 (3)	-2.294838 (3)	-
4d	0.5	-6.125908 (-5)	6	-9.080874 (1)	2.920390 (3)	-4.214640 (4)	2.957122 (4)	-3.233687 (3)	-3.239672 (3)	-
5d	0	-8.153463 (-5)	6	-8.822469 (1)	2.660686 (3)	-3.278500 (4)	2.073906 (3)	2.188639 (4)	-1.197448 (4)	-
6d	0	-9.638096 (-5)	5	-9.837691 (1)	3.548735 (3)	-5.733432 (4)	5.199802 (4)	-1.880275 (4)	-	-
4f	0	3.430110 (-6)	6	-8.877817 (1)	2.735603 (3)	-3.792017 (4)	2.414505 (5)	-3.076405 (4)	-2.105890 (5)	-
5f	1	-1.036580 (-4)	6	-8.855610 (1)	2.692853 (3)	-3.396777 (4)	2.573611 (4)	-1.487663 (3)	-3.884909 (3)	-
6f	0.5	-1.480772 (-4)	6	-8.645421 (1)	2.495874 (3)	-2.787871 (4)	7.102947 (3)	1.714989 (4)	-1.069723 (4)	-
5g	0.5	4.384522 (-6)	6	-8.849531 (1)	2.705931 (3)	-3.675688 (4)	2.215534 (5)	-7.483400 (4)	-1.726774 (3)	-
6g	0	1.029567 (-5)	7	-8.918294 (1)	2.755909 (3)	-3.765652 (4)	2.189035 (5)	2.107816 (4)	-1.720243 (5)	7.874019 (4)
6h	0	1.425577 (-7)	6	-5.322143 (1)	-4.029780 (2)	5.724290 (4)	-1.011869 (6)	6.487566 (6)	-2.680109 (6)	-

where $\theta_{n\ell} = I_{n\ell} / kT$. Substituting for the photoionization cross-section from eq.(8.11), viz.,

$$a_{n\ell}(u) = \frac{C}{u^p} \sum_{k=0}^{m} \frac{b_k}{u^k} \; , \; b_0 = 1 ,$$

in eq.(8.17), we obtain

$$\beta_{n\ell}(T) = D_{n\ell}(T) \, I_{n\ell}^3 \, C \times \sum_{k=0}^{m} b_k \, S_{2-p-k}(\theta_{n\ell}) \qquad \ldots(8.18)$$

where we have introduced the function

$$S_\mu(x) = \int_1^\infty u^\mu e^{-xu} \, du ; \qquad \ldots(8.19)$$

no restrictions are imposed on the value of μ. The following relations are to be used in eq.(8.18):

$$\omega_{n\ell} = 2(2\ell+1),$$

$$\omega_n = 2n^2,$$

$$\omega_i = 1 , \qquad \ldots(8.20)$$

and for $I_{n\ell}$ in Rydbergs and T in K,

$$\theta_{n\ell} = 157,890 \; I_{n\ell} / T , \qquad \ldots(8.21)$$

$$D_{n\ell}(T) = 2.062 \times 10^{11} \frac{\omega_{n\ell}}{\omega_i} \, T^{-3/2} \, e^{\theta_{n\ell}} \; cm^3 \, s^{-1} \, Ryd^{-3} \qquad \ldots(8.22)$$

6. EVALUATION OF $S_\mu(x)$

$S_\mu(x)$ need be evaluated only for integral and half-integral values of μ. In these special cases, $S_\mu(x)$ reduces to well-known functions.

6.1. Integral values of μ

We put $\mu = m$ where m is an integer. For $m \geq 0$, we have the function (Abramowitz and Stegun, 1965, p.228)

$$\alpha_m(x) = \int_1^\infty u^m \cdot e^{-xu}\, du$$

$$= m! \frac{e^{-x}}{x^{m+1}} \sum_{k=0}^{m} \frac{x^k}{k!} . \qquad \ldots(8.23)$$

For $m < 0$ and $m' = |m|$, we have the m'^{th} exponential integral (Abramowitz and Stegun, 1965, p.228):

$$E_{m'}(x) \equiv \int_1^\infty \frac{e^{-xu}}{u^{m'}}\, du. \qquad \ldots(8.24)$$

By using the recurrence relation (Abramowitz and Stegun, 1965, p.229)

$$m' E_{m'+1}(x) = e^{-x} - x E_{m'}(x), \qquad \ldots(8.25)$$

we obtain an expression for $E_{m'}(x)$ in terms of the exponential integral $E_1(x)$ (Pagurova, 1961, p.ix):

$$E_{m'}(x) = P_{m'}(x) \cdot e^{-x} + \frac{(-x)^{m'-1}}{(m'-1)!} E_1(x) \qquad \ldots(8.26)$$

where

$$P_{m'}(x) = \frac{1}{(m'-1)!} \sum_{k=0}^{m'-2} (m'-k-2)!\,(-x)^k \qquad \ldots(8.27)$$

Rational approximations to $E_1(x)$ exist and greatly simplify its evaluation. We use approximations due to Cody and Thacher (1968) which give an accuracy of 14S.

6.2. Half-integral values of μ

We put $\mu = m+1/2$ where m is an integer. For $m \geq 0$, the function $\alpha_m(x)$ can be generalized to give

$$\alpha_{m+\frac{1}{2}}(x) = \int_1^\infty u^{m+\frac{1}{2}} e^{-xu}\, du$$

$$= R_m(x) \cdot e^{-x} + \frac{\Gamma(m+3/2)}{x^{m+3/2}}\, erfc(\sqrt{x}) \qquad \ldots(8.28)$$

where

$$R_m(x) = \frac{\Gamma(m+3/2)}{x} \sum_{k=0}^{m} \frac{x^{-k}}{\Gamma(m+3/2-k)} \qquad \ldots(8.29)$$

and erfc(x) is the complementary error function

$$erfc(x) = \frac{2}{\sqrt{\pi}} \int_x^\infty e^{-u^2} du. \qquad \ldots(8.30)$$

For $m < 0$ and $m' = |m|-1$, the general exponential integral (Pagurova, 1961, p.ix) can be written as

$$E_{m'+1/2}(x) = \int_1^\infty \frac{e^{-xu}}{u^{m'+1/2}}\, du$$

$$= Q_{m'}(x) \cdot e^{-x} + \frac{\pi}{\sqrt{x}} \frac{(-x)^{m'}}{\Gamma(m'+\frac{1}{2})} \operatorname{erfc}(\sqrt{x}) \quad \ldots(8.31)$$

where

$$Q_{m'}(x) = \frac{1}{\Gamma(m'+1/2)} \sum_{k=0}^{m'-1} (-x)^k \, \Gamma(m'-k-1/2). \quad \ldots(8.32)$$

6.3. Asymptotic expansions

Numerical calculations with eqs.(8.26) and (8.31) become impractical for large values of m or x. This is due to the fact that, under these conditions,

$$P_{m'}(x) \cdot e^{-x} \simeq -\frac{(-x)^{m'-1}}{(m'-1)!} E_1(x)$$

and

$$Q_{m'}(x) \cdot e^{-x} \simeq -\frac{\pi}{\sqrt{x}} \frac{(-x)^{m'}}{\Gamma(m'+\frac{1}{2})} \operatorname{erfc}(\sqrt{x}).$$

The use of asymptotic expansions solves this problem. For large values of x, we have the well-known relation (Pagurova, 1961, p.xi),

$$E_\mu(x) = \frac{e^{-x}}{x}\left[1 + \frac{1}{\Gamma(\mu)}\sum_{k=1}^{m}(-1)^k\frac{\Gamma(\mu+k)}{x^k} + R_\mu(m,x)\right] \quad \ldots(8.33)$$

where

$$|R_\mu(m,k)| < \frac{\Gamma(\mu+m+1)}{\Gamma(\mu)} \cdot \frac{1}{x^{m+1}} \cdot \quad \ldots(8.34)$$

For large values of both x and μ, it is more convenient to use (Pagurova, 1961, p.xii)

$$E_\mu(x) \doteq \frac{e^{-x}}{x+\mu}\left[1 + \frac{\mu}{(x+\mu)^2} + \frac{\mu(\mu-2x)}{(x+\mu)^4} + \frac{\mu(6x^2-8\mu x+\mu^2)}{(x+\mu)^6}\right] + R_\mu(x) \quad \ldots(8.35)$$

where

$$R_\mu(x) = \mu\int_1^\infty e^{-xu}\left[-24x^3u^3 + 58\mu x^2u^2 - 22\mu^2xu + \mu^3\right] / \left[u^\mu(xu+\mu)^8\right] du \quad \ldots(8.36)$$

and

$$|R_\mu(x)| < \frac{e^{-x}}{x}\frac{\mu}{(x+\mu)^8}\left|-24x^3 + (-72+58\mu)x^2 + (x+1)(-114+116\mu-22\mu^2) + \mu^3\right| \quad \ldots(8.37)$$

The asymptotic expansion (8.35) is particularly useful since its accuracy depends on the value of $x+\mu$. It is thus also applicable to large x and small μ, as is expansion (8.33). Although, in this case, expansion (8.33) may give more accurate results than expansion (8.35), the accuracy obtained with the latter is more than sufficient for our purpose. We will thus use eq.(8.35) in all the calculations where the asymptotic expansion of the general exponential integral is required.

6.4. Accuracy

In Fig.8.5, we compare the accuracy obtained when $E_m(x)$ and $E_{m+1/2}(x)$ are calculated with the exact relations (8.26) and (8.31) and when $E_\mu(x)$ is calculated with the asymptotic expansion (8.35). The minimum accuracy, obtained for $x+\mu \simeq 15$, is of $\sim$4S. If for $x+\mu < 15$, we use the exact expressions and, for $x+\mu > 15$, the asymptotic expansion, the accuracy of $E_m(x)$ and $E_{m+1/2}(x)$ will be better than 4S and will increase as we move away from $x+\mu = 15$ in either directions ($x+\mu \gtrless 15$). It should be noted that if the exact expression is used to calculate $E_{m+1/2}(x)$ for $x+\mu < 40$, a minimum accuracy of 6S is obtained for half-integral values of μ. However, such accuracy is not necessary since the photoionization cross-sections are not known to better than 2-3S (see Section 8 of this Chapter).

7. COMPARISON WITH HYDROGENIC VALUES

We calculate the radiative recombination rate coefficients of the average states n from the rate coefficients of the individual $n\ell$ states with the formula

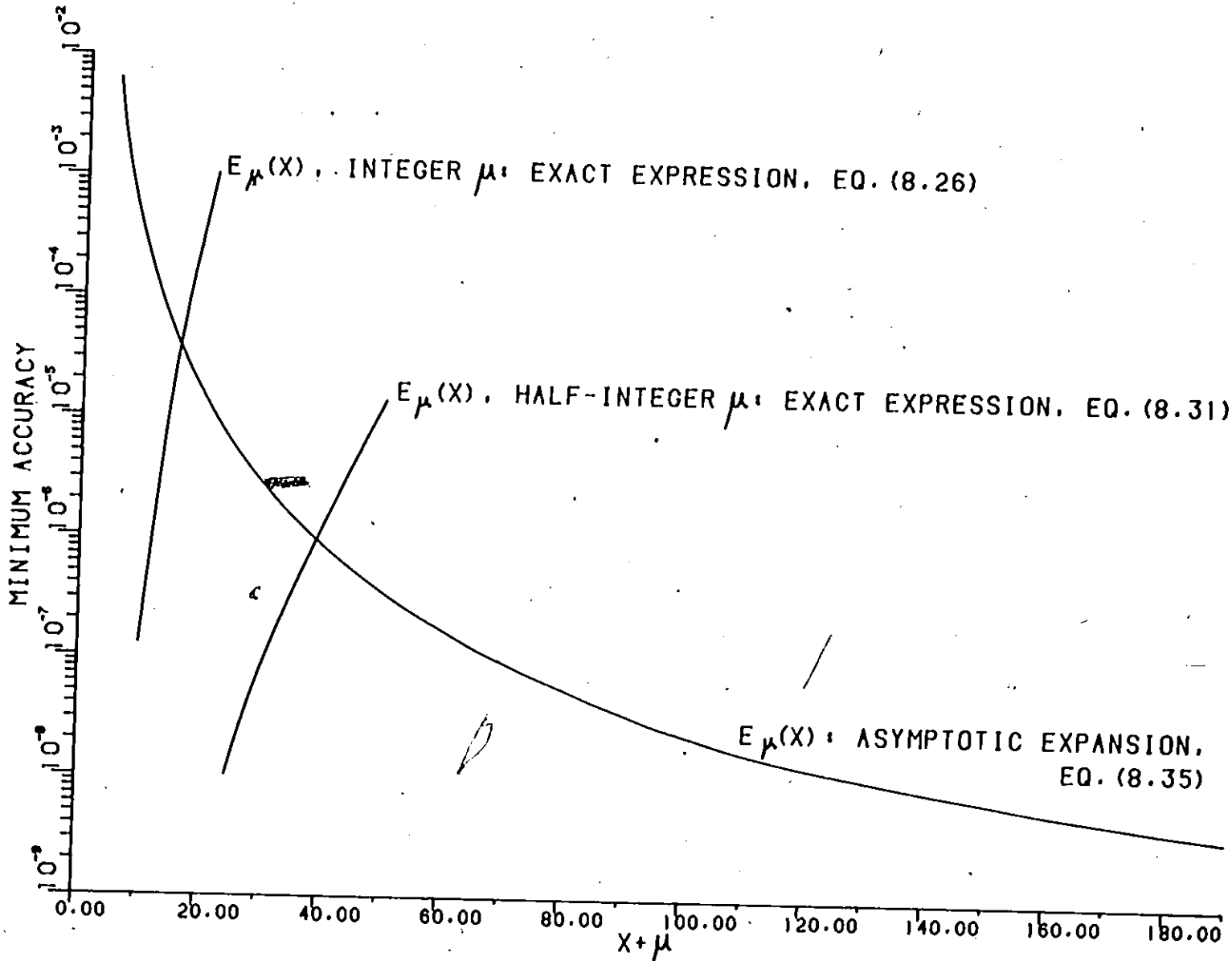

FIGURE 8.5 - APPROXIMATE MINIMUM ACCURACY EXPECTED FROM VARIOUS METHODS OF CALCULATING $E_\mu(X)$.

$$\beta_n = \sum_{\ell} \beta_{n\ell} \qquad \ldots(8.38)$$

This relation is written down by analogy with three-body recombination rate coefficients where a similar formula is derived (see Section 2 of Chapter VII).

The values of β_n obtained in this way are compared in Fig.8.6 with the hydrogenic values calculated with Seaton's (1959) work. At low values of n, there is some difference between the hydrogenic and the lithium-like rate coefficients but, as n increases, the latter approach the hydrogenic values.

8. ACCURACY OF THE RATE COEFFICIENTS

The final accuracy of the radiative recombination rate coefficients depends on the accuracy of several intermediate steps: the numerical evaluation of the function $S_\mu(x)$, the choice of the parameters used in the semi-empirical representation of the photoionization cross-sections, and finally the values of the cross-sections. $S_\mu(x)$ is accurate to 4S or better and the parameters chosen provide in most cases an accuracy in the rate coefficients of about 3S for $T \leq 1{,}000{,}000$ K and 4S for $T \leq 500{,}000$ K. The accuracy of the rate coefficients is thus limited by the cross-sections used, especially since these are calculated from approximate methods.

The photoionization cross-sections of the s and p states are calculated from the Coulomb approximation applied to bound-free transitions. In the case of bound-bound transitions, the CA gives good results. The

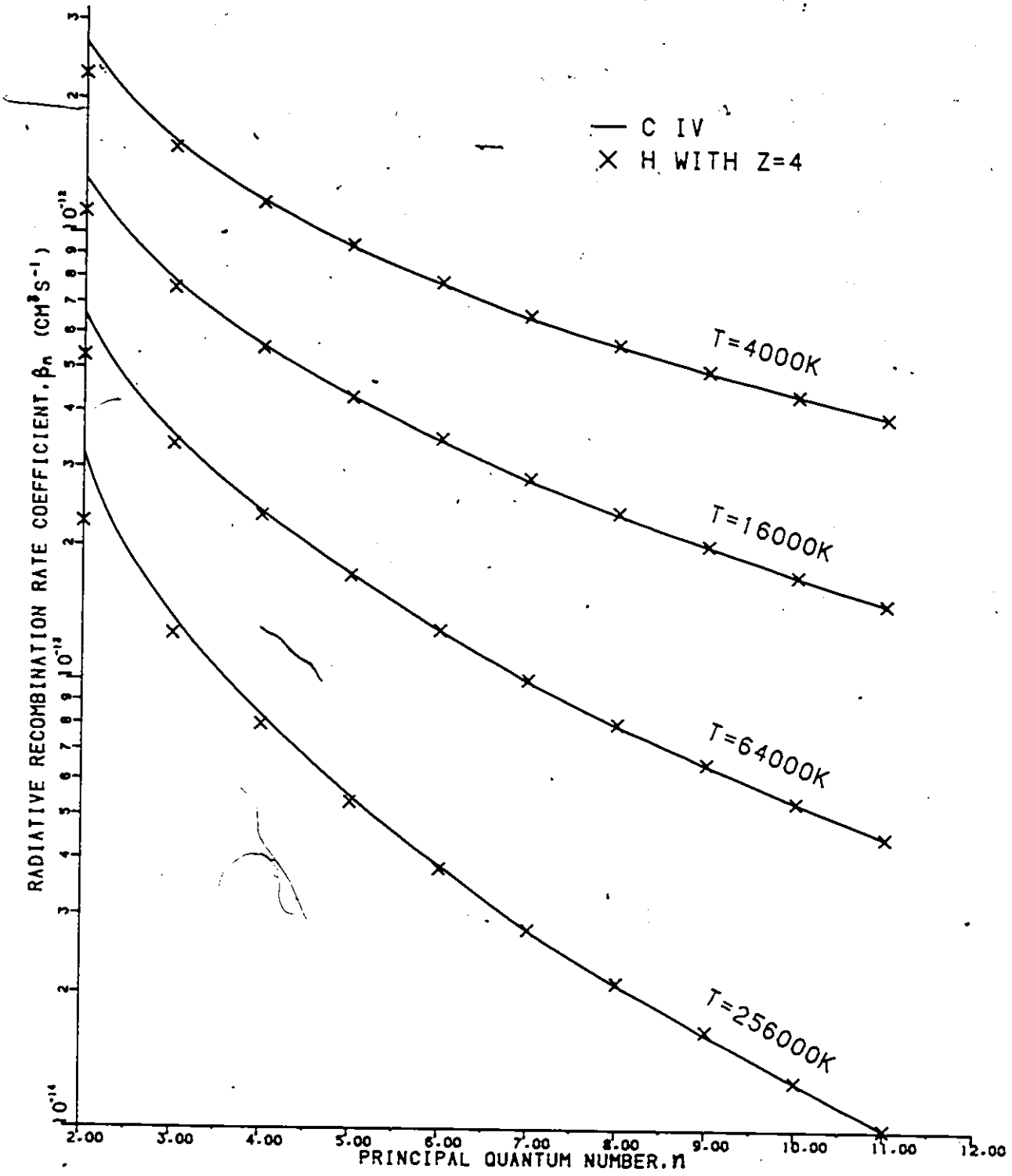

FIGURE 8.6 - COMPARISON OF THE RADIATIVE RECOMBINATION RATE COEFFICIENT OF THE LITHIUM-LIKE ION C IV WITH A HYDROGENIC ION WITH Z=4.

uncertainty arising from the use of the approximation was estimated by comparing lithium-like oscillator strengths calculated from the CA with the tables of critically evaluated values published by Martin and Wiese (1976b). Apart from a few exceptions, the CA values were found to be systematically lower than the Martin and Wiese values; furthermore, in most cases errors of ~15% were observed, the maximum error being ~25%. Assuming that the error estimates for the bound-bound transitions are applicable to the bound-free transitions, we assign an error of ~15% arising from the use of the CA.

Using the CA for bound-free transitions also introduces an additional source of error which is not present when dealing with bound-bound transitions. This uncertainty comes from the extrapolation of the quantum defect function $\mu_\ell(\epsilon)$ to positive energy states of the valence electron. $\mu_\ell(\epsilon)$ is calculated with Seaton's (1966b) quantum defect theory (see Section 9.1 of Chapter III) which is reasonably accurate if a sufficient number of high quality data on the energy states are available. Some data are available for the s and p states of C IV, N V, and O VI from which extrapolation is possible but, as discussed in Section 9.1 of Chapter III, not enough data are available to have a highly accurate extrapolation. However, since the cross-section behaves as

$$a_{n\ell}(u) \sim \cos^2 \pi \left[n^* + \mu_{\ell'}(\epsilon') + \chi(n^*\ell;\epsilon'\ell') \right] \quad \ldots(8.39)$$

and since $\mu_{\ell'}(\epsilon') < n^*$ by at least a factor of ten, the effect of the error in $\mu_{\ell'}(\epsilon')$ on the cross-section remains within reasonable bounds.

The smaller the value of ℓ' is, the more data on energy states are available and the better is the extrapolation of $\mu_{\ell'}(\epsilon')$. Furthermore, the larger the value of ℓ' is, the smaller the absolute value of $\mu_{\ell'}(\epsilon')$ becomes. Thus taking $\Delta\mu_{\ell'}(\epsilon') = \pm 0.01$ for all values of ℓ' is a reasonable estimate for the error in $\mu_{\ell'}(\epsilon')$. With this value, the error in

$$\cos^2 \pi [n^* + \mu_{\ell'}(\epsilon') + \chi(n^*\ell ; \epsilon'\ell')]$$

is found to be $\sim$5% in most cases, with a maximum value of $\sim$10%. Since other elements of eq.(8.4), such as the functions $G(n^*\ell;\epsilon'\ell')$ and $\chi(n^*\ell;\epsilon'\ell')$, could be in error, we fix the error in the cross-section arising from the approximate representation of the final continuum state at $\sim$10%. The total error in the photoionization cross-sections and thus in the radiative recombination rate coefficients of the s and p states is thus estimated to be $\sim$25%.

Since the cross-sections of the d and higher ℓ-value states were obtained from the hydrogenic calculations of Burgess (1964), and since Burgess' work gives results accurate to 5S, the error in these cross-sections depends on how close to hydrogenic the lithium-like d and higher states of C IV, N V, and O VI are. The quantum defects of these states are very small; for example, the quantum defects of the bound d states are approximately equal to 0.003. The departures of the rate coefficients from the hydrogenic values should thus be very small; we can expect an accuracy of at least 2-3S in the rate coefficients of the d and higher states of C IV, N V, and O VI.

The error in the average rate coefficients β_n calculated from eq.(8.38) will be dominated by the 25% error in the rate coefficients of the s and p states. Comparison of the hydrogenic and exact values of β_n in Fig.8.6 shows that an error of 25% in the s and p states is compatible with the results.

It should be noted that the values of the radiative recombination rate coefficients calculated in this work are accurate to within the limits previously mentioned as long as the energy of the incident photon is small enough that no inner-shell electrons are photoionized.

Chapter IX

RESULTS ON POPULATION INVERSION, COMPARISON WITH LINE INTENSITIES IN WOLF-RAYET SPECTRA, AND CONCLUSIONS

C IV lines are very prominent in the spectra of the WC category of the Wolf-Rayet stars as is evidenced in the tracings of the spectra of Wolf-Rayet stars obtained by Smith (1955) and reproduced in part in Figs.9.18 to 9.20. We have thus carried out detailed calculations on this ion. In Fig.9.1, the Grotrian diagram of C IV is shown and the transitions among states with $n \leq 6$ giving rise to lines in the visible region of the spectrum are also shown. We have concentrated our attention to these transitions since the level scheme used in this model (see Fig.3.2) can only resolve the ℓ-value splitting of states with $n \leq 6$.

The adiabatic cooling of the plasma was simulated with the model outlined in Section 7 of Chapter III, and the population densities of the excited states of C IV after cooling were calculated with the CR model. Population inversions were found to occur in many of the transitions of this ion. Plots of the gain α' versus T_e for the inversely populated transitions of interest to us were made for a series of values of n_e. Typical results for the transitions 6s→5p, 6p→5d, 6d→5p, 6f→5d, 6g→5f, and 6h→5g are shown in Figs.9.2 to 9.9. These plots were then used to determine the contours of equal α' on a n_e, T_e plot. The final results for the transitions 6s→5p, 6p→5d, 6d→5p, 6f→5d, 6g→5f, and 6h→5g are shown in Figs.9.10 to 9.15. It will be noticed that these contours

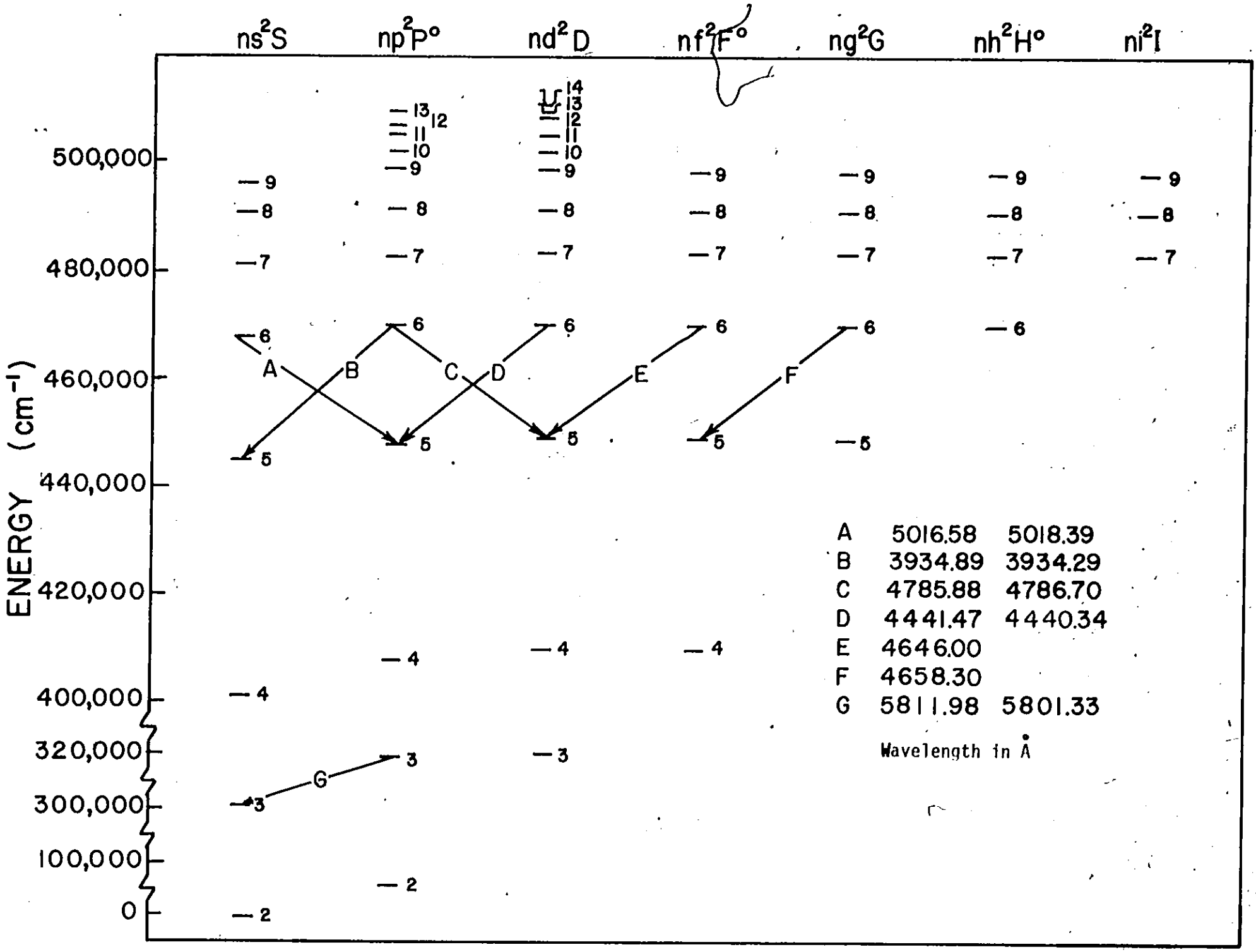

Figure 9.1 - Grotrian diagram of C IV.

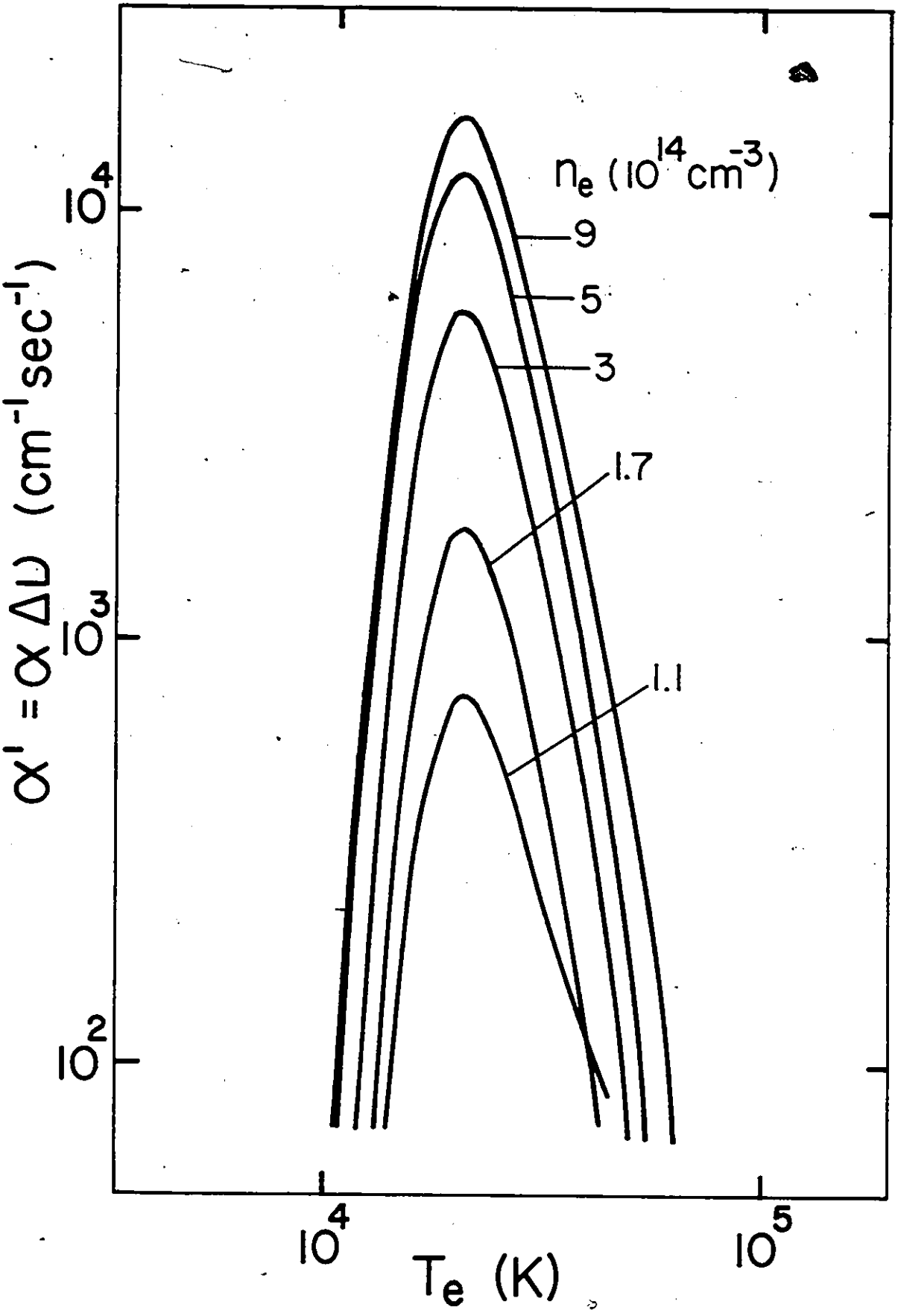

Figure 9.2 - Typical α' versus T_e plot for the 6s→5p transition of C IV.

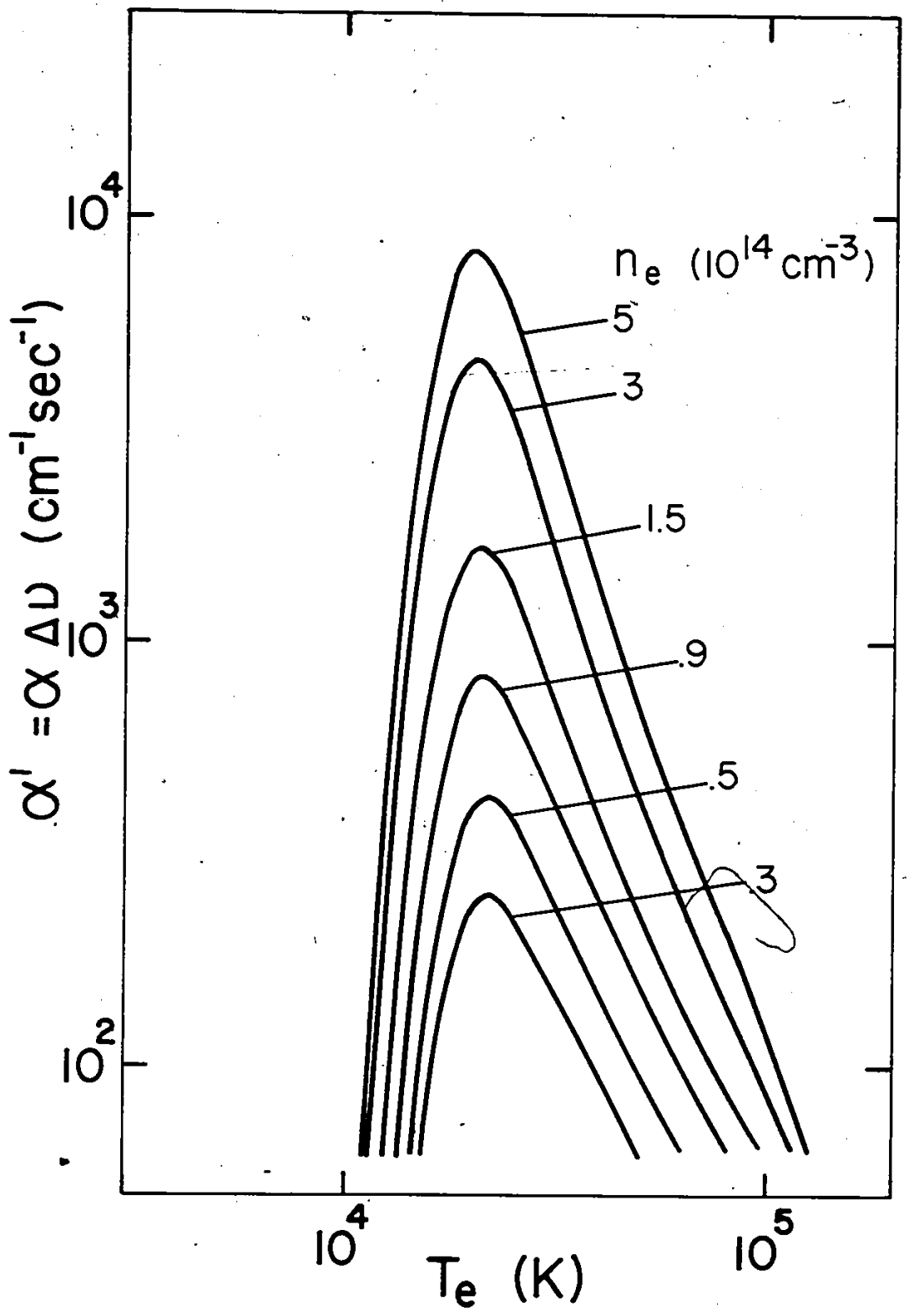

Figure 9.3 - Typical α' versus T_e plot for the 6p->5d transition of C IV.

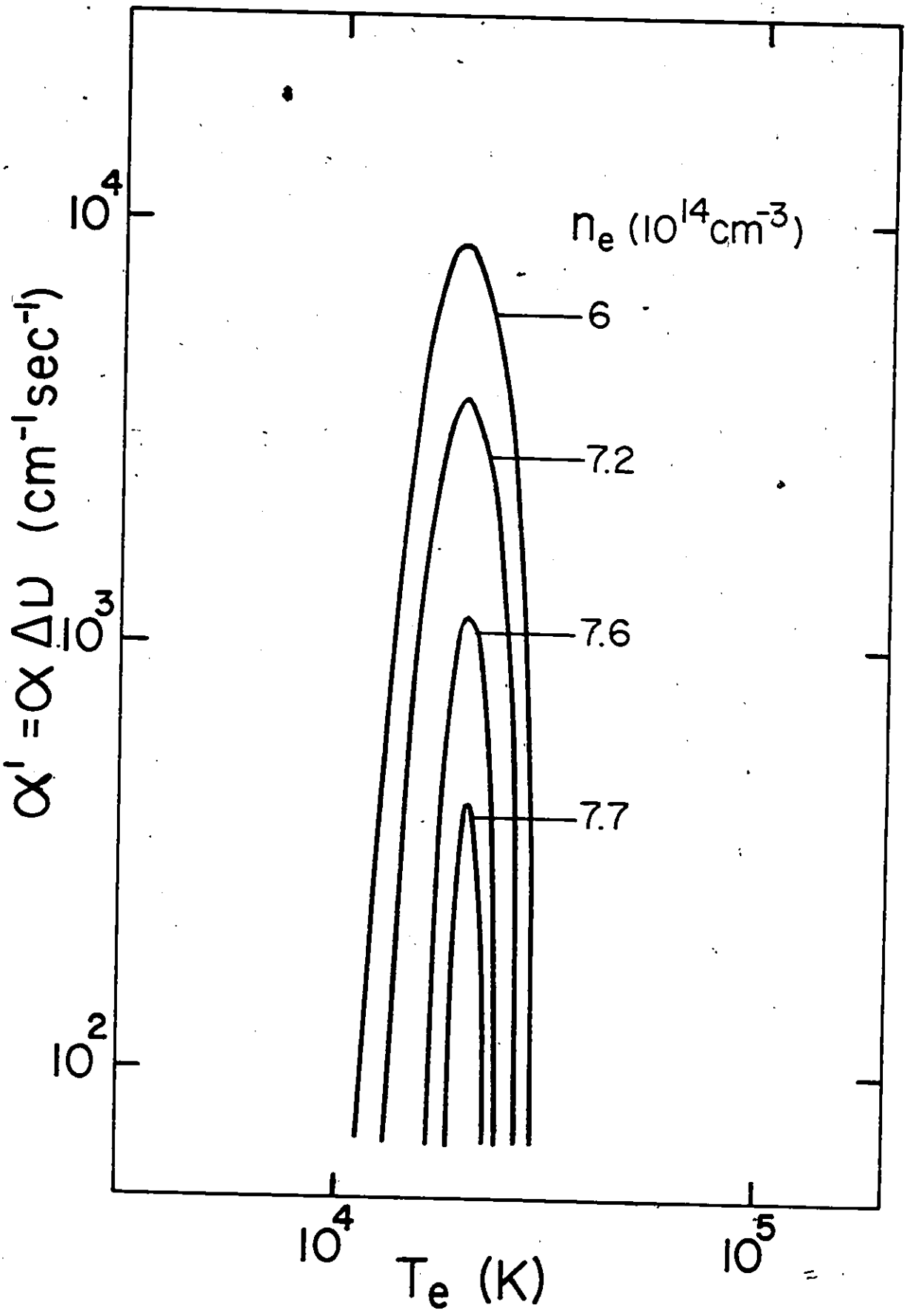

Figure 9.4 - Typical α' versus T_e plot for the 6d->5p transition of C IV.

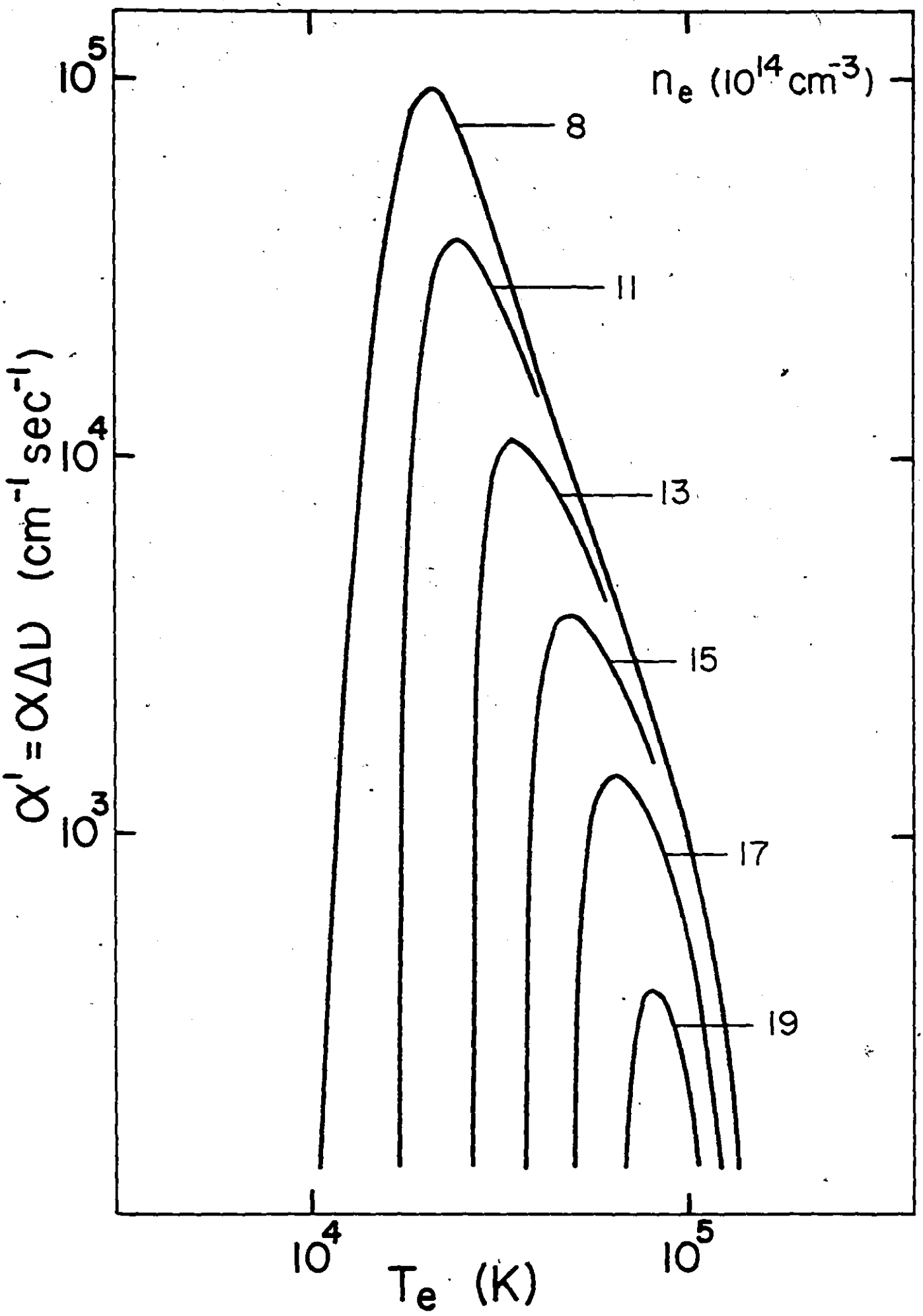

Figure 9.5 - Typical α' versus T_e plot for the 6f->5d transition of C IV.

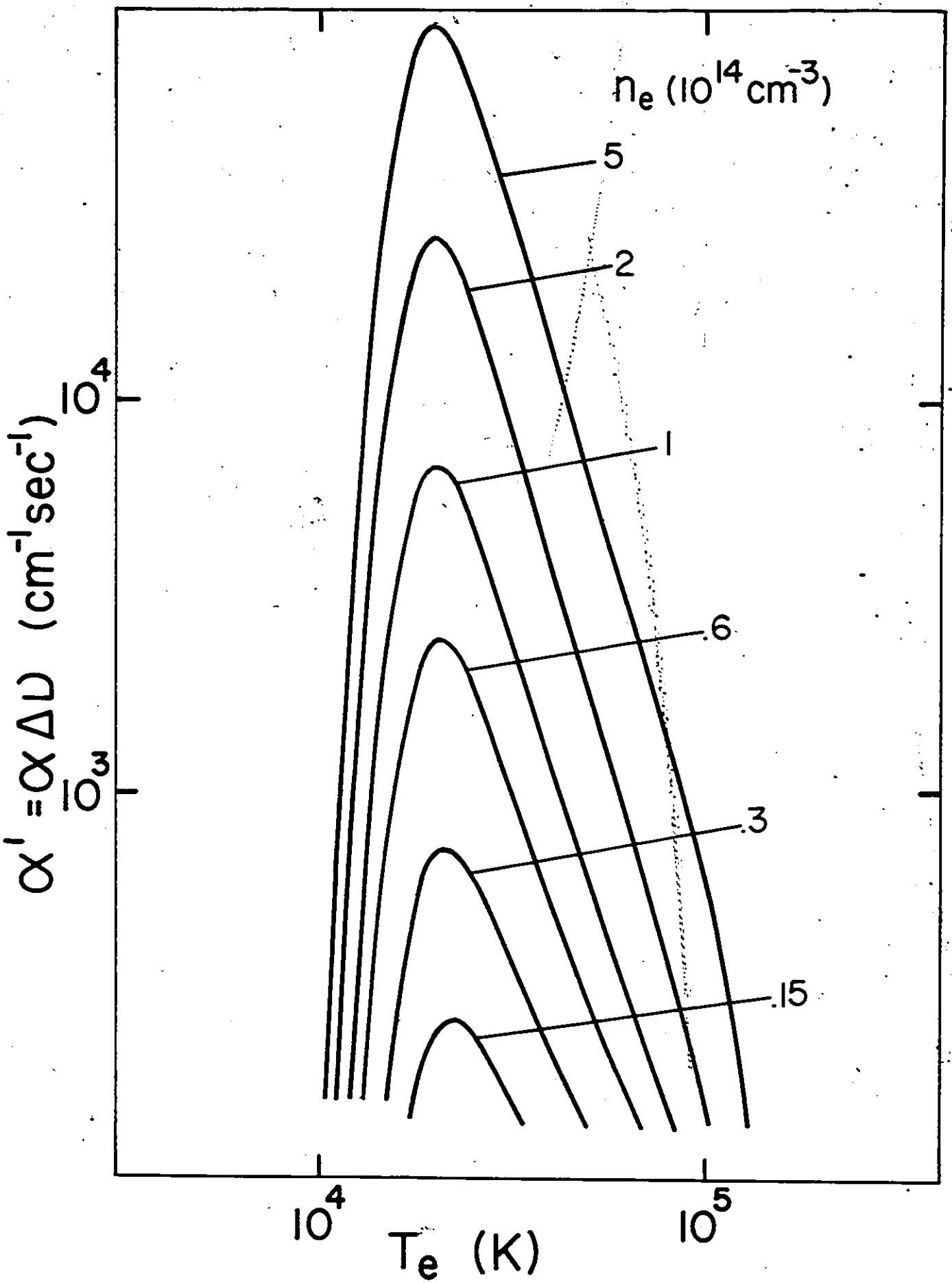

Figure 9.6 - Typical α' versus T_e plot for the 6f->5d transition of C IV.

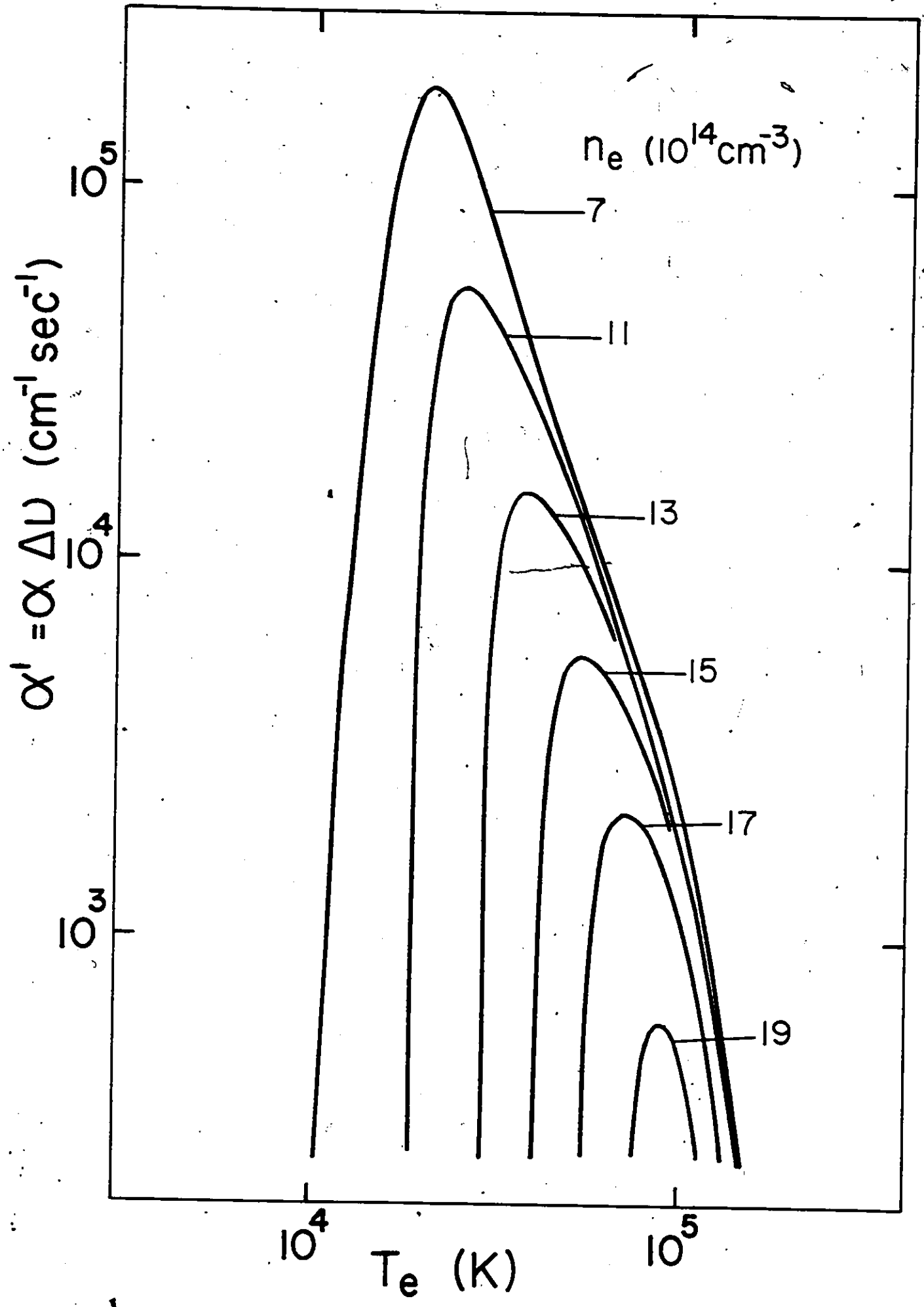

Figure 9.7 - Typical α' versus T_e plot for the 6g->5f transition of C IV.

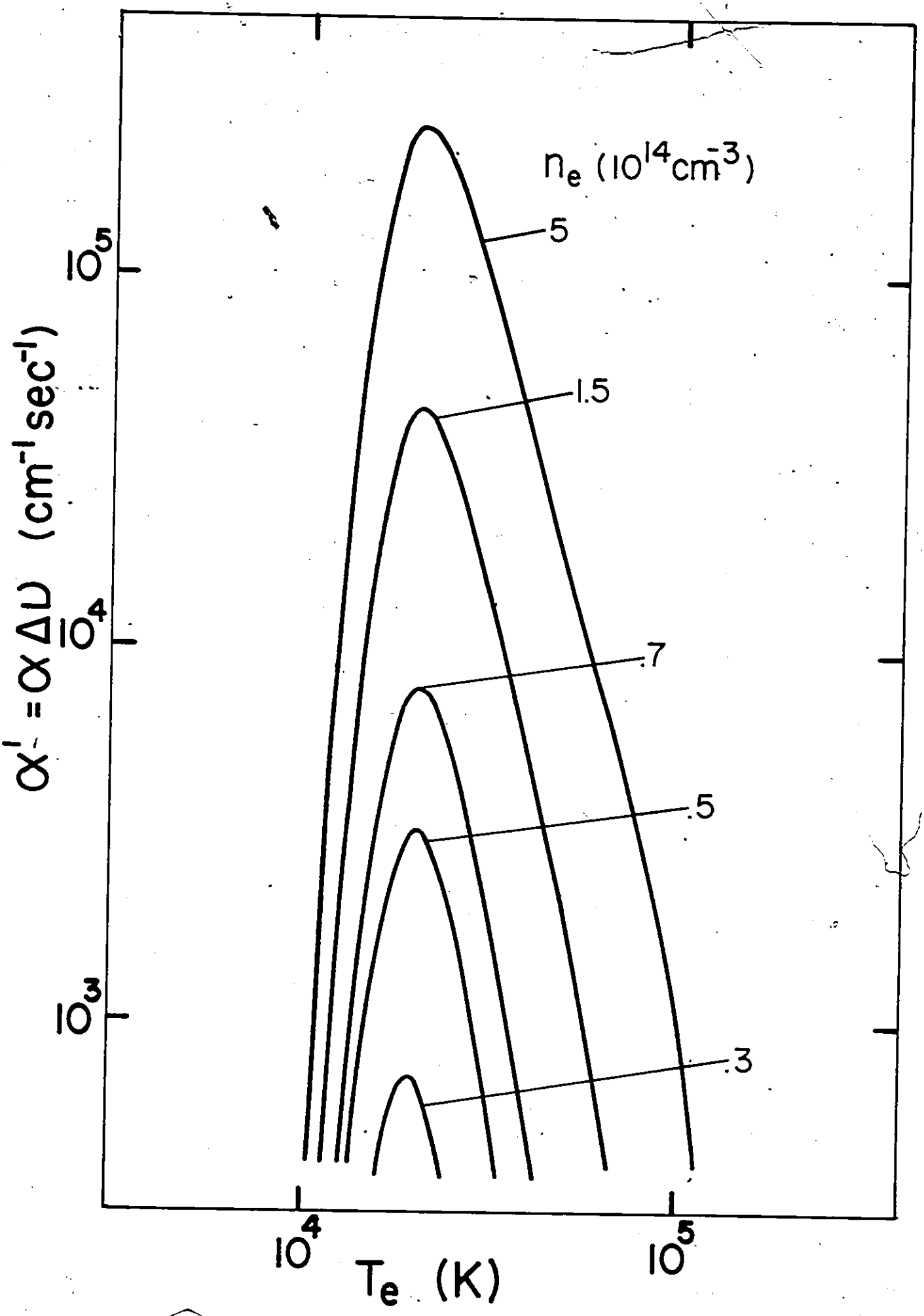

Figure 9.8 - Typical α' versus T_e plot for the 6g->5f transition of C IV.

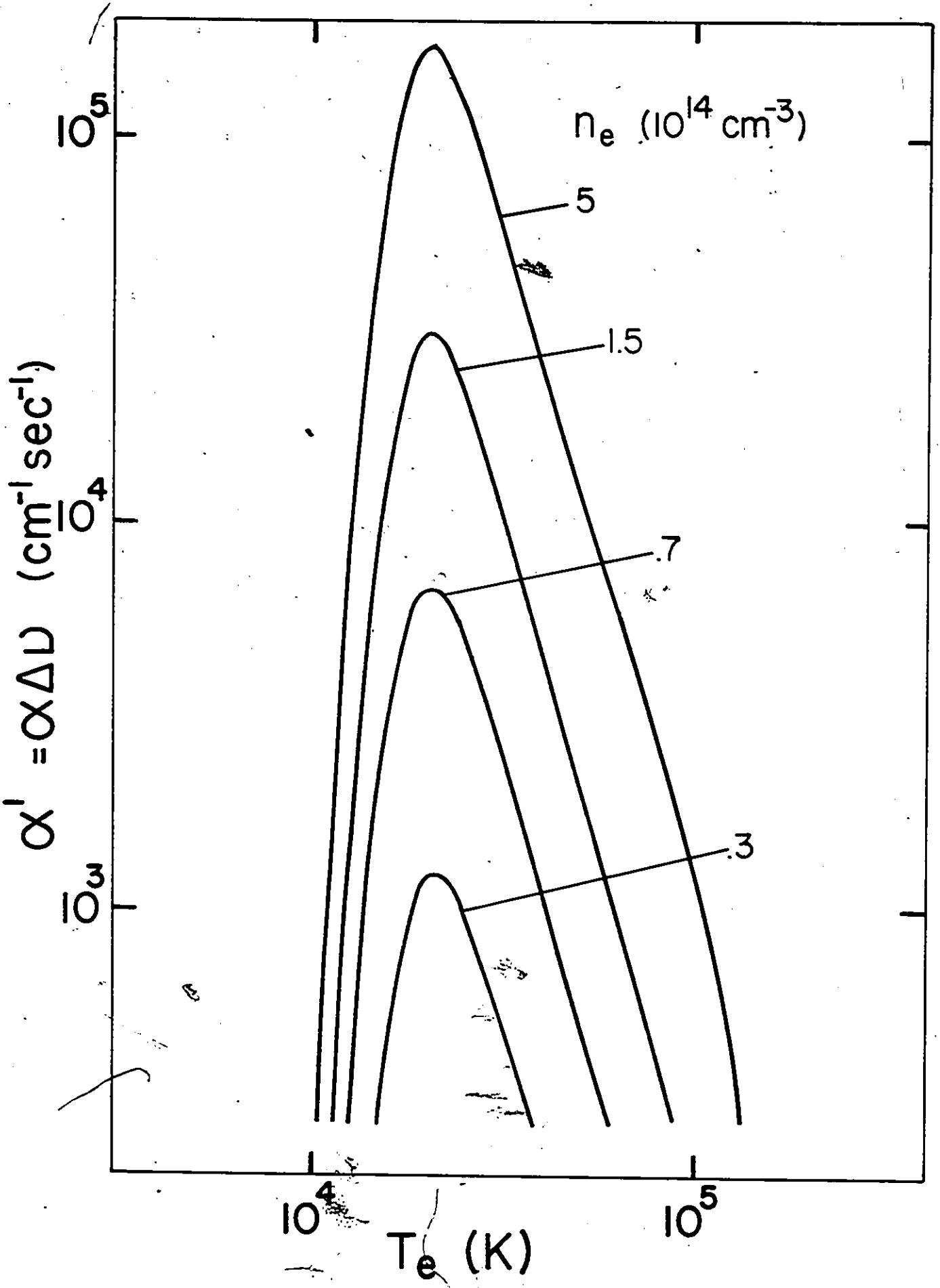

Figure 9.9 - Typical α' versus T_e plot for the 6h->5g transition of C IV.

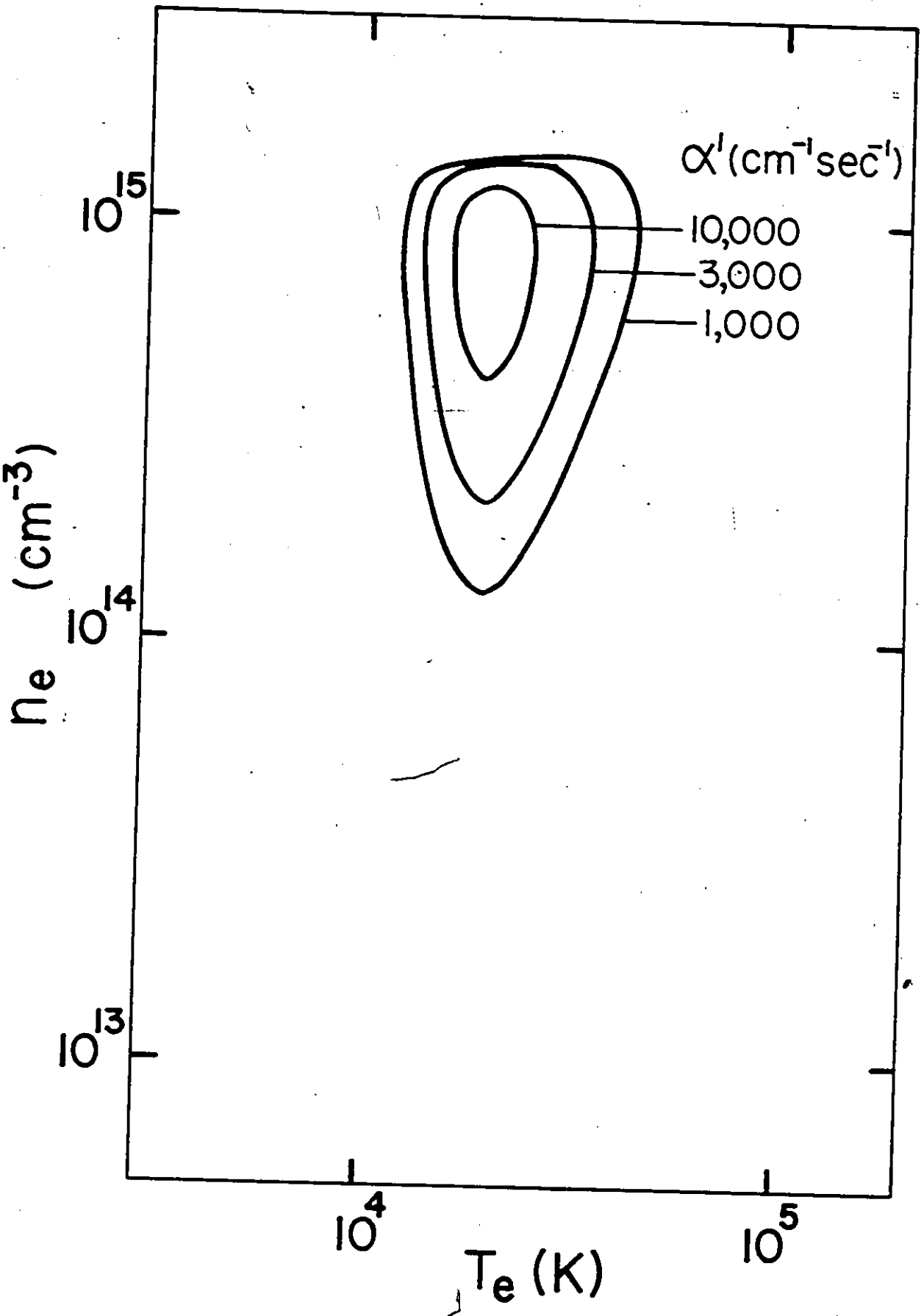

Figure 9.10 - n_e-T_e diagram for the 6s->5p transition of C IV.

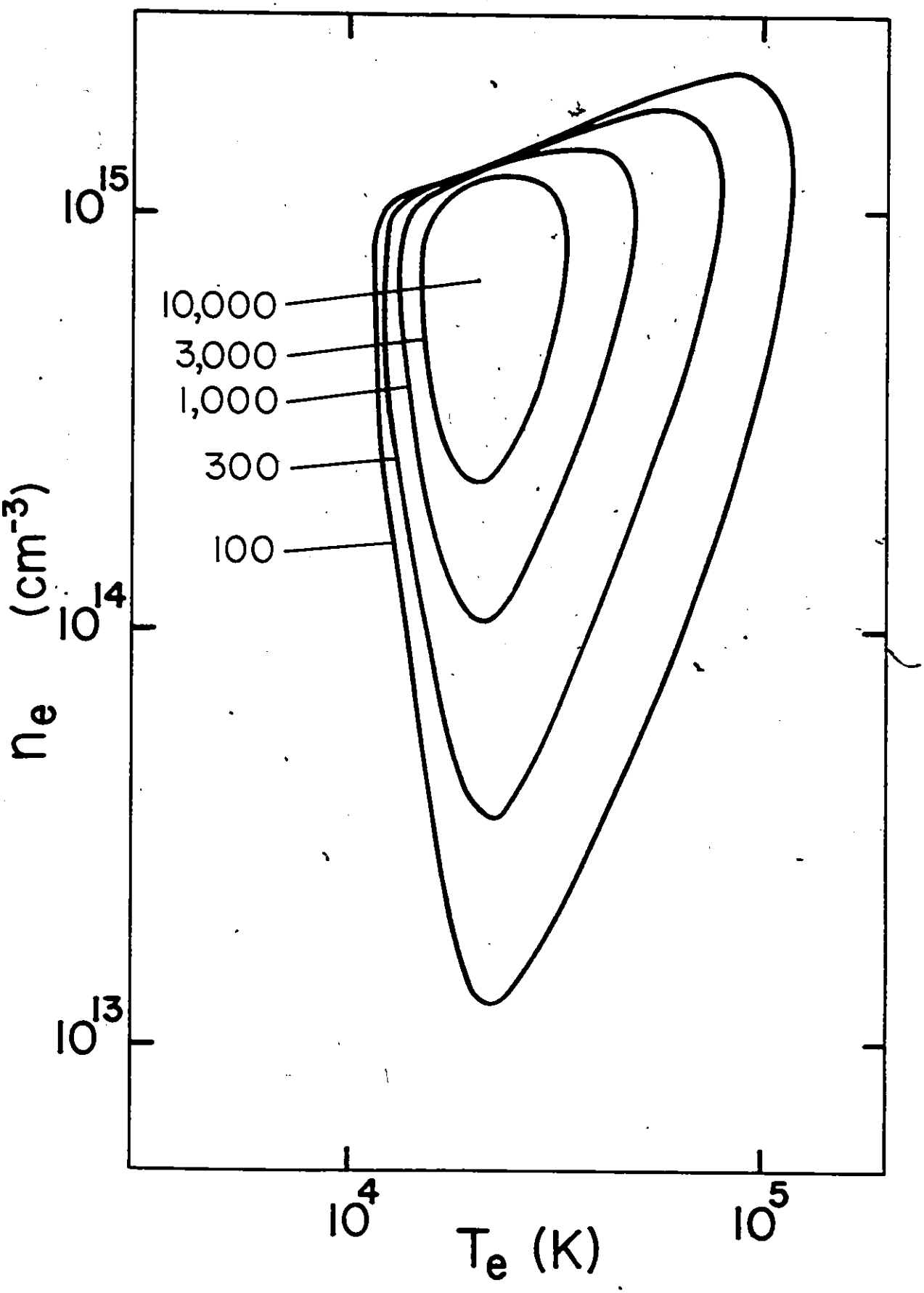

Figure 9.11 - n_e-T_e diagram for the 6p->5d transition of C IV.

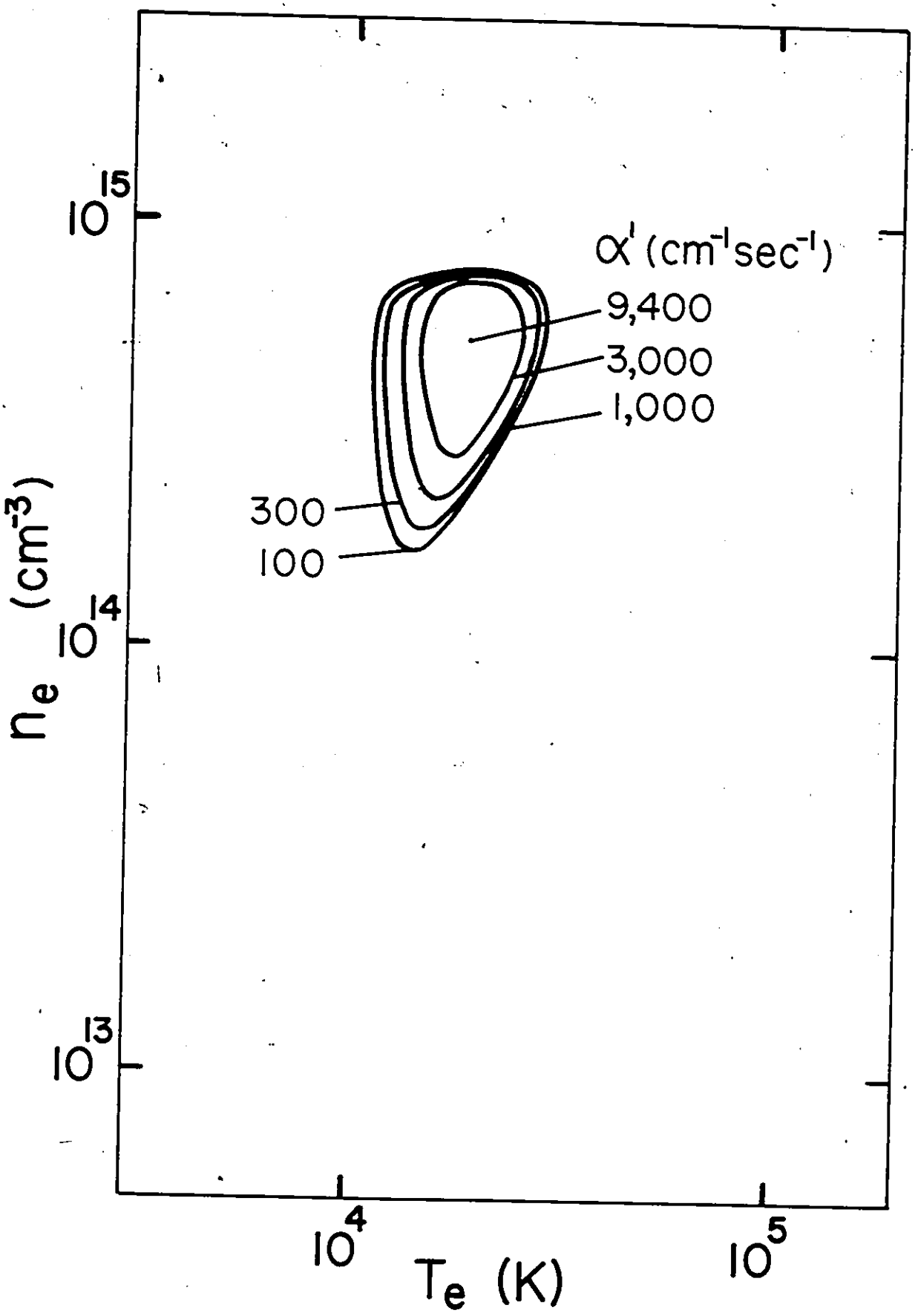

Figure 9.12 - n_e-T_e diagram for the 6d->5p transition of C IV.

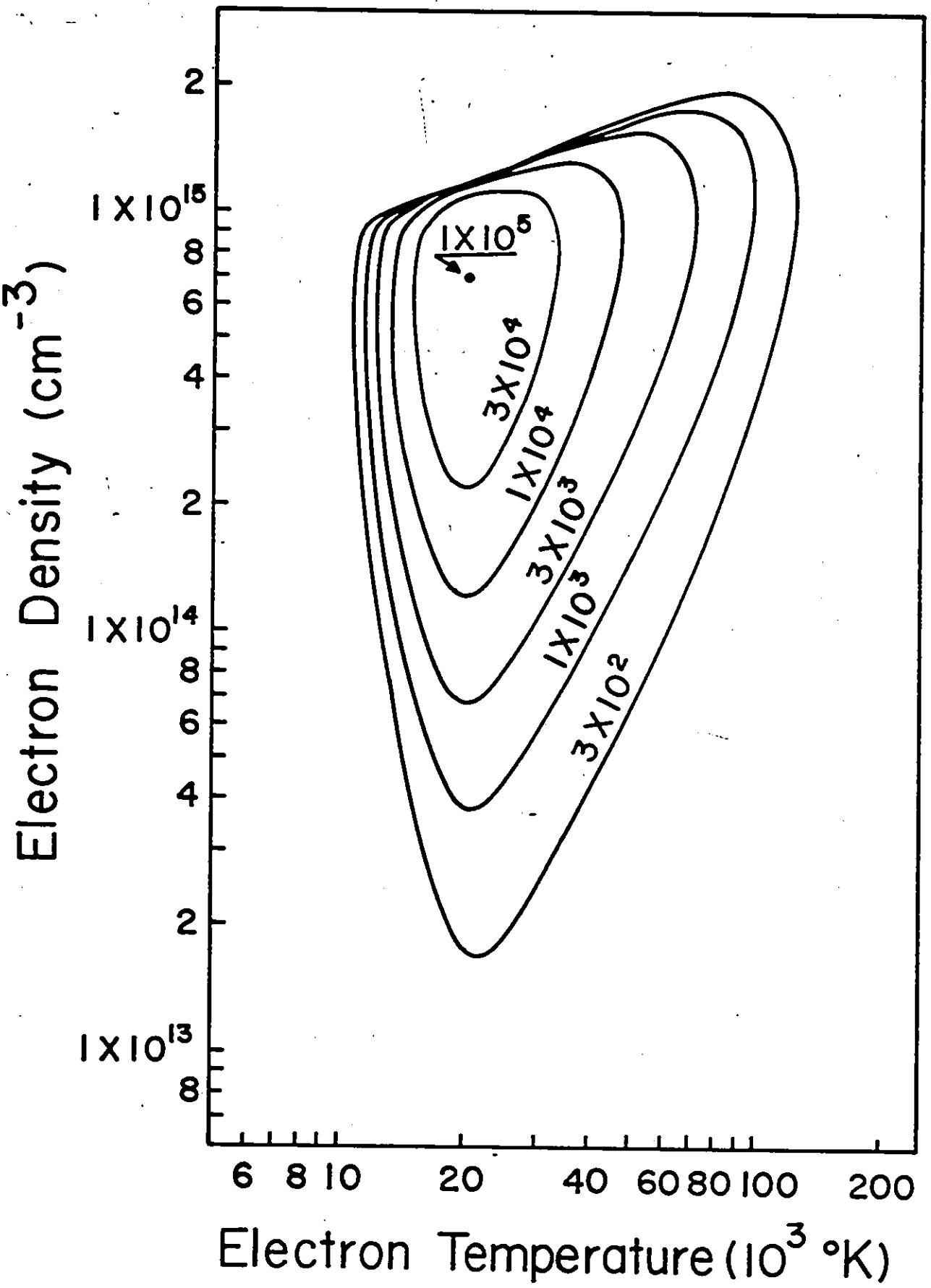

Figure 9.13 - n_e-T_e diagram for the 6f->5d transition of C IV (λ4646).

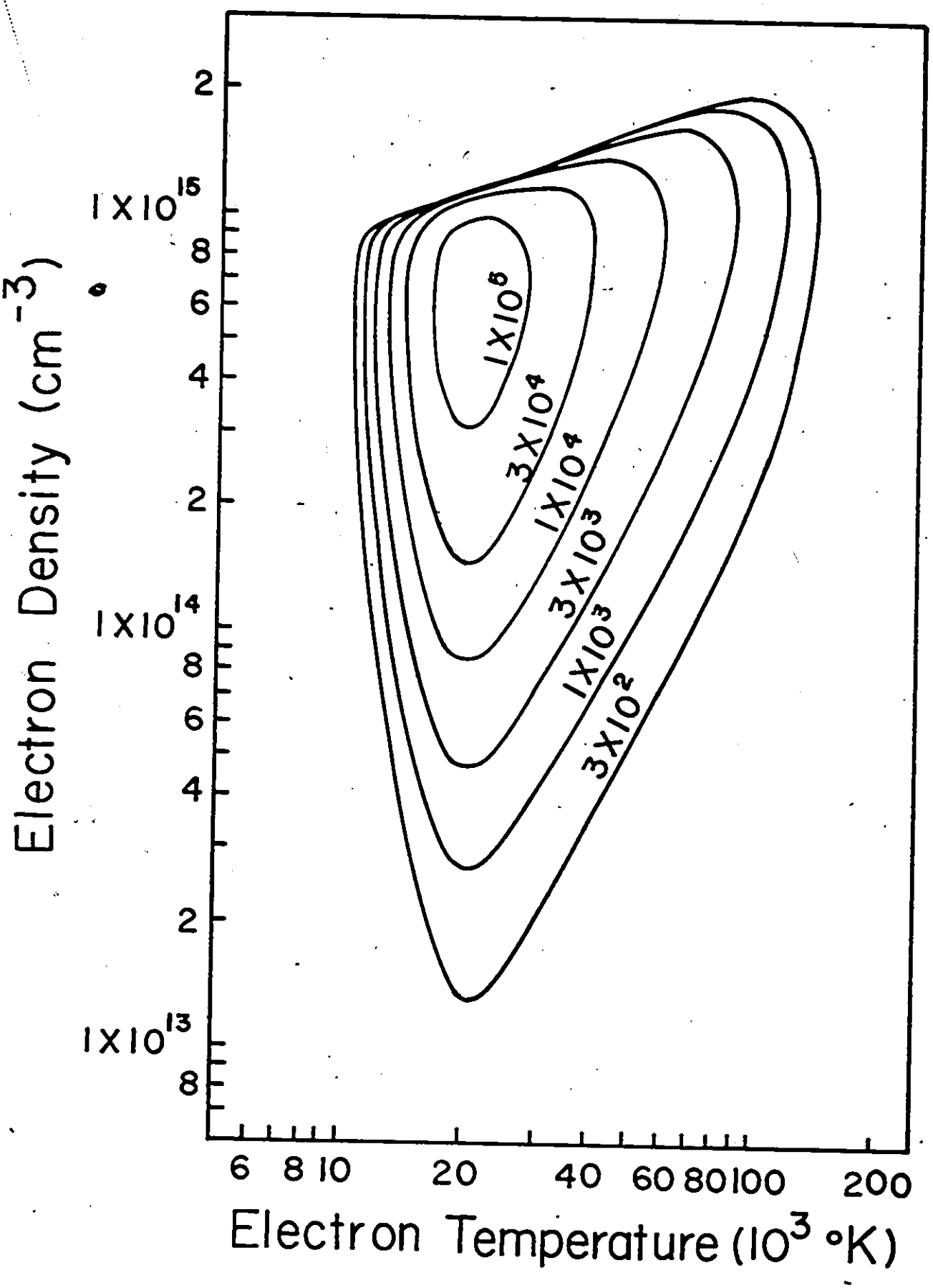

Figure 9.14 - n_e-T_e diagram for the 6g->5f transition of C IV (λ4658).

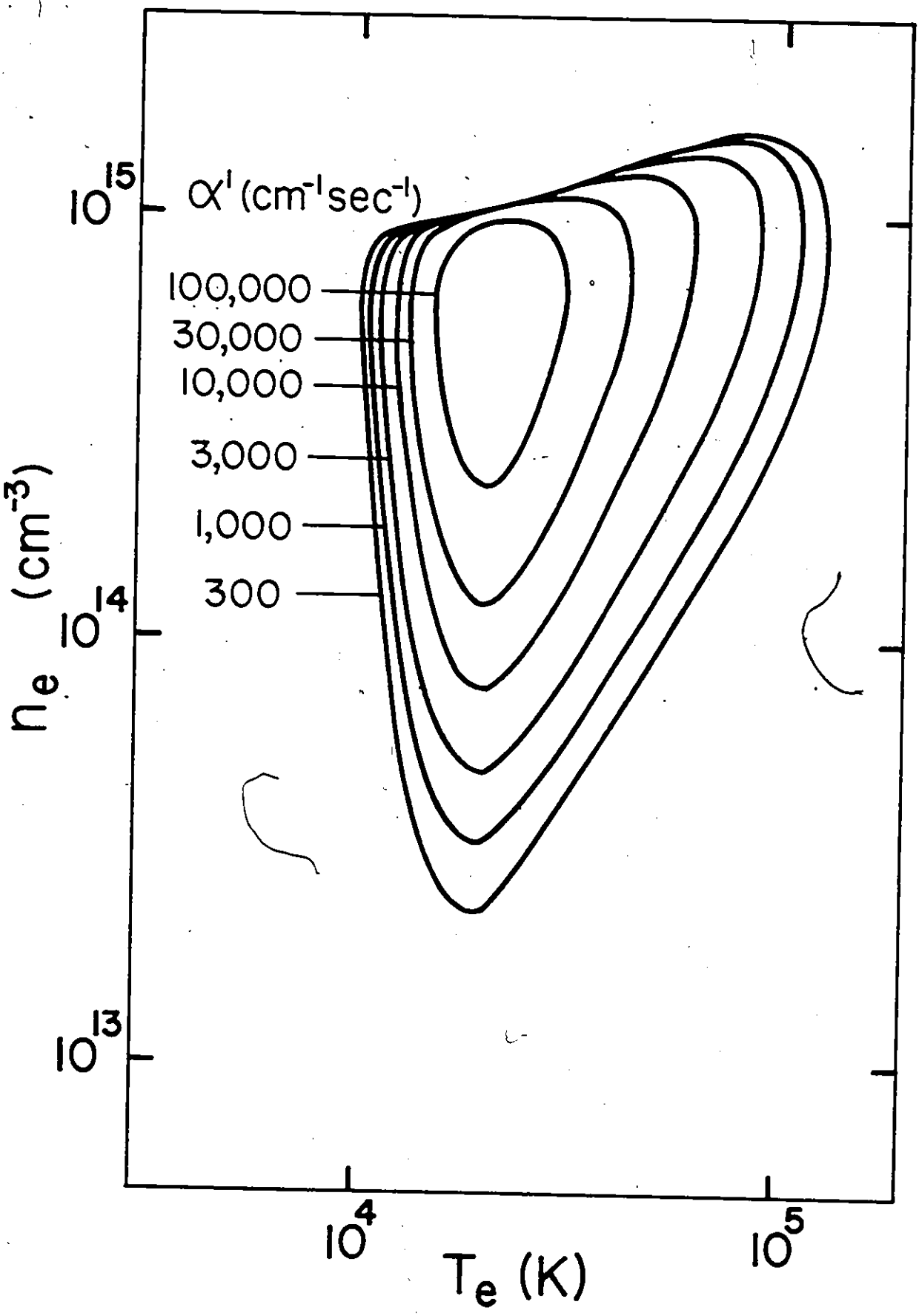

Figure 9.15 - n_e-T_e diagram for the 6h->5g transition of C IV.

are very similar to those obtained for He II λ4686 by Varshni and Lam (1976): the gain decreases very rapidly at high values of n_e, decreases less rapidly at low values of T_e, and decreases slowly at high values of T_e and low values of n_e.

The $6\ell' \rightarrow 5\ell$ inversely populated transitions can be separated in two broad categories: the $\Delta\ell = +1$ transitions (6s→5p, 6p→5d) with a gain $\alpha'_{max} \sim 10^4$ cm^{-1}s^{-1} and the $\Delta\ell = -1$ transitions (6f→5d, 6g→5f, 6h→5g) with a gain $\alpha'_{max} \sim 10^5$ cm^{-1} s^{-1}. The $\Delta\ell = -1$ transition 6d→5p is relatively unimportant and has a much smaller region of population inversion on the n_e-T_e diagram. Of the transitions shown in Fig.9.1, the 6g→5f (4658Å) and the 6f→5d (4646Å) transitions are the most prominent. The maximum value of α' is largest for these two transitions: $\alpha' \sim 10^5$ cm^{-1}s^{-1} for $T_e \simeq 20{,}000$K and $n_e \simeq 7 \times 10^{14}$ cm^{-3}. Laser action will thus be most intense for these transitions.

An analysis of the limitations of the model used in these calculations is now necessary if we are to assess correctly the relevance of these results to physical observations. The model is based on several approximations, the most important of which are:

i. the plasma undergoes rapid cooling (or rapid expansion) (see Section 5.2 of Chapter I);

ii. the expansion of the plasma occurs under adiabatic conditions (see Section 5.3 of Chapter I);

iii. QSS conditions prevail in the plasma (see Section 4.1.h of Chapter I);

iv. the plasma is optically thin; this condition is less realistic since some degree of radiation reabsorption is likely to occur in the plasma.

Departures from these conditions will affect the comparison of the theoretical results with physical observations.

Given a plasma which satisfies these approximations, the accuracy of the calculated results will then depend on the accuracy of the rate coefficients used in the coupled rate equations of the CR model. In these calculations, the electron impact excitation rate coefficients have the largest uncertainties, estimated to be a factor of about four. In comparison, the uncertainties in the other coefficients are negligible. Consequently, we have investigated the effect of the uncertainties in the electron impact excitation rate coefficients on the gain of the transitions considered in this work. This procedure should provide a good estimate of the validity of these calculations.

The electron impact excitation rate coefficients have been varied by factors of up to ten, and model calculations have been carried out with these values of the rate coefficients. Qualitatively, the general behavior of the population inversion scheme and the shape of the n_e-T_e diagrams are left unchanged. Quantitatively, a change in the electron impact excitation rate coefficients of a factor of four results in a change in the gain of the transitions of interest by a factor of five or less, depending on the transition considered, the temperature and the free electron density of the plasma.

The uncertainties in the values of other quantities such as δ or n_i should only have a refining effect on the results. The general population inversion scheme is unaffected by uncertainties in the rate coefficients or in other quantities.

Under appropriate conditions, the previously mentioned results are applicable to both laboratory and astrophysical plasmas. In particular, we consider the bearing of these results on the spectra of Wolf-Rayet stars, which are known to have an expanding envelope of hot ionized gases.

When the speed of expansion of the plasma is low, the expansion will be closer to being isothermal than adiabatic. However, as the speed of expansion increases, the expansion will become more and more nearly adiabatic, and certain spectral lines can then be expected to display laser action. Let us compare this expectation with the spectra of various classes of WC stars. WC8 stars have relatively sharp lines; since the widths of the lines in an expanding shell arise from the Doppler effect, the speed of expansion of the plasma must be low and the degree of laser action is also expected to be low. The lines become wider in WC7 stars, indicating that the speed of ejection is greater than in WC8 stars; correspondingly, the degree of laser action is also expected to be greater. The lines become still wider in WC6 stars; we thus expect the degree of laser action to further increase. We compare these expectations with the observed data on the spectra of WC stars.

A bright emission feature at about $\lambda 4650$ has been known in Wolf-Rayet spectra for the last hundred years or so. A few years after the

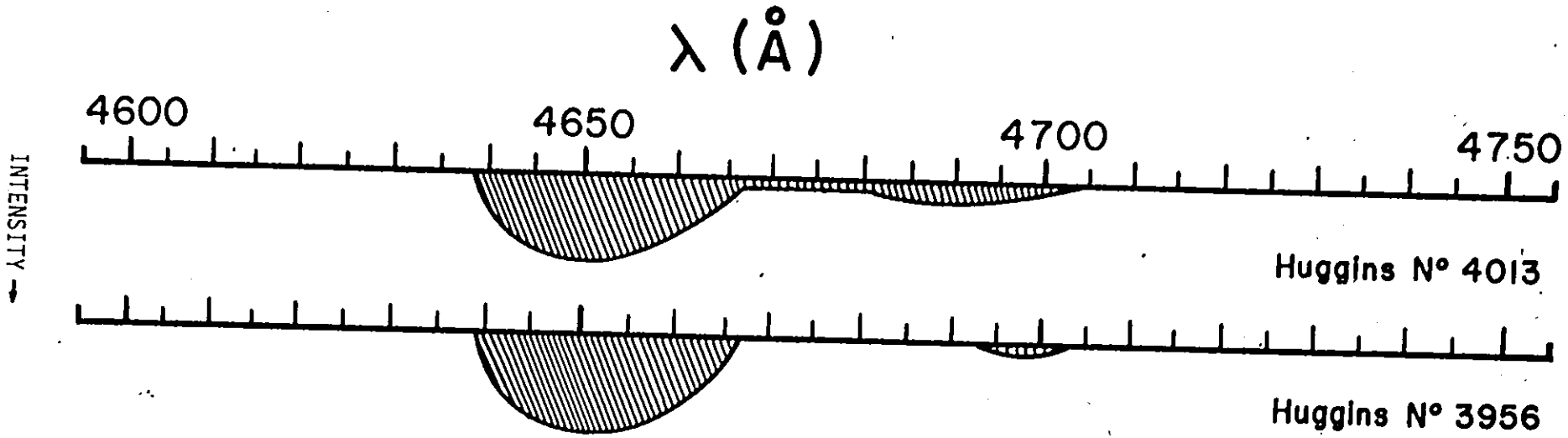

Figure 9.16 - Spectra of the Wolf-Rayet stars BD+35°4013 and BD+36°3956 as reported by Huggins and Huggins (1891).

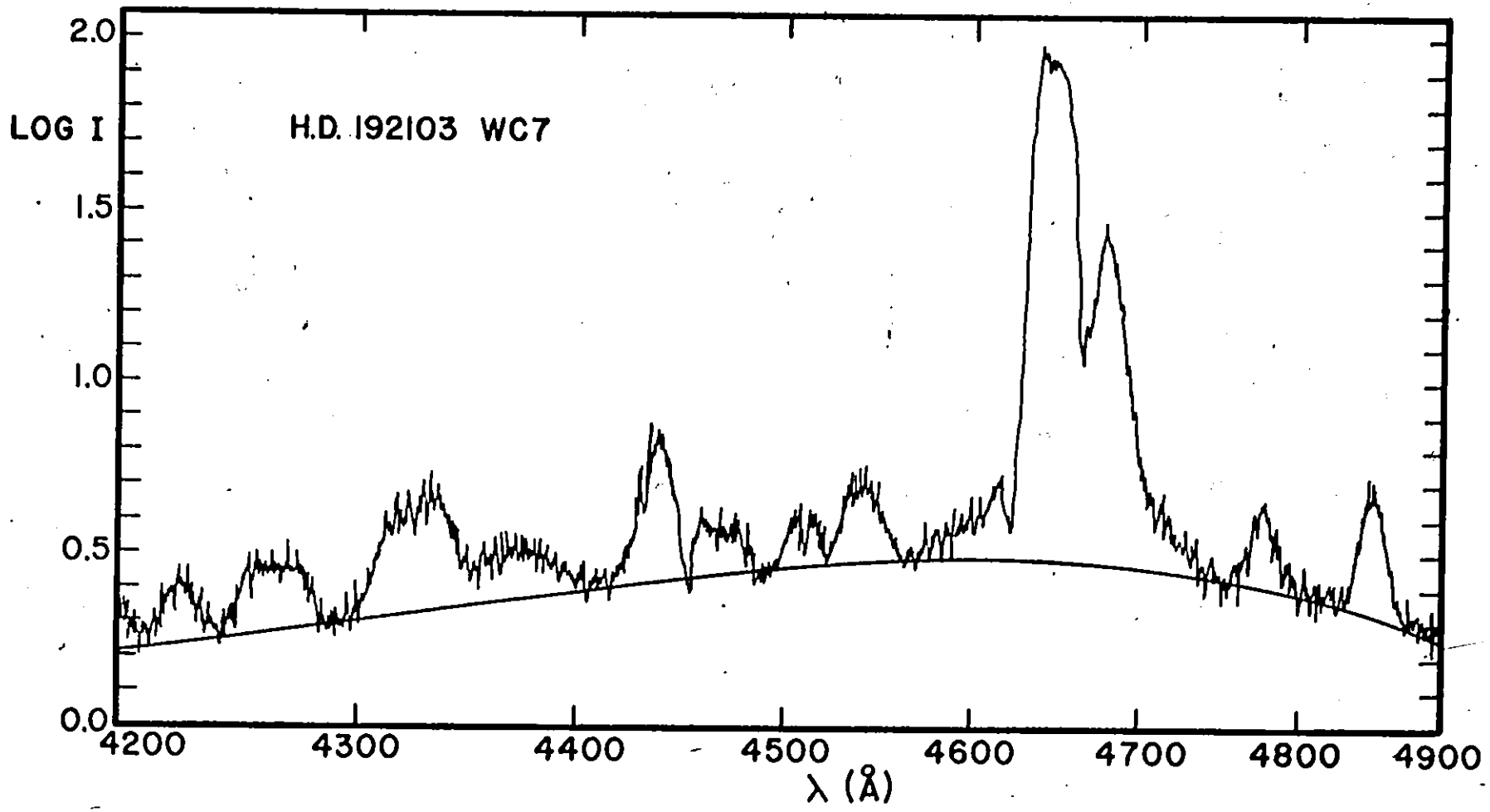

Figure 9.17 - Tracing of the spectrum of a WC7 star for the wavelength region λλ4200-4900 from Underhill (1959).

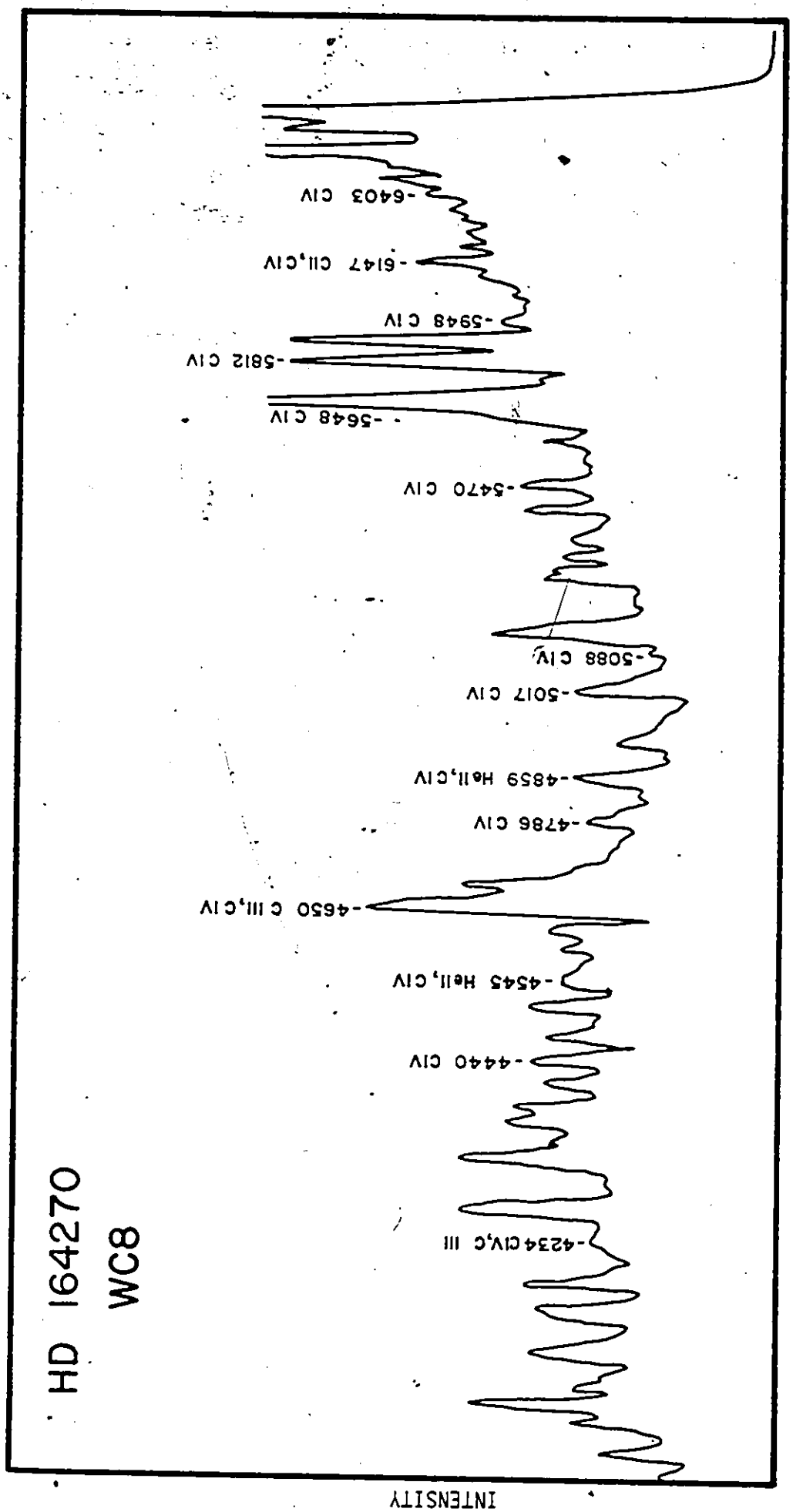

Figure 9.18 - Tracing of the spectrum of the WC8 star HD 164270 from Smith (1955).

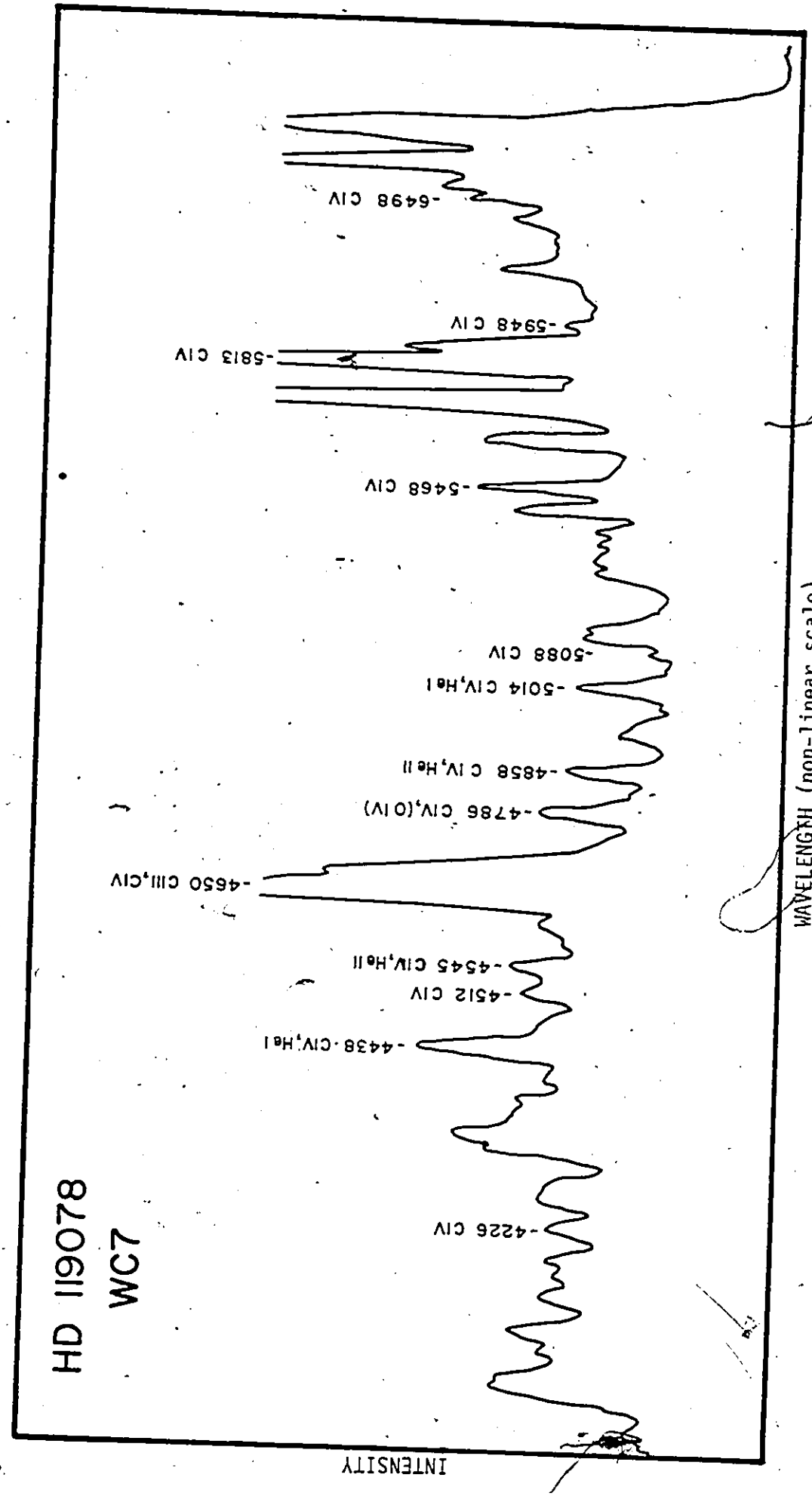

Figure 9.19 - Tracing of the spectrum of the WC7 star HD 119078 from Smith (1955).

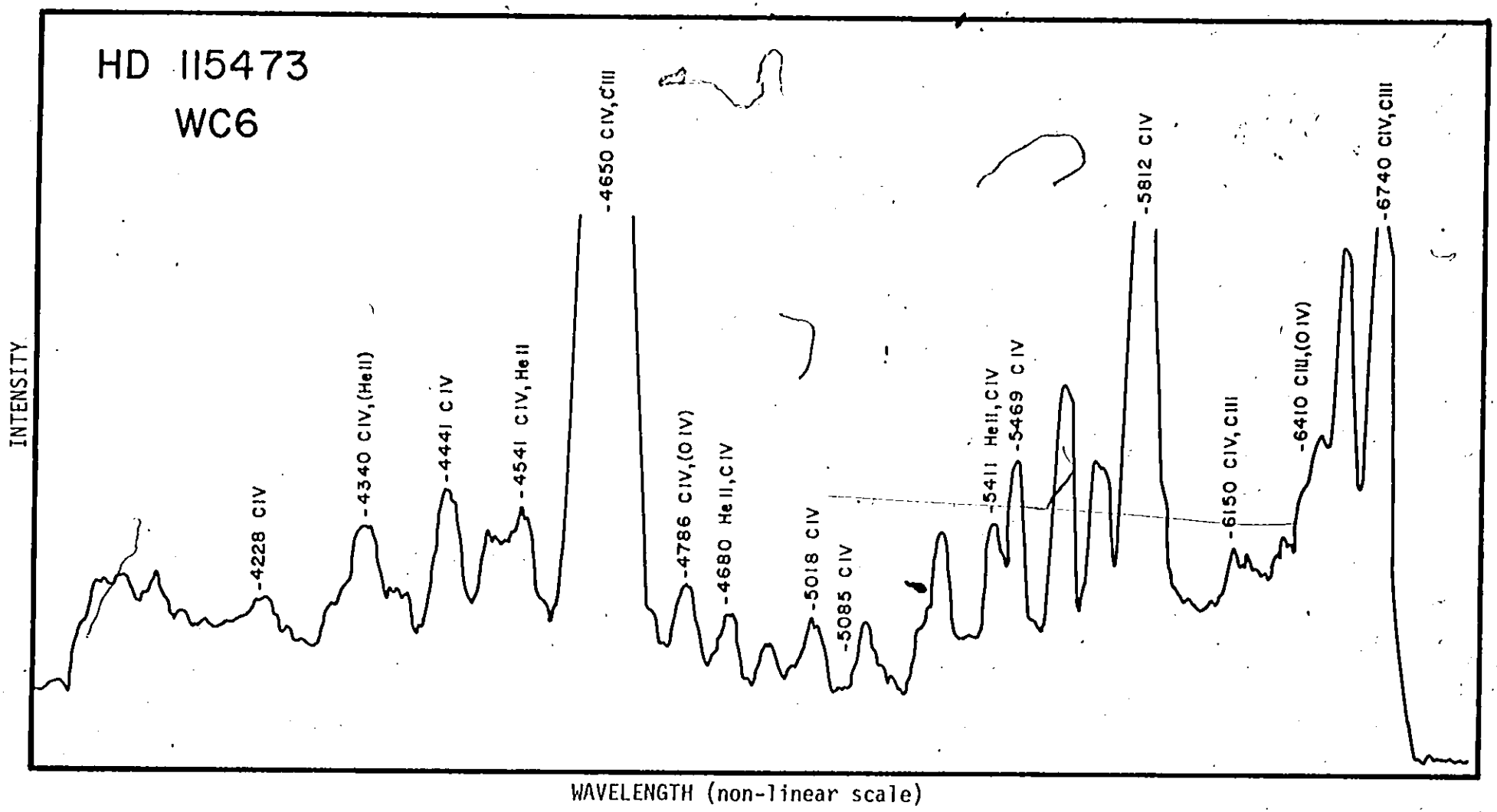

Figure 9.20 - Tracing of the spectrum of the WC6 star HD 115473 from Smith (1955).

discovery of Wolf and Rayet (1867) of the bright lines in the spectra of BD+35°4001, BD+35°4013, and BD+36°3956, Vogel (1873, 1883) described their spectra in more detail. He found that both BD+36°3956 and BD+35°4013 have a wide bright blue band with a maximum at about λ4640. Copeland in 1884 (quoted in Huggins and Huggins, 1891) measured the position of the maximum in BD+35°4013 to be at λ4654 and that in BD+36°3956 to be at λ4649. Huggins and Huggins (1891) found the position of maximum to be practically the same in the two cases, namely λ4650. The spectra of these two stars as reported by Huggins and Huggins (1891) are reproduced in Fig.9.16.

The curious behavior of the relative intensities of λ4650 and λ4686 in classical Wolf-Rayet spectra has been known for the last 50 years (Plaskett, 1924). Plaskett (1924) was struck by the remarkable variations in the relative intensities of these two lines and noted 'The ratio of 4650 C^+ to 4686 He^+ is also peculiar, as the marked discontinuity at the third group where the ratio abruptly increases tenfold distinctly shows. Examination of the spectra clearly indicates that this is almost entirely due to the sudden increase in the strength of the carbon band. Even supposing the interval between the second and third groups to be greater than between the earlier ones, still the change in the strength of enhanced carbon at 4650 is more abrupt than shown by any other element and there must be some physical reason which makes ionized carbon behave in this unique manner.' Varshni (1977) pointed out that such variations can be readily understood on the basis of laser action.

Over the years, the spectra of Wolf-Rayet stars have been investi-

gated by many workers. However, very few tracings have been published. In Fig.9.17, we reproduce a tracing of the spectrum of a WC7 star for the wavelength region λλ4200–4900 from a paper by Underhill (1959). The strong line at λ4650 is very prominent.

Smith (1955) carried out a series of detailed spectroscopic observations of the southern Wolf-Rayet stars. Portions of his tracings of the spectra of three Wolf-Rayet stars are reproduced in Figs.9.18 to 9.20. In these figures, we have indicated the C IV lines identified by Smith (1955). The behavior of the emission line at λ4650 is remarkable. As we go from a WC8 star to a WC6 star, this emission line shows a great increase in its intensity. This observation can now be understood in the light of our calculations. Our results show that in C IV, the 4650 Å line will show the strongest population inversion and consequent laser action under adiabatic expansion. Thus we find that as the speed of expansion increases from WC8 to WC6 stars, the laser action in C IV λ4650 becomes greater, leading to a rapid increase in the intensity of this line.

It will also be noticed from Figs.9.18 to 9.20 that another line of C IV arising from the 3p -> 3s transition, namely λλ5801, 5812, also shows an increase in intensity as we go from WC8 to WC6 stars. However, our calculations do not show a population inversion for this transition. This may be due to the breakdown of one of the previously mentioned assumptions on which the model calculations are based. Indeed, if we assume that a certain reabsorption of radiation occurs within the plasma (which is probably more realistic for stellar conditions), we find that laser action is possible in this line and in the λ4650 lines.

In conclusion, we find that the C IV λλ4646,4658 lines arising from the 6f → 5d and 6g → 5f transitions respectively, display strong population inversions and should be excellent candidates for producing laser action in laboratory plasmas cooled by adiabatic expansion techniques. In the astrophysical context, the behavior of the line C IV λ4650 observed in the WC category of the Wolf-Rayet stars is found to be in agreement with that expected from the model calculations. The present investigation thus provides an understanding of the unusual strength of the C IV λ4650 emission in Wolf-Rayet stars, and provides a strong basis for believing that laser action is responsible for it. It also raises the possibility that certain other unusually strong emission lines observed in Wolf-Rayet stars may also be due to laser action.

Appendix A

CRITERIA FOR THE APPLICABILITY OF MAXWELL-BOLTZMANN STATISTICS

1. UPPER LIMIT ON n_e

In a plasma of free electron density n_e cm^{-3}, an electron occupies an effective volume of $1/n_e$ cm^3. Representing this volume by a sphere, the average distance between two electrons is given by

$$\bar{d} = \left(\frac{6}{\pi n_e}\right)^{1/3}. \qquad \ldots(A.1)$$

The mean de Broglie wavelength of the electron is obtained from

$$\lambda_{DB} = \frac{h}{m\bar{v}} \qquad \ldots(A.2)$$

where the average velocity of an electron satisfying Maxwell-Boltzmann statistics is given by

$$\bar{v} = \sqrt{\frac{8kT}{\pi m}}. \qquad \ldots(A.3)$$

Maxwell-Boltzmann statistics will apply to free electrons in a plasma if the following condition holds (Vedenov, 1965, p.235):

$$\lambda_{DB} \ll \bar{d}. \qquad \ldots(A.4)$$

Combining eqs.(A.1), (A.2), (A.3), and (A.4), we obtain the condition

$$n_e \ll \frac{6}{\pi h^3}\left(\frac{8\,m\,k\,T}{\pi}\right)^{3/2}. \qquad \ldots(A.5)$$

Numerically,

$$n_e \ll 1.2 \times 10^{15}\ T^{3/2}\ \ cm^{-3}. \qquad \ldots(A.6)$$

This upper limit on n_e is shown graphically in Fig.A.1.

2. LOWER LIMIT ON n_e

The distribution of the free electrons will be Maxwellian if a sufficient number of elastic collisions occurs between them. An expression for the "self-collision time" t_c of a group of particles interacting with each other has been derived by Spitzer (1956, p.78). t_c provides a measure of the time that is required to reduce substantially any lack of isotropy in the velocity distribution of the particles and to allow the distribution of the kinetic energies to approach a Maxwellian distribution. For electrons,

$$t_c = \frac{0.266}{\ell n\,\Lambda}\ \frac{T^{3/2}}{n_e}\ \ sec. \qquad \ldots(A.7)$$

where T is in Kelvin, n_e in cm^{-3}, and Λ is proportional to the number of electrons in a sphere of radius λ_D, the Debye length. $\ell n\,\Lambda$ is sometimes referred to as the Coulomb logarithm. It shows little variation; for most plasma parameters, $5 \leq \ell n\,\Lambda \leq 35$. Tables of $\ell n\,\Lambda$ for collisions of

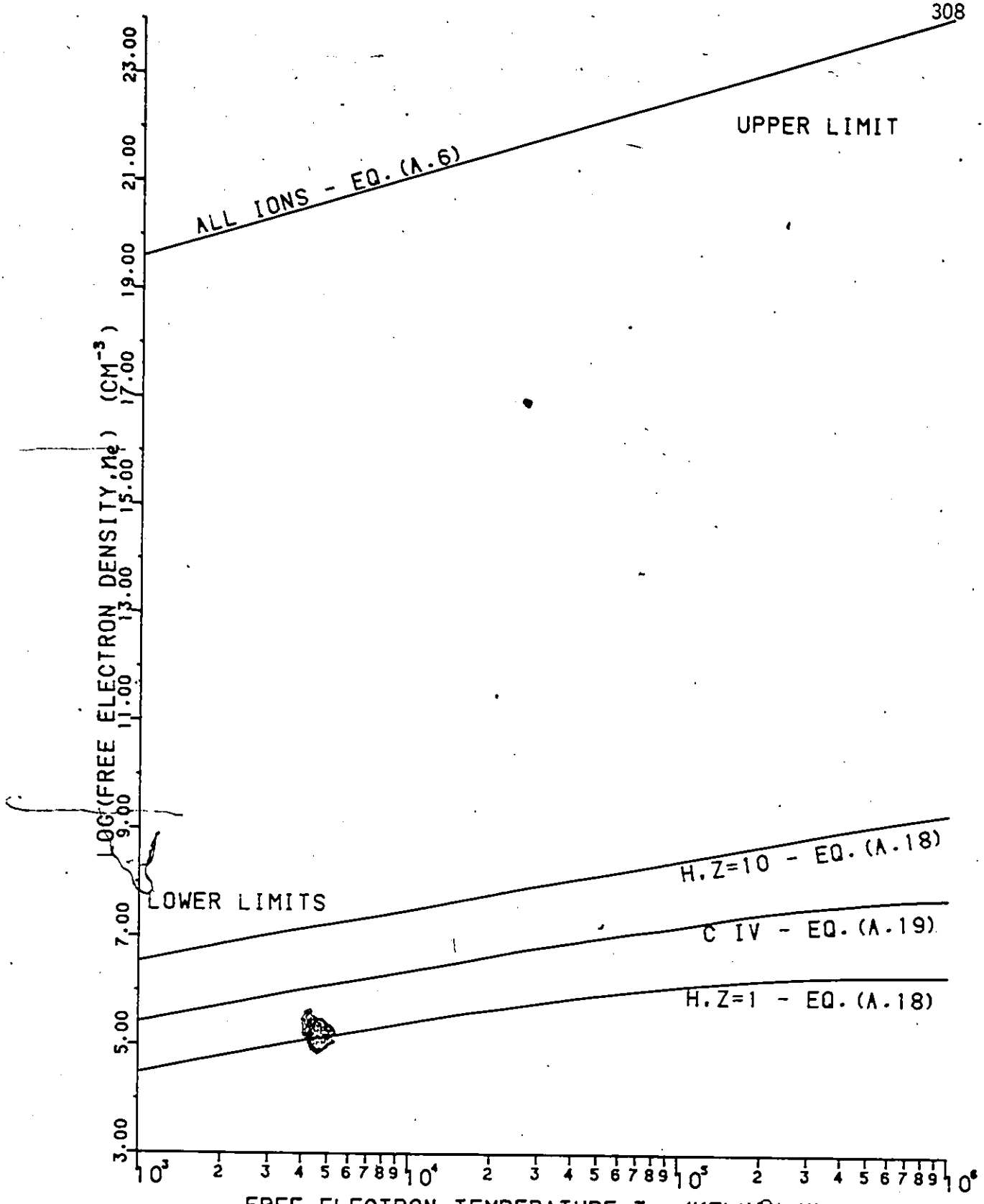

FIGURE A.1 - APPROXIMATE LIMITS OF APPLICABILITY OF MAXWELL-BOLTZMANN STATISTICS TO FREE ELECTRONS IN A PLASMA

electrons and particles of charge +e, corrected for quantum mechanical effects, are given by Spitzer (1956, p.73) and Mitchner and Kruger (1973, p.59).

The lifetime of a free electron in a low density plasma is determined by radiative recombination which predominates over three-body recombination. It is given by (Böhm, 1960, p.97)

$$t_f = \frac{1}{\sigma_{RR}\, n_i} \sqrt{\frac{m}{3kT}} \qquad \ldots(A.8)$$

where σ_{RR} is the cross-section for radiative recombination, n_i is the population density of the ions mainly responsible for electron capture, and all other symbols have their usual meaning.

A Maxwellian distribution will be established if the free electrons undergo sufficient elastic collisions before recombining with an ion. This will occur if

$$t_f \gg t_c . \qquad \ldots(A.9)$$

Substituting eqs.(A.7) and (A.8) in the above, we obtain

$$n_e \gg \frac{0.266}{\ln \Lambda} \sqrt{\frac{3k}{m}}\; T^2 n_i \sigma_{RR}. \qquad \ldots(A.10)$$

The cross-section for radiative recombination into level n, σ_n^{RR}, can be obtained by the principle of detailed balancing (see Section 6 of Chapter II) from the cross-section for photoionization from level n, σ_n^{PI} (Drawin, 1963):

$$\sigma_n^{RR} = \left(\frac{h\nu}{mvc}\right)^2 \frac{\omega_n}{\omega_i}\,\sigma_n^{PI} \qquad \ldots(A.11)$$

where v is the velocity of the free electron, ν the frequency of the emitted or absorbed photon, and all other symbols have their usual meaning. The cross-section for photoionization of a hydrogenic ion of core charge Z from level n is given by (Seaton, 1959)

$$\sigma_n^{PI} = \frac{2^6\alpha}{3\sqrt{3}}\,(hcR)^3\,\pi a_0^2\,\frac{Z^4}{n^5}\,\frac{g_{II}(n,\nu)}{(h\nu)^3} \qquad \ldots(A.12)$$

where $g_{II}(n,\nu)$, the Kramers-Gaunt factor, is of order unity. We put

$$g_{II}(n,\nu) \simeq 1. \qquad \ldots(A.13)$$

Using eqs.(A.11), (A.12), (A.13), $\omega_i = 1$, $\omega_n = 2n^2$, the energy conservation relation

$$h\nu = \tfrac{1}{2} mv^2 + I_n\,, \qquad \ldots(A.14)$$

the ionization potential of level n

$$I_n = hRc\,\frac{Z^2}{n^2}\,, \qquad \ldots(A.15)$$

and the average velocity of the free electron Maxwellian distribution from eq.(A.3), criterion (A.10) becomes

$$n_e \gg \frac{5.83\times10^{-7}}{\ln\Lambda}\,\frac{Z^4}{n^3}\,n_i\,\frac{T}{T + 124{,}000\,Z^2/n^2}\,. \qquad \ldots(A.16)$$

The cross-section for radiative recombination is largest for recombination into the ground state; we thus put

$$n = n_{gd} . \qquad \ldots(A.17)$$

The maximum value of n_i is n_A, the density of element A in the monatomic plasma; in this work, we use $n_A = 10^{14}\ cm^{-3}$.

For hydrogenic ions ($n_{gd} = 1$), eq.(A.16) thus becomes

$$n_e \gg \frac{5.8 \times 10^7}{\ln \Lambda} \quad \frac{Z^4 T}{T + 124{,}000\, Z^2} . \qquad \ldots(A.18)$$

This lower limit on n_e is given graphically in Fig.A.1 for atomic hydrogen and for a hydrogenic ion with Z=10. For lithium-like ions ($n_{gd} = 2$), we obtain

$$n_e \gg \frac{7.3 \times 10^6}{\ln \Lambda} \quad \frac{Z^4 T}{T + 31{,}000\, Z^2} . \qquad \ldots(A.19)$$

This limit is given for C IV in Fig.A.1. For all cases of interest to us, we find that the free electrons satisfy a Maxwellian distribution for $n_e > 10^{10}\ cm^{-3}$.

Appendix B

EVALUATION OF THE PARTITION FUNCTION

The partition function of an X-times ionized atom (ion X) is given by

$$U^{(x)} = \sum_{p=1}^{\infty} \omega_p^{(x)} \, e^{-E_{1p}^{(x)}/kT} \qquad \ldots(B.1)$$

where $\omega_p^{(x)}$ is the statistical weight of level p of ion X and $E_{1p}^{(x)}$ is the energy separation of the ground and p^{th} state of ion X. For $E_{1p}^{(x)}$ in Rydbergs and T in Kelvin,

$$\frac{E_{1p}^{(x)}}{kT} = 157,890 \, \frac{E_{1p}^{(x)}}{T} \, . \qquad \ldots(B.2)$$

For low values of T, eq.(B.1) can then be approximated by the statistical weight of the ground state:

$$U^{(x)} \simeq \omega_1^{(x)} \, . \qquad \ldots(B.3)$$

If the first few excited states are energetically very close to the ground state, they must also be included in the sum (B.1).

As T increases, the exponential term in eq.(B.1) tends to one since $E_{1p}^{(x)}$ remains finite in all cases. $U^{(x)}$ is then proportional to the sum of the statistical weights of all the levels p of ion X. This sum

diverges as p tends to infinity. It must thus be truncated, and this can be done in a number of ways, some of which are mentioned by Griem (1964, p.140). The easiest method is the nearest-neighbour approximation which is used, for example, by Drawin (1970b). It consists in finding the last bound state of ion X, as determined from the maximum physical size the ion can assume in a plasma of density n_A. Assuming circular orbits, and denoting the mean distance between the ions by $\langle d^+ \rangle$, the last bound state is given by

$$p_{max} = \sqrt{\frac{Z \langle d^+ \rangle}{2 a_0}} \qquad \ldots(B.4)$$

where a_0 is the Bohr radius and Z the core charge of the ion. If ion X is the dominant species in the plasma,

$$\langle d^+ \rangle \simeq \left(\frac{6}{\pi n^{(x)}} \right)^{1/3} \qquad \ldots(B.5)$$

for spherical ions; $n^{(x)}$ is the population density of ion X in cm^{-3}. Combining eqs.(B.4) and (B.5), we then obtain

$$p_{max} \simeq \frac{1.08 \times 10^4 \sqrt{Z}}{[n^{(x)}]^{1/6}} \qquad \ldots(B.6)$$

For $n^{(x)} = 10^{14}$ cm^{-3},

$$p_{max} \simeq 50 \sqrt{Z}. \qquad \ldots(B.7)$$

It should be noted that the presence of neighbouring ions will perturb the high-lying quantum states of each ion. Thus the energy eigenvalues and hence the radii of these states will be different from those of an isolated ion. Eq.(B.6) is thus an approximation to the actual last bound state of the ion. It should also be noted that if eq.(B.3) is used for all temperatures, the relative population densities of the levels of ion X obtained from this value of $U^{(x)}$ will be correct for any constant temperature. This is due to the fact that the population densities are all proportional to the same value of $U^{(x)}$ for a given temperature and ionic density. However, the absolute values of the population densities will be in error. We use this last approximation in these calculations.

Appendix C

EVALUATION OF CROSS-SECTION INTEGRALS

1. $\underline{I_1 = \int_a^b \ln x \, e^{-x} \, dx}$ ...(C.1)

To evaluate this integral, we first expand the exponential in a power series:

$$I_1 = \int_a^b \ln x \left[\sum_{n=0}^{\infty} (-1)^n \frac{x^n}{n!} \right] dx. \qquad \text{...(C.2)}$$

Interchanging the order of integration and summation,

$$I_1 = \sum_{n=0}^{\infty} \frac{(-1)^n}{n!} \int_a^b x^n \ln x \, dx. \qquad \text{...(C.3)}$$

From Selby (1970, p.434),

$$I_1 = \sum_{n=0}^{\infty} \frac{(-1)^n}{n!} \left[\frac{x^{n+1}}{n+1} \left(\ln x - \frac{1}{n+1} \right) \right]_a^b \qquad \text{...(C.4)}$$

$$= \ln x \sum_{n=0}^{\infty} (-1)^n \frac{x^{n+1}}{(n+1)!} \Big|_a^b - \sum_{n=0}^{\infty} (-1)^n \frac{x^{n+1}}{(n+1)(n+1)!} \Big|_a^b$$

$$= \ln x \cdot S_1(x) \Big|_a^b - T_1(x) \Big|_a^b . \qquad \text{...(C.5)}$$

We evaluate the series

$$S_1(x) = \sum_{n=0}^{\infty} (-1)^n \frac{x^{n+1}}{(n+1)!} . \qquad \text{...(C.6)}$$

It can be very easily shown to be given by

$$S_1(x) = 1 - e^{-x}. \qquad \ldots(C.7)$$

The other series is

$$T_1(x) = \sum_{n=0}^{\infty} (-1)^n \frac{x^{n+1}}{(n+1)\cdot(n+1)!} \qquad \ldots(C.8)$$

which can be rewritten as

$$T_1(x) = -\sum_{n=1}^{\infty} (-1)^n \frac{x^n}{n\cdot n!}. \qquad \ldots(C.9)$$

From the definition of the exponential integral (Abramowitz and Stegun, 1965, p.229),

$$E_1(x) = -\gamma - \ln x + \sum_{n=1}^{\infty} (-1)^{n+1} \frac{x^n}{n\cdot n!}, \qquad \ldots(C.10)$$

we obtain

$$T_1(x) = \gamma + \ln x + E_1(x) \qquad \ldots(C.11)$$

where $\gamma = 0.5772156649$ is Euler's constant. Substituting for $S_1(x)$ and $T_1(x)$ from eqs.(C.7) and (C.11) respectively, eq.(C.5) becomes

$$I_1 = e^{-a} \ln a - e^{-b} \ln b + E_1(a) - E_1(b). \qquad \ldots(C.12)$$

In particular,

$$\int_a^\infty \ln x\, e^{-x}\, dx = e^{-a} \ln a + E_1(a). \qquad \ldots(C.13)$$

2. $\underline{I_2 = \int_a^b \ln x / x\; e^{-x}\, dx}$ $\qquad \ldots(C.14)$

Expanding the exponential in a power series, and interchanging the order of integration and summation, we obtain

$$I_2 = \sum_{n=0}^{\infty} \frac{(-1)^n}{n!} \int_a^b x^{n-1} \ln x\, dx$$

$$= \int_a^b \frac{\ln x}{x} dx + \sum_{n=1}^{\infty} \frac{(-1)^n}{n!} \int_a^b x^{n-1} \ln x\, dx. \qquad \ldots(C.15)$$

From Selby (1970, p.434),

$$I_2 = \frac{1}{2} \ln^2 x \Big|_a^b + \sum_{n=1}^{\infty} \frac{(-1)^n}{n!} \left[\frac{x^n}{n} \left(\ln x - \frac{1}{n} \right) \right]_a^b$$

$$= \frac{1}{2} \ln^2 x \Big|_a^b + \ln x\, S_2(x) \Big|_a^b - T_2(x) \Big|_a^b \qquad \ldots(C.16)$$

where $S_2(x) = \sum_{n=1}^{\infty} (-1)^n \frac{x^n}{n \cdot n!}$ $\qquad \ldots(C.17)$

$$T_2(x) = \sum_{n=1}^{\infty} (-1)^n \frac{x^n}{n^2 \cdot n!}. \qquad \ldots(C.18)$$

From eq.(C.10),

$$S_2(x) = -\gamma - \ln x - E_1(x). \qquad \ldots(C.19)$$

The series (C.18) is evaluated by first differentiating it with respect to x:

$$\frac{dT_2(x)}{dx} = \sum_{n=1}^{\infty} (-1)^n \frac{x^{n-1}}{n \cdot n!} . \qquad \ldots(C.20)$$

From eq.(C.10),

$$\frac{dT_2(x)}{dx} = -\frac{1}{x}\left[\gamma + \ln x + E_1(x)\right]. \qquad \ldots(C.21)$$

Integrating this equation, we obtain

$$T_2(x) = -\gamma \ln x - \frac{1}{2}\ln^2 x - \int^x \frac{E_1(t)}{t}\,dt + C_1 \qquad \ldots(C.22)$$

where C_1 is a constant of integration. The lower limit of integration of the integral of eq.(C.22) is chosen such that its constant of integration is zero, and its contribution to C_1 is also zero. The lower limit $t \to \infty$ satisfies this condition; eq.(C.22) thus becomes

$$T_2(x) = -\gamma \ln x - \frac{1}{2}\ln^2 x + \int_x^{\infty} \frac{E_1(t)}{t}\,dt + C_1 . \qquad \ldots(C.23)$$

It is not necessary to evaluate C_1 since we are interested in the difference $T_2(b) - T_2(a)$. Substituting eqs.(C.19) and (C.23) in eq.(C.16), we obtain

$$I_2 = \Big[\frac{1}{2}\ln^2 x - \ln x\left(\gamma + \ln x + E_1(x)\right)$$

$$+ \gamma \ln x + \frac{1}{2}\ln^2 x - \epsilon_1(x) - C_1\Big]_a^b \qquad \ldots(C.24)$$

where $\epsilon_1(x) = \int_x^\infty \frac{E_1(t)}{t}\, dt$. ...(C.25a)

Thus

$$I_2 = E_1(a) \ln a - E_1(b) \ln b + \epsilon_1(a) - \epsilon_1(b), \quad \text{...(C.26)}$$

and, in particular,

$$\int_a^\infty \frac{\ln x}{x} e^{-x}\, dx = \ln a\, E_1(a) + \epsilon_1(a). \quad \text{...(C.27)}$$

3. $\epsilon_1(\theta) = \int_\theta^\infty E_1(x)/x\, dx$ ...(C.25b)

3.1. Analytical approximations

This integral cannot be evaluated analytically since $E_1(x)$ has no closed analytical form. However, if approximate expressions are used to represent $E_1(x)$ in integral (C.25b), approximate analytical expressions can be obtained for $\epsilon_1(\theta)$. We use the following analytical approximations to represent $E_1(x)$ (Abramowitz and Stegun, 1965, p.231):

$0 \leq x \leq 1$:

$$E_1(x) \simeq \sum_{n=0}^{5} a_n x^n - \ln x + \varepsilon(x) \quad \text{...(C.28)}$$

where $a_0 = -0.57721566$

$a_1 = 0.99999193$

$a_2 = -0.24991055$

$a_3 = 0.05519968$

$a_4 = -0.00976004$

$a_5 = 0.00107857$

$|\varepsilon(x)| < 2 \times 10^{-7}$.

$1 \leq x \leq 10$:

$$E_1(x) \simeq \frac{e^{-x}}{x} \frac{x^2 + ax + b}{x^2 + cx + d} + \frac{e^{-x}}{x} \varepsilon(x) \qquad \ldots(C.29)$$

where $a = 2.334733$

$b = 0.250621$

$c = 3.330657$

$d = 1.681534$

$|\varepsilon(x)| < 5 \times 10^{-5}$.

$x \geq 10$:

We use eq.(C.29) with the following parameters:

$a = 4.03640$

$b = 1.15198$

$c = 5.03637$

$d = 4.19160$

$|\varepsilon(x)| < 10^{-7}$.

This approximation is labelled eq.(C.30).

Eq.(C.25b) is then evaluated as follows:

$0 \leq \theta \leq 1$:

$$\epsilon_1(\theta) \simeq \int_\theta^1 \frac{\text{eq.(C.28)}}{x}\, dx + \epsilon_1(1)\ ; \qquad \ldots(C.31)$$

$1 \leq \theta \leq 10$:

$$\epsilon_1(\theta) \simeq \int_\theta^{10} \frac{\text{eq.(C.29)}}{x}\, dx + \epsilon_1(10)\ ; \qquad \ldots(C.32)$$

$\theta \geq 10$:

$$\epsilon_1(\theta) \simeq \int_\theta^{\infty} \frac{\text{eq.(C.30)}}{x}\, dx. \qquad \ldots(C.33)$$

$\epsilon_1(1)$ and $\epsilon_1(10)$ used in eqs.(C.31) and (C.32) respectively must be known to an accuracy comparable to that of the integral to which they are added to.

3.2. Evaluation of the integrals

$0 \leq \theta \leq 1$:

$$\int_\theta^1 \frac{\text{eq.(C.28)}}{x}\, dx = \int_\theta^1 \sum_{n=0}^{5} a_n x^{n-1}\, dx - \int_\theta^1 \frac{\ln x}{x}\, dx$$

$$= \left[a_0 \ln x + \sum_{n=1}^{5} \frac{a_n}{n} x^n - \frac{1}{2} \ln^2 x \right]_\theta^1$$

$$= A + \frac{1}{2} \ln^2 \theta - a_0 \ln \theta - \sum_{n=1}^{5} \frac{a_n}{n} \theta^n \qquad \ldots(C.34)$$

where $A = \sum_{n=1}^{5} \frac{a_n}{n} = 0.89121224.$ $\qquad \ldots(C.35)$

$\theta \geq 10$:

Equations (C.32) and (C.33) involve the evaluation of the same integral over different limits of integration. We first evaluate the integral (C.33):

$$\int_\theta^\infty \frac{\text{eq.(c.30)}}{x}\, dx = \int_\theta^\infty \frac{e^{-x}}{x^2}\, \frac{x^2+ax+b}{x^2+cx+d}\, dx. \qquad \ldots(C.36)$$

We rewrite eq.(C.36) to get

$$\epsilon_1(\theta) \propto \int_\theta^\infty \frac{x^2+ax+b}{x^2(x+\alpha)(x+\beta)}\, e^{-x}\, dx \qquad \ldots(C.37)$$

where $-\alpha$ and $-\beta$ are the roots of x^2+cx+d, α and $\beta > 0$, $\alpha < \beta$, and

$$\alpha = \frac{c}{2} - \sqrt{\left(\frac{c}{2}\right)^2 - d}$$

$$\beta = \frac{c}{2} + \sqrt{\left(\frac{c}{2}\right)^2 - d}\,. \qquad \ldots(C.38)$$

Separating the denominator of the R.H.S. of eq.(C.37) by partial fractions, we obtain

$$\frac{x^2+ax+b}{x^2(x+\alpha)(x+\beta)} = \frac{c_1}{x+\alpha} + \frac{c_2}{x+\beta} + \frac{c_3}{x} + \frac{c_4}{x^2} \qquad \ldots(C.39)$$

where

$$c_1 = \frac{\alpha^2 - \alpha a + b}{\alpha^2(\beta-\alpha)}$$

$$c_2 = -\frac{\beta^2 - \beta a + b}{\beta^2(\beta-\alpha)}$$

$$c_3 = \frac{a}{\alpha\beta} - \frac{(\alpha+\beta)\,b}{\alpha^2\beta^2}$$

$$c_4 = \frac{b}{\alpha\beta}\,.$$

Substituting eq.(C.39) in eq.(C.37), and using the following integrals (Abramowitz and Stegun, 1965, pp.228-230)

$$\int_\theta^\infty \frac{e^{-x}}{x+\alpha}\,dx = e^{\alpha}\,E_1(\theta+\alpha)$$

$$\int_\theta^\infty \frac{e^{-x}}{x^2}\,dx = \frac{e^{-\theta}}{\theta} - E_1(\theta), \qquad \ldots(C.40)$$

we obtain

$$\int_\theta^\infty \frac{\text{eq.(C.30)}}{x}\,dx = d_1 E_1(\alpha+\theta) + d_2 E_1(\beta+\theta) + d_3 E_1(\theta) + d_4 \frac{e^{-\theta}}{\theta} \qquad \ldots(C.41)$$

where

$$d_1 = c_1 e^{\alpha}$$

$$d_2 = c_2 e^{\beta}$$

$$d_3 = c_3 - \frac{b}{\alpha\beta}$$

$$d_4 = c_4\,.$$

From the values of a, b, c, and d of eq.(C.30), the following numerical values of the parameters are obtained:

α = 1.0520153

β = 3.9843540

$d_1 = -1.7537327$

$d_2 = -1.0907011$

$d_3 = 0.35792351$

$d_4 = 0.27483028.$ ...(C.42)

$1 \leq \theta < 10$:

Integral (C.32) is now evaluated as follows:

$$\int_\theta^\infty \frac{\text{eq.(C.29)}}{x}\,dx = \int_\theta^\infty \frac{\text{eq.(C.29)}}{x}\,dx - \int_{10}^\infty \frac{\text{eq.(C.29)}}{x}\,dx. \quad \ldots(C.43)$$

Since eq.(C.29) has the same analytical form as eq.(C.30), we use eq.(C.41) with the following parameters to evaluate eq.(C.43):

$\alpha = 0.62044334$

$\beta = 2.7102127$

$d_1 = -1.8794966$

$d_2 = -1.2420263$

$d_3 = 0.94419706$

$d_4 = 0.14904308.$ ...(C.44)

Then eq.(C.43) becomes

$$\int_\theta^{10} \frac{\text{eq.(C.29)}}{x}\,dx = d_1 E_1(\alpha+\theta) + d_2 E_1(\beta+\theta)$$

$$+ d_3 E_1(\theta) + d_4 \frac{e^{-\theta}}{\theta} - B \quad \ldots(C.45)$$

where $B = d_1 E_1(\alpha+10) + d_2 E_1(\beta+10) + d_3 E_1(10) + d_4 \frac{e^{-10}}{10}$

$$B = 0.35280 \times 10^{-6}. \qquad \ldots(C.46)$$

3.3. Accurate evaluation of $\epsilon_1(1)$ and $\epsilon_1(10)$

The values of $\epsilon_1(1)$ and $\epsilon_1(10)$ required in the evaluation of eqs.(C.31) and (C.32) can be calculated to any desired accuracy by numerical integration. We obtain these indirectly by first evaluating the function $G(1,\theta)$ defined in Section 4 of Chapter II with numerical integration. The values of $\epsilon_1(\theta)$ can then be obtained from eq.(2.35). This procedure gives the values

$$\epsilon_1(1) = 0.978432 \times 10^{-1}$$

$$\epsilon_1(10) = 0.35277326 \times 10^{-6}. \qquad \ldots(C.47)$$

3.4. Accuracy of the approximations (C.31), (C.32), and (C.33)

The accuracy of these approximations depends on the accuracy of the analytical approximations used to represent $E_1(x)$, eqs.(C.28), (C.29), and (C.30). The maximum accuracy that can be obtained is thus $|\varepsilon(x)|$. The actual accuracy is smaller than this value because the approximation is integrated over $x = \theta \to \infty$ to obtain $\epsilon_1(\theta)$.

We study each approximation separately.

$0 \leq \theta \leq 1$:

From eq.(C.28),

$$|\mathcal{E}(x)| < 2 \times 10^{-7}.$$

Since this is the error in $E_1(x)$, the error in $\epsilon_1(\theta)$ will be greater for the smallest value of $\epsilon_1(\theta)$ within the range $0 \leq \theta \leq 1$. This value occurs at $\theta = 1$. We then obtain

$$\epsilon_1(1) = 0.0978432$$

by numerical integration, and

$$\epsilon_1(1) = 0.0978432$$

from the approximate expression (C.31). The smallest error estimate

$$|\Delta \epsilon_1| \sim 2 \times 10^{-7} \qquad \ldots(C.48)$$

is thus reasonable in this case. This gives an accuracy of at least 5-6S.

$1 \leq \theta \leq 10$:

From eq.(C.29),

$$|\mathcal{E}(x)| < 5 \times 10^{-5}$$

and the error in $E_1(x)$ is given by

$$|\Delta E_1(x)| < 5 \times 10^{-5} \frac{e^{-x}}{x}. \qquad \ldots(C.49)$$

For large x,

$$E_1(x) \sim \frac{e^{-x}}{x} , \qquad \ldots(C.50)$$

and we have

$$\left|\frac{\Delta E_1(x)}{E_1(x)}\right| \lesssim 5 \times 10^{-5}. \qquad \ldots(C.51)$$

For x = 1, eq.(C.50) is not a very good representation of $E_1(x)$, and the evaluation of the ratio (C.51) from eqs.(C.49) and (C.29) yields

$$\left|\frac{\Delta E_1(1)}{E_1(1)}\right| < 8 \times 10^{-5}. \qquad \ldots(C.52)$$

The largest uncertainty of eq.(C.32) will occur for $\theta = 1$ since the range of integration $x = \theta \to \infty$ for $1 \leq \theta \leq 10$ is then at its maximum extent. The value (C.52) can then be taken to be the minimum value of

$$\left|\frac{\Delta \epsilon_1(x)}{\epsilon_1(x)}\right| \gtrsim 8 \times 10^{-5}. \qquad \ldots(C.53)$$

The maximum accuracy obtainable with eq.(C.32) is thus 4S. Evaluating $\epsilon_1(1)$ and $\epsilon_1(10)$ with eq.(C.32), and comparing these with the values (C.47) obtained by numerical integration, we do obtain an accuracy of 4S over the range $1 \leq \theta \leq 10$.

$\theta \geq 10$:

From eq.(C.30),

$$|\mathcal{E}(x)| < 10^{-7},$$

and the error in $E_1(x)$ is given by

$$|\Delta E_1(x)| < 10^{-7}\frac{e^{-x}}{x} \qquad \ldots(C.54)$$

Following the reasoning of eqs.(C.49) to (C.53), the minimum value of $|\Delta\epsilon_1(x)| / \epsilon_1(x)$ is

$$\left|\frac{\Delta\epsilon_1(x)}{\epsilon_1(x)}\right| \gtrsim 10^{-7}. \qquad \ldots(C.55)$$

By evaluating $\epsilon_1(\theta)$ with eq.(C.33), and comparing these values with the more accurate ones obtained by numerical integration or by eq.(C.60), we obtain the actual accuracy of eq.(C.33):

θ	Accuracy
10	6S
100	5S
200	4S
1000	3S

...(C.56)

As θ increases, the accuracy of eq.(C.33) decreases; however, since we consider values of $\theta \lesssim 100$ in this work, eq.(C.33), for this range of values of θ, has an accuracy of 5S.

4. THE FUNCTION $\epsilon_1'(\theta)$

For large values of θ, it is easier to evaluate the function

$$\epsilon_1'(\theta) = e^{\theta}\,\epsilon_1(\theta) \qquad \ldots(C.57)$$

Using the analytical expression (C.41) in eq.(C.33), and substituting in the above equation, we obtain

$$\epsilon_1'(\theta) = d_1 e^{\theta} E_1(\alpha+\theta) + d_2 e^{\theta} E_1(\beta+\theta)$$

$$+ d_3 e^{\theta} E_1(\theta) + \frac{d_4}{\theta} \qquad \ldots(C.58)$$

where α, β, d_1, d_2, d_3, and d_4 are given by eq.(C.42), and

$$e^{\theta} E_1(\theta+r) \simeq \frac{e^{-r}}{\theta+r}\left[1 - \frac{1!}{\theta+r} + \frac{2!}{(\theta+r)^2} - + \cdots\right]. \qquad \ldots(C.59)$$

However, as θ increases, the accuracy of eq.(C.33), and hence of eq.(C.58), decreases. It is then preferable to evaluate $\epsilon_1(\theta)$ by substituting the asymptotic expansion of the exponential integral (eq.C.59 with $r = 0$) in eq.(C.25b). We then obtain

$$\epsilon_1'(\theta) \simeq \frac{1}{\theta^2}\left[1 - (1+\tfrac{1}{2})\frac{2!}{\theta}\right.$$

$$\left. + (1+\tfrac{1}{2}+\tfrac{1}{3})\frac{3!}{\theta^2} - + \cdots\right]. \qquad \ldots(C.60)$$

For sufficiently large values of θ, this equation can be evaluated to any desired accuracy by including more terms in the sum. This expression was used to evaluate $\epsilon_1'(200)$ and $\epsilon_1'(1000)$ to estimate the accuracy of approximation (C.33) at large values of θ.

Appendix D

LEAST SQUARES FITS

1. THE METHOD

Suppose that a finite number n of data points $y_i = y(x_i)$, $i = 1, 2, \ldots, n$ are the values of an unknown function $y(x)$ at the points x_i, $i = 1, 2, \ldots, n$. We approximate the function $y(x)$ by a function $f(x)$ which is a function of m adjustable parameters a_k, $k = 1, 2, \ldots, m$:

$$f(x; a_1, a_2, \ldots, a_m) \simeq y(x). \qquad \ldots(D.1)$$

At the points x_i, the function $f(x)$ has the values $f_i = f(x_i)$, $i = 1, 2, \ldots, n$. Defining the residuals

$$R_i = y_i - f_i \; ; \; i = 1, 2, \ldots, n, \qquad \ldots(D.2)$$

the values of the parameters a_k can be evaluated within the least squares approximation by requiring that

$$\sum_{i=1}^{n} R_i^2 = \sum_{i=1}^{n} (y_i - f_i)^2 \qquad \ldots(D.3)$$

be a minimum. This requirement imposes the conditions

$$\frac{\partial}{\partial a_k} \left[\sum_{i=1}^{n} R_i^2 \right] = 0 \; ; \; k = 1, 2, \ldots, m \qquad \ldots(D.4)$$

which can be rewritten as

$$\sum_{i=1}^{n} R_i \frac{\partial R_i}{\partial a_k} = 0 \; ; \; k = 1, 2, \ldots, m$$

or $$\sum_{i=1}^{n} (y_i - f_i) \frac{\partial f_i}{\partial a_k} = 0 \; ; \; k = 1, 2, \ldots, m. \qquad \ldots(D.5)$$

These conditions minimize the difference between the actual values y_i and the approximate values f_i of the function $y(x)$ at the points x_i.

However, if $y(x)$ varies over several orders of magnitude, the approximation $f(x)$ will not have the same relative accuracy for all values of $y(x)$: it will be less accurate for small values of $y(x)$. In such cases, it is better to consider the relative residuals

$$r_i = \frac{y_i - f_i}{y_i} \; ; \; i = 1, 2, \ldots, n. \qquad \ldots(D.6)$$

Requiring that

$$\sum_{i=1}^{n} r_i^2 = \sum_{i=1}^{n} \left(\frac{y_i - f_i}{y_i} \right)^2 \qquad \ldots(D.7)$$

be a minimum, we obtain the conditions

$$\sum_{i=1}^{n} r_i \frac{\partial r_i}{\partial a_k} = 0 \; ; \; k = 1, 2, \ldots, m$$

or $$\sum_{i=1}^{n} \frac{1}{y_i} \left(1 - \frac{f_i}{y_i} \right) \frac{\partial f_i}{\partial a_k} = 0 \; ; \; k = 1, 2, \ldots, m. \qquad \ldots(D.8)$$

The minimization conditions (D.5) or (D.8) are solved for the fit parameters a_k.

2. EXTRAPOLATION OF THE QUANTUM DEFECTS

We use the notation of Chapter III. We have N known values of ϵ_n, $n = 1, 2, \ldots, N$ which are calculated from the quantum defects $\mu_n = \mu(\epsilon_n)$ with eq.(3.7). These values satisfy the expression (3.20):

$$Tan(\pi \mu_{n\ell}) = A_\ell(\epsilon_n)\, Y_\ell(\epsilon_n) \qquad \ldots(D.9)$$

where $A_\ell(\epsilon_n)$ is calculated with eq.(3.10) and $Y_\ell(\epsilon_n)$ is given by eq.(3.17):

$$Y_\ell(\epsilon_n) = \sum_{i=0}^{p} \alpha_i \epsilon_n^i \;/\; \left[1 + \sum_{m=1}^{q} \beta_m \epsilon_n^m\right] \qquad \ldots(D.10)$$

where α_i, $i = 0, 1, \ldots, p$ and β_m, $m = 1, 2, \ldots, q$ are the fit parameters. We rewrite eq.(D.9) as

$$G_\ell(\epsilon_n) = Y_\ell(\epsilon_n) \qquad \ldots(D.11)$$

where $$G_\ell(\epsilon_n) = \frac{Tan(\pi \mu_{n\ell})}{A_\ell(\epsilon_n)} . \qquad \ldots(D.12)$$

can be evaluated from the known values of ϵ_n. We thus approximate the function $G_\ell(\epsilon_n)$ with the function $Y_\ell(\epsilon_n)$. To simplify the evaluation of the fit parameters, we rewrite eqs.(D.10) and (D.11) as

$$\sum_{i=0}^{p} \alpha_i \epsilon_n^i - G_\ell(\epsilon_n) \sum_{m=1}^{q} \beta_m \epsilon_n^m = G_\ell(\epsilon_n) \qquad \ldots(D.13)$$

and we say that we approximate the values of $G_\ell(\epsilon_n)$ with the L.H.S. of eq.(D.13). The residuals are then given by

$$R_n = G_\ell(\epsilon_n) - \sum_{i=0}^{p} \alpha_i \epsilon_n^i + G_\ell(\epsilon_n) \sum_{m=1}^{q} \beta_m \epsilon_n^m \; ; \; n = 1, 2, \ldots, N \qquad \ldots(D.14)$$

and the required derivatives by

$$\frac{\partial R_n}{\partial \alpha_k} = -\epsilon_n^k \; ; \; k = 0, 1, \ldots, p \; ;$$

$$\frac{\partial R_n}{\partial \beta_j} = G_\ell(\epsilon_n) \epsilon_n^j \; ; \; j = 1, 2, \ldots, q. \qquad \ldots(D.15)$$

From eq.(D.5), the minimization conditions are then given by

$$\alpha_k : \sum_{n=1}^{N} \left\{ \sum_{i=0}^{p} \alpha_i \epsilon_n^i - G_\ell(\epsilon_n) \sum_{m=1}^{q} \beta_m \epsilon_n^m - G_\ell(\epsilon_n) \right\} \epsilon_n^k = 0 \; ; \; k = 0, 1, \ldots, p \; ;$$

$$\beta_j : \sum_{n=1}^{N} \left\{ \sum_{i=0}^{p} \alpha_i \epsilon_n^i - G_\ell(\epsilon_n) \sum_{m=1}^{q} \beta_m \epsilon_n^m - G_\ell(\epsilon_n) \right\} G_\ell(\epsilon_n) \epsilon_n^j = 0 \; ; \; j = 1, 2, \ldots, q. \qquad \ldots(D.16)$$

which become

$$\alpha_k : \sum_{i=0}^{p} \left[\sum_{n=1}^{N} \epsilon_n^{i+k} \right] \alpha_i - \sum_{m=1}^{q} \left[\sum_{n=1}^{N} G_\ell(\epsilon_n)\, \epsilon_n^{m+k} \right] \beta_m$$

$$= \left[\sum_{n=1}^{N} G_\ell(\epsilon_n)\, \epsilon_n^{k} \right]; \; k = 0, 1, \ldots, p;$$

$$\beta_j : \sum_{i=0}^{p} \left[\sum_{n=1}^{N} \epsilon_n^{i+j} \right] \alpha_i - \sum_{m=1}^{q} \left[\sum_{n=1}^{N} G_\ell^2(\epsilon_n)\, \epsilon_n^{m+j} \right] \beta_m$$

$$= \left[\sum_{n=1}^{N} G_\ell^2(\epsilon_n)\, \epsilon_n^{j} \right]; \; j = 1, 2, \ldots, q. \qquad \ldots(D.17)$$

We thus obtain a set of p+q+1 linear equations which can easily be solved for the p+q+1 fit parameters.

3. PHOTOIONIZATION CROSS-SECTIONS

We use the notation of Chapter VIII. The photoionization cross-section data $a_i(U_i)$, i = 1, 2, ..., n are fitted to an expression of the form (eq.8.11)

$$a_i(u_i) = \frac{C}{u_i^P} \left[1 + \frac{b_1}{u_i} + \frac{b_2}{u_i^2} + \cdots + \frac{b_m}{u_i^m} \right] \qquad \ldots(D.18)$$

where C and b_k, k = 1, 2, ..., m are the fit parameters. We rewrite this equation as

$$a_i(u_i) = \sum_{k=0}^{m} \frac{d_k}{u_i^{k+P}} \qquad \ldots(D.19)$$

where $d_o = c$

$$d_k = c\, b_k \quad ; k = 1, 2, \ldots, m.$$

Since the cross-section varies over several orders of magnitude, relative residuals are used in this fit:

$$r_i = 1 - \sum_{k=0}^{m} \frac{d_k}{a_i\, u_i^{k+p}} \quad ; \; i = 1, 2, \ldots, n. \qquad \ldots(D.20)$$

The required derivatives are given by

$$\frac{\partial r_i}{\partial d_j} = \frac{-1}{a_i\, u_i^{j+p}} \quad ; j = 0, 1, \ldots, n. \qquad \ldots(D.21)$$

From eq.(D.8), the minimization conditions are

$$\sum_{i=1}^{n} \left[1 - \sum_{k=0}^{m} \frac{d_k}{a_i\, u_i^{k+p}} \right] \frac{1}{a_i\, u_i^{j+p}} = 0 \; ;$$

$$j = 0, 1, \ldots, m \; ; \qquad \ldots(D.22)$$

which can be rewritten as

$$\sum_{k=0}^{m} \left[\sum_{i=1}^{n} \frac{1}{a_i^2\, u_i^{k+2p+j}} \right] d_k = \sum_{i=1}^{n} \frac{1}{a_i\, u_i^{p+j}} \; ;$$

$$j = 0, 1, \ldots, m. \qquad \ldots(D.23)$$

We thus have a set of m+1 linear equations which can be easily solved for the m+1 fit parameters.

4. COLLISIONAL EXCITATION CROSS-SECTIONS

We use the notation of Chapter VI. Since we are dealing with cross-sections, we again use relative residuals. We have two different expressions for optically allowed and forbidden transitions.

4.1. Allowed transitions

The collisional excitation cross-section data $\sigma_i(U_i)$, i = 1, 2, ..., n are fitted to an expression of the form (eq.6.6)

$$\sigma_i(u_i) = k\alpha \frac{u_i - \phi}{u_i^2} \ln(1.25\beta u_i) \qquad \ldots(D.24)$$

where α, β, and ϕ are the fit parameters. The relative residuals are given by

$$r_i = 1 - \frac{k\alpha}{\sigma_i} \frac{u_i - \phi}{u_i^2} \ln(1.25\beta u_i);$$

$$i = 1, 2, \ldots, n \qquad \ldots(D.25)$$

and the required derivatives by

$$\frac{\partial r_i}{\partial \alpha} = -\frac{k}{\sigma_i} \frac{u_i - \phi}{u_i^2} \ln(1.25\beta u_i)$$

$$\frac{\partial r_i}{\partial \beta} = -\frac{k\alpha}{\sigma_i} \frac{u_i - \phi}{u_i^2} \frac{1}{\beta}$$

$$\frac{\partial r_i}{\partial \phi} = \frac{k\alpha}{\sigma_i u_i^2} \ln(1.25\beta u_i). \qquad \text{...(D.26)}$$

From eq.(D.8), the minimization conditions are

$$\alpha: \sum_{i=1}^{n} \left[1 - \frac{k\alpha}{\sigma_i} \frac{u_i - \phi}{u_i^2} \ln(1.25\beta u_i) \right] \times \frac{u_i - \phi}{\sigma_i u_i^2} \ln(1.25\beta u_i) = 0$$

$$\beta: \sum_{i=1}^{n} \left[1 - \frac{k\alpha}{\sigma_i} \frac{u_i - \phi}{u_i^2} \ln(1.25\beta u_i) \right] \times \frac{u_i - \phi}{\sigma_i u_i^2} = 0$$

$$\phi: \sum_{i=1}^{n} \left[1 - \frac{k\alpha}{\sigma_i} \frac{u_i - \phi}{u_i^2} \ln(1.25\beta u_i) \right] \times \frac{\ln(1.25\beta u_i)}{\sigma_i u_i^2} = 0 \qquad \text{...(D.27)}$$

which can be rewritten as

$$\alpha = \left\{ \sum_{i=1}^{n} \frac{u_i - \phi}{\sigma_i u_i^2} \ln(1.25\beta u_i) \right\} \Big/ \left\{ k \sum_{i=1}^{n} \left[\frac{u_i - \phi}{\sigma_i u_i^2} \ln(1.25\beta u_i) \right]^2 \right\} \qquad \text{...(D.28)}$$

$$\ln\beta = \left\{ \sum_{i=1}^{n} \frac{u_i - \phi}{\sigma_i u_i^2} \left[\frac{1}{k\alpha} - \frac{u_i - \phi}{\sigma_i u_i^2} \ln(1.25 u_i) \right] \right\} \Big/ \left\{ \sum_{i=1}^{n} \left[\frac{u_i - \phi}{\sigma_i u_i^2} \right]^2 \right\} \qquad \text{...(D.29)}$$

$$\phi = \left\{ \sum_{i=1}^{n} \frac{\ln(1.25\beta u_i)}{\sigma_i u_i^2} \left[\frac{\ln(1.25\beta u_i)}{\sigma_i u_i} - \frac{1}{k\alpha} \right] \right\}$$

$$/\left\{\sum_{i=1}^{n}\left[\frac{\ln(1.25\,\beta u_i)}{\sigma_i u_i^2}\right]^2\right\}. \qquad \ldots(D.30)$$

These three equations are solved by an iterative procedure: from an initial estimate of α_0 and β_0, ϕ_0 is calculated with eq.(D.30); from β_0 and ϕ_0, α_1 is calculated with eq.(D.28); from ϕ_0 and α_1, β_1 is calculated with eq.(D.29). This procedure is repeated until sufficient accuracy is attained.

4.2. Forbidden transitions

The collisional excitation cross-section data $\sigma_i(U_i)$, $i = 1, 2, \ldots, n$ are fitted to an expression of the form (eq.6.11)

$$\sigma_i(u_i) = k\alpha\,\frac{u_i - \phi}{u_i^2} \qquad \ldots(D.31)$$

where α and ϕ are the fit parameters. Using relative residuals, and following the steps of eqs.(D.24) to (D.30), the minimization conditions can be easily shown to be

$$\alpha = \left\{\sum_{i=1}^{n}\frac{u_i-\phi}{\sigma_i u_i^2}\right\} / \left\{k\sum_{i=1}^{n}\left[\frac{u_i-\phi}{\sigma_i u_i^2}\right]^2\right\} \qquad \ldots(D.32)$$

$$\phi = \left\{\sum_{i=1}^{n}\frac{1}{\sigma_i u_i^2}\left[\frac{1}{\sigma_i u_i} - \frac{1}{k\alpha}\right]\right\} / \left\{\sum_{i=1}^{n}\left[\frac{1}{\sigma_i u_i^2}\right]^2\right\}. \qquad \ldots(D.33)$$

Again, these two equations are solved by an iterative procedure: from an initial estimate of ϕ_0, α_0 is calculated with eq.(D.32), and substituted in eq.(D.33) to obtain ϕ_1. This procedure is repeated until sufficient accuracy is attained.

Appendix E

CALCULATION OF THE GAUNT FACTOR g

A more accurate expression than g = 1 is obtained for the Gaunt factor by transforming eq.(2.8) to the form of eq.(2.12). With eq.(2.11), the two hypergeometric functions of eq.(2.8) can be expressed as polynomials:

$$ {}_2F_1\left(-n', -n+1; 1; -\frac{4nn'}{(n-n')^2}\right) $$

$$ = \sum_{k=0}^{n'} \frac{(-1)^k}{k!^2} \frac{n'!}{(n'-k)!} \frac{(n-1)!}{(n-1-k)!} \left[\frac{4nn'}{(n-n')^2}\right]^k ; \qquad \ldots(E.1) $$

$$ {}_2F_1\left(-n'+1, -n; 1; -\frac{4nn'}{(n-n')^2}\right) $$

$$ = \sum_{k=0}^{n'-1} \frac{(-1)^k}{k!^2} \frac{(n'-1)!}{(n'-1-k)!} \frac{n!}{(n-k)!} \left[\frac{4nn'}{(n-n')^2}\right]^k . \qquad \ldots(E.2) $$

For large n and n', these series are dominated by the last terms and we thus evaluate them by carrying out the summation in the reverse direction, starting with the last term. Using $\Delta = n-n'$, eqs.(E.1) and (E.2) become:

$$ {}_2F_1\left(-n', -n+1; 1; -\frac{4nn'}{\Delta^2}\right) $$

$$ = (-1)^{n'} \frac{(n-1)!}{(\Delta-1)!\, n'!} \left(\frac{4nn'}{\Delta^2}\right)^{n'} \gamma_1(n', n) \qquad \ldots(E.3) $$

where

$$\gamma_1(n',n) = 1 - \left(\frac{\Delta}{4}\frac{n'}{n}\right) + \frac{1}{2!}\frac{\Delta}{\Delta+1}\frac{(n'-1)^2}{n'^2}\left(\frac{\Delta}{4}\frac{n'}{n}\right)^2 - \frac{1}{3!}\frac{\Delta^2}{(\Delta+1)(\Delta+2)}\frac{(n'-1)^2(n'-2)^2}{n'^4}\left(\frac{\Delta}{4}\frac{n'}{n}\right)^3 + \cdots ; \quad \ldots(E.4)$$

$$2F_1\left(-n'+1, -n; 1; -\frac{4nn'}{\Delta^2}\right) = (-1)^{n'-1}\frac{n!}{(\Delta+1)!\,(n'-1)!}\left(\frac{4nn'}{\Delta^2}\right)^{n'-1}\gamma_2(n',n) \quad \ldots(E.5)$$

where

$$\gamma_2(n',n) = 1 - \frac{\Delta}{\Delta+2}\frac{(n'-1)^2}{n'^2}\left(\frac{\Delta}{4}\frac{n'}{n}\right) + \frac{1}{2!}\frac{\Delta^2}{(\Delta+2)(\Delta+3)}\frac{(n'-1)^2(n'-2)^2}{n'^4}\left(\frac{\Delta}{4}\frac{n'}{n}\right)^2 - + \cdots \quad \ldots(E.6)$$

We also define a correction factor $\delta(n)$ in such a way that all factorials can be written as

$$n! = \sqrt{2\pi n}\; n^n e^{-n}\,\delta(n) \quad \ldots(E.7)$$

For large n, $\delta(n)$ is obtained from the Stirling asymptotic formula for the gamma function (Abramowitz and Stegun, 1965, p.257):

$$\delta(n) \simeq 1 + \frac{1}{12n} + \frac{1}{288n^2} - \frac{139}{51,840\,n^3} - \cdots . \quad \ldots(E.8)$$

For small values of n, $\delta(n)$ is evaluated from eq.(E.7). Substituting eqs.(E.3) to (E.8) in eq.(2.8), and comparing the resulting equation with eq.(2.12), we obtain

$$g = \frac{\sqrt{3}}{2}\, 16^{n'} \left(\frac{n}{n+n'}\right)^{2n+2n'} \gamma_3(n', n)$$

$$\times \left[\gamma_1^2(n', n) - \frac{1}{16}\left(\frac{\Delta}{\Delta+1}\right)^2 \gamma_2^2(n', n)\right] \qquad \ldots(E.9)$$

where $$\gamma_3(n', n) = \left[\frac{\delta(n)}{\delta(n')\,\delta(\Delta)}\right]^2. \qquad \ldots(E.10)$$

BIBLIOGRAPHY

Abramowitz, M. and Stegun. I.A., 1965, Handbook of Mathematical Functions with Formulas, Graphs and Mathematical Tables, Dover Publications, New York.

Allen, C.W., 1961, Mém. Soc. R. Sci. Liège, 4, 241.

Bates, D.R. and Damgaard, A., 1949, Phil. Trans. Roy. Soc. London, A242, 101.

Bates, D.R. and Kingston, A.E., 1963, Planet. Space Sci., 11, 1.

Bates, D.R., Kingston, A.E., and McWhirter, R.W.P., 1962a, Proc. Roy. Soc., A267, 297.

Bates, D.R., Kingston, A.E., and McWhirter, R.W.P., 1962b, Proc. Roy. Soc., A270, 155.

Bely, O., 1962, C. R. Acad. Sci. Paris, 254, 3075.

Bely, O., 1965, C. R. Acad. Sci. Paris, 261, 909.

Bely, O., 1966a, Proc. Phys. Soc., 88, 587.

Bely, O., 1966b, Annales d'Astrophys., 29, 683.

Bely, O. and Petrini, D., 1970, Astron. and Astrophys., 6, 318.

Bely, O. and Van Regemorter, H., 1970, Ann. Rev. Astron. and Astrophys., 8, 329.

Bethe, H.A. and Salpeter, E.E., 1957, Quantum Mechanics of One- and Two-electron Atoms, Academic Press, New York.

Böhm, K.-H., 1960, in Stellar Atmospheres, edited by J.L. Greenstein, University of Chicago Press, Chicago, p.88.

Boland, B.C., Jahoda, F.C., Jones, T.J.L., and McWhirter, R.W.P., 1970, J. Phys. B 3, 1134.

Bradbury, J.N., Sharp, T.E., Mass, B., and Varney, R.N., 1973, Nucl. Instr. and Methods, 110, 75.

Burgess, A., 1958, Mon. Not. Roy. Astron. Soc., 118, 477.

Burgess, A., 1961, Mém. Soc. Roy. Sci. Liège, 4, 299.

Burgess, A., 1964, Mem. R. Astr. Soc., 69, 1.

Burgess, A. and Seaton, M.J., 1958, Rev. Mod. Phys., 30, 992.

Burgess, A. and Seaton, M.J., 1960, Mon. Not. Roy. Astron. Soc., 120, 121.

Burke, P.G., Tait, J.H., and Lewis, B.A., 1966, Proc. Phys. Soc., 87, 209.

Caves, T.C. and Dalgarno, A., 1972, J. Quant. Spectrosc. Radiat. Transfer, 12, 1539.

Cody, W.J. and Thacher, H.C. Jr, 1968, Mathematics of Computation, 22, 641.

Condon, E.U. and Shortley, G.H., 1957, The Theory of Atomic Spectra, Cambridge University Press, New York.

Copeland, 1884, Mon. Not. Roy. Astron. Soc., 45, 91.

Crossley, R.J.S., 1969, Advances in Atomic and Molecular Physics, 5, 237.

Davis, J. and Morin, S., 1970, J. Chem. Phys., 52, 4410.

Dewhurst, R.J., Jacoby, D., Pert, G.J., and Ramsden, S.A., 1976, Phys. Rev. Lett., 37, 1265.

Drawin, H.W., 1961, Z. Physik, 164, 513.

Drawin, H.W., 1962, Z. Physik, 168, 238.

Drawin, H.W., 1963, Atomic Cross-Sections for Inelastic Electronic Collisions, Euratom-C.E.A. Report No. EUR-CEA-FC-236.

Drawin, H.W., 1964, Z. Naturforsch., 19a, 1451.

Drawin, H.W., 1966, Collision and Transport Cross-Sections, Euratom-C.E.A. Report No. EUR-CEA-FC-383.

Drawin, H.W., 1969a, Z. Physik, 225, 470.

Drawin, H.W., 1969b, Z. Physik, 225, 483.

Drawin, H.W., 1969c, Z. Naturforsch., 24a, 1492.

Drawin, H.W., 1970a, High Temperatures - High Pressures, 2, 359.

Drawin, H.W., 1970b, J. Quant. Spectrosc. Radiat. Transfer, 10, 33.

Drawin, H.W., 1971, Phys. Lett., 34A, 151.

Drawin, H.W., 1975, in Progress in Plasmas and Gas Electronics, Volume I, edited by R. Rompe and M. Steenbeck, Akademie-Verlag, Berlin, p.591.

Drawin, H.W. and Emard, F., 1970, Instantaneous Population Densities of the Excited Levels of Hydrogen Atoms, Hydrogen-like Ions, and Helium Atoms in Optically Thin and Thick Non-LTE Plasmas, Euratom-C.E.A. Report No. EUR-CEA-FC-534.

Drawin, H.W. and Emard, F., 1972, Z. Physik, 253, 100.

Drawin, H.W. and Emard, F., 1973, Plasma Physik, 13, 143.

Drawin, H.W. and Emard, F., 1974, Z. Physik, 270, 59.

Elwert, G., 1952, Z. Naturforsch., 7a, 703.

Fano, U. and Cooper, J.W., 1968, Rev. Mod. Phys., 40, 441.

Flower, D.R., 1971, J. Phys. B, 4, 697.

Fuhr, J.R. and Wiese, W.L., 1971, Bibliography on Atomic Transition Probabilities (July 1969 through June 1971), Nat. Bur. Stand. (U.S.), Spec. Publ. 320, Suppl. 1.

Fuhr, J.R. and Wiese, W.L., 1973, Bibliography on Atomic Transition Probabilities (July 1971 through June 1973), Nat. Bur. Stand. (U.S.), Spec. Publ. 320, Suppl. 2.

Fujimoto, T., Sugiyama, I., and Fukuda, K., 1972, Mem. Faculty of Engin., Kyoto University, 34, part 2, 249.

Geltman, S., Rudge, M.R.H., and Seaton, M.J., 1963, Proc. Phys. Soc., 81, 375.

Giovanelli, R.G., 1948, Austral. J. Sci. Research, 1, 275.

Glennon, B.M. and Wiese, W.L., 1966, Bibliography on Atomic Transition Probabilities, Nat. Bur. Stand. (U.S.), Misc. Publ. 278.

Goldberg, L., 1935, Astrophys. J., 82, 1.

Goldberg, L., 1936, Astrophys. J., 84, 11.

Gol'dfarb, V.M., Il'ina, E.V., Kostygova, I.E., and Luk'yanov, G.A., 1969, Opt. Spektrosk., 27, 204 [1969, Optics and Spectrosc., 27, 108].

Gol'dfarb, V.M., Il'ina, E.V., Kostygova, I.E., Luk'yanov, G.A., and Silant'ev, V.A., 1966, Opt. Spektrosk., 20, 1085 [1966, Optics and Spectrosc., 20, 602].

Gordiets, B.F., Dymova, I.A., and Shelepin, L.A., 1971, Zh. Prikl. Spektrosk., 15, 205.

Gordiets, B.F., Gudzenko, L.I., and Shelepin, L.A., 1966, Zh. Tekh. Fiz., 36, 1622 [1967, Sov. Phys. - Tech. Phys., 11, 1208].

Gordiets, B.F., Gudzenko, L.I., and Shelepin, L.A., 1968, Zh. Eksp. Teor. Fiz., 55, 942 [1969, Sov. Phys. - JETP, 28, 489].

Gordon, W., 1929, Ann. Physik, 2, 1031.

Green, A.E.S., Sellin, D.L., and Zachor, A.S., 1969, Phys. Rev., 184, 1.

Green, L.C., Rush, P.P., and Chandler, C.D., 1957, Astrophys. J. Suppl., 3, 37.

Griem, H.R., 1964, Plasma Spectroscopy, McGraw-Hill, New York.

Gryzinski, M., 1959, Phys. Rev., 115, 374.

Gudzenko, L.I., Filippov, S.S., and Shelepin, L.A., 1966, Zh. Eksp. Teor. Fiz., 51, 1115 [1967, Sov. Phys. - JETP, 24, 745].

Gudzenko, L.I., Mamachun, A.T., and Shelepin, L.A., 1967, Zh. Tekh. Fiz., 37, 833 [1967, Sov. Phys. - Tech. Phys., 12, 598].

Gudzenko, L.I. and Shelepin, L.A., 1963, Zh. Eksp. Teor. Fiz., 45, 1445 [1964, Sov. Phys. - JETP, 18, 998].

Gudzenko, L.I. and Shelepin, L.A., 1965, Dokl. Akad. Nauk SSSR, 160, 1296 [1965, Sov. Phys. - Dokl., 10, 147].

Gudzenko, L.I., Shelepin, L.A., and Yakovlenko, S.I., 1974, Usp. Fiz. Nauk, 114, 457 [1975, Sov. Phys. - Usp., 17, 848].

Hayes, M.A., 1975, J. Phys. B, 8, L8.

Henry, R.J.W., 1970, Astrophys. J., 161, 1153.

Henry, R.J.W., 1974, J. Phys. B, 7, L439.

Henry, R.J.W. and Lipsky, L., 1967, Phys. Rev., 153, 51.

Herzberg, G., 1944, Atomic Spectra and Atomic Structure, Dover Publications, New York.

Hidalgo, M.B., 1968, Astrophys. J., 153, 981.

Hoffmann, P. and Bohn, W.L., 1972, Z. Naturforsch., 27a, 878.

House, L.L., 1964, Astrophys. J. Suppl., 8, 307.

Huggins, W. and Huggins, M., 1891, Proc. Roy. Soc., 49, 33.

Irons, F.E. and Peacock, N.J., 1974, J. Phys. B, 7, 1109.

Ivanova, A.V., 1964, Optics and Spectrosc., 16, 502.

John, T.L. and Morgan, D.J., 1973, Phys. Lett., 45A, 135.

Kelly, P.S., 1964, J. Quant. Spectrosc. Radiat. Transfer, 4, 117.

Kenney, J.F. and Keeping, E.S., 1954, Mathematics of Statistics, Part One, 3rd edition, Van Nostrand, New York.

Kingston, A.E. and Lauer, J.E., 1966a, Proc. Phys. Soc., 87, 399.

Kingston, A.E. and Lauer, J.E., 1966b, Proc. Phys. Soc., 88, 597.

Kirkwood, J.G., 1932, Phys. Z., 33, 521.

Kulander, J.L., 1970, J. Quant. Spectrosc. Radiat. Transfer, 10, 299.

Kunze, H.-J., 1971, Phys. Rev., A3, 937.

Kunze, H.-J. and Johnston, W.D. III, 1971, Phys. Rev., A3, 1384.

Layzer, D., 1959, Ann. Physik, 8, 271.

Leibowitz, E.M., 1972, J. Quant. Spectrosc. Radiat. Transfer, 12, 299.

Lengyel, B.A., 1966, Introduction to Laser Physics, John Wiley, New York.

Lindgård, A. and Nielsen, S.E., 1977, Atomic Data and Nuclear Data Tables, 19, 533.

Lotz, W., 1967, Z. Physik, 206, 205.

Lotz, W., 1968, Z. Physik, 216, 241.

Luk'yanov, G.A., 1977, Zh. Tech. Fiz., 47, 600 [1977, Sov. Phys. - Tech. Phys., 22, 361].

Marr, G.V. and Creek, D.M., 1968, Proc. Roy. Soc., A304, 245.

Martin, G.A. and Wiese, W.L., 1976a, Phys. Rev., A13, 699.

Martin, G.A. and Wiese, W.L., 1976b, J. Phys. Chem. Ref. Data, 5, 537.

Massey, H.S.W. and Burhop, E.H.S., 1952, Electronic and Ionic Impact Phenomena, Clarendon Press, Oxford.

McCoyd, G.C. and Milford, S.N., 1963, Phys. Rev., 130, 206.

McWhirter, R.W.P., 1965, in Plasma Diagnostic Techniques, edited by R.H. Huddlestone and S.L. Leonard, Academic Press, New York, p.201.

McWhirter, R.W.P. and Hearn, A.G., 1963, Proc. Phys. Soc., 82, 641.

Menzel, D.H. and Pekeris, C.L., 1935, Mon. Not. Roy. Astron. Soc., 96, 77.

Mewe, R., 1972, Astron. Astrophys., 20, 215.

Miles, B.M. and Wiese, W.L., 1970, Bibliography on Atomic Transition Probabilities (January 1916 through June 1969), Nat. Bur. Stand. (U.S.), Spec. Publ. 320.

Missavage, D.W. and Manson, S.T., 1972, Phys. Lett., 38A, 85.

Mitchner, M. and Kruger, C.H. Jr, 1973, Partially Ionized Gases, Wiley-Interscience, New York.

Moiseiwitsch, B.L. and Smith, S.J., 1968, Rev. Mod. Phys., 40, 238.

Moore, C.E., 1949, Atomic Energy Levels, Vol.I, Nat. Stand. Ref. Data Ser., Nat. Bur. Stand. (U.S.), NSRDS-NBS 35.

Moore, C.E., 1970, Selected Tables of Atomic Spectra, CI, CII, CIII, CIV, CV, CVI, Nat. Stand. Ref. Data Ser., Nat. Bur. Stand. (U.S.), NSRDS-NBS 3, Sec.3.

Moore, C.E., 1971, Selected Tables of Atomic Spectra, NIV, NV, NVI, NVII, Nat. Stand. Ref. Data Ser., Nat. Bur. Stand. (U.S.), NSRDS-NBS 3, Sec.4.

Norcross, D.W., 1969, J. Phys. B, 2, 1300.

Norcross, D.W. and Stone, P.M., 1968, J. Quant. Spectrosc. Radiat. Transfer, 8, 655.

Novotny, E., 1973, Introduction to Stellar Atmospheres and Interiors, Oxford University Press, New York.

Olver, F.W.J., 1974, Asymptotics and Special Functions, Academic Press, New York.

Oxenius, J., 1970a, Z. Naturforsch., 25a, 101.

Oxenius, J., 1970b, Z. Naturforsch., 25a, 1302.

Pagurova, V.I., 1961, Tables of the Exponential Integral $E_\nu(x)=\int_1^\infty e^{-xu}u^{-\nu}du$, Pergamon Press, New York.

Peach, G., 1967, Mem. R. Astr. Soc., 71, 13.

Petrini, D., 1972, Astron. Astrophys., 17, 410.

Plaskett, J.S., 1924, Publ. Dominion Astrophys. Obs., 2, 346.

Presnyakov, L.P. and Urnov, A.M., 1975, Sov. Phys. - JETP, 41, 31.

Rainville, E.D., 1960, Special Functions, MacMillan, New York.

Rudge, M.R.H. and Schwartz, S.B., 1966, Proc. Phys. Soc., 88, 563.

Russell, H.N., 1936, Astrophys. J., 83, 129.

Sato, K., Shiho, M., Hosokawa, M., Sugawara, H., Oda, T., and Sasaki, T., 1977, Phys. Rev. Lett., 39, 1074.

Schwartz, S.W., 1971, Unpublished.

Seaton, M.J., 1955, C. R. Acad. Sci. Paris, 240, 1317.

Seaton, M.J., 1958a, Mon. Not. Roy. Astron. Soc., 118, 504.

Seaton, M.J., 1958b, Rev. Mod. Phys., 30, 979.

Seaton, M.J., 1959, Mon. Not. Roy. Astron. Soc., 119, 81.

Seaton, M.J., 1962, in Atomic and Molecular Processes, edited by D.R. Bates, Academic Press, New York, p.414.

Seaton, M.J., 1966a, Proc. Phys. Soc., 88, 801.

Seaton, M.J., 1966b, Proc. Phys. Soc., 88, 815.

Selby, S.M., editor, 1970, CRC Standard Mathematical Tables, 18th edition, The Chemical Rubber Co., Cleveland.

Shaw, J.F., Mitchner, M., and Kruger, L.H., 1970a, Phys. Fluids, 13, 325.

Shaw, J.F., Mitchner, M., and Kruger, L.H., 1970b, Phys. Fluids, 13, 339.

Shoub, E., 1977, Astrophys. J. Suppl., 34, 259.

Smith, H.J., 1955, Ph.D. Thesis, Dept. of Astronomy, Harvard University, Cambridge.

Spiegel, M.R., 1968, Mathematical Handbook of Formulas and Tables, McGraw-Hill, New York.

Spitzer, L. Jr, 1956, Physics of Fully Ionized Gases, Interscience Publishers, New York.

Stevefelt, J. and Robben, F., 1972, Phys. Rev., A5, 1502.

Suckewer, S., 1970, Phys. Lett., 33A, 110.

Taylor, A.J. and Lewis, B.A., 1965, A.E.R.E. Report No. R5061.

Taylor, B.N., Parker, W.H., and Langenberg, D.N., 1969, Rev. Mod. Phys., 41, 375.

Tiwari, P., Hashim, M.A., and Ojha, S.P., 1975, Can. J. Phys., 53, 1524.

Trefftz, E., 1963, Proc. Roy. Soc., A271, 379.

Tully, J.A., 1973, Can. J. Phys., 51, 2047.

Tully, J.A. and Petrini, D., 1974, J. Phys. B, 7, L231.

Underhill, A.B., 1959, Publ. Dominion Astrophys. Obs., 11, 209.

Unsöld, A., 1977, The New Cosmos, 2nd edition, Springer-Verlag, Berlin.

Van Regemorter, H., 1962, Astrophys. J., 136, 906.

Varsavsky, C.M., 1963, Planet. Space Sci., 11, 1001.

Varshni, Y.P., 1977, Astrophys. Space Sci., 46, 443.

Varshni, Y.P. and Lam, C.S., 1976, Astrophys. Space Sci., 45, 87.

Vedenov, A.A., 1965, in Reviews of Plasma Physics, Volume I, edited by M.A. Leontovich, Consultants Bureau, New York, p.312.

Vogel, H.C., 1873, Berichte K. Sächs. Ges. der Wiss., p.556 (Dec.).

Vogel, H.C., 1883, Publicationen Astrophys. Observ. Potsdam, 4, No. 14, 17.

Weiss, A.W., 1963, Astrophys. J., 138, 1262.

White, H.E. and Eliason, A.Y., 1933, Phys. Rev., 44, 753.

Wiese, W.L., Smith, M.W., and Glennon, B.M., 1966, Atomic Transition Probabilities - Hydrogen through Neon (A Critical Data Compilation), Vol.I, Nat. Stand. Ref. Data Ser., Nat. Bur. Stand. (U.S.), NSRDS-NBS 4.

Wigner, E., 1931, Phys. Z., 32, 450.

Willett, C.S., 1974, Gas Lasers: Population Inversion Mechanisms, Pergamon Press, New York.

Wolf, R. and Rayet, G., 1867, Comptes Rendus, 65, 292.

Zemtsov, Yu.K., 1971, Thesis for Candidate's Degree, Scientific-Research Institute for Nuclear Physics, Moscow State University.